THE PREDICTION OF SAILING YACHT PERFORMANCE.

by

J.C. Sainsbury

A THESIS SUBMITTED FOR THE DEGREE OF

DOCTOR OF PHILOSOPHY

IN THE FACULTY OF ENGINEERING,

UNIVERSITY OF SOUTHAMPTON.

October 1965.

PREFACE

The work described in this Thesis was started as an attempt to analyse, in a General manner, the windward performance of sailing yachts; at the same time it was intended to produce a more accurate and general method of predicting the Optimum Windward Performance of a sailing yacht than that in use at the time which was based on the work of D.S.M. Davidson, published in his well known paper 'Some Experimental Studies of the Sailing Yacht' in 1936.

In the very early stages of the analysis it was thought that the main lack of data was in the field of sail aerodynamics, as very little useful published work was available; wind tunnel experiments then being undertaken as part of the University's Yacht Research programme have to a large extent eased this problem, and some results from these experiments have been used in the work to estimate the performance of a yacht using the analysis developed in PART 1.

A considerable number of yacht hulls had been tested in towing tanks, principally at the Davidson Laboratory in the U.S.A., and at the National Physical Laboratory and at Saunders Roe Division of Westland Aircraft Ltd. in the U.K., so that a large amount of useful data was thought to be available for use in the analysis. It soon became evident however, that although a large amount of experimental data had been collected, it was for the most part shielded by security

requirements of designers, and in any case did not give a sufficiently broad picture of the properties of sailing yacht hulls for use in a general analysis of the type being developed.

The high cost of using commercial towing tanks made it necessary to design and construct a small towing tank facility at the University for use in experimental work with yacht hulls in order to obtain the data in the form required for the analysis. PART 2 is a description of the design, construction, development and evaluation work necessary to bring this facility to a standard suitable for producing the required hull data.

PART 3 describes and studies the results of model tests made to obtain the data required for the performance analysis, together with some other experimental work undertaken as a start to the further understanding of the properties of sailing yacht hulls.

This work could not have been undertaken without the constant encouragement and support of Prof. E.J. Richards, and the Pallisades Foundation who provided financial support.

Staff of the Department of Aeronautics and Astronautics workshop erected the towing tank, for which Mr.L. Dykes produced the detailed drawings; the Electronics were designed by Mr. G.A. Allcock and built by the staff of the Aero-Electronics workshop.

The Author wishes place on record his deep indebtedness to Mr. T. Tanner, whose assistance and guidance proved of inestimable value.

CONTENTS

PART 3 Model Experiments

LIST OF FIGURES

LIST OF TABLES

TERMS AND SYMBOLS

Gimcrack Technique	A method of predicting the Optimum Windward Performance of a sailing yacht, based on Davidson's work of Ref. 9 which included full scale trials of the yacht 'GIMCRACK'.
Hull Characteristics (Hydro-dynamic characteristics)	Properties of the hull in terms of hydro-dynamic coefficients.
Sail Characteristics (Aerodynamic characteristics)	Properties of the sails in terms of Aeordynamic coefficients.
$V/\sqrt{L}$	Speed-Length Ratio: ratio of Course speed in knots to square root of waterline length in feet.
A.U.W.	All up weight of yacht (Displacement)
L.C.G.	Longitudinal Centre of Gravity
V.C.G.	Vertical centre of gravity
Sea Axes	A set of axes with the x-y plane parallel to the sea surface, the x axis along the course.
Body Axes	A set of axes with the x-y plane perpendicular to the vessel's centre line plane, the z axis vertical and the x axis in the centre line plane
Body/Sea Axes	A set of axes with the x-y plane parallel to the sea surface and the x axis in the vessel's centreline plane.
Hull Inclination	Attitude of the hull in heel and leeway

Optimum windward performance Optimum windward ability Optimum V_{MG} Best V_{MG}	Maximum speed to windward at any value of the true wind velocity.
Sail Setting Sail sheeting	A measure of the manner in which sails are sheeted in terms of the angle between tack and clew.
Sail Configuration	The number and arrangement of sails on the yacht
Sail Planform	The shape of the sailplan in profile when all sails are sheeted in to the centreline.
Section shape (of sails) Chord shape (of sails)	Shape of sail in section
Sail Cut	The shape given to a sail by the sailmaker during manufacture.
Weather Helm	Rudder Angle to Leeward (Tiller angle to Windward) to prevent vessel from departing from course to windward.
Lee Helm	Rudder Angle to windward (Tiller angle to leeward) to prevent vessel from departing from course to leeward.
Envelope Curve (for V_{MG})	Curve showing Best V_{MG} for vessel against True Wind speed with one sail sheeting position, resulting from curves showing vessels windward performance at several heel angles.
Boundary Curve (for V_{MG})	Curve showing Best V_{MG} for vessel against True Wind velocity, taking into account all possible sail sheeting positions (obtained by taking the enevlope curve of the Envelope Curve above).

V_S	Course Velocity of Yacht
γ	Angle between the yachts course and the Apparent Wind.
V_T	Velocity of True Wind
V_A	Velocity of Apparent Wind
β	Angle between the Apparent wind and the course.
V_{MG}	Speed made good to windward (speed to windward) component of vessels course velocity giving progress in a direction 180° to direction of the True Wind.
λ	Angle of Leeway
$\beta-\lambda$	Angle of incidence of yacht to Apparent Wind
θ	Angle of Heel
δ_F	Sheeting angle for Foresail of Sloop Rig. Angle between line joining tack and clew of Foresail and C.L.
δ_M	Sheeting angle for Mainsail of Sloop Rig. Angle between boom and C.L.
F_X, F_Y, F_Z	Components of Aerodynamic Force on sails referred to x,y,z, axes of Body/Sea axes system.
F_{Xw}, F_{Yw}, F_{Zw}	Components of Hydrodynamic Force on Yacht's hull referred to x.y.z. axes of Body/Sea axes system.
M_X, M_Y, M_Z	Moments due to aerodynamic force on sails referred to x,y,z, axes of Body/Sea axes system.
M_{Xw}, M_{Yw}, M_{Zw}	Moments due to hydrodynamic force on yacht's hull referred to x,y,z, axes of Body/Sea axes system.
C_X, C_Y, C_Z	Aerodynamic Coefficients referring to force components F_X, F_Y, F_Z.

C_{Xw}, C_{Yw}, C_{Zw}	Hydrodynamic Coefficients referring to Force components F_{Xw}, F_{Yw}, F_{Zw}.
K_X, K_Y, K_Z	Aerodynamic Coefficients referring to moments M_X, M_Y, M_Z.
K_{Xw}, K_{Yw}, K_{Zw}	Hydrodynamic Coefficients referring to moments M_{Xw}, M_{Yw}, M_{Zw}.
ρ_A	Air Density
ρ_W	Water Density
S	Characteristic Sail Area
P	Characteristic length for sails
A	Characteristic Hull Area
Q	Characteristic length for Hull
C_L	Lift Coefficient
C_D	Drag Coefficient
R_T	Total Resistance
R_R	Residuary Resistance
R_F	Frictional Resistance
C_T	Total Resistance Coefficient.
C_R	Residuary Resistance Coefficient
C_F	Friction Resistance Coefficient.
W.S.	Wetted Surface
L.W.L.	Load waterline
W.L.	Waterline

PART 1

THE PREDICTION OF SAILING YACHT PERFORMANCE

CHAPTER 1: INTRODUCTION

Before the publication of K.S.M. Davidsons well-known paper 'Some Experimental Studies of the Sailing Yacht' (Ref. 9) in 1936, anomalies had been observed in the performance of sailing yachts 'on the wind' and before the wind. Tank Test of yachts had been undertaken in an effort to assess performance, but restricted to the upright condition with the hull making no leeway: both yachtsmen and experts were surprised to find that although the hull showing better capabilities in the condition equivalent to running free from the test results was actually preferable when on the run, it could well prove less reliable when sailing close-hauled.

Most yachtsmen still agree that races are 'won or lost on the windward leg', so that this common reversal of predictions was worrying. Davidson therefore undertook tank tests in an attempt to determine the reasons for the 'anomaly' and after establishing a viable means of using small models in a model basin he showed that it was necessary to take into account the hulls characteristics

when travelling with leeway and heel, as actually occurred when 'on the wind'. He followed this by establishing the now accepted fact that a complete assessment of the yacht's performance can only be achieved by considering the balance of forces due to the effects of air and water on the sails and hull.

By measuring the pertinent angles and velocities on a full size yacht sailing its best to windward and comparing them with the results of tank tests on a model hull of the same vessel, Davidson was able to determine the forces on the sails and hence the aerodynamic coefficients of the sails for optimum windward performance of that yacht.

These 'Gimcrack' Coefficients, named after the yacht to which they refer, were used by Davidson to assess the windward performance of other yachts.

It is clear from the paper, that Davidson realised the limited application of the coefficients, and that the sailplan and cut might affect the values, Stevens Institute have continued to use the Gimcrack Coefficients, albeit in a modified form, in their routine predictions for the performance of sailing yachts.

It would appear that this method of performance prediction is a means of comparing the performance of hulls following tank tests. Using the method, the Stevens Tank has accumulated great experience in assessing the capabilities of yachts and although the continued use of such a method cannot be said to promote actual understanding of sailing yacht behaviour, it's very continuance for some 30 years virtually unchanged must lead to the belief that when carried out by experienced personnel, it produces the correct order of comparison, which

is confirmed by the performance of the actual yachts when racing. Certainly a great amount of work on full scale measurement and its comparison with tank results at Stevens following the original work did not lead to any appreciable change in the method.

At about the same time that Davidson undertook his now classic work on yacht performance, Sir Richard Fairey, in connection with a challenge for the America's Cup, was promoting research into sails in the wind tunnel at Hayes, Middlesex. Although a very great number of sail measurements were made and a vast amount of analysis of water and air conditions when racing undertaken, it is evident from the paper and results available that although the inter-relation between hull and sails was realised, it was not fully understood.

Following the advent of the Yacht Research Council in 1963, work on yacht performance was recommenced in the United Kingdom at the Ship Division of the National Physical Laboratory, and at Saunders Roe Ltd.

At the National Physical Laboratory, the windward performance of the 5.5 metre Yacht YEOMAN was measured and compared with the predicted ability as calculated from the results of tank tests using the Gimcrack procedure. Despite some doubts concerning the method of deciding when YEOMAN was sailing at 'best speed to

windward', and the difference in results with different helmsmen, the large scatter in full scale results, and the difference possible in a model prediction curve when varying assumptions of hull flow state were used, the results of this work were declared to show that this method of prediction would give a reasonable estimate of a yacht's actual windward performance. (Ref. 13)

Following what was thought to be a proof of the Stevens procedure, work was put in hand at Saunders Roe Ltd. in Cowes, to study the performance of a Dragon Class Yacht in an attempt to produce better results from this class in the next Olympic Games. A wide range of tank test results were used with the aid of the Gimcrack analysis to give curves of 'Best windward performance' with the yacht under various conditions of weight and trim, (Refs. 1 & 2).

P.V. McKinnon remarks in a letter now held in the yacht Research Council files at Southampton University, that a compariosn of the results of the N.P.L. and Saunders Roe experiments indicates that a Dragon was capable of a better Windward performance than a 5.5 metre, a known fallacy. A possible reason for this other than the inherent tolerance of the analysis is that the two series of experiments were undertaken in different tanks and that different flow states round the hulls were assumed.

Saunders Roe Ltd. have continued to use a revised and extended Gimcrack analysis to compare the windward performance of a number of sailing craft, and the technique must be assumed to give the correct order of ability due to its continued use; the simplicity and evident usefulness of Davidsons original work in assessing comparative performance when handled by experienced personnel at the same establishment must be considered the reason for its continued use by the Davidson Labratory and the intention of Saunders Roe Ltd, (ref. 4) to continue with it.

Despite this advantage in routine analysis of commercial hull tests, the Gimcrack method was evolved as a first stage in a much wider investigation; it takes no account of variations in the sail characteristics which must occur due to shape, planform and configuration, and setting angles, nor does it attempt to relate the hull and sail forces in other than a relatively crude manner.

Several attempts have been made to improve the Gimcrack type of analysis while retaining the same general form, notably Barkla (Ref. 23) and Crewe (Ref. 3).

Tanner returned to the basic balance of hull and sail forces in an attempt to determine the true geometry and mechanics of sailing to windward. Simplifying the problem to one

of a yacht sailing only in the upright condition, equivalent to a light displacement vessel held upright by the crew, he showed how the basic geometry of windward sailing allied with the results of wind tunnel sail tests and tank hull tests could be used to obtain a predicted curve giving the yacht's best speed to windward at any true wind condition. (Ref. 24)

As in the case of the Gimcrack analysis, this method of performance prediction resulted in a 'boundary' curve giving the maximum possible speed to windward over the range of wind speeds; it might be expected that only when very carefully sailed and with optimum sail sheeting and helmsmanship would this performance actually reach the optimum boundary; the 'setting-up' of the yacht's sailing geometry and mechanics when under way would still be entirely at the whim of the helmsman.

In his work Tanner laid the foundation for a fresh and more basic approach to the problem of yacht performance analysis and prediction along lines which showed promise of considerable extension and generalisation.

The work described in the following chapters uses a similar basic approach but is extended and generalised to give a wider application to both the practical yachtsman interested in setting up and sailing his craft at maximum efficiency, and for use in studies of the mechanics of windward sailing for sail

propelled vessels.

It is widely recognised that the helmsman is all important during windward sailing; it would be difficult if not impossible at this stage to deal mathematically with the technique and thinking of the helmsman, moreover, if racing, the presence and activity of other craft together with tactics becomes as important as obtaining the maximum speed to windward of which the yacht is capable when sailing alone. From the practical sailor's point of view a method of analysis which uses the sailing geometry together with the mechanics of hull and sails in order to assist the helmsman in setting up his craft for optimum windward sailing is likely to prove of value. Such analysis must give the helmsman the required information in terms of physical quantities which he can control and measure while sailing.

If an analysis of windward sailing is to be of use in the study of performance, it must be possible to use basic characteristics of the hull and sails to predict the performance, and be sufficiently general to allow its use in assessing the effects of changes in a single perameter.

CHAPTER 2: THE PERFORMANCE ANALYSIS

2.1 Setting up the Problem

A yacht will normally sail in water with tidal drift or other currents and waves, together with wind conditions which are unstable in velocity and direction.

An analysis of the vessels performance under such conditions introduces a great complexity of variables and handling. It is true to say that understanding of the behaviour of powered ships in a seaway is not yet complete so that to introduce such complications together with the associated effects on sail characteristics, especially when the latter are allied with unstable airflow conditions must be considered impracticable at this stage when even the performance of the yacht in steady state is not fully understood and analysed.

The problem as in the work of writers discussed previously, has therefore been set as that of calculating and analysing the performance for a yacht in a steady state of sailing. While this general solution may be applied to all points of sailing, it is used here to consider the vessels optimum windward performance in terms of the relevant variables which are chosen in order to allow direct use of results from model tests and reference to measurable particulars of the yacht.

Windward performance is the ultimate goal of the analysis, due to the general agreement among racing yachtsmen that 'races are won or lost on the windward leg', and that it is this area of sailing, the most difficult to solve, which has occupied the attention of many previous studies in the field of yacht performance.

The analysis of a yacht's performance involves study of the sailing geometry, the hull characteristics and the sail characteristics, which must be chosen and combined to give the performance in terms of the requirements previously set out.

2.2. The Geometry

Consider a yacht sailing in steady conditions with velocity V_S along a course making an angle γ with the true wind, velocity V_T. Fig. 1 shows this situation for a vessel sailing so that γ is less than 90°. In this case the relative wind approaching the sails is V_A, which makes an angle β with the course. When γ is less than 90°, the yacht will have a 'speed made good to windward' of V_{MG}, and it is this quantity which represents directly the windward ability of the yacht.

A similar velocity diagram may be drawn for γ greater than 90°.

Fig. 2 shows a sailing vessel superimposed on the velocity diagram of Fig. 1. Due to the hull making leeway, the vessel's

centreline is inclined at an angle λ to windward of the course; the angle of leeway; the direction of the relative wind with the yacht's centreline is $\beta - \lambda$.

If wind tunnel measurements of sail characteristics are to be used in analysing sailing yacht performance, then the quantities used must be those applicable to tunnel experiments.

A yacht while sailing may well operate under conditions where the true wind has a velocity gradient above the sea surface due to a boundary layer effect. A number of measurements have been made of this gradient and it has been shown to exist well out to sea where the wind travels over a large stretch of open water; measured gradients in these conditions have been shown to depend on the sea state but to vary widely under approximately similar conditions. In the presence of land, the question is more complicated and a number of experiments have indicated that no gradient exists.

Attempts have been made in a wind tunnel to simulate the gradient by means of a wire mesh in order to study its effects on sail characteristics; an alternative method might be to correct wind tunnel results in a uniform air stream for a gradient effect but in either case it is necessary to know the gradient in question.

For the present analysis it is assumed that no gradient exists and wind tunnel results used are those applicable to a uniform air stream.

In the wind tunnel, the air velocity represents V_A and the sail model is turned so that its centreline is at a known angle to the direction of V_A: i.e. $\beta - \lambda$. The required components of sail force and associated moments may be measured using either direction of V_A or the yacht's centreline as a principal axis, and from these measurements the relevant aerodynamic coefficients may be calculated.

The aerodynamic forces and coefficients are likely to depend on $\beta - \lambda$, V_A, the angle of heel θ ,mastrake, the sail configuration and planform, the section shape of the sails and other factors due to the 'cut', the sail cloth, and the setting angles of the sails in relation to one another and the vessels centreline.

For one particular suit of sails, it may be assumed that the variables can be reduced to V_A, θ , $\beta - \lambda$, mastrake and the sail setting angles, i.e. that the effects of sail cut and cloth are always the same for constant V_A, θ , $\beta - \lambda$, mastrake and sail setting.

The most common rig in use today is the sloop, in which case it is possible to define the sail setting in terms of the angles between the chord of each sail foot and the yacht's centreline; i.e. as δ_F, and δ_M for foresail and mainsail respectively, see Fig. 3.

In the case of other sail configurations, the number of sail sheeting angles necessary as variables will depend on the number of independent sails employed, i.e. the sail configuration, and the analysis may be extended to cover all possible combinations.

It may be noted that all the variables now remaining may be set or measured directly on the yacht: V_A the wind velocity, θ the angle of heel, $\beta-\lambda$ the direction of the relative wind to the centreline, the trim, and the angle between the foot of each sail and the centreline.

In the model towing tank the model is run at speed V_S along a course at which the centreline is inclined at an angle of leeway λ ; the hydrodynamic coefficients may be measured with respect to the course or the hull centreline as a principal axis. These characteristics might be expected to vary with V_S; λ , θ , trim, the hull shape, the hull weight and C.G. position and rudder angle. For a particular vessel these variables will be reduced to V_S, λ , θ , all of which may be referred to and measured at the yacht.

If a balance of sail and hull characteristics similar to but more extensive than that of Tanner (ref. 24) is to be made, a suitable set of axes must be chosen. Tanner and all other writers have used the vessel's course as one principal axis, enabling the relation of all results directly to the geometry and the setting up of a set of 'sea' axes with the x axis along the course, the y axis perpendicular to the course, and the z axis vertical. It has already been seen that if wind tunnel results are to be related directly to the yacht they must be connected with $\beta-\lambda$ as β is not known until the analysis has been undertaken and the necessary λ established. It is possible to refer the sail characteristics to the angle β , as in the case of Tanner, but this is arranged mathematically and does

not allow the acutal sail setting on the yacht to be derived for the performance found. It is therefore, a pre-requisite that one axis of the set should be along the vessel's centreline; this could lead to the use of a set of Body Axes with the x axis along the centreline, the y axis perpendicular to the centreline and the z axis perpendicular to the xy plane, possibly along a 'vertical' mast. However, on considering a vessel heeled, the axes are inclined to the sea plane and lose a simple connection with the geometry.

This suggests the use of a set of 'Body-Sea' axes as shown in Fig. 4 with the axis along the centreline considered positive looking forward, the y axis perpendicular to the centreline considered positive looking down. As the xy plane is parallel to the Sea plane, a direct connection with the geometry is obtained while the physical quantities used for reference to the yacht are referred to the vessel's reference planes.

The origin of such an axes system is best placed at some known and easily determined physical position on the yacht so that the moment characteristics may be related to the vessel during wind tunnel and tank experiments. A convenient location might be the point where the mast centreline passes through the deck centreline, or some similar position.

2.3 Breakdown of hydrodynamic and aerodynamic forces acting on the yacht.

The resultant aerodynamic forces on the yacht's sails may be broken down into three components parallel to the three reference axes, together with three associated moments referred to these axes.

The same is true for the hydrodynamic components.

Fig. 5 illustrates how the force components and moments may be defined for a yacht using the system of Body-Sea axes developed earlier. In the figure, the static balance between the vessels weight and buoyancy has been omitted as this may be considered automatic and does not appear in the dynamic balance.

Aerodynamic Components

F_X is the component, of sail force, along + Ox.

F_Y is the component, of sail force, along + Oy.

F_Z is the component, of sail force, along + Oz.

M_X is the moment, of sail force, about Ox tending to heel the vessel

M_Y is the moment, of sail force, about Oy tending to trim the vessel by the bow.

M_Z is the moment, of sail force, about Oz tending to rotate the vessel on to the wind.

Hydrodynamic components

F_{Xw} is the component, of hull force, along - Ox.

F_{Yw} is the component, of hull force, along - Oy.

F_{Zw} is the component, of hull force, along - Oz.

M_{Xw} is the moment, about Ox tending, to right the vessel.

M_{Yw} is the moment, about Oy tending, to trim the vessel by the stern.

M_{Zw} is the moment, about Oz tending, to rotate the vessel off the wind.

Although the static balance of weight and buoyancy is not included, the hull when underway and heeled will possess a certain righting moment which is included under M_{Xw}.

2.4 Complete Balance Equations

With the yacht in a steady sailing state, the complete dynamic balance conditions may be stated as follows:

$$F_X = F_{Xw} \qquad M_X = M_{Xw}$$

$$F_Y = F_{Yw} \qquad M_Y = M_{Yw}$$

$$F_Z = F_{Zw} \qquad M_Z = M_{Zw}$$

These forces and moments may conveniently be expressed in

terms of non-dimensional coefficients as:

$$F_X = C_X \cdot \tfrac{1}{2} \cdot \rho_A \cdot S \cdot V_A^2 \qquad M_X = K_X \cdot \tfrac{1}{2} \cdot \rho_A \cdot S \cdot P \cdot V_A^2$$

$$F_Y = C_Y \cdot \tfrac{1}{2} \cdot \rho_A \cdot S \cdot V_A^2 \qquad M_Y = K_Y \cdot \tfrac{1}{2} \cdot \rho_A \cdot S \cdot P \cdot V_A^2$$

$$F_Z = C_Z \cdot \tfrac{1}{2} \cdot \rho_A \cdot S \cdot V_A^2 \qquad M_Z = K_Z \cdot \tfrac{1}{2} \cdot \rho_A \cdot S \cdot P \cdot V_A^2$$

$$F_{Xw} = C_{Xw} \cdot \tfrac{1}{2} \cdot \rho_W \cdot A \cdot V_S^2 \qquad M_{Xw} = K_{Xw} \cdot \tfrac{1}{2} \cdot \rho_W \cdot A \cdot Q \cdot V_S^2$$

$$F_{Yw} = C_{Yw} \cdot \tfrac{1}{2} \cdot \rho_W \cdot A \cdot V_S^2 \qquad M_{Yw} = K_{YW} \cdot \tfrac{1}{2} \cdot \rho_W \cdot A \cdot Q \cdot V_S^2$$

$$F_{Zw} = C_{Zw} \cdot \tfrac{1}{2} \cdot \rho_W \cdot A \cdot V_S^2 \qquad M_{Xw} = K_{Xw} \cdot \tfrac{1}{2} \cdot \rho_W \cdot A \cdot Q \cdot V_S^2$$

----------(1)

where C_X, C_Y, C_Z, C_{Xw}, C_{Yw}, C_{Zw}, K_X, K_Y, K_Z, K_{Xw}, K_{Yw}, K_{Zw} are non-dimensional coefficients, the suffix $_W$ referring to water quantities.

In the above:

ρ_A is the air density

S is a 'characteristic' sail area.

P is a 'characteristic' length for the sail plan

ρ_W is the water density

A is a 'characteristic' area for the hull.

Q is a 'characteristic' length for the hull.

The choice of sail area to use for S in the expressions may be made from: the total sail area, the sail area as obtained from a rating rule, or the plan form area excluding overlap. In comparing the characteristics of various sail plans, a preference may be felt for one or other of the areas; probably if in connection with a racing yacht the rating area might be applicable, but for the present purpose any of the alternatives may be taken as 'characteristic'. In the work of later chapters, the total area has been used.

The choice of A could be either a wetted surface or a profile area; as both these areas are liable to alter with speed, leeway and heel, the applicable condition for measurement must be stated. In the work of later chapters, the wetted surface area in the static zero heel condition has been used.

The characteristic lengths for sail plan and hull likewise present a choice of possible quantities; possible values for P may be the mean chord for the sailplan, the foot length of the sailplan or the height of the sailplan; later work uses the height. Q may be taken as the mean chord of the wetted profile or the waterline length; as before, the condition for measurement must be given; later work takes Q as the waterline length in the static, zero heel condition.

In coefficient form, the balance conditions of (1) may be written as:

$$C_X \cdot \tfrac{1}{2} \cdot \rho_A \cdot S \cdot V_A^2 = C_{Xw} \cdot \tfrac{1}{2} \cdot \rho_W \cdot A \cdot V_S^2$$

$$C_Y \cdot \tfrac{1}{2} \cdot \rho_A \cdot S \cdot V_A^2 = C_{Yw} \cdot \tfrac{1}{2} \cdot \rho_W \cdot A \cdot V_S^2$$

$$C_Z \cdot \tfrac{1}{2} \cdot \rho_A \cdot S \cdot V_A^2 = C_{Zw} \cdot \tfrac{1}{2} \cdot \rho_W \cdot A \cdot V_S^2$$

$$K_X \cdot \tfrac{1}{2} \cdot \rho_A \cdot S \cdot P \cdot V_A^2 = K_{Xw} \cdot \tfrac{1}{2} \cdot \rho_W \cdot A \cdot Q \cdot V_S^2$$

$$K_Y \cdot \tfrac{1}{2} \cdot \rho_A \cdot S \cdot P \cdot V_A^2 = K_{Yw} \cdot \tfrac{1}{2} \cdot \rho_W \cdot A \cdot Q \cdot V_S^2$$

$$K_Z \cdot \tfrac{1}{2} \cdot \rho_A \cdot S \cdot P \cdot V_A^2 = K_{Zw} \cdot \tfrac{1}{2} \cdot \rho_W \cdot A \cdot Q \cdot V_S^2$$

By rearranging each of these equations to give expressions for $\frac{\rho_W \cdot A \cdot V_S^2}{\rho_A \cdot S \cdot V_A^2}$, the complete balance equation becomes:

$$\frac{C_X}{C_{Xw}} = \frac{C_Y}{C_{Yw}} = \frac{C_Z}{C_{Zw}} = \frac{P \cdot K_X}{Q \cdot K_{Xw}} = \frac{P \cdot K_Y}{Q \cdot K_{Yw}} = \frac{P \cdot K_Z}{Q \cdot K_{Zw}} = \frac{\rho_W \cdot A \cdot V_S^2}{\rho_A \cdot S \cdot V_A^2} \qquad \text{----------(3)}$$

Values of C_X, C_Y, C_Z, C_{Xw}, C_{Yw}, C_{Zw}, K_X, K_Y, K_Z, K_{Xw}, K_{Zw} may be obtained for the sails and hull of a yacht under consideration, from wind tunnel and tank experiments at various values of V_S and V_A:

A,S,P,Q, for any vessel may be set out as described previously; ρ_W and ρ_A are known for a particular air and water state.

2.5 Simplified balance equations.

The coefficients for one vessel will, however, vary due to the attitudes of sails and hull as discussed earlier, and a complete measurement of all the coefficients would require extremely sophisticated wind tunnel and tank instrumentation which has not as yet been fully developed.

This fact together with the complexity of matching all the coefficient variations with the complete balance equation (3), and the geometry leads to the necessity of simplifying the balance conditions to ensure that the balance is undertaken for the quantities that have greatest effect on the performance.

It is generally agreed that the yacht's leeway and heel are important factors governing performance, as the sideforce and resistance of the hull, and the equivalent sail characteristics dictate largely the sailing speed which may vary widely with changes in them.

From experience it is found that trim changes and displacement changes are less important. The yawing 'balance' of a yacht depends on the rudder application, the sail sheeting and fore and aft location of the sail plan, so that this can well be considered as a separate condition.

It is considered that the following simplifications may now be assumed in a first analysis of the balance.

(1) The vertical balance is affected by the vertical force from the sails, the vertical component of hydrodynamic force on the hull and changes in hull buoyancy, which may result in a change of waterline. The value of these quantities and any changes which may result in other characteristics have not as yet been studied so that the effect of this balance on the characteristics of sails and hull must be considered small and the balance omitted.

(2) It is assumed that the yacht is perfectly 'balanced' with the rudder angle locked so that this balance may be omitted. A study into whether it is desirable to have weather or lee helm as an aid to performance (Ref. 14) indicates that rudder application can have an effect on the performance, this can however be studied by considering the application as producing a different set of hull characteristics and putting them through the simplified analysis, if desired. It is therefore assumed that the balance of $M_Z = M_{Zw}$ may be omitted.

(3) The yacht when sailing experiences moments from the sails, hull, and rudder, acting about Oy. Small changes in trim are likely to have a negligible effect on the sail characteristics and only a small effect on hull characteristics. The variation of hull

characteristics with trim has not yet been studied in detail, but if the the effects are important, they may be taken into account by loading the model in a similar manner to the procedure for tank testing at Saunders Roe and the Davidson Laboratory (Ref. 10, 5). It is therefore assumed that the balance $M_Y = M_{Yw}$ may be omitted for a simplified analysis.

The complete equations for the simplified balance conditions, from (1) are now seen to be:

$$F_X = F_{Xw}$$

$$F_Y = F_{Yw}$$

$$M_X = M_{Xw}$$

Or in coefficient form:

$$C_X \cdot \tfrac{1}{2} \cdot \rho_A \cdot S \cdot V_A^2 = C_{Xw} \cdot \tfrac{1}{2} \cdot \rho_W \cdot A \cdot V_S^2 \quad \text{----------(4)}$$

$$C_Y \cdot \tfrac{1}{2} \cdot \rho_A \cdot S \cdot V_A^2 = C_{Yw} \cdot \tfrac{1}{2} \cdot \rho_W \cdot A \cdot V_S^2 \quad \text{----------(5)}$$

$$K_X \cdot \tfrac{1}{2} \cdot \rho_A \cdot S \cdot P \cdot V_A^2 = K_{Xw} \cdot \tfrac{1}{2} \cdot \rho_W \cdot A \cdot V_S^2 \quad \text{----------(6)}$$

The simultaneous solution of equations (4), (5), and (6) together with the geometry will give a balanced sailing condition and the performance at that sailing condition.

(4), (5), and (6) may be rearranged to give:

$$\frac{A.\rho_W.V_S^2}{S.\rho_A.V_A^2} = \frac{C_X}{C_{Xw}} = \frac{C_Y}{C_{Yw}} = \frac{P.K_X}{Q.K_{Xw}}$$

Any combination of these may be used to calculate the balance: the following three conditions are covenient:

$$\frac{C_Y}{C_X} = \frac{C_{Yw}}{C_{Xw}} \qquad \text{——————————(7)}$$

$$\frac{C_Y}{C_{Yw}} = \frac{P.K_X}{Q.K_{Xw}} \qquad \text{——————————(8)}$$

$$\frac{C_Y}{C_{Yw}} = \frac{A.\rho_W.V_S^2}{S.\rho_A.V_A^2}$$

and as $\frac{\rho_W}{\rho_A}$ has a reasonably constant value of 835, then:

$$\frac{C_Y}{C_{Yw}} = \frac{835.A.V_S^2}{S.V_A^2} \qquad \text{——————————(9)}$$

Equation (7) provides the balance of forces

Equation (8) connects the balance of forces and moments

Equation (9) connects the balanced sailing conditions with the geometry.

To provide for a complete definition of the sailing condition for the geometry, one further geometric quantity is required, which may conveniently be β. The solution of the balance equations must therefore allow for the emergence of β.

2.6 Graphical Solution of Balanced Sailing Condition

Results of wind tunnel and tank experiments will show the appropriate coefficients, in terms of the parameters affecting them, as graphs for which no simple expression is likely to be available. A graphical method of solution is therefore desirable and to reduce the complexity of such a solution, it is convenient to assume that sail characteristics are unaffected by the value of V_A, i.e. that Reynolds Number and effect of changes in V_A on the sail shape and twist and flow through the material may be neglected. Data covering this is very limited and it will be possible to allow for changes in sail characteristics with V_A later.

If the sails are considered sheeted home in one position so that the value of δ_F and δ_M is constant, then the sail characteristics for this sheeting position may, in order to be immediately applicable to the analysis, be expressed as curves showing values of K_X, C_Y, and $\beta - \lambda$, for varying $\frac{C_Y}{C_X}$. Fig. 6 shows this for the sails of an 'X' class One Design yacht as calculated from the data

contained in Ref. 28 extrapolated to 15° heel by the method outlined in App. 1 to this part at, $\delta_M = 5°$, $\delta_F = 17\frac{1}{2}°$. Similar graphs would show the sail characteristics for this sail sheeting at other heel angles.

It is well known that the hull characteristics may vary widely with V_S, so that it is necessary here to have these for a number of course velocities.

For the hull, the characteristics at a particular angle of heel will appear similar to those in Fig. 7, as curves showing values of K_{Xw}, C_{Yw}, and λ for several values of V_S. The curves of Fig. 7 are taken from the results of experiments on a 'Dragon' class hull described in Part 3. These tests were made at four different model velocities indicated in the figure and are commented on in Part 3.

It is now possible to combine the sail and hull characteristics to obtain a balanced sailing state for the yacht.

From Figs. 6 & 7, it is possible to determine values of C_Y, C_{Yw}, K_X and K_{Xw} for which $\frac{C_Y}{C_X}$ and $\frac{C_{Yw}}{C_{Xw}}$ are identical, at each value of V_S. e.g.:

from Fig. 5, at $\frac{C_Y}{C_X} = 4$, $C_Y = 0.96$, and $K_X = 0.337$.

from Fig. 6, at $\frac{C_{Yw}}{C_{Xw}} = 4$, $C_{Yw} = 0.0262$, and $K_{Xw} = 0.0085$, at a Full scale course velocity of 9.46 ft/sec.

C_Y, C_{Yw}, K_X, K_{Xw}, may be obtained from the figures for a number of values for $\frac{C_Y}{C_X}$ and $\frac{C_{Yw}}{C_{Xw}}$ and set out as shown in Table 1 below:

TABLE 1

$\frac{C_Y}{C_X} = \frac{C_{Yw}}{C_{Xw}}$	sail characteristics		hull characteristics at V_S (f.s.) = 9.46		balance quantities at V_S (f.s.) = 9.46	
	C_Y	K_X	C_{Yw}	K_{Xw}	$\frac{C_Y}{C_{Yw}}$	$\frac{P.K_X}{Q.K_{Xw}}$
2.6	1.53	0.53	0.017	0.0092	90.2	89.5
3.0	1.25	0.44	0.0198	0.0090	63.2	76.0
3.5	1.07	0.38	0.023	0.0088	46.5	67.0
4.0	0.96	0.337	0.0262	0.0085	36.5	61.5
4.5	0.87	0.030	0.0295	0.0082	29.5	57.0

it is assumed in compiling the table that $\frac{P}{Q} = 1.55$.

Having tabulated the required quantities, they may be combined in order to satisfy equation 8 of the balance conditions; it will be noted that equation 7 has been satisfied already by taking values of C_Y, C_{Yw}, K_X, K_{Xw} at identical values of $\frac{C_Y}{C_X}$, equal to $\frac{C_{Yw}}{C_{Xw}}$.

The final columns of Table 1 will therefore show $\frac{C_Y}{C_{Yw}}$ and $\frac{P.K_X}{Q.K_{Xw}}$ at each value of $\frac{C_Y}{C_X}$ (equal to $\frac{C_{Yw}}{C_{Xw}}$). (in the table, $\frac{P}{Q}$ has been assumed equal to 1.55, the actual value for a DRAGON as found in Chapter 4).

Equation 8 is finally satisified when the last two columns show the same figure. Obviously in the case shown, this point lies between $\frac{C_Y}{C_X}$ of 2.6 and 3.0, and the true value can be found as the crossing point for curves of $\frac{C_Y}{C_{Yw}}$ and $\frac{P.K_X}{Q.K_{Xw}}$ drawn to a base of $\frac{C_Y}{C_X}$ (equal to $\frac{C_{Yw}}{C_{Xw}}$) as shown in Fig. 8, although the crossing point is nearly at the lower limit of $\frac{C_Y}{C_X}$ as shown by the sail curves, the curves of Fig. 8 have been continued well beyond to show their characteristic shapes.

The crossing point is shown ringed and gives: $\frac{C_Y}{C_{Yw}} = 88.6$, $\frac{C_Y}{C_X} = 2.65$

It remains to satisfy equation 9 and this is achieved when:

$$\frac{V_S}{V_A} = \sqrt{\frac{C_Y.S}{C_{Yw}.A.835}}$$

As the balance has been established for a known value of V_S, then the condition set by equation 9 is met when:

$$V_A = V_S \cdot \sqrt{\frac{C_{Yw} \cdot A \cdot 835}{C_Y \cdot S}}$$

Assuming $\frac{A}{S}$ for the DRAGON is 0.556, (the value found in Chapter 4), then:

$$V_A = 9.46 \cdot \sqrt{\frac{0.556 \times 835}{\frac{C_Y}{C_{Yw}}}}$$

$$= 9.46 \cdot \frac{21.55}{\sqrt{88.6}}$$

$$= 21.7 \ \frac{sec}{ft.}$$

It is now known that at an apparent wind velocity of 21.7 $\frac{ft}{sec}$, the yacht will sail at a heel angle of 15° with a course velocity of 9.46 $\frac{ft}{sec.}$

To enable the complete geometry to be specified, it is necessary to obtain the value of β :

Now, at the balance point, $\frac{C_Y}{C_X} = 2.65$, and on referring to Fig.6 for the sails it is seen that at the value of $\frac{C_Y}{C_X}$, $\beta - \lambda = 32.4°$,

On referring to Fig. 7 for the hull, at $\frac{C_{Yw}}{C_{Xw}} = 2.65$, $\lambda = 3.70°$

therefore $\beta = 36.1°$.

The sailing condition for the yacht may now be specified:

$V_A = 21.7$ $\frac{ft}{sec}$, $V_S = 9.46$ $\frac{ft}{sec}$, $\beta = 36.1°$, $\theta = 15°$, for a sail sheeting of $\delta_M = 5°$, $\delta_F = 17\frac{1}{2}°$.

By use of the geometry, the true wind velocity V_T and the vessel's spped to windward V_{MG} may be calculated:

Frpm Fig. 1, it can be shown that $V_T = V_A \cdot \frac{\text{Sin } \beta}{\text{Cos. } \gamma}$

and $V_{MG} = V_S \cdot \text{Cos } \gamma$.

again, from Fig. 1, it may be shown that:

$$\sin \gamma = \frac{\sin \beta}{\sqrt{1 + \left(\frac{V_S}{V_A}\right)^2 - 2. \frac{V_S}{V_A}.\text{Cos}\beta}}$$

so giving γ, the remaining qnantity necessary for calculation of V_T and V_{MG}.

In the previous example, $\sin \gamma = \frac{\sin \beta}{\sqrt{1 + 0.19 - 0.87 \times 0.808}}$

giving $\gamma = 57.8°$

so that from the expressions above, $V_T = 21.7 \times \frac{0.589}{0.848} = 15.5$ ft/sec.

$V_{MG} = 9.46 \times 0.533 = 5.03$ ft/sec

$= 2.97$ knots.

2.7 Extension of Solution to Give Windward Performance for the Yacht

The balanced sailing position for which V_T and V_{MG} were found in the last section is unlikely to be the optimum speed to windward for the vessel at the particular V_T with the chosen sail setting. As the hull and sail characteristics are available at three known heel angles, it is now possible to determine balance positions for each V_S at each of the heel angles. The result is a series of curves as shown in Fig. 9 and the envelope of these curves will give the vessels optimum performance over the complete range of V_T and heel for the particular sail sheeting considered. The curves shown in Fig. 9 were obtained during work connected with Chapter 4, using sail data and hull data given Appendices 1 & 2.

Although the envelope curve in Fig. 9 represents the yacht's best windward performance with the particular sail setting considered, if these sheeting angles are changed, then a number of such curves may be plotted, and it is the envelope of these which will give the boundary curve showing the yacht's true optimum windward performance.

Note on hull data

During model tests, the model is likely to be run at several course velocities covering the range likely to be applicable to the range of V_T in which the vessel is designed to sail. At any particular

heel angle, therefore, data may be required for a number of values of V_S for each heel angle, it is possible to provide data in the form shown in Appendix 2 to this part, as curves of C_{Yw} and K_{Xw} against V_S for constant values of $\frac{C_{Yw}}{C_{Xw}}$ on one graph, and λ against V_S on a second graph. This enables the coefficients C_{Yw}, K_{Xw}, and λ to be read off for a series of $\frac{C_{Yw}}{C_{Xw}}$ at the required value of V_S.

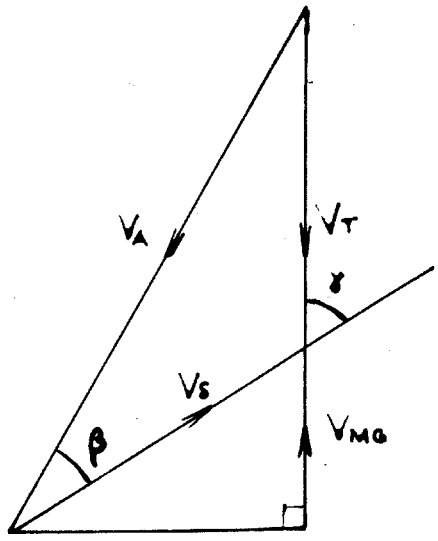

fig 1 velocity vector diagram

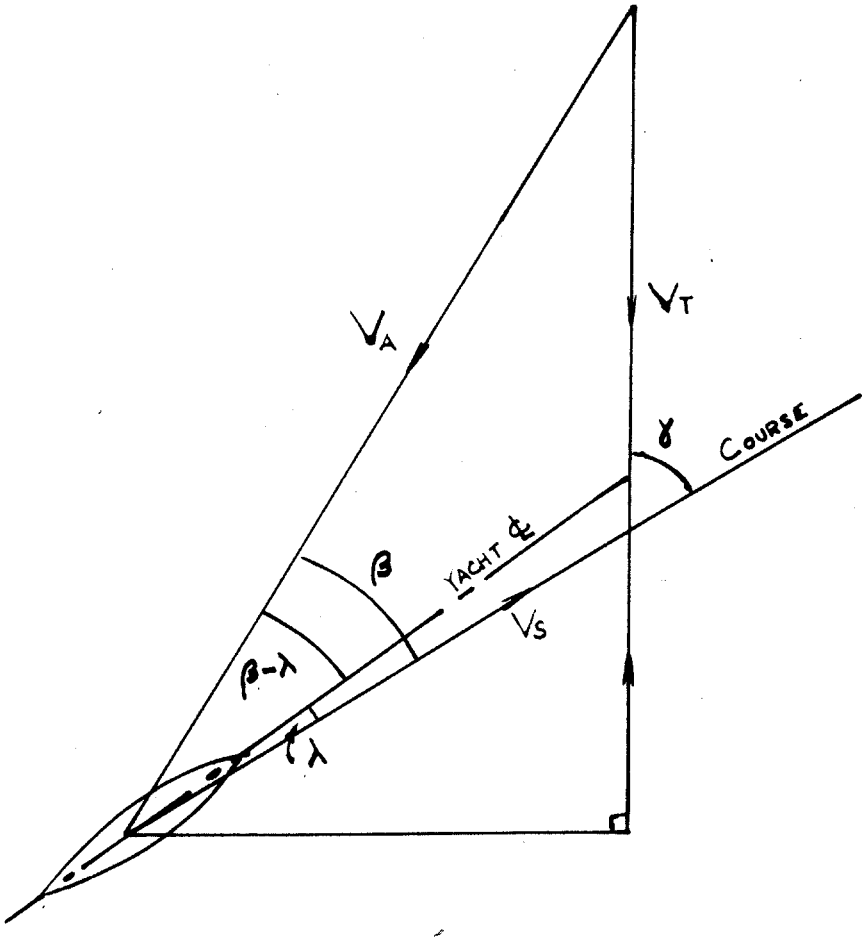

fig 2 the geometry

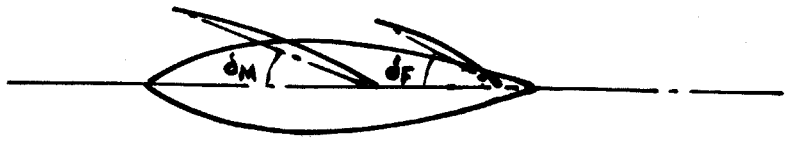

fig 3 sail sheeting definitions
yacht is upright

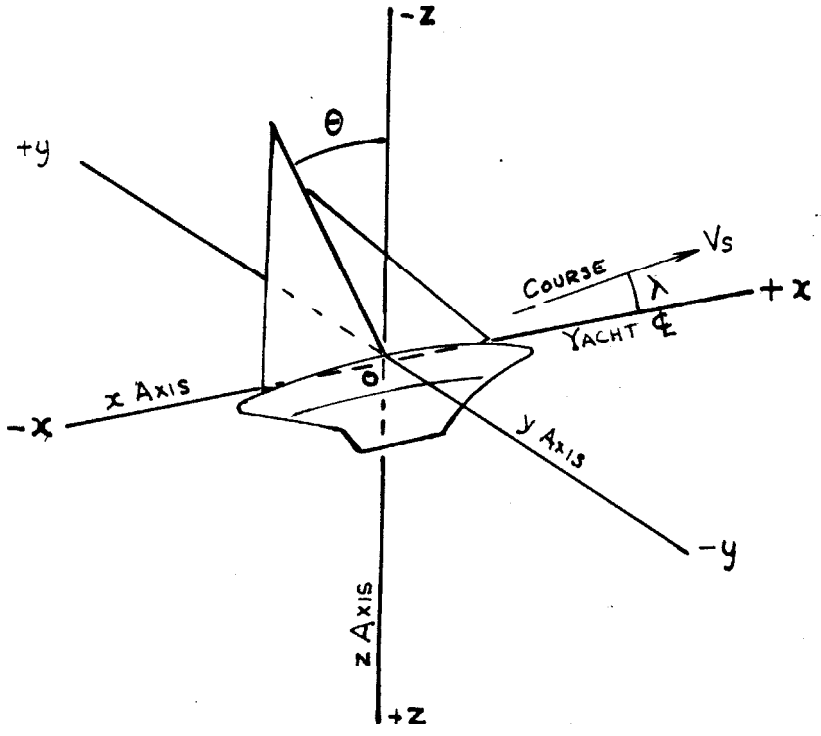

fig 4 body sea axes
yacht at heel θ°, leeway λ°
starboard tack.

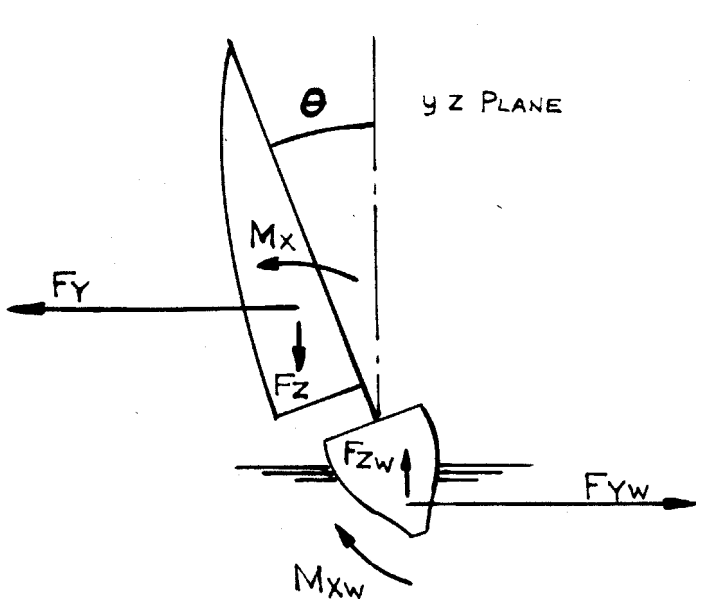

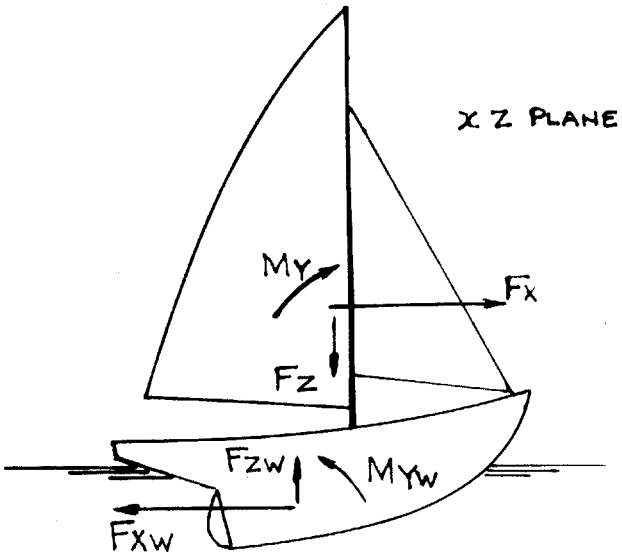

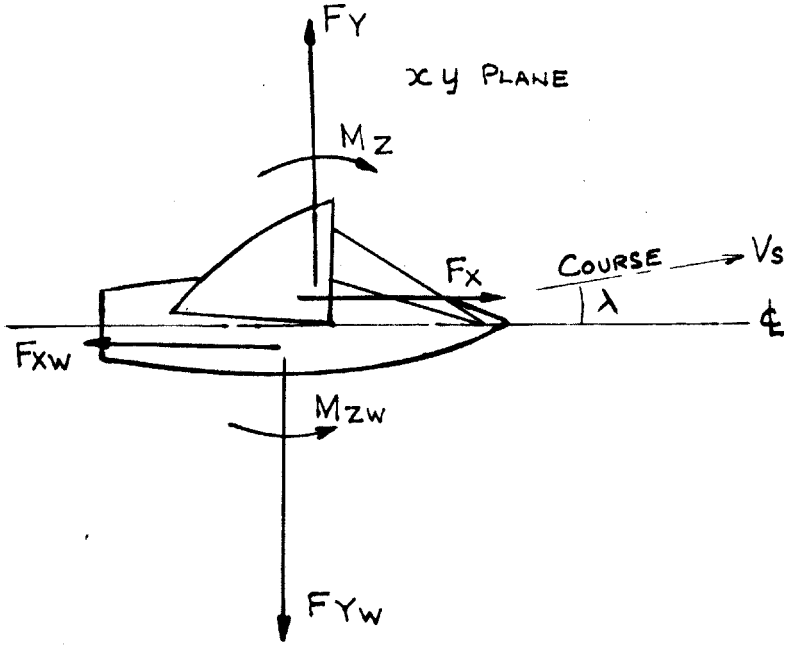

fig 5 diagrammatic representation of dynamic force and moment components on yacht.

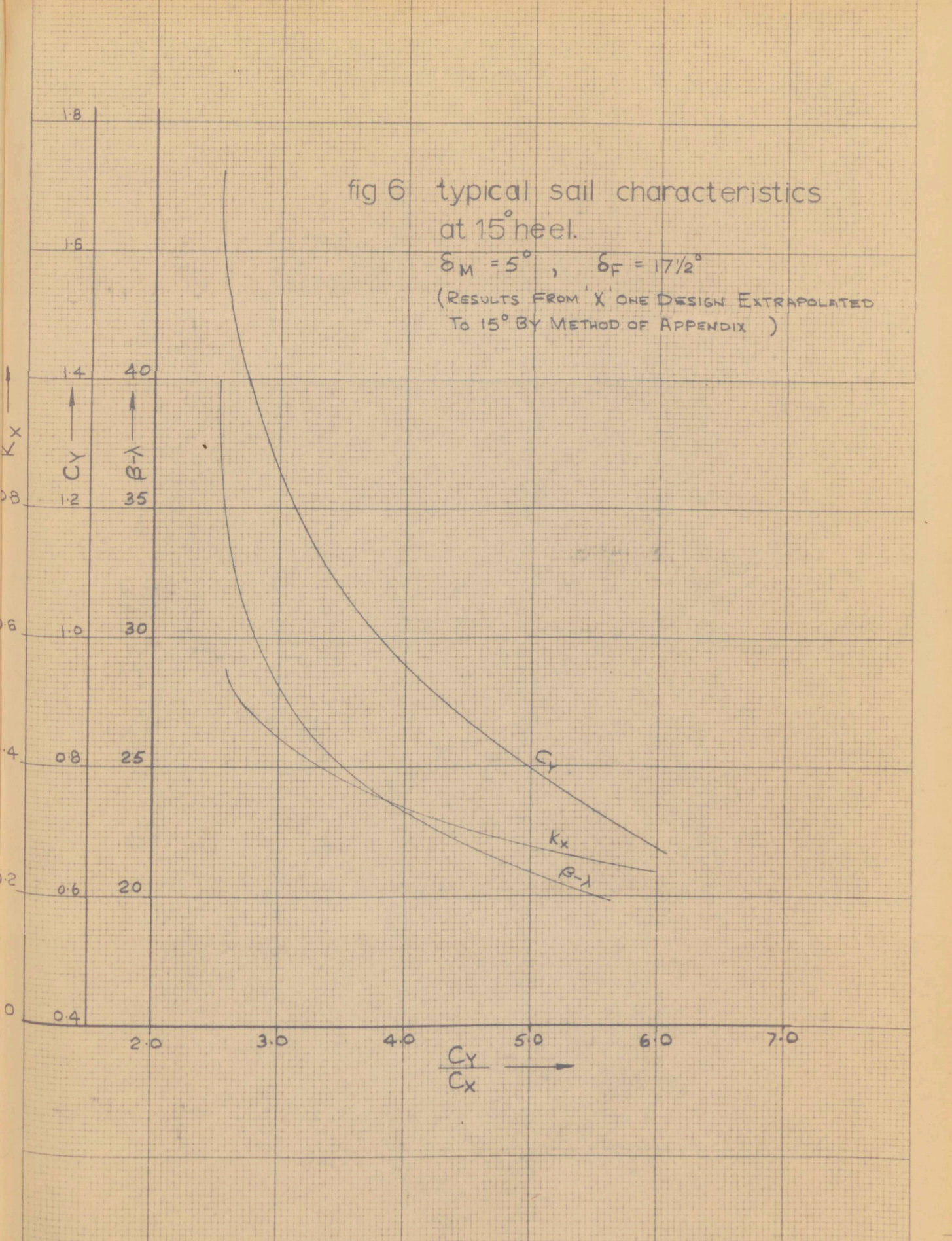
fig 6 typical sail characteristics at 15° heel.
$\delta_M = 5°$, $\delta_F = 17\frac{1}{2}°$
(Results from 'X' one Design Extrapolated To 15° By Method of Appendix)
1·8
1·6
1·4
1·2
1·0
0·8
0·6
0·4
40
35
30
25
20
C_Y
$\beta - \lambda$
K_X
C_Y
K_X
$\beta - \lambda$
2·0
3·0
4·0
5·0
6·0
7·0
$\frac{C_Y}{C_X}$

fig 7 typical hull characteristics
dragon hull at 15° heel.

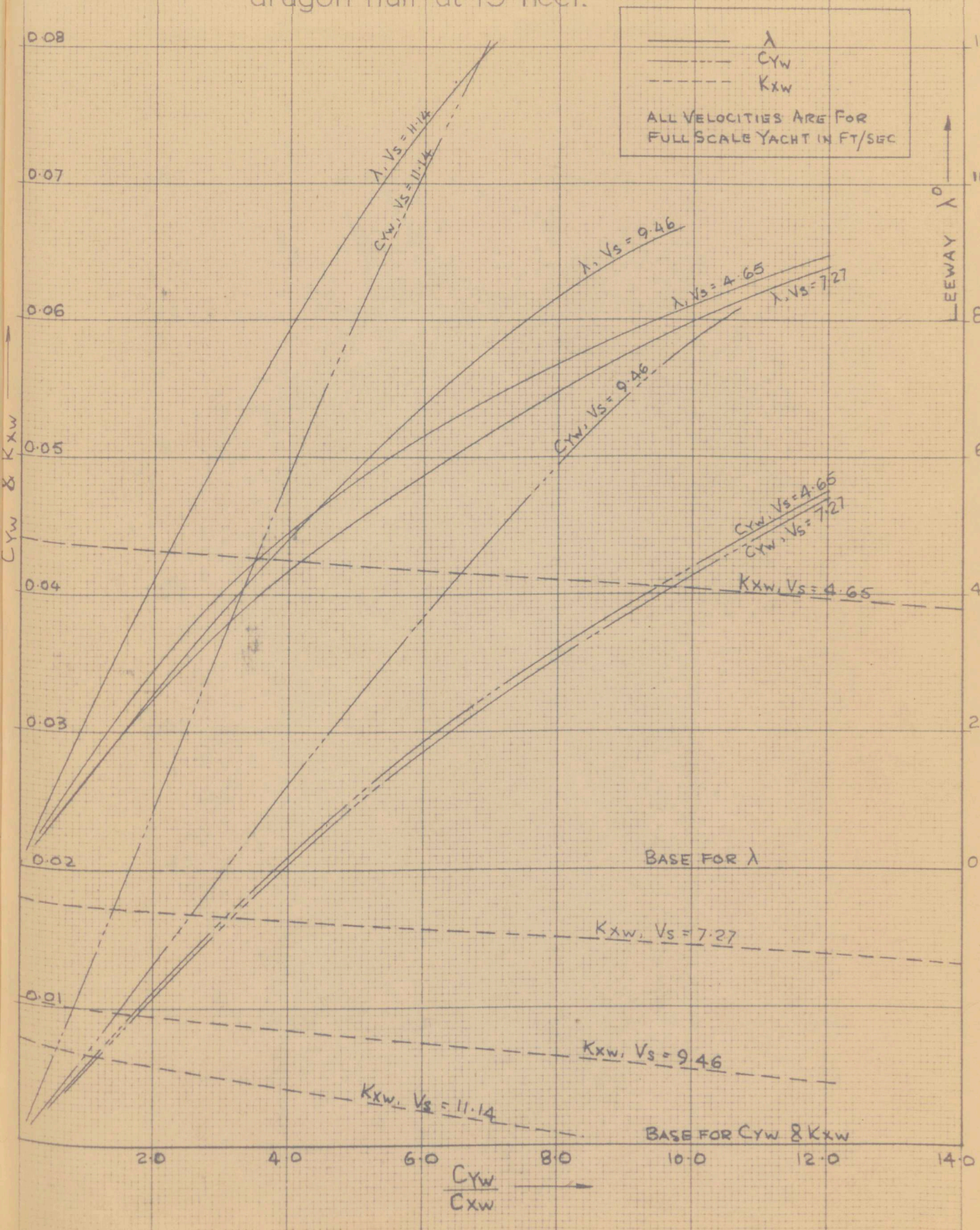

fig 8 obtaining balanced sailing position for yacht.

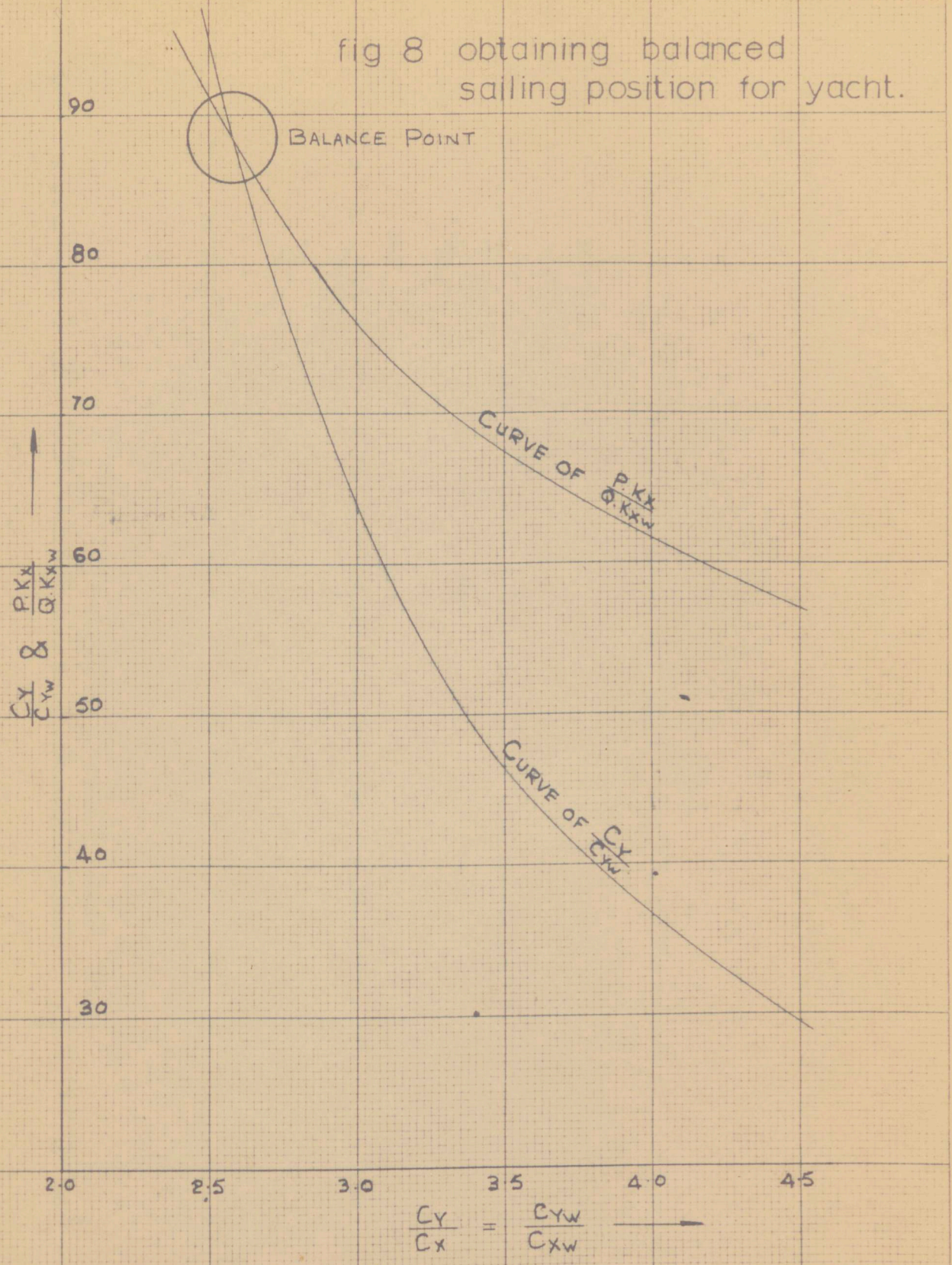

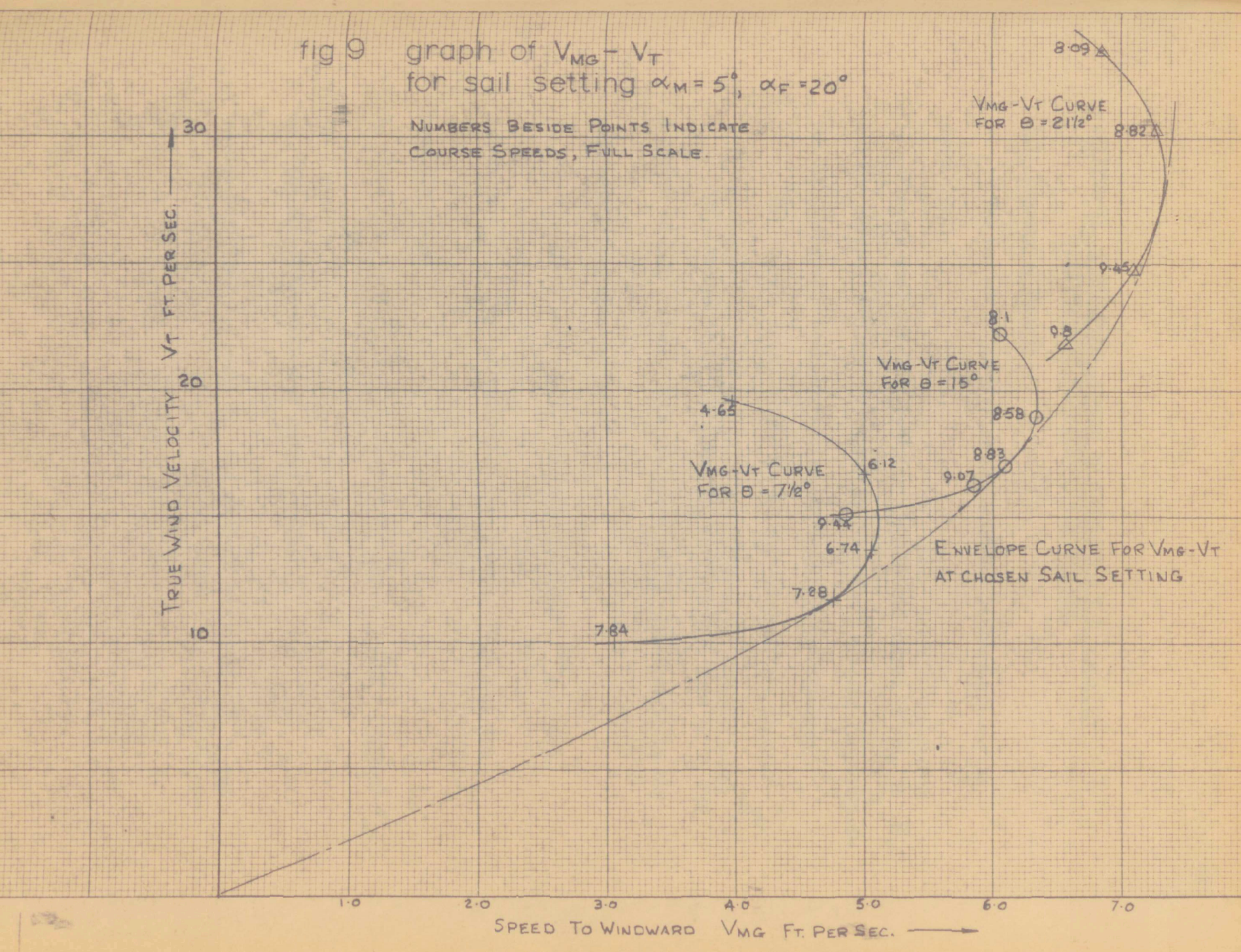
fig 9 graph of $V_{MG} - V_T$ for sail setting $\alpha_M = 5°$, $\alpha_F = 20°$
Numbers beside points indicate course speeds, full scale.
True Wind Velocity V_T ft. per sec.
30
20
10
1·0
2·0
3·0
4·0
5·0
6·0
7·0
Speed to Windward V_{MG} ft. per sec.
V_{MG}-V_T Curve for θ = 21½°
8·09
8·82
9·45
V_{MG}-V_T Curve for θ = 15°
8·1
9·8
8·58
8·83
9·07
V_{MG}-V_T Curve for θ = 7½°
4·65
6·12
9·44
6·74
7·88
7·84
Envelope Curve for V_{MG}-V_T at chosen sail setting

CHAPTER 3: A PRACTICAL METHOD OF PREDICTING THE WINDWARD PERFORMANCE FROM MODEL TEST RESULTS.

3.1 Summary of Method

The method of predicting the windward performance may be summarised:

1. Select a sail sheeting position (particular values of δ_F & δ_M) and for several heel angles covering the likely sailing range obtain the following sail characteristics and hull characteristics:

   (a) Curves of C_Y, ($\beta - \lambda$), K_X, plotted to a base of $\frac{C_Y}{C_X}$.

   (b) Curves of C_{Yw}, λ , and K_{Xw} plotted to a base of V_S for a number of $\frac{C_{Yw}}{C_{Xw}}$ values, with the range of $\frac{C_Y}{C_X}$ appropriate to the sail characteristics in (a) above.

2. For the first heel angle, tabulate $\frac{C_Y}{C_{Yw}}$ and $\frac{P.K_X}{Q.K_{Xw}}$ for values of $\frac{C_Y}{C_X} = \frac{C_{Yw}}{C_{Xw}}$ at several course speeds (V_S) over the possible range.

3. Plot $\frac{C_Y}{C_{Yw}}$ and $\frac{P.K_X}{Q.K_{Xw}}$ to a base of $\frac{C_Y}{C_X}$ (= $\frac{C_{Yw}}{C_{Xw}}$) for each V_S.

4. Take the intersection of curves showing $\frac{C_Y}{C_{Yw}}$ and $\frac{P.K_X}{Q.K_{Xw}}$, the balance positions for each V_S and read off values of $\frac{C_Y}{C_{Yw}}$ and $\frac{C_Y}{C_X}$.

5. Calculate V_A from :

$$V_A = V_S \sqrt{\frac{835.A.C_{Y_W}}{S.C_Y}}$$

6. Calculate $\beta = (\beta - \lambda) + \lambda$, the values of the component angles being taken from the data of item (1) at the value of $\frac{C_Y}{C_X}$ and $\frac{C_{Y_W}}{C_{X_W}}$ given by item (4).

7. Use geometry to obtain V_T and V_{MG} for each balance point from:

$$V_{MG} = V_S . \cos\gamma \quad , \text{ and } \quad V_T = V_A . \frac{\sin\beta}{\sin\gamma}$$

(where, $\sin\gamma = \frac{\sin\beta}{\sqrt{1 + \left(\frac{V_S}{V_A}\right)^2 - 2.\frac{V_S}{V_A}.\cos\beta}}$)

8. Plot V_T to a base of V_{MG} for the heel angle θ considered.

9. Repeat operations (2) to (8) for each selected heel angle, so that a curve of V_T to V_{MG} is obtained for each θ. The envelope of these curves gives the optimum windward performance of the yacht with the values of δ_M and δ_F chosen.

10. Repeat items (1) to (9) to give envelope curves for a wide range of sail sheeting covering the values of δ_M and δ_F in which

the optimum performance might be expected with the chosen sails.

3.2 Example Solution

In practice the calculation for each sheeting position chosen may be effected rapidly as demonstrated in the example below which gives the optimum performance curve at one sheeting position ($\delta_M = 5°$, $\delta_F = 20°$) as shown in Fig. 9:

Sail Data at $\theta = 7\frac{1}{2}°$ is given in Fig. 29, (Appendix 1), and the Hull Data at $\theta = 7\frac{1}{2}°$ is given in Fig. 37, (Appendix 2). From this data, Table 2 shown below may be compiled for a number of course speeds; only sufficient values of $\frac{C_Y}{C_{Y_W}}$ and $\frac{P.K_X}{Q.K_{X_W}}$ need be calculated to give good curves for determination of balance points.

TABLE 2

$\frac{C_Y}{C_X}$	C_Y	K_X	V_S = 6.12 ft/sec.				V_S = 7.84 ft/sec.			
			C_{Yw}	K_{Xw}	$\frac{C_Y}{C_{Yw}}$	$\frac{P.K_X}{Q.K_{Xw}}$	C_{Yw}	K_{Xw}	$\frac{C_Y}{C_{Yw}}$	$\frac{P.K_X}{Q.K_{Xw}}$
2.5	1.615	0.575	0.0122	0.0131			0.0131	0.0071	123	125
3.0	1.32	0.480	0.0142	0.0129			0.0149	0.0069	89	108
3.5	1.11	0.40	0.0168	0.0127			0.0180	0.0067	62	92.5
4.0	0.97	0.345	0.0186	0.0125	52	42.7	0.0203	0.0065		
4.5	0.875	0.310	0.0202	0.0124	43.4	38.8				
5.0	0.805	0.290	0.0223	0.0123	36.1	36.6				
5.5	0.740	0.270	0.0242	0.0122	30.6	34.4				
6.0	0.695	0.260	0.0260	0.0121						

$\frac{C_Y}{C_X}$	C_Y	K_X	V_S = 6.74 ft/sec				V_S = 4.65 ft/sec.			
			C_{Yw}	K_{Xw}	$\frac{C_Y}{C_{Yw}}$	$\frac{P.K_X}{Q.K_{Xw}}$	C_{Yw}	K_{Xw}	$\frac{C_Y}{C_{Yw}}$	$\frac{P.K_X}{Q.K_{Xw}}$
2.5	1.615	0.575								
3.0	1.32	0.480	0.0143	0.0103	92	72				
3.5	1.11	0.40	0.0168	0.0101	66	61				
4.0	0.97	0.345	0.0187	0.0099	52	54				
4.5	0.875	0.31	0.0203	0.0048	43	49				
5.0	0.805	0.290					0.0239	0.0221	33.7	20.4
5.5	0.740	0.270					0.0259	0.0220	28.6	19.0
6.0	0.695	0.260					0.0278	0.0219	25	18.4
7.0	0.60	0.245					0.0315	0.0215	19	17.7
			V_S = 7.28 ft/sec							
2.5	1.615	0.575	0.0127	0.0087	127	102.5				
3.0	1.32	0.48	0.0149	0.0086	89	86.5				
3.5	1.11	0.40	0.017	0.0085	65.2	73.0				
4.0	0.97	0.345	0.019	0.0083	51	64.3				

NOTE. Sufficient values of $\frac{C_Y}{C_{Yw}}$ and $\frac{P.K_X}{Q.K_{Xw}}$ have been calculated to give intersection point for curves in Fig. 10.

Curves of $\frac{C_Y}{C_{Yw}}$ and $\frac{P.K_X}{Q.K_{Xw}}$ as found in Table 2 are plotted for each V_S to give balance points as shown in Fig. 10.

The values of V_T and V_{MG} for each balance point are now calculated, and it is simplest to set out the calculation in a standard form as illustrated in Fig. 11, which shows the procedure for $V_S = 6.74$ ft/sec.

When V_T and V_{MG} have been calculated for each balance point, curves of V_T against V_{MG} for $\theta = 7\frac{1}{2}^o$ can be plotted as in Fig. 9.

The remaining heel angles have been treated similarly and the envelope curve gives the yacht's optimum performance for sail sheeting $\delta_M = 5°$; $\delta_F = 20°$.

fig 10 balanced sailing positions at 7½° heel and one sail sheeting:- $\alpha_M = 5°$ $\alpha_F = 20°$

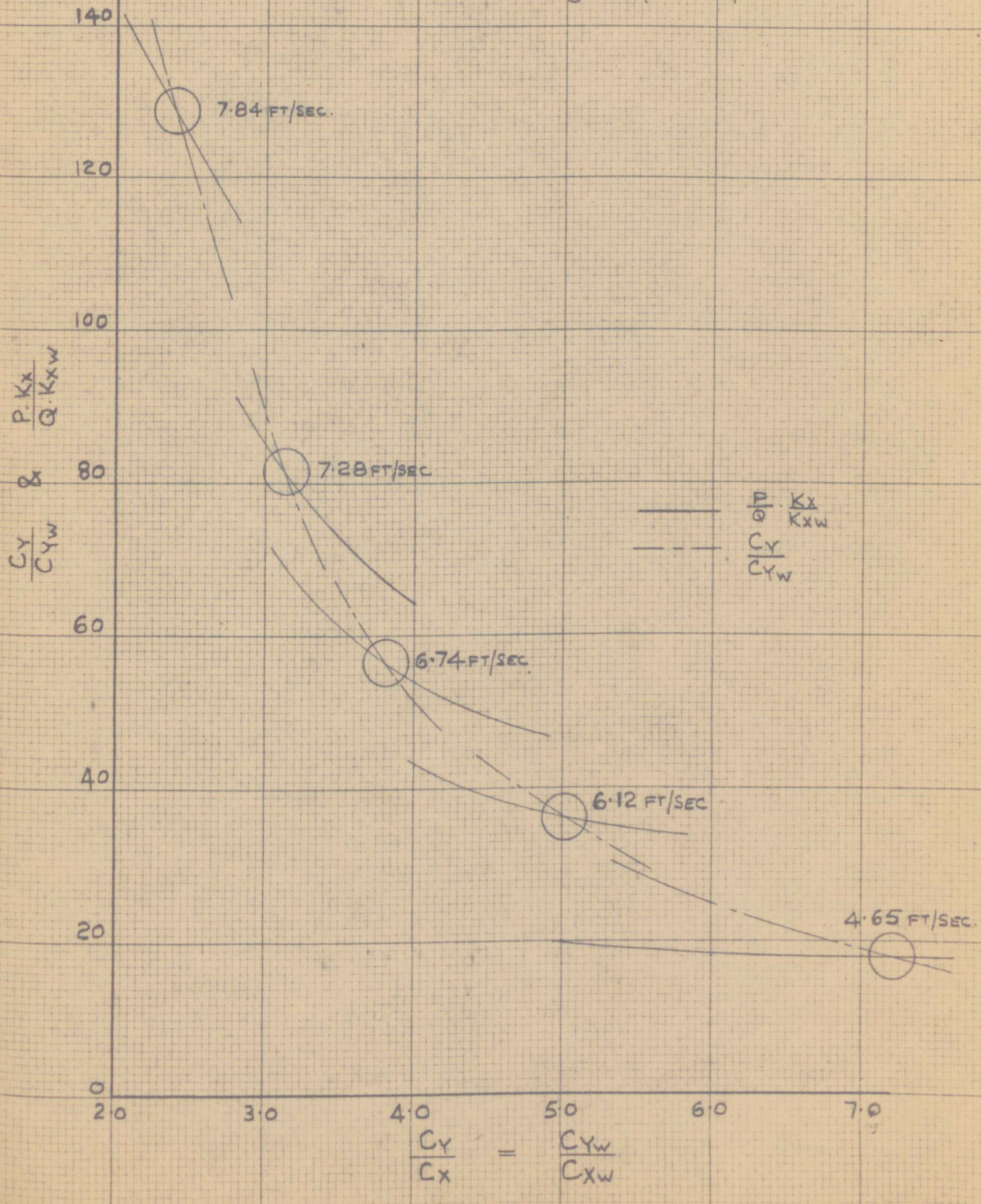

Fig. 11 CALCULATION FOR V_T AND V_{MG} AT EACH BALANCE POSITION.

$\delta_M = 5^\circ$, $\delta_F = 7\frac{1}{2}^\circ$.

(1) Balance $\frac{C_Y}{C_X}$ $(= \frac{C_{Yw}}{C_{Xw}})$ $= 3.78$

(2) Model $V_S = 2.75$ Full Scale $V_S = \sqrt{\text{Scale Factor}} \cdot 2.75 = 6.74$ Ft/sec.
$= 3.98$ Knots.

(3) $\beta - \lambda = 24.1^\circ$

(4) $\lambda = 3.8^\circ$

(5) $\beta = (\beta - \lambda) + \lambda = 27.9^\circ$ $\sin\beta = 0.468$, $\cos\beta = 0.884$

(6) $\frac{C_Y}{C_{Yw}}$ at balance $= 57.0 \cdot \sqrt{\frac{C_Y}{C_{Yw}}} = 7.55$.

(7) $\sqrt{835 \cdot \frac{A}{S}} = 21.55$ (for Dragon)

(8) $V_A = \frac{V_S}{\sqrt{\frac{C_Y}{C_{Yw}}}} \cdot 21.55 = \frac{6.74}{7.55} \cdot 21.55 = 19.24$ ft/sec.

(9) $\frac{V_S}{V_A} = \frac{6.74}{19.24} = 0.35$

(10) $\sin\gamma = \frac{\sin\beta}{\sqrt{1 + (\frac{V_S}{V_A})^2 - 2 \cdot \frac{V_S}{V_A} \cdot \cos\beta}} = \frac{0.468}{\sqrt{1 + 0.0[illegible] - 0.7 \times 0.884)}}$

(11) $\gamma = 41.3^\circ$ $\cos\gamma = 0.751$

(12) $V_{MG} = V_S \cdot \cos\gamma = 6.74 \times 0.751 = 5.06$ ft/sec. $= 2.99$ knots.

(13) $V_T = V_A \cdot \frac{\sin\beta}{\sin\beta} = 19.24 \cdot \frac{0.468}{0.66} = 13.63$ ft/sec. $= 8.08$ knots.

CHAPTER 4: PERFORMANCE PREDICTION FOR A YACHT

The practical method of predicting performance described in the previous chapter has been used to predict the optimum windward ability of a yacht having the hull characteristics obtained in Part 3, and detailed in Appendix 2, and sail characteristics detailed in Appendix 1.

The sail characteristics have been assumed as applicable to a 'Dragon' sail plan and physical quantities used in the calculations are those for this class of vessel: Sail Area (S) = 286.2 sq.ft., Mast height (P) = 32.4 ft.

The Hull characteristics refer to the All-up-weight and C.G. location of the experiments described in Part 3, where the Waterline Length (Q) was 20.85 ft., the Wetted Area (A) was 159.2 sq. ft.

These gave the value of $(\frac{P}{Q})$ used in the analysis as 1.55 and $\frac{A}{S}$ as 0.556.

Curves of optimum V_{MG} to V_T were obtained in a similar manner to the example calculation given in the previous chapter at the following sail sheeting combinations which were available from the data of Ref. 28, with use of a wind tunnel test velocity = 20 ft. per sec:

δ_M constant,	δ_F varying	δ_M varying,	δ_F constant
5 degs. ,	20 degs.	5 degs.,	17½ degs.
5 degs. ,	17½ degs.	10 degs.,	17½ degs.
5 degs. ,	15 degs.	15 degs.,	17½ degs.
5 degs. ,	10 degs.		
5 degs. ,	7½ degs.		

Tables of balanced sailing positions are given in Appendix 3, and envelope curves showing optimum performance at each of the above sheeting positions were drawn from these. These envelope curves are shown in Fig. 12, together with their boundary curve which gives the yacht's optimum windward performance for the sheeting variations used.

It may be seen that at the lower end of the true wind velocity range, a sheeting of $\delta_M = 5°$ with δ_F between 15° and 17½° is suitable, while in the medium range of V_T, $\delta_M = 5°$, $\delta_F = 15°$ is preferable; at the higher true wind velocities however, the ideal value of δ_F falls to 10°.

It is interesting to plot curves of V_{MG} against the sheeting angle of the foresail at various values of V_T and these are shown in Fig. 13, for the mainsail constant at 5°. The advantage of tightening the foresail sheeting as the wind velocity increases is clearly shown.

A similar plot in Fig. 14 shows the effect of tightening the mainsail while the foresail is maintained at $\delta_F = 17\frac{1}{2}^\circ$, the near optimum position for the low to medium V_T range. It is unfortunate that the sail characteristics at lower values of δ_M are not available as it seems likely from Fig. 14 that the windward performance could be improved by sheeting the mainsail harder, especially at the lower end of the V_T range.

The figures considered together show that the optimum windward performance of the yacht is controlled by the actual sheeting of the foresail and mainsail together with their sheeting relative to one another. If sail characteristics were available for a larger range of sheetings it is likely that a better performance would be found, but the limited sail data used in the calculations illustrate that the performance is very sensitive to mainsail sheeting, and perhaps less sensitive to foresail sheeting for this particular suit of sails.

In the sail experiments of Ref. 28, the effect of foresail sheeting variation was restricted to a fixed mainsail angle of 5° and the effect of mainsail variation to a foresail angle of $17\frac{1}{2}^\circ$. A complete study of the effects of sail sheeting appears to require a wider range of mainsail-foresail sheeting combinations. It would

then be possible to plot diagrams similar to those of Fig. 13 & 14, but with several curves at each value of V_T within the range considered.

It must be noted here that the above results apply only to sails having the characteristics given in Ref. 28 for which no chord shapes are given, and that with sails of different cut the results may differ considerably.

Comparison of the Predicted Optimum Windward Performance from Present Analysis with that from previous work

It is possible to compare the predicted windward performance from Fig. 12 with that predicted for 'Yeoman' (Ref. 13) and that resulting from the previous work with the 'Dragon' model at Saunders Roe Ltd. (Ref. 1); Fig. 15 shows this comparison in terms of V_{MG} and V_T.

It may be seen that the Saunders Roe 'Dragon' prediction indicates that a 'Dragon' class yacht has a superior windward performance to a 5.5 Metre yacht, a situation with which experienced yachtsmen are likely to disagree; this was in fact the subject of P. V. Mackinnon's letter to which reference was made in Chapter 1.

The prediction resulting from the present analysis shows the 'Dragon' to have an inferior windward performance to the 5.5 Metre over most of the V_T range.

The curves of $V_{MG} \sim V_T$, for 'Yeoman' and from Fig. 12, are seen to be similar in shape, coming to a maximum value of V_{MG} at a certain V_T, the maximum V_{MG} for the 'Dragon' being greater than that for the 5.5 Metre and occurring at a larger V_T, indicative of the better 'heavy weather' performance attributed to 'Dragons'.

If it may be assumed that the predicted curve for 'Yeoman', which Ref. 13 shows to be the boundary curve of the performance points measured during trials, is correctly positioned, then the predicted curve for the 'assumed Dragon' of Fig. 12 appears to be reasonably positioned relative to it.

It is shown in Part 3, Chapter 23, that the measured Lift Coefficients during the two series of experiments on the 'Dragon' hull are similar, but that the predicted full scale resistance coefficients differ considerably; the reasons for this difference are discussed in that Chapter, and it would appear that the lower full scale Resistance Coefficients resulting from the measurements, assumptions, and scaling adopted in the present work are responsible for the difference in windward performance appearing in Fig. 15.

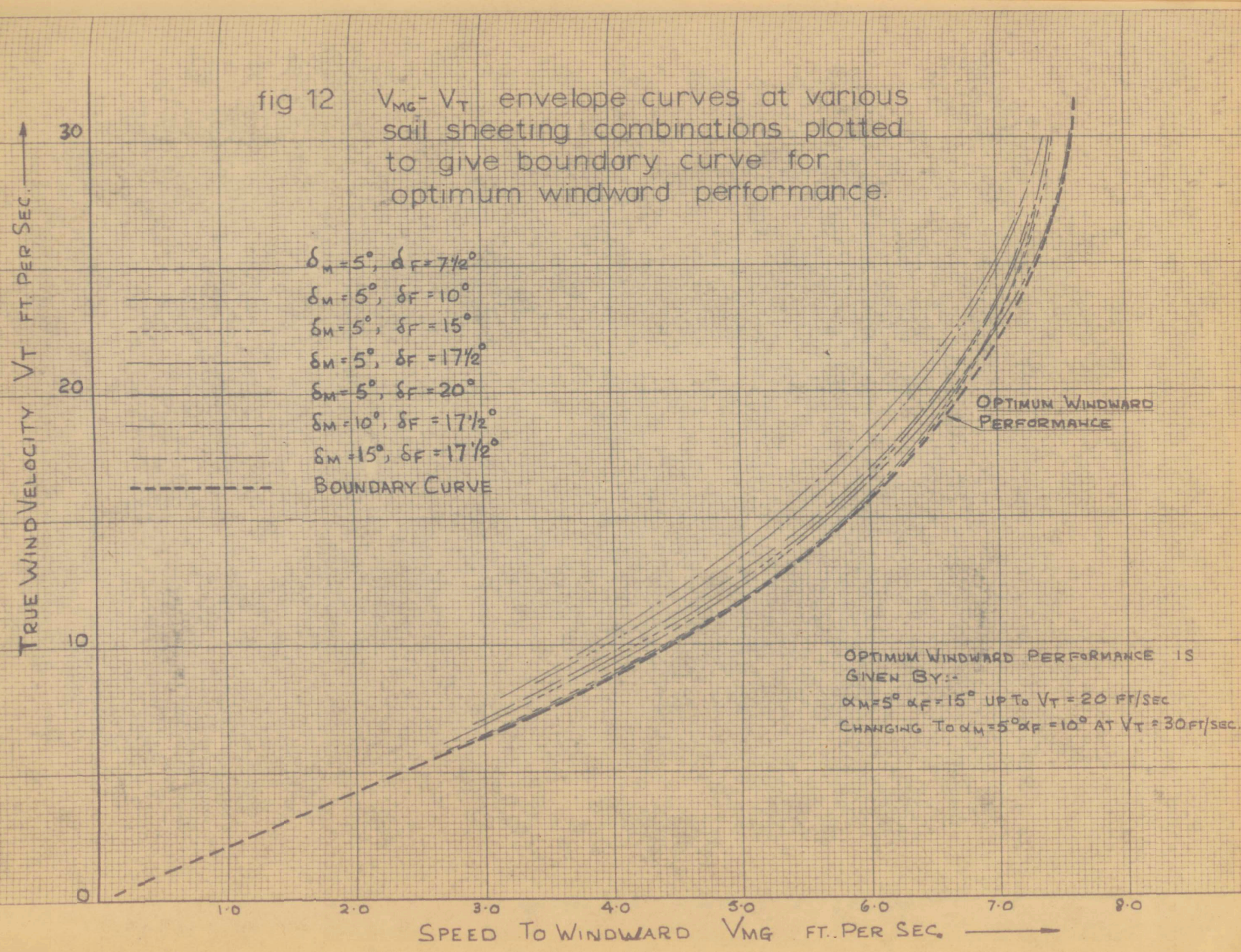
fig 12 V_{MG} - V_T envelope curves at various sail sheeting combinations plotted to give boundary curve for optimum windward performance.
$\delta_M = 5°$, $\delta_F = 7\frac{1}{2}°$
$\delta_M = 5°$, $\delta_F = 10°$
$\delta_M = 5°$, $\delta_F = 15°$
$\delta_M = 5°$, $\delta_F = 17\frac{1}{2}°$
$\delta_M = 5°$, $\delta_F = 20°$
$\delta_M = 10°$, $\delta_F = 17\frac{1}{2}°$
$\delta_M = 15°$, $\delta_F = 17\frac{1}{2}°$
BOUNDARY CURVE
OPTIMUM WINDWARD PERFORMANCE
OPTIMUM WINDWARD PERFORMANCE IS GIVEN BY:-
$\alpha_M = 5°$ $\alpha_F = 15°$ UP TO $V_T = 20$ FT/SEC
CHANGING TO $\alpha_M = 5°$ $\alpha_F = 10°$ AT $V_T = 30$ FT/SEC.
TRUE WIND VELOCITY V_T FT. PER SEC.
0
10
20
30
1·0
2·0
3·0
4·0
5·0
6·0
7·0
8·0
SPEED TO WINDWARD V_{MG} FT. PER SEC.

fig 13 effect on windward performance of varying foresail sheeting.

$V_{MG} - \delta_F$ FOR VARYING α_F AT CONSTANT V_T

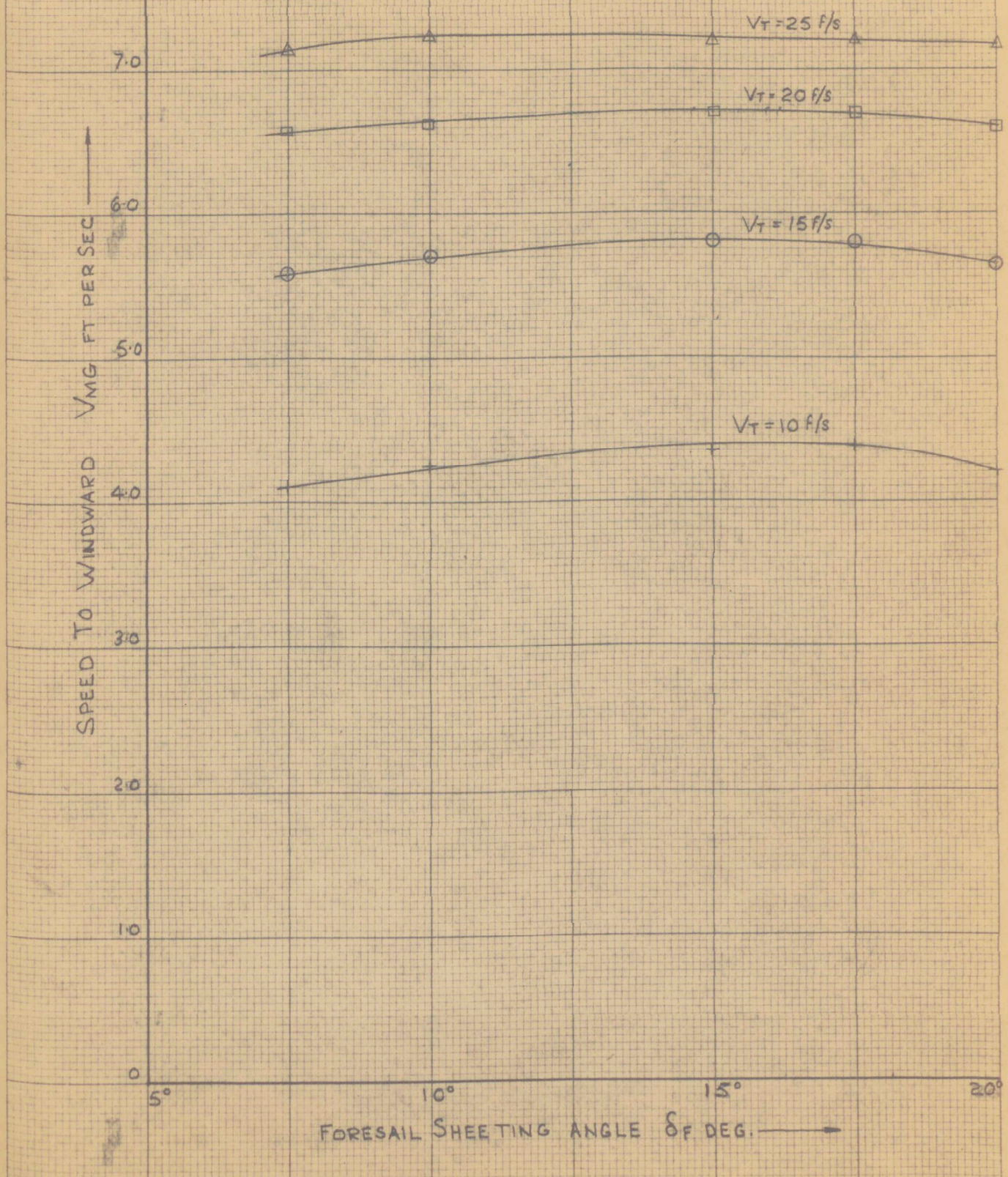

fig 14 effect on windward performance of varying mainsail sheeting.

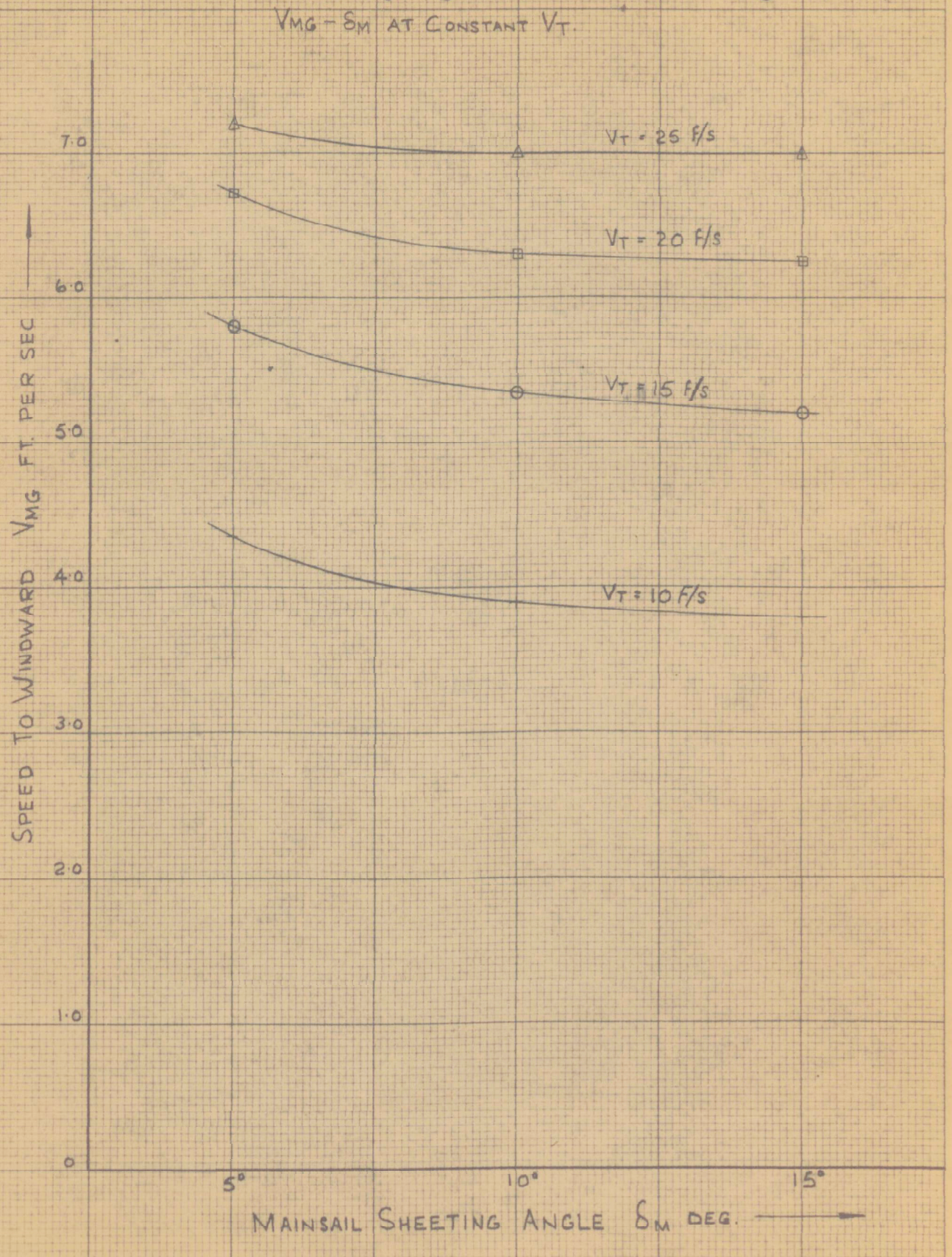

fig 15 windward performance of 'dragon' as predicted from present work compared with measured performance of 'yeoman' and previous prediction for 'dragon'

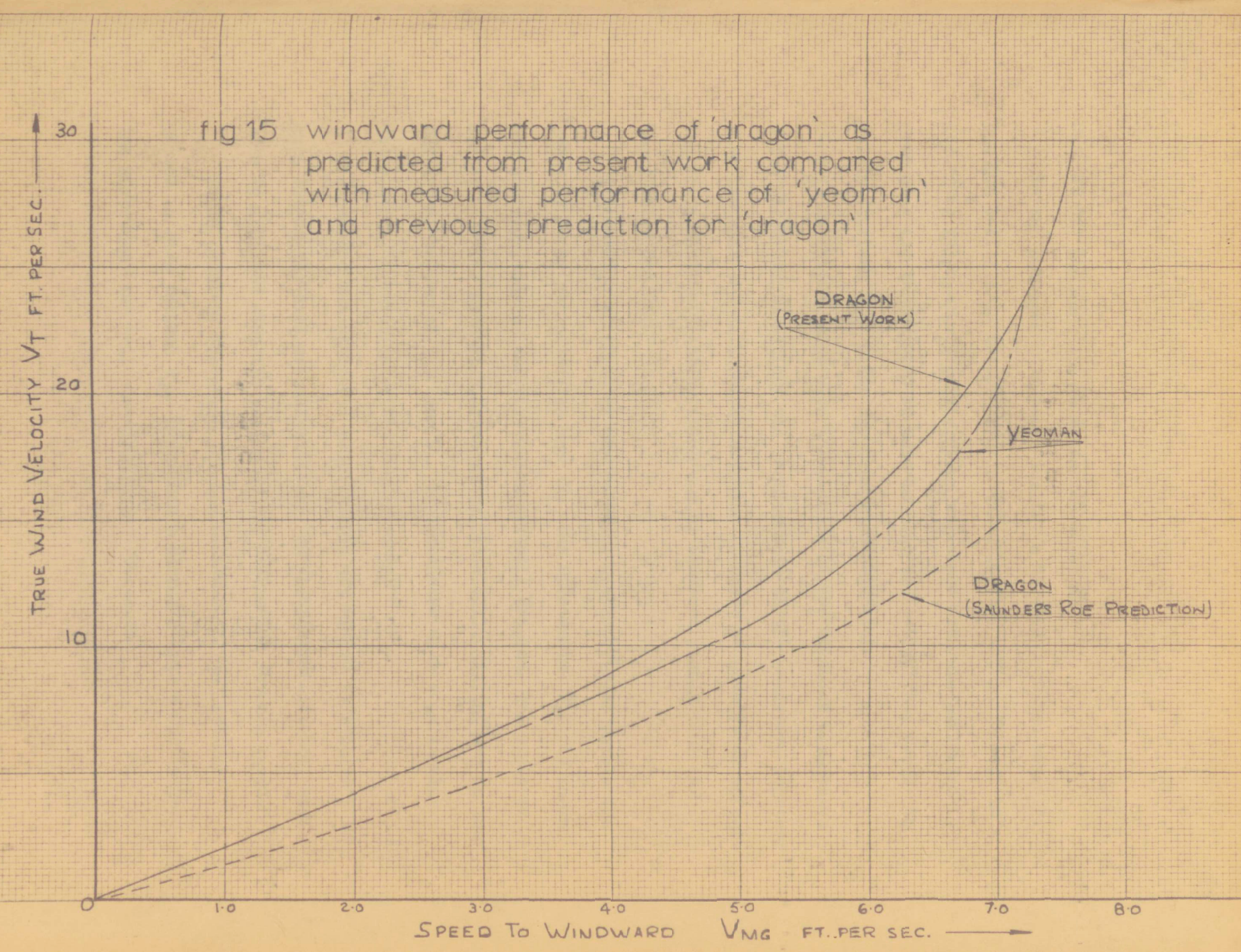

CHAPTER 5: THE ANALYSIS AS AN AID TO HELMSMEN

To the helmsman of a yacht racing, a knowledge of the vessel's optimum performance to windward is valuable, but not sufficient in itself to allow him to gain maximum advantage from the analysis producing it; in addition he must be able to 'set up' the yacht to obtain 'optimum V_{MG}' under any true wind conditions.

To do this he must have a knowledge of the relevant parameters which allow him to satisfy the requirements of the geometry, together with the hull and sail characteristics in terms of quantities affecting the yacht's capability which can be measured easily from on board while sailing.

A knowledge of three of the relevant quantities will enable the geometry to be satisfied; at any V_T the obtainable V_{MG} is known and the magnitude of one relevant angle will complete the requirements; $\beta-\lambda$ is easily measured on board while sailing and at the particular values of V_{MG} and V_T, is associated with a particular value of λ, so satisfying the requirements.

To ensure the sail/hull requirements are met it is necessary to know either the sail or hull attitude, or the characteristics, and this is achieved when the sail sheeting angles and $\beta-\lambda$ are known.

It is possible therefore for the helmsman to 'set up' his vessel to give optimum V_{MG} if he has a simple relative wind direction instrument and sail sheeting angle indicators.

It has already been seen that the necessary values of sail sheeting: δ_M and δ_F appear in, and are essential to the analysis and it remains to use a 'reverse' process in order to arrive at $(\beta - \lambda)$ associated with 'best V_{MG}' for a number of V_T values.

In the performance prediction given in the previous chapter, the sail sheeting for 'best V_{MG}' over the middle portion of the V_T range was found to be $\delta_M = 5°$, $\delta_F = 15°$; detailed results for balanced sailing positions are available at a heel angle of 15° which may be considered as appropriate to the middle range of V_T, and reference to the tabulated results for $\delta_M = 5°$, $\delta_F = 15°$ at 15° heel contained in Appendix 3 allows the plotting of curves showing V_{MG}, V_A, γ, $\beta-\lambda$, and λ against various values of course velocity V_S, see Fig. 16a.

Fig. 16b shows the envelope curve of optimum V_{MG} together with its component curves of V_{MG} against V_T for various V_S at the heel angles considered. At 15° heel, the optimum value of V_{MG} where the envelope curve touches the component curve for this heel angle is seen to be 8.90 ft/sec. occurring at a V_T of 16.70 ft/sec.

Returning to Fig. 16a, values of the other quantities may be obtained for this V_{MG} and the relevant value of $\beta-\lambda$ is seen to be 27.0°. V_S, V_A, λ, and γ at optimum V_{MG} may be obtained in a similar manner if required and are shown in the Figure.

In a similar manner the envelope curves for $\delta_M = 5°$, δ_F $17\frac{1}{2}°$ and $\delta_M = 5°$, $\delta_F = 10°$, may be used together with the appropriate

data at $7\frac{1}{2}^{o}$ and $21\frac{1}{2}^{o}$ heel from Appendix 3 to give values of all relevant quantities, in particular β-λ, for the lower and higher portions of the V_T range. These results are shown in Fig. 17a & b and 18a & b.

The values of β-λ, δ_M and δ_F to give optimum V_{MG} over the full range of V_T may now be presented in tabular or graphical form to the helmsman.

Fig. 19 shows the variation of V_A, V_S, β-λ, λ, β, and γ for optimum V_{MG} over the range of V_T appearing from the performance prediction of the previous chapter. While the true variation of the quantities is somewhat indeterminate due to data being available at only three heel angles, it appears likely that the angles have a linear variation, the required β, β-λ, and γ reducing as V_T increases, while λ increases with V_T.

fig 16a obtaining values of $\beta-\lambda$, λ, V_S, V_A, γ, for opt. V_{MG} at $V_T = 16{\cdot}7$ FT/SEC. $\theta = 15°$, $\delta_M = 5°$, $\delta_F = 15°$

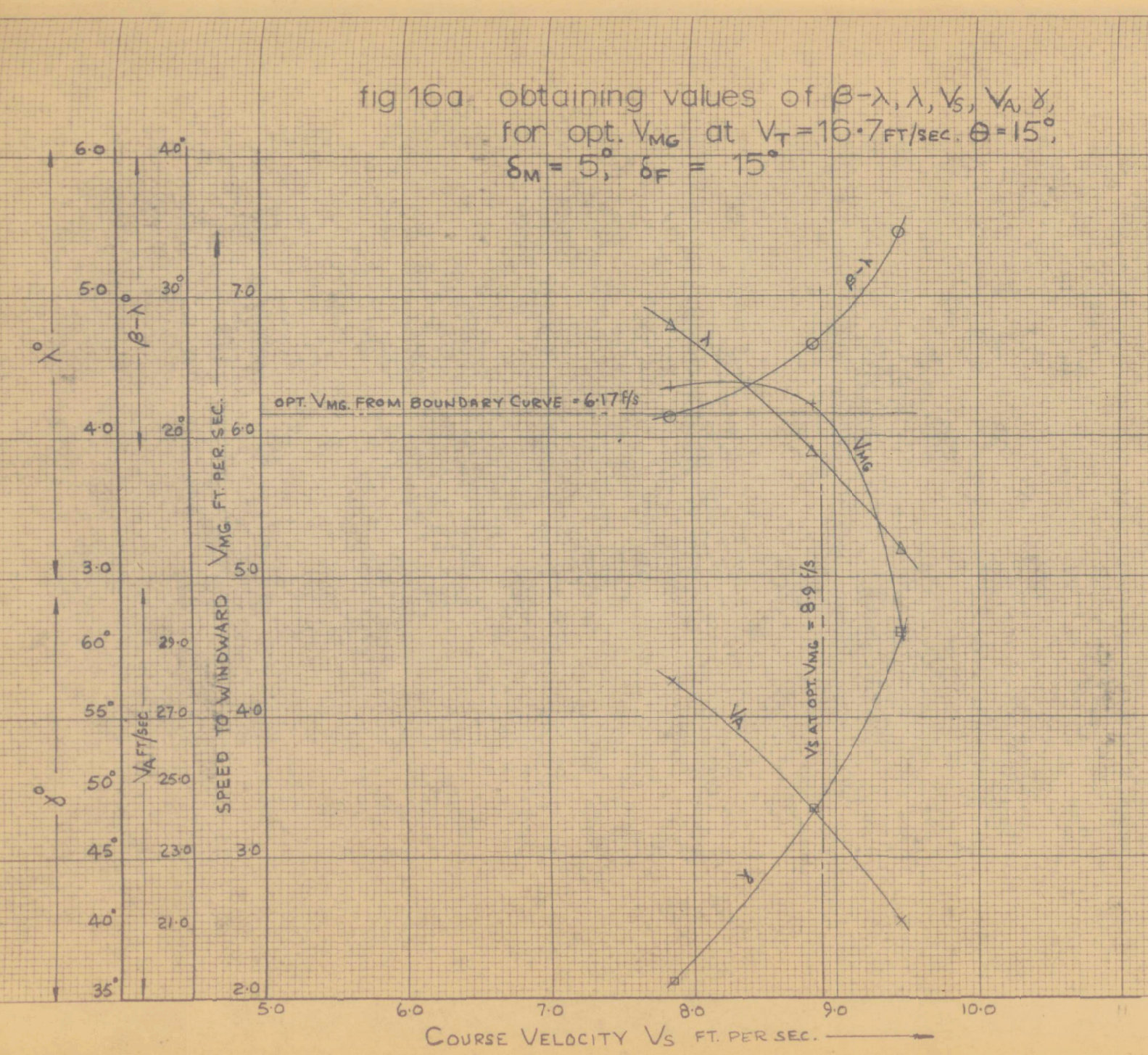

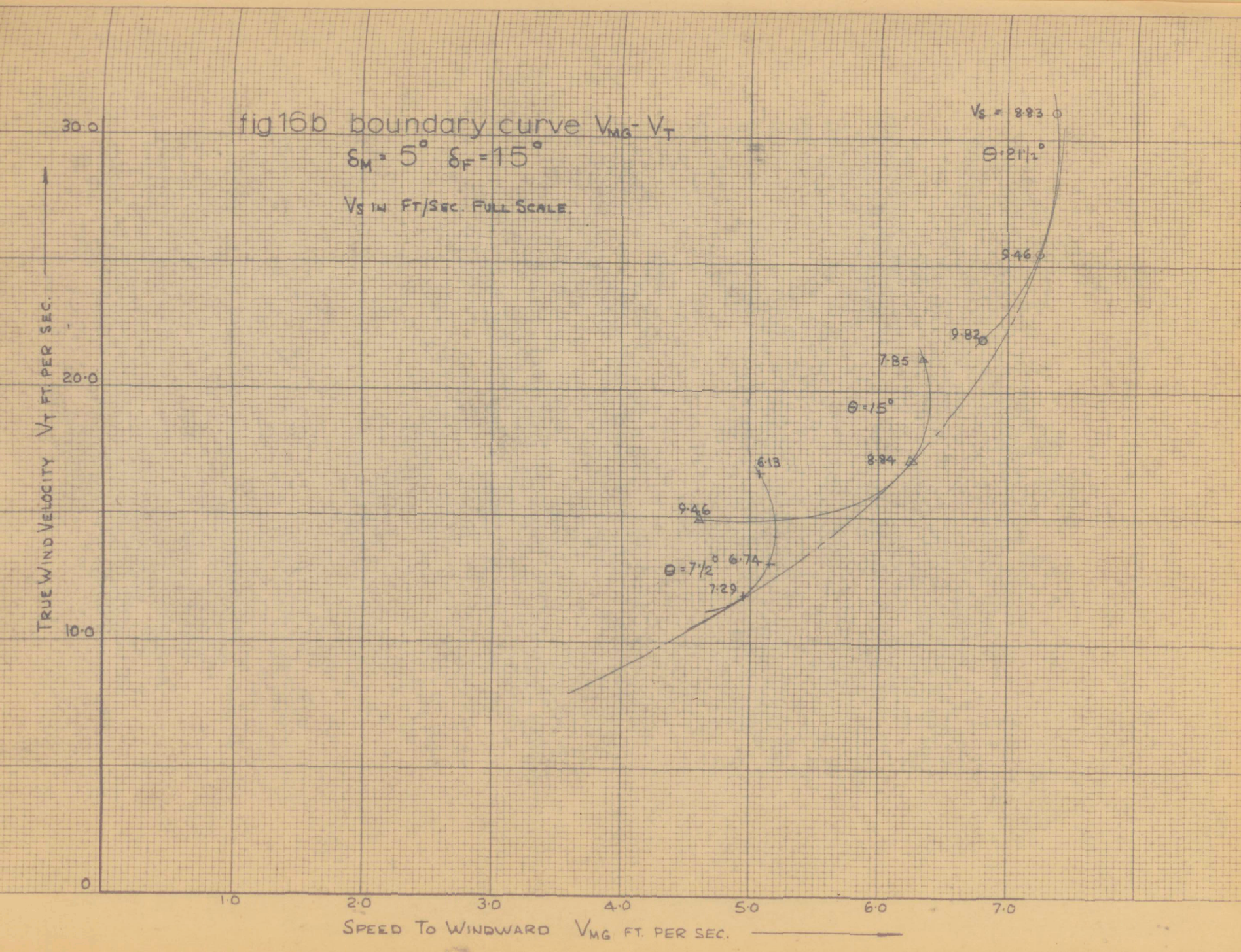
fig 16b boundary curve V_{MG} - V_T
$\delta_M = 5°$ $\delta_F = 15°$
V_S IN FT/SEC. FULL SCALE.
V_S = 8.83
θ = 22½°
9.46
9.82
7.85
θ = 15°
8.84
6.13
9.46
θ = 7½°
6.74
7.29
30.0
20.0
10.0
0
TRUE WIND VELOCITY V_T FT. PER SEC.
1.0
2.0
3.0
4.0
5.0
6.0
7.0
SPEED TO WINDWARD V_{MG} FT. PER SEC.

fig 17a obtaining values of $\beta-\lambda$, λ, V_S, V_A, γ, for opt. V_{MG} at $V_T = 11{\cdot}3$ FT/SEC, $\theta = 7\frac{1}{2}°$ $\delta_M = 5°$; $\delta_F = 17\frac{1}{2}°$.

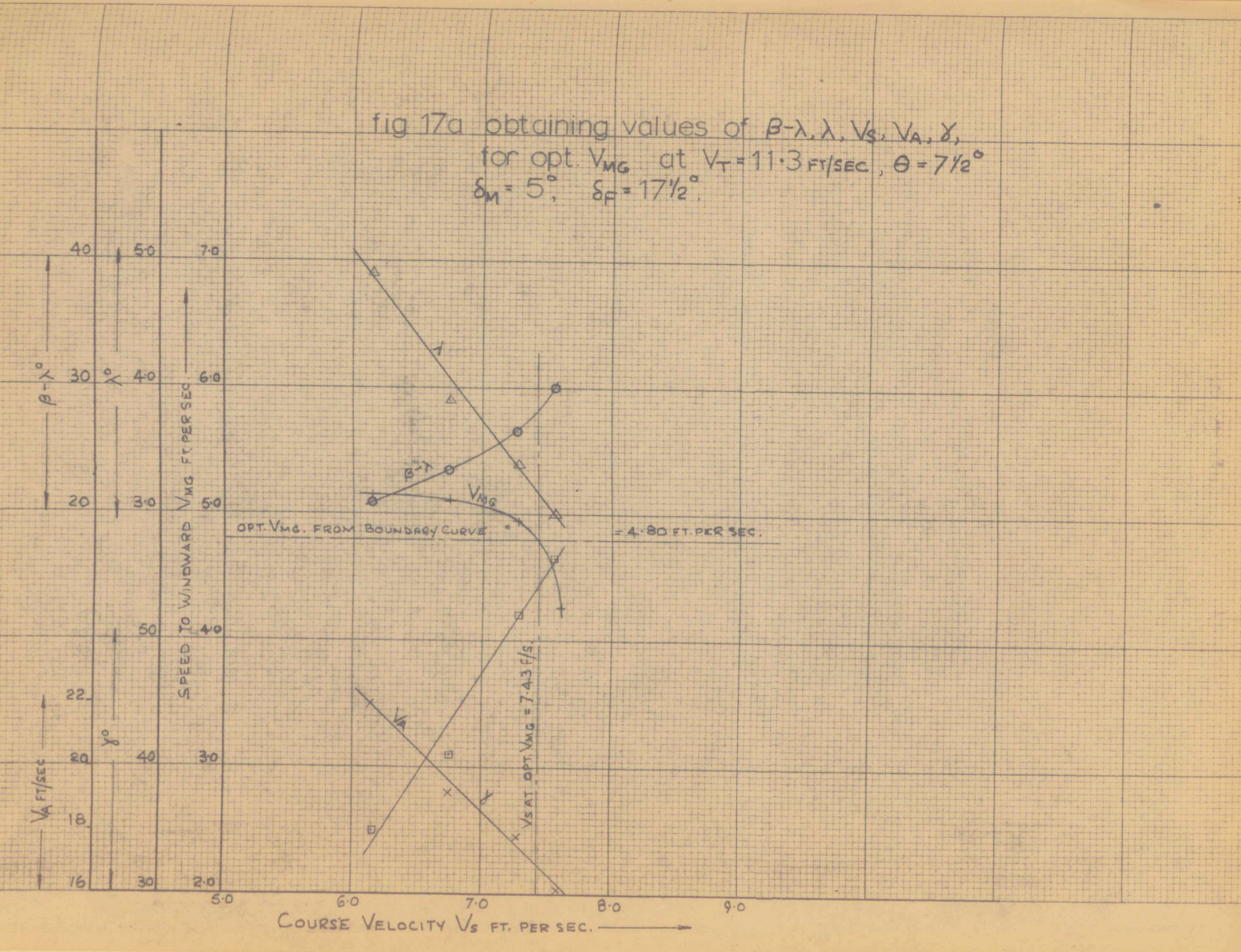

fig 17b boundary curve V_{MG} - V_T

$\delta_M = 5°$, $\delta_F = 17\frac{1}{2}°$

V_S IN FT/SEC. FULL SCALE.

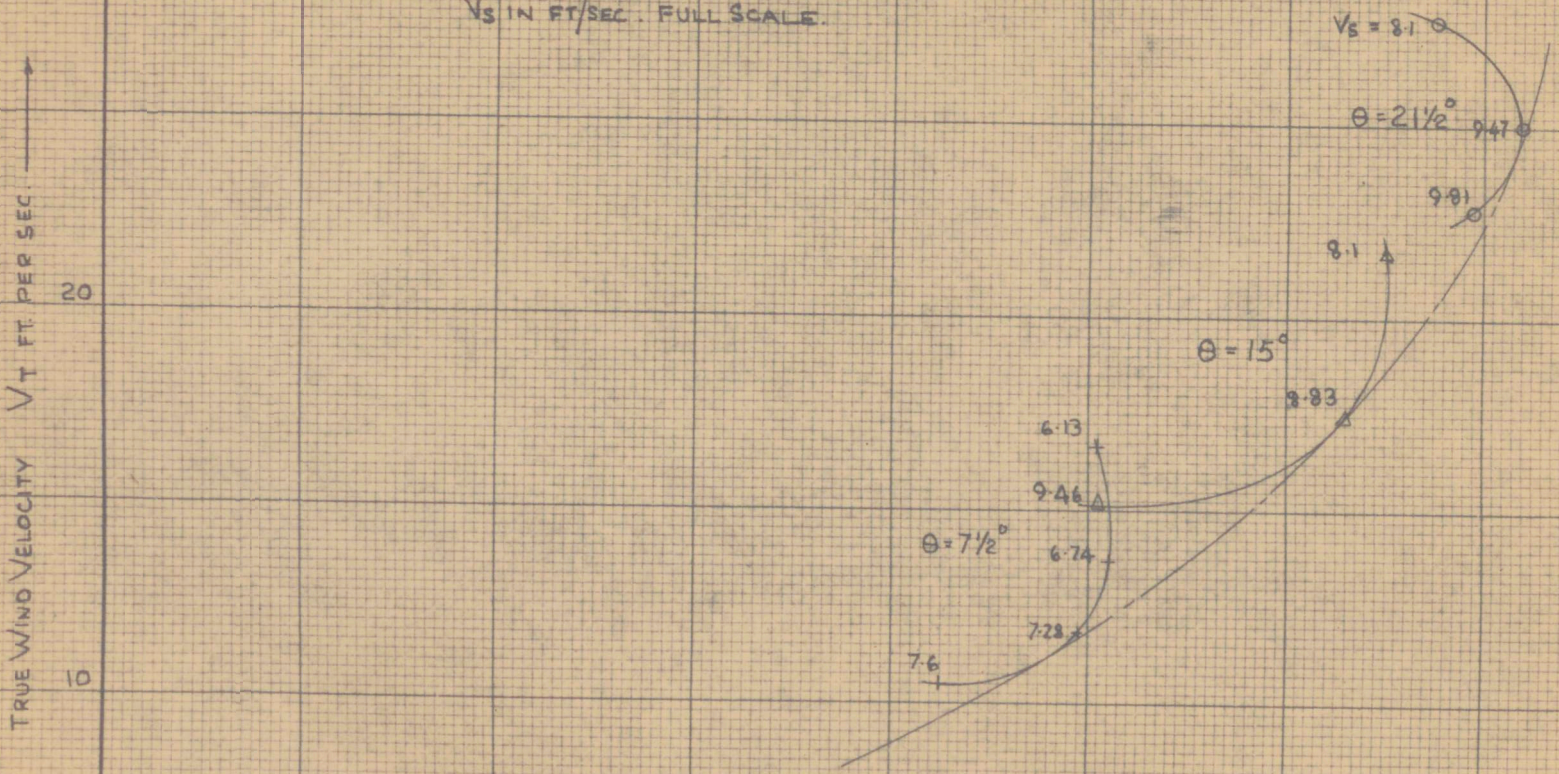

TRUE WIND VELOCITY V_T FT. PER SEC.

0 10 20 30

1.0 2.0 3.0 4.0 5.0 6.0 7.0 8.0

SPEED TO WINDWARD. V_{MG} FT. PER SEC.

fig18a obtaining values of $\beta-\lambda$, λ, V_S, V_A, γ, for opt. V_{MG} at $V_T = 25.7_{FT/SEC}$, $\theta = 21\frac{1}{2}^\circ$ $\delta_M = 5^\circ$, $\delta_F = 10^\circ$.

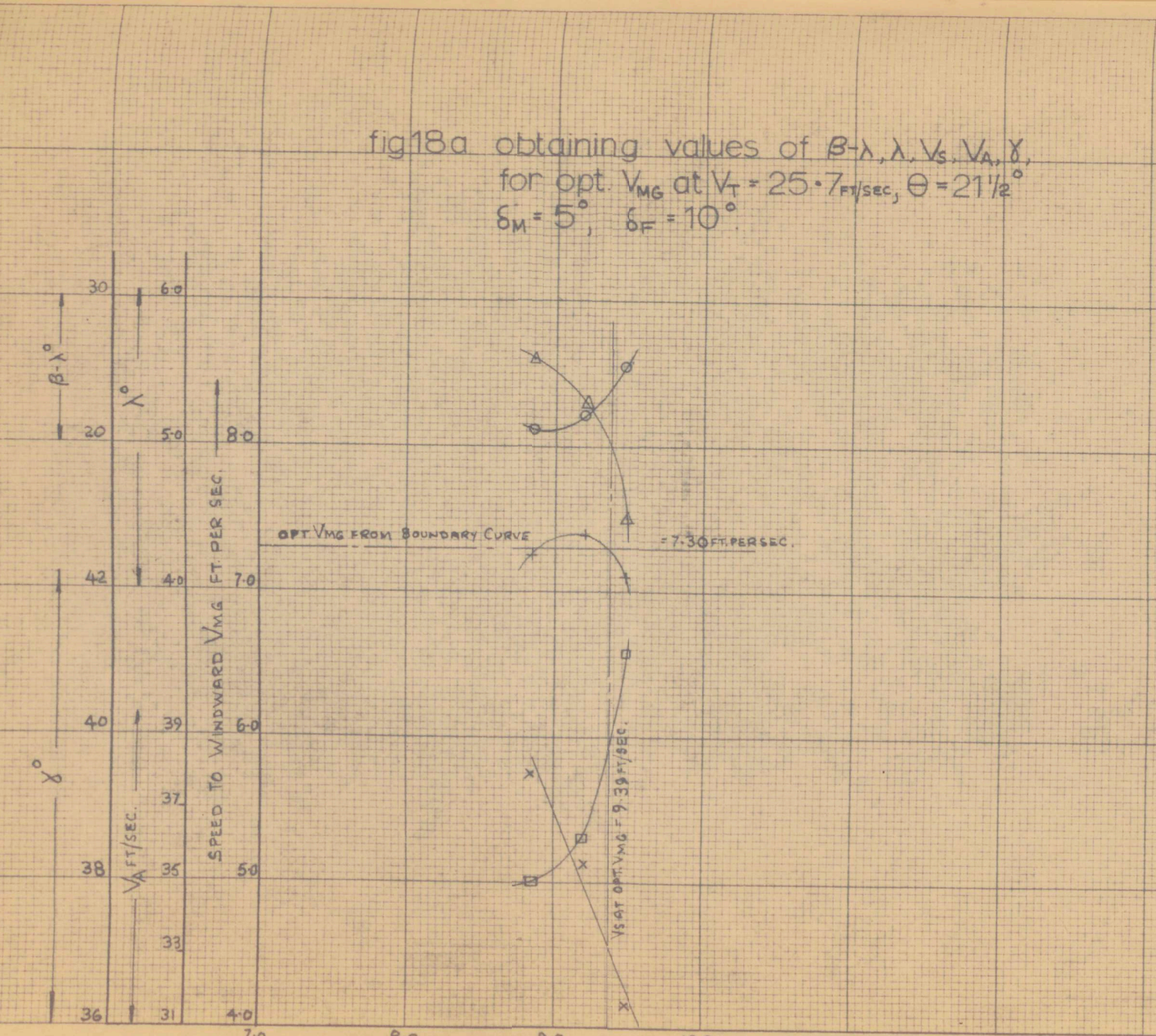

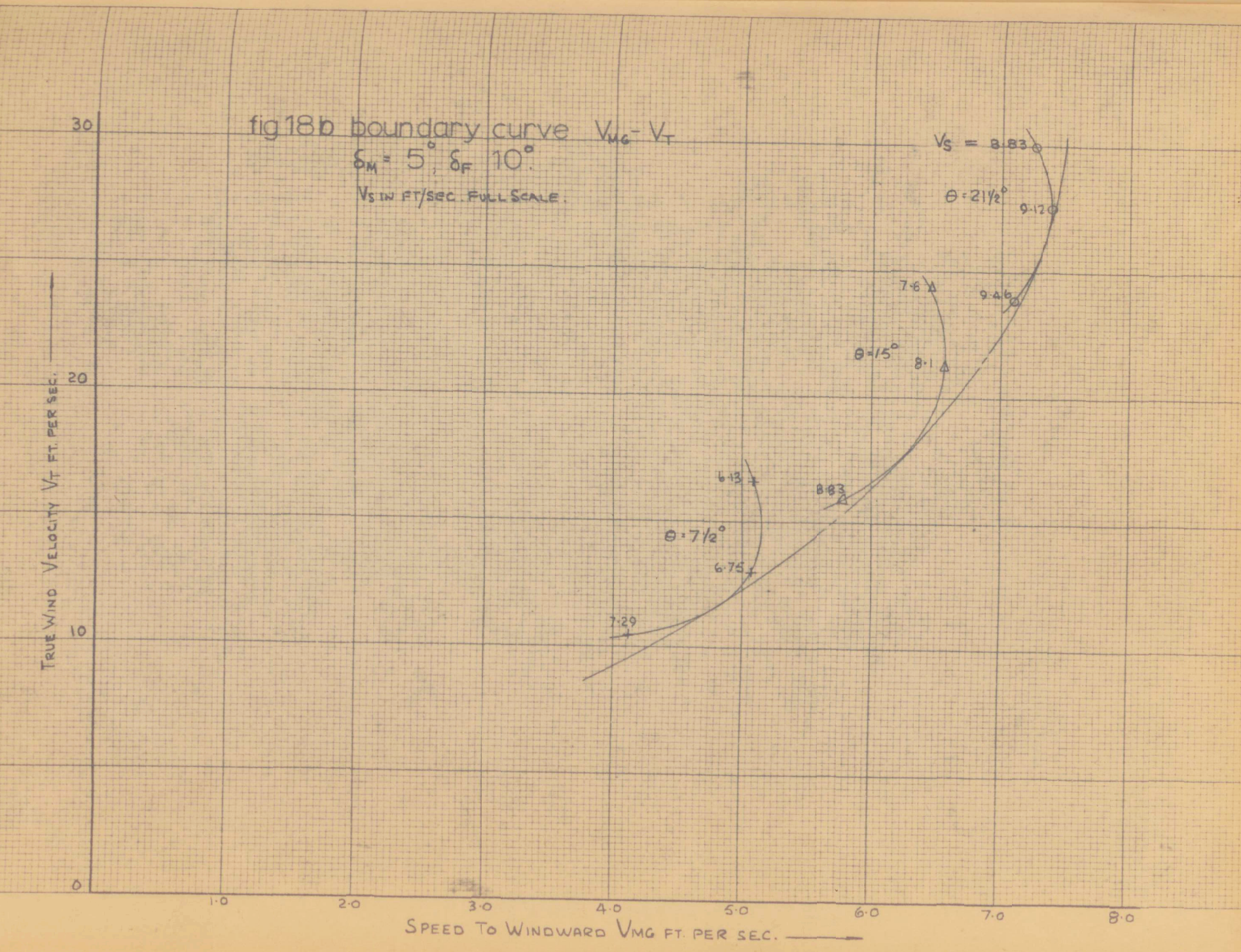
fig 18b boundary curve V_{MG} - V_T
$\delta_M = 5°$, δ_F 10°.
V_S IN FT/SEC. FULL SCALE.
V_S = 8.83
θ = 21½°
9.12
7.6
9.46
θ = 15°
8.1
6.13
8.83
θ = 7½°
6.75
7.29
30
20
10
0
TRUE WIND VELOCITY V_T FT. PER SEC.
1.0
2.0
3.0
4.0
5.0
6.0
7.0
8.0
SPEED TO WINDWARD V_{MG} FT. PER SEC.

fig 19 conditions for optimum V_{MG}

$\beta - \lambda$, λ, V_S FOR RANGE OF V_T

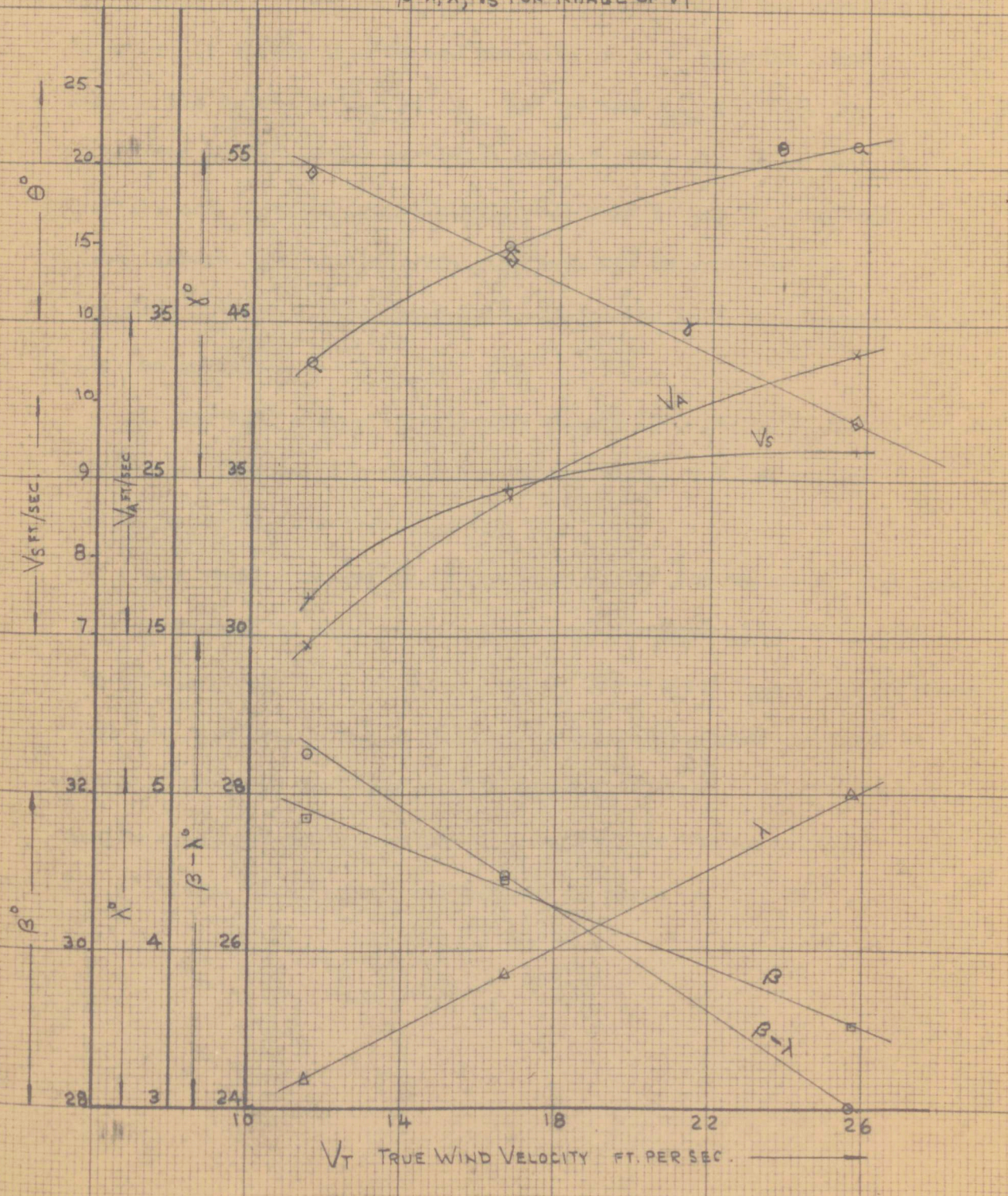

CHAPTER 6: SAIL AND HULL PROPERTIES TO GIVE BEST WINDWARD PERFORMANCE

Using the values of V_S, λ , and V_T obtained in the previous chapter, it is possible to use the hull data of Appendix 2 and obtain the values of C_{Y_w} and C_{X_w} for optimum V_{MG}, see Fig. 20. Again due to data being available at only three angles of heel, the results are somewhat indeterminate, although it may be seen that with increasing true wind strength, as might be expected, the required C_{Y_w} and C_{X_w} become greater due to the increased course velocity and leeway.

If the hull characteristics are placed in terms of C_L and C_D plotted against λ , for the three values of V_T, and the optimum points inserted, the result is Fig. 21.

In a similar manner it is possible to use the values of β-λ, and V_T (V_A assumed to have no effect on characteristics) together with the data Appendix 1 to obtain C_X and C_Y for optimum V_{MG}. Fig. 22 shows that the required C_Y and C_X fall as V_T increases, again as might be expected from the decrease in β-λ found in Fig. 19. It is interesting to note that the variation of C_X appears to be linear.

In terms of C_L and C_D the pattern is shown in Fig. 23.

fig 20 hull coefficients for optimum V_{MG}

C_{YW} AND C_{XW}

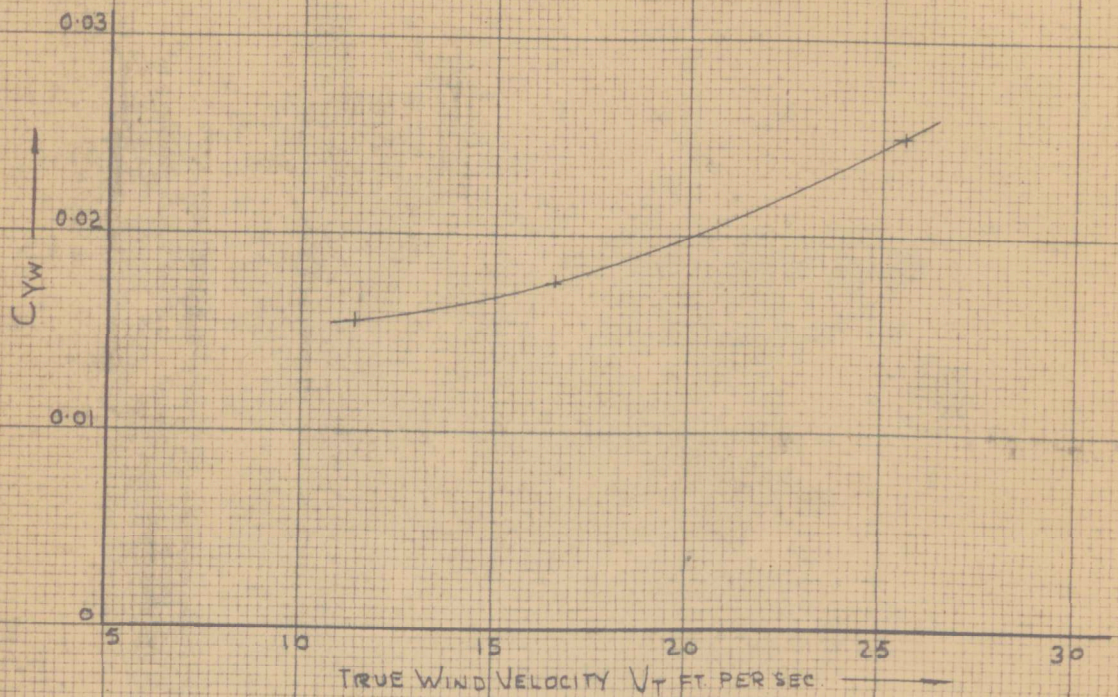

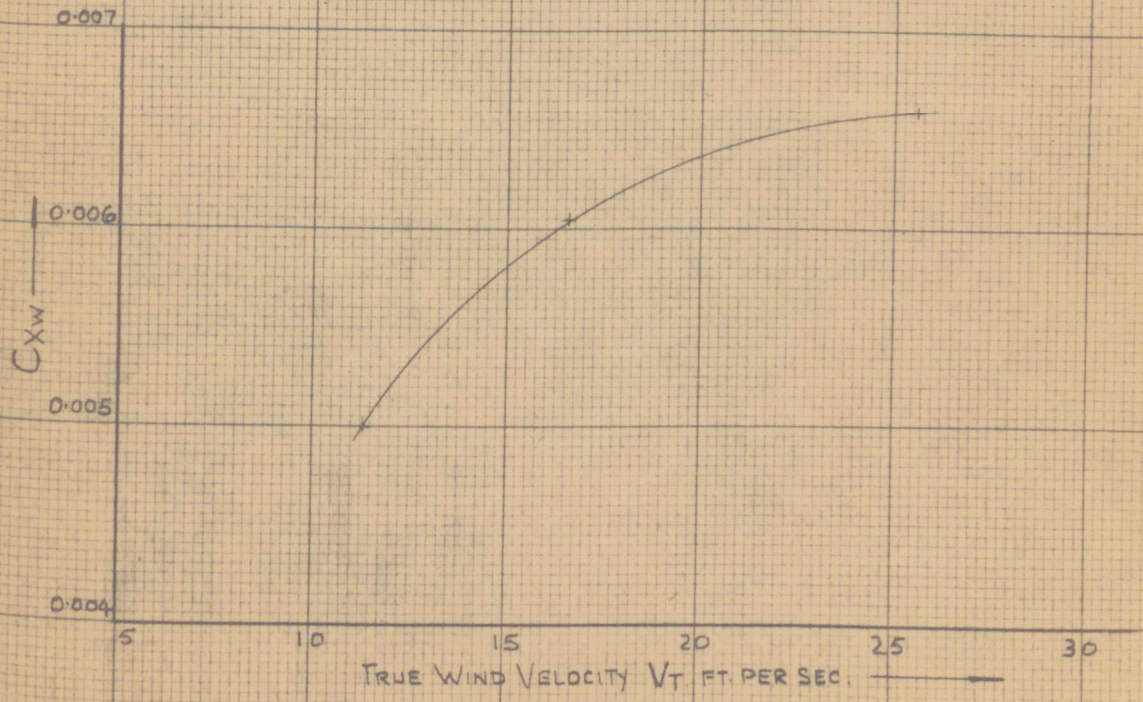

fig 21 hull coefficients for optimum V_{MG}

C_L AND C_D

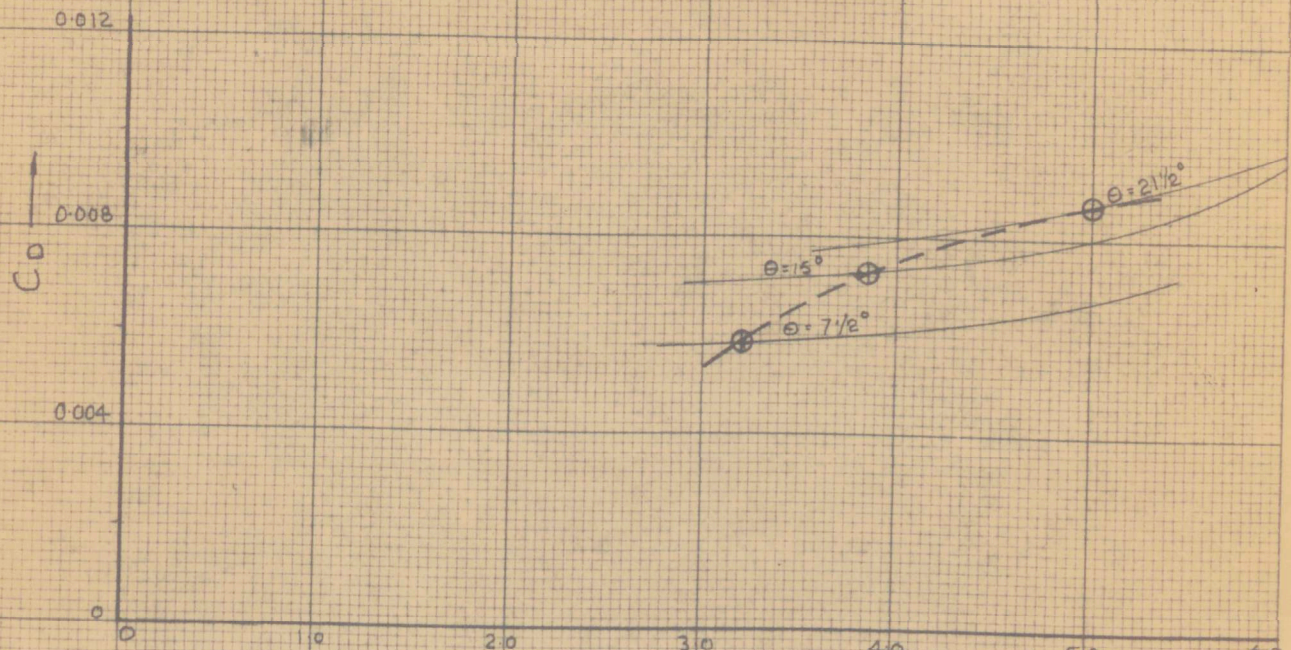

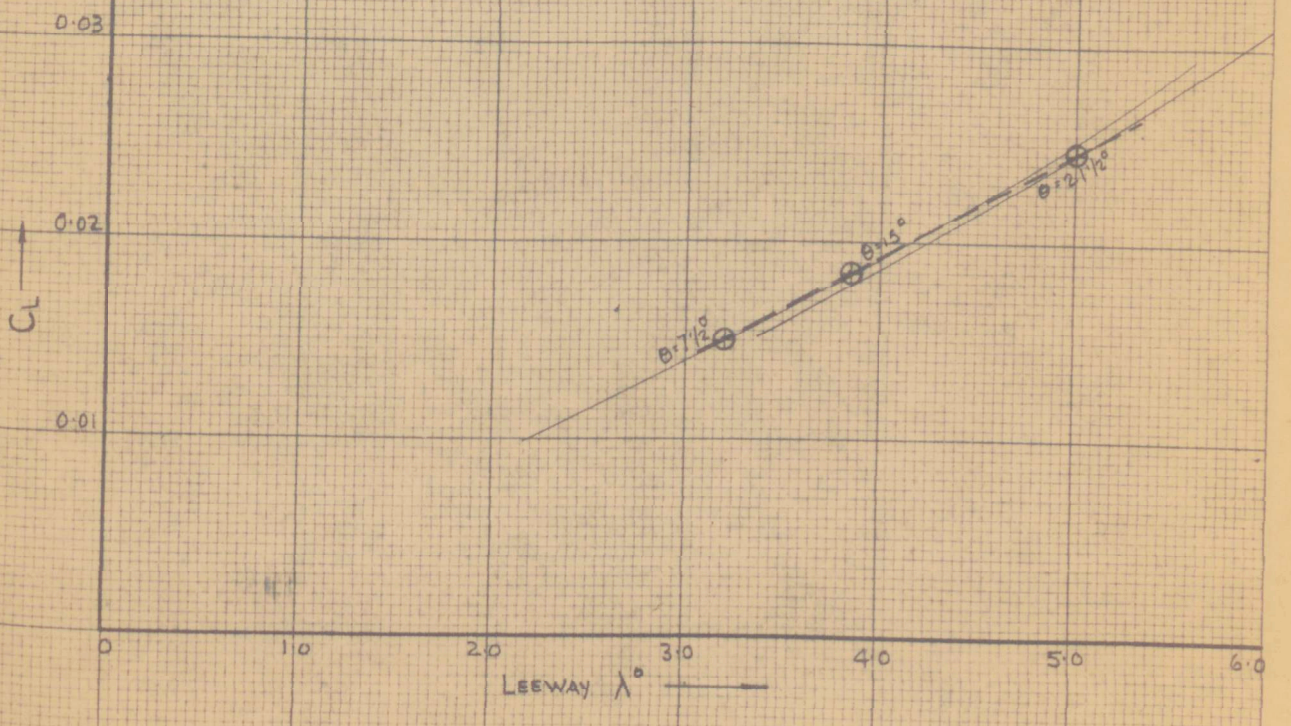

fig 22 sail coefficients for optimum V_{MG}

C_Y AND C_X.

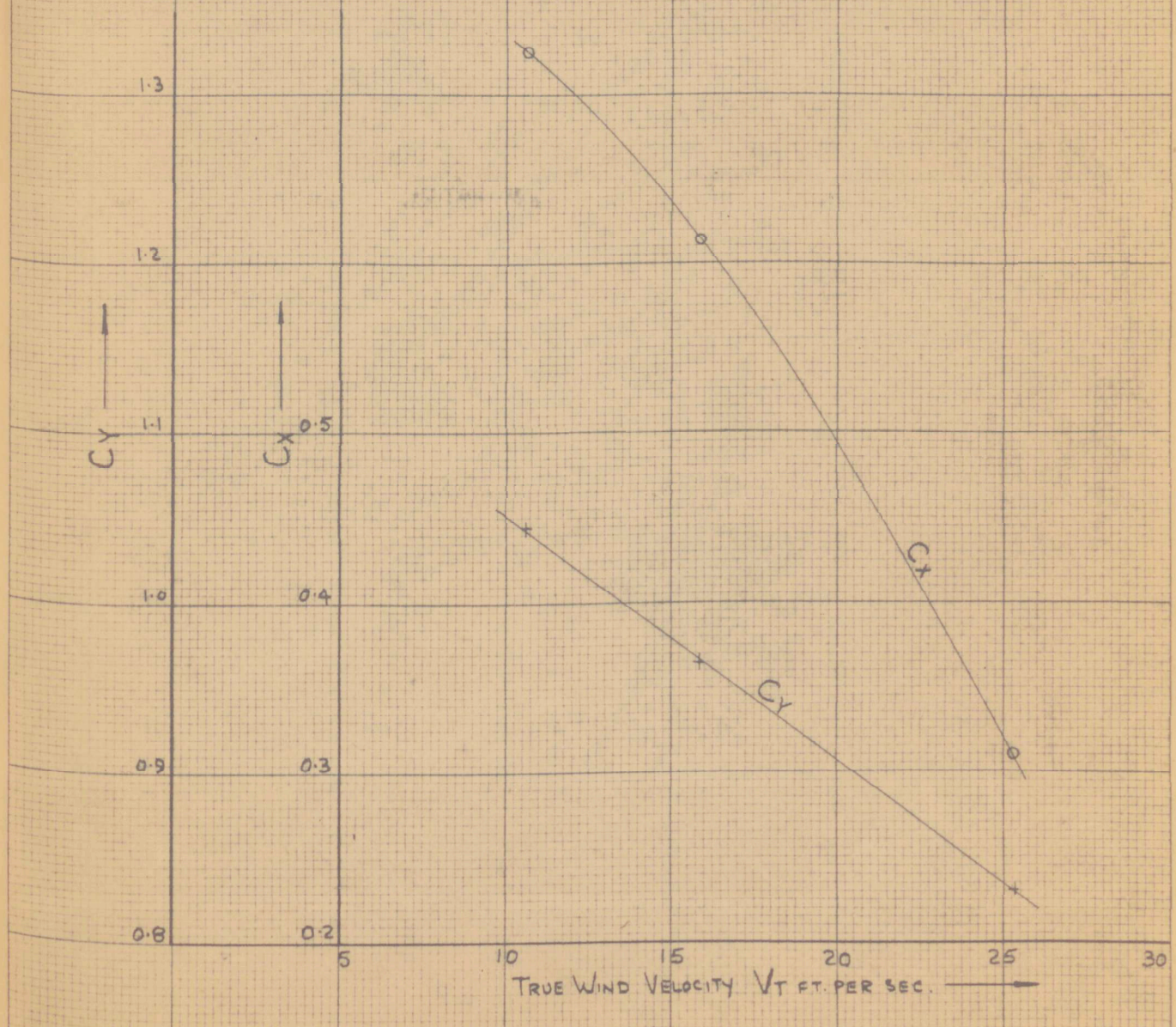

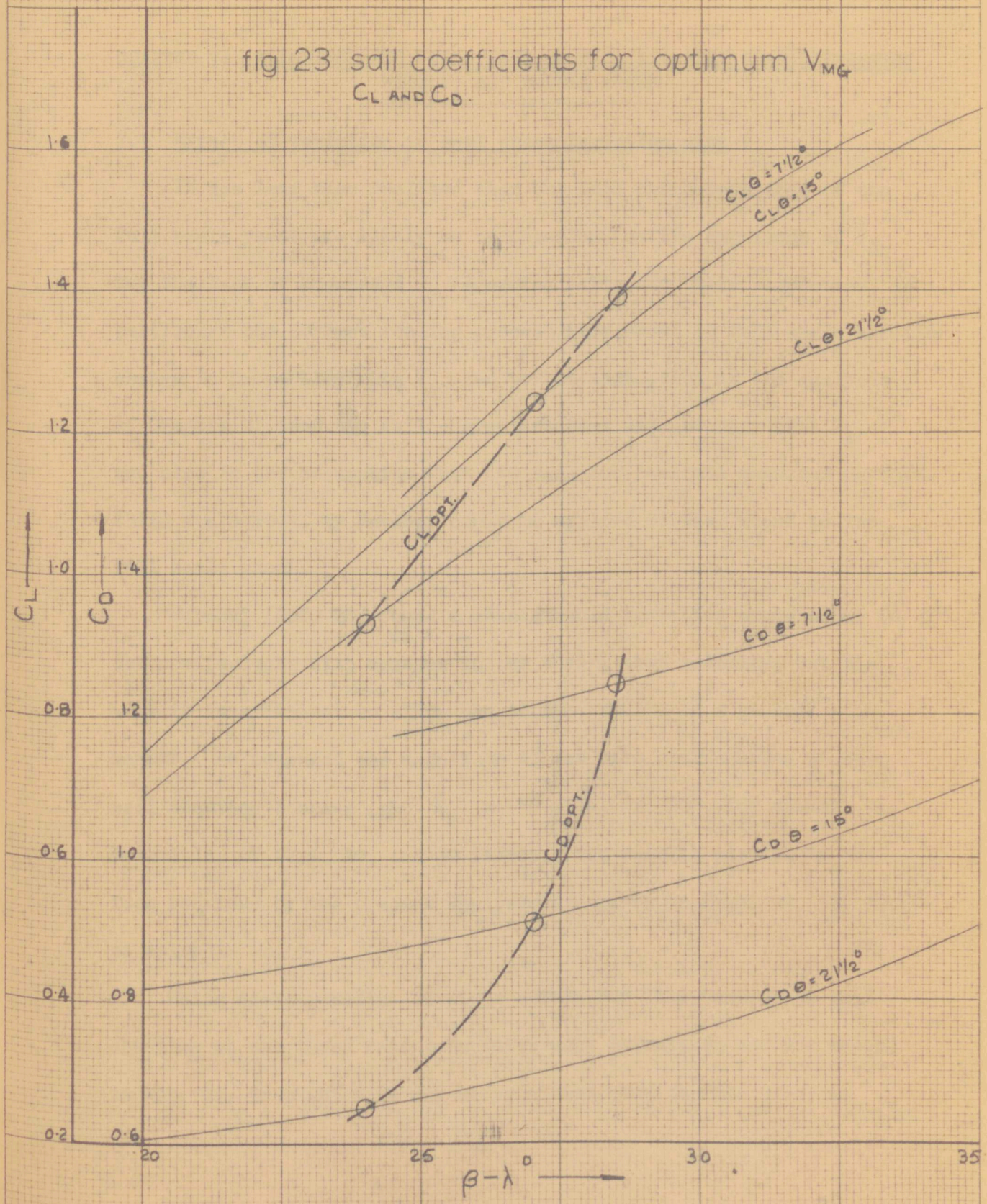
fig 23 sail coefficients for optimum V_{MG}
C_L AND C_D.
C_L
C_D
1·6
1·4
1·2
1·0
0·8
0·6
0·4
0·2
1·4
1·2
1·0
0·8
0·6
$C_L\theta = 7\frac{1}{2}°$
$C_L\theta = 15°$
$C_L\theta = 21\frac{1}{2}°$
C_L OPT.
$C_D\theta = 7\frac{1}{2}°$
C_D OPT.
$C_D\theta = 15°$
$C_D\theta = 21\frac{1}{2}°$
20
25
30
35
$\beta - \lambda°$

CHAPTER 7: ALLOWANCE FOR VARIATIONS OF SAIL AND HULL CHARACTERISTICS WITH V_A AND RUDDER ANGLE

7.1 Effect of variation in sail characteristics with V_A

It has long been realised that the sail characteristics of the full scale yacht are likely to be dependent on the magnitude of V_A but the lack of knowledge regarding sails and their properties, in particular the correct scaling process from model to full scale and the change in properties with V_A, led to the assumption in the analysis of Chapter 2, that the sail characteristics did not vary with V_A, and also to the assumption that the sail coeffecients measured on the third scale model by Marchaj could be applied as they stand to the full scale yacht.

Marchaj (Ref. 28) found a considerable variation could occur in the coeffecients with changes in the tunnel test velocity, but his work is insufficient to allow use of the results in a general manner. He measured the magnitude of the sail coeffecients at one sail sheeting combination, $\delta_M = 5°$, $\delta_F = 20°$, for tunnel velocities of 17.1, 20, and 30 ft/sec., the results plotted in the form required by the present analysis are given in Figs. 29, 33, 34, of Appendix No. 1.

Using these results, envelope curves for this particular sail sheeting at the three test velocities were calculated and are shown in Fig. 24, from which it may be seen that considerable error in

optimum V_{MG} can result; a comparison of Figures 12 and 24 shows that these variations in V_{MG} are of similar magnitude to those due to changes in foresail and mainsail sheeting, so illustrating the importance of further knowledge regarding the variation of sail characteristics with wind velocity.

If the true characteristics for a wide range of wind velocity were known, it would be possible to obtain the envelope curves for V_{MG} at several values of V_T, and hence V_A, for each sail sheeting position and so determine the corrected envelope curves for the appropriate values of V_A over the V_T range. When these corrected envelope curves are available the optimum windward performance boundary curve may be fitted and the reverse process undertaken to provide information required by the helmsman.

7.2 Effect of rudder application

The brief experiments described in Part. 3 to assess the effect of rudder application on the hull characteristics together with the data of Ref. 14, suggest that the optimum windward performance of a yacht may well be found with the use of a small amount of weather helm.

Available data is insufficient to allow its use in the analysis for the hull under consideration but if the required information were available, the envelope curve for each sail sheeting position could be further corrected by the use of the hull characteristics at a number of rudder angles, and hence the optimum boundary curve and

rudder condition obtained for any true wind velocity.

This information would then be available to the designer whose task it would be to 'balance' the vessel to give the necessary heel angle at each true wind velocity, perhaps with the aid of tunnel and tank experiments.

fig 24 variation in V_{MG} with V_A used in sail experiments
sail sheeting $\delta_M = 5°$, $\delta_F = 20°$

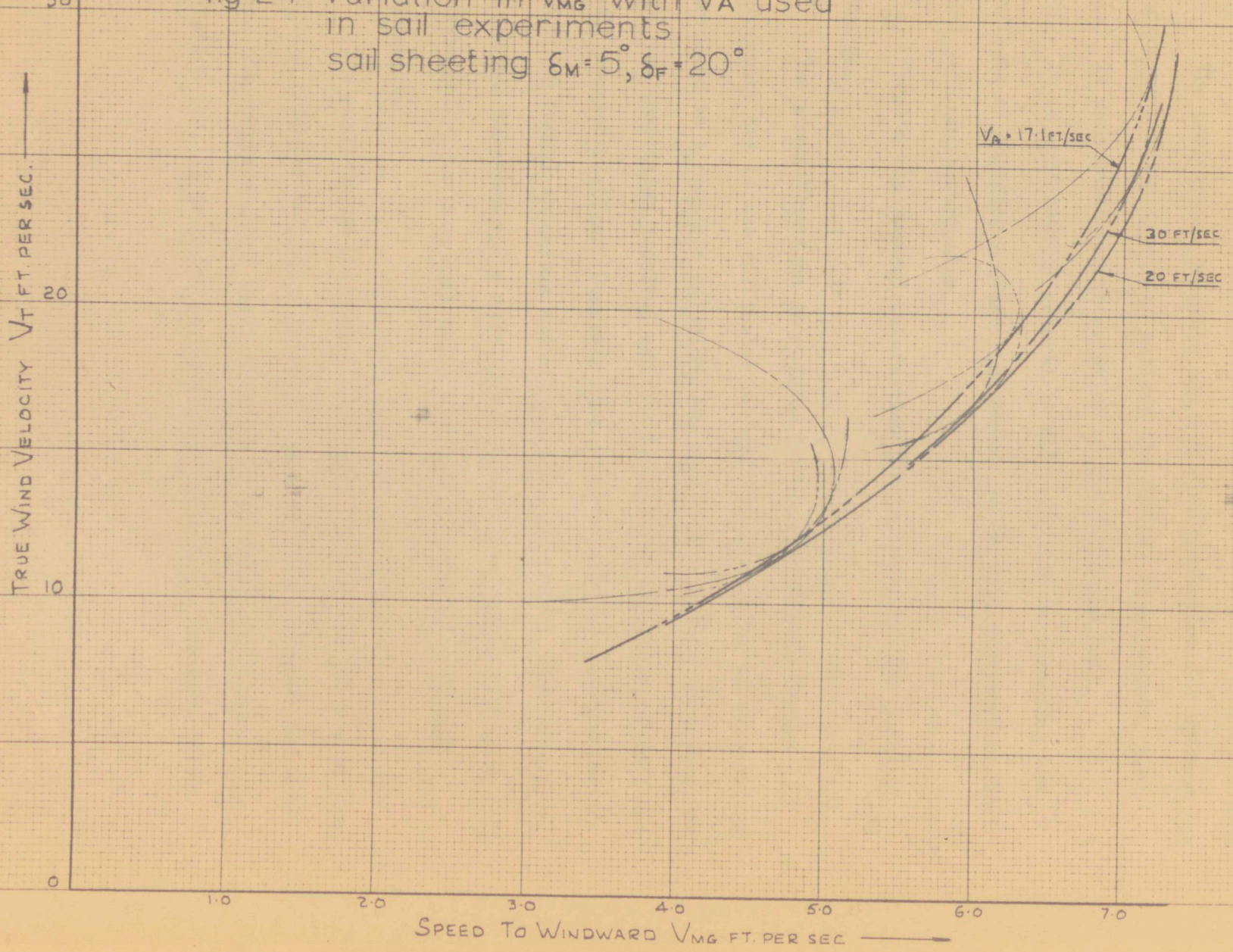

CHAPTER 8: CONCLUSIONS AND RECOMMENDATIONS

The performance anlaysis and method of prediction for optimum windward ability appear to satisfy the initial requirements, i.e:

(a) It uses basic characteristics of the sails and hull.

(b) It is sufficiently general to allow its use in assessing the effects of changing a single parameter, using data expressed as hull and sail characteristics.

(c) Permits the desired information for 'setting up' the yacht to emerge.

The simplifications introduced during the analysis became necessary due to the difficulty of handling the number of expressions involved in a complete solution, and due to the lack of data concerning the quantities involved and the appropriate variation of hull and sail characteristics. Complete data will require more sophisticated tank and tunnel apparatus and experimental techniques, involving six component balances and a much larger range of variables including full coverage of trim (for hull and sails) rudder, and depth of hull immersion.

The analysis in its present form appears suitable for use with a digital computer and hence it should be possible to process the data from the complete model tests in terms of the complete balance equation (No. 3) in order to obtain the optimum V_{MG} boundary curve.

Using the simplified method, the labour involved in determining balance positions and the boundary curve is not excessive when carried out graphically by hand, but would become so if a further balance of equation No. 3 were considered, so that the use of a computer appears essential.

It is recommended therefore that the required programming be carried out for the complete solution while allowing the processing of the simplified solution until the sophistication of tank and tunnel, together with the understanding of the scaling and effects of such variables as V_A and rudder application is sufficient to allow the former's use.

The simplified anlaysis may be made more complete by taking into account the effects of changes in the wind tunnel test velocity V_A, and rudder as suggested in the previous chapter.

The model tests described in Part 3 were undertaken in order to provide data required for the analysis omitting the balance of the yacht in trim. In carrying out such work for use with the performance prediction for an actual yacht, it would be possible to allow approximately for the downward force and trimming moment of the sails by applying the appropriate loading and moments to the hull under test, following the practice in connection with tank test work for use with 'the Gimcrack' technique (Refs. 5 & 10).

It is interesting to note that it appears possible to ignore the balance of yawing moments in a first treatment and to consider them in a similar manner to that described in the last chapter. In fact this may have advantages as the correct balance of the yacht under the optimum conditions may be obtained from later model tests after the optimum rudder application for best V_{MG} has been taken from the prediction. This balance is likely to vary with the True wind velocity and will only hold for windward work; balance for off the wind sailing, which has not been considered here, may be rather different so leading to a possible requirement for a means of altering the longitudinal location of the sailplan on the hull while under way.

The quantitative accuracy of the analysis will depend almost wholly on the accuracy with which the full scale hull and sail c aracteristics and their variation will all the parameters can be predicted. It is essential therefore that the necessary work is carried through to promote a fuller understanding of the problems involved in this area. Even when this has been achieved, only the quantitative performance of the yacht in steady conditions will result so that although the 'best windward performance' boundary curve is probably very near the truth at the lower end of the V_T ran_e, it is likely to become increasingly optimistic as V_T increases due to the unsteady wind and sea states associated with higher true wind velocities.

The problems discussed above apply also to all other present methods of windward performance prediction, based on established techniques and the analysis described in this part is likely to be of considerably greater inherent accuracy and generalised use due to its more general nature and consideration of a greater number of parameters.

APPENDIX NO. 1: SAIL DATA FOR USE IN CALCULATIONS

Marchaj (Ref. 28) has carried out experiments to determine the characteristics of the 'soft' sails of a 1/3 scale model of an 'X' class yacht's sails. He measured the Lift and Drag and Heeling Moment for the terrylene sails in the upright condition over a wide range of sail sheeting positions and $(\beta - \lambda)$. He also measured, for one sheeting position, the same quantities at a heel angle of 20°, and for three different apparent wind velocities.

The data contained in Ref. 28 is insufficient as it stands for direct application to the analysis of Part 1, in order to calculate the vessel's optimum windward performance; but by making certain assumptions and undertaking some manipulation a complete set of sail characteristics has been developed.

From the data of Ref. 28 it was desired to obtain curves of C_X, C_Y and K_X at heel angles of $7\frac{1}{2}°$, 15°, and $21\frac{1}{2}°$ for use with the hull characteristics obtained during the work described in Part 3.

Ref. 29 reports a careful evaluation by the yacht research staff at the University of Southampton of some wind tunnel experiments made on a small model having a sloop rig and 'solid' metal sails. It was considered at the time that little change in value of the coefficients occurred for the first 10° heel, and that beyond a heel angle of 20° they fell off rapidly.

In deriving sail characteristics from Ref. 28, it has therefore been assumed that the coefficients at $7\frac{1}{2}°$ heel may be taken as those obtained by Marchaj in the upright condition.

From Marchaj's data, it was possible to calculate C_X, C_Y and K_X for the vessel at $7\frac{1}{2}°$ (assumed those at 0°).

For the particular sail sheeting used by Marchaj in the measurements at 20° heel, a study of the results showed that for all values showed that for all values of $(\beta - \lambda)$ used, the average value of the coefficients was approximately 0.85 of their values at 0° heel.

By use of the above, Fig. 25 was produced to give an assumed curve to give values of coefficients at angles of 15° and $21\frac{1}{2}°$. From the curve it has been assumed that at 15° heel each coefficient has 0.95 of its value at 0°, and that at $21\frac{1}{2}°$ heel, each coefficient has 0.82 of its value at 0°.

Sail data calculated from Ref. 28 using the assumptions detailed above is presented in the form required for the performance analysis in Figs. 26 to 34. Figs. 26, 27, 28, 29, 30, give the sail characteristics for $7\frac{1}{2}°$ heel with δ_M maintained constant while δ_F varies from $7\frac{1}{2}°$ to 20°. Figs. 30, 31, 32, are for $7\frac{1}{2}°$ heel, δ_F remaining constant at $17\frac{1}{2}°$ while δ_M varies from 5° to 15°.

These have been given for $\theta = 7\frac{1}{2}°$ only; at 15° heel for any particular value of $\frac{C_Y}{C_X}$ and $(\beta - \lambda)$ the coefficients K_X and C_Y are 0.95 of the graphed values. At $21\frac{1}{2}°$ heel for any particular $\frac{C_Y}{C_X}$ and $(\beta - \lambda)$ the coefficients K_X and C_Y are 0.82 of the graphed values.

Note: data of Figs. 26 to 32 inclusive all refer to a test wind velocity of 20 ft/sec.

Figs. 29,33, 34, show characteristics for three different apparent wind velocities in the wind tunnel. For $\delta_M = 5°$, $\delta_F = 20°$. Again the values refer to a heel angle of $7\frac{1}{2}°$, and at any particular value of $\frac{C_Y}{C_X}$ and $(\beta - \lambda)$, the C_Y and K_X at 15° and 21½ heel will be 0.95 and 0.82 respectively of the values graphed.

fig 25 assumed fall of sail coefficients with heel.

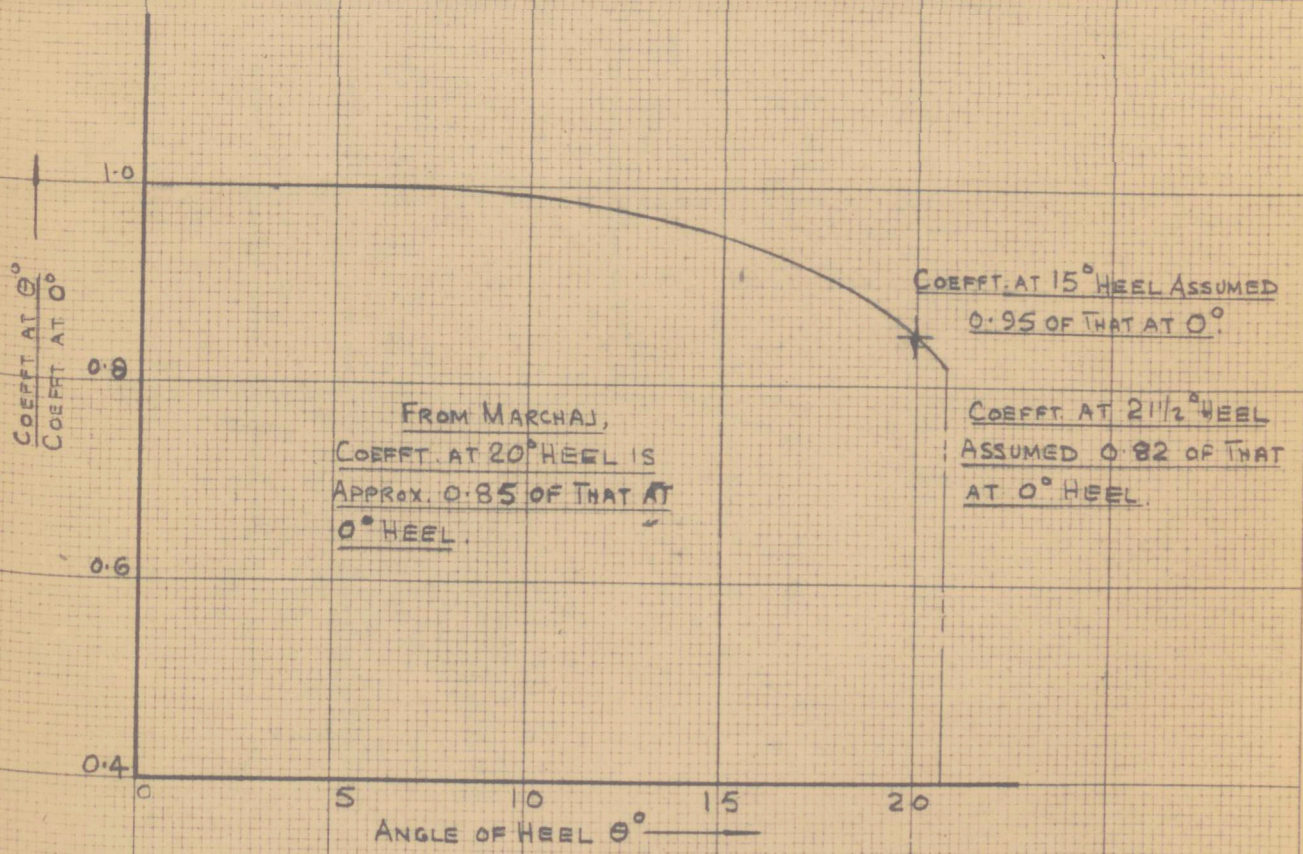

fig 26 sail coefficients at 7½° heel

$\delta_M = 5°$, $\delta_F = 7\frac{1}{2}°$

$V_A = 20$ FT/SEC.

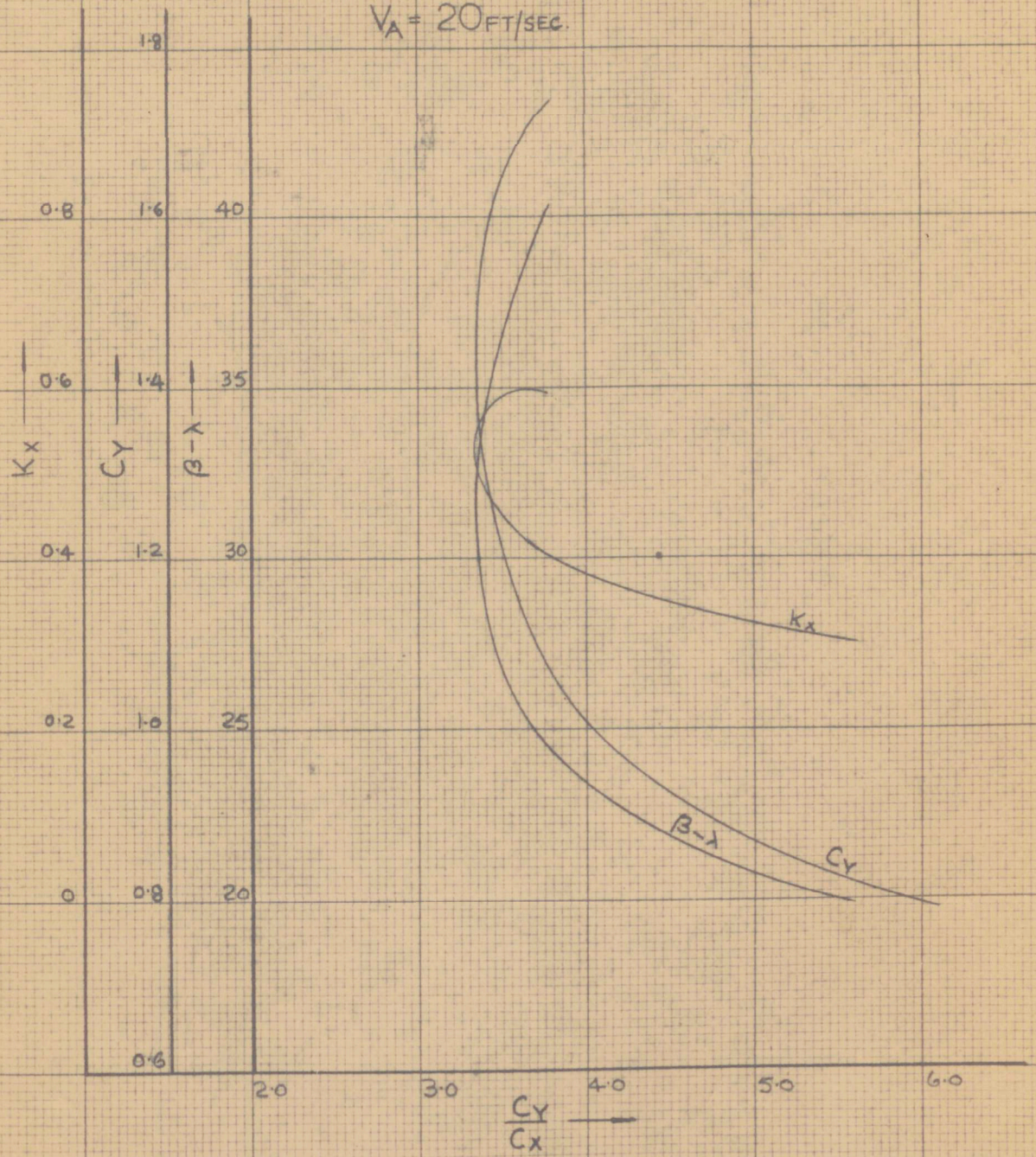

fig 27 sail coefficients at 7½° heel.

$\delta_M = 5°$, $\delta_F = 10°$

$V_A = 20$ FT/SEC.

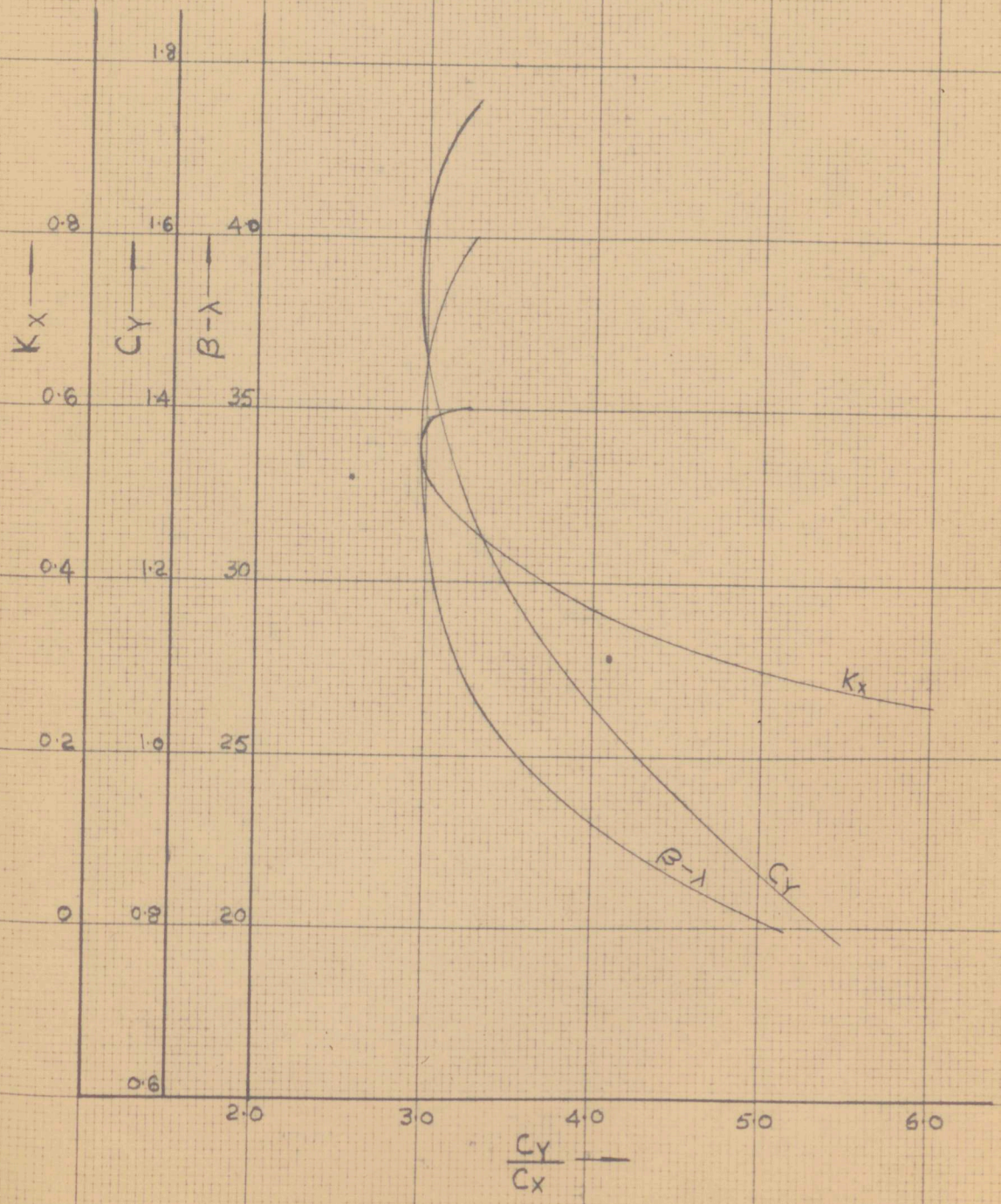

fig 28 sail coefficients. at 7½° heel.

$\delta_M = 5°$, $\delta_F = 15°$

$V_A = 20$ FT/SEC.

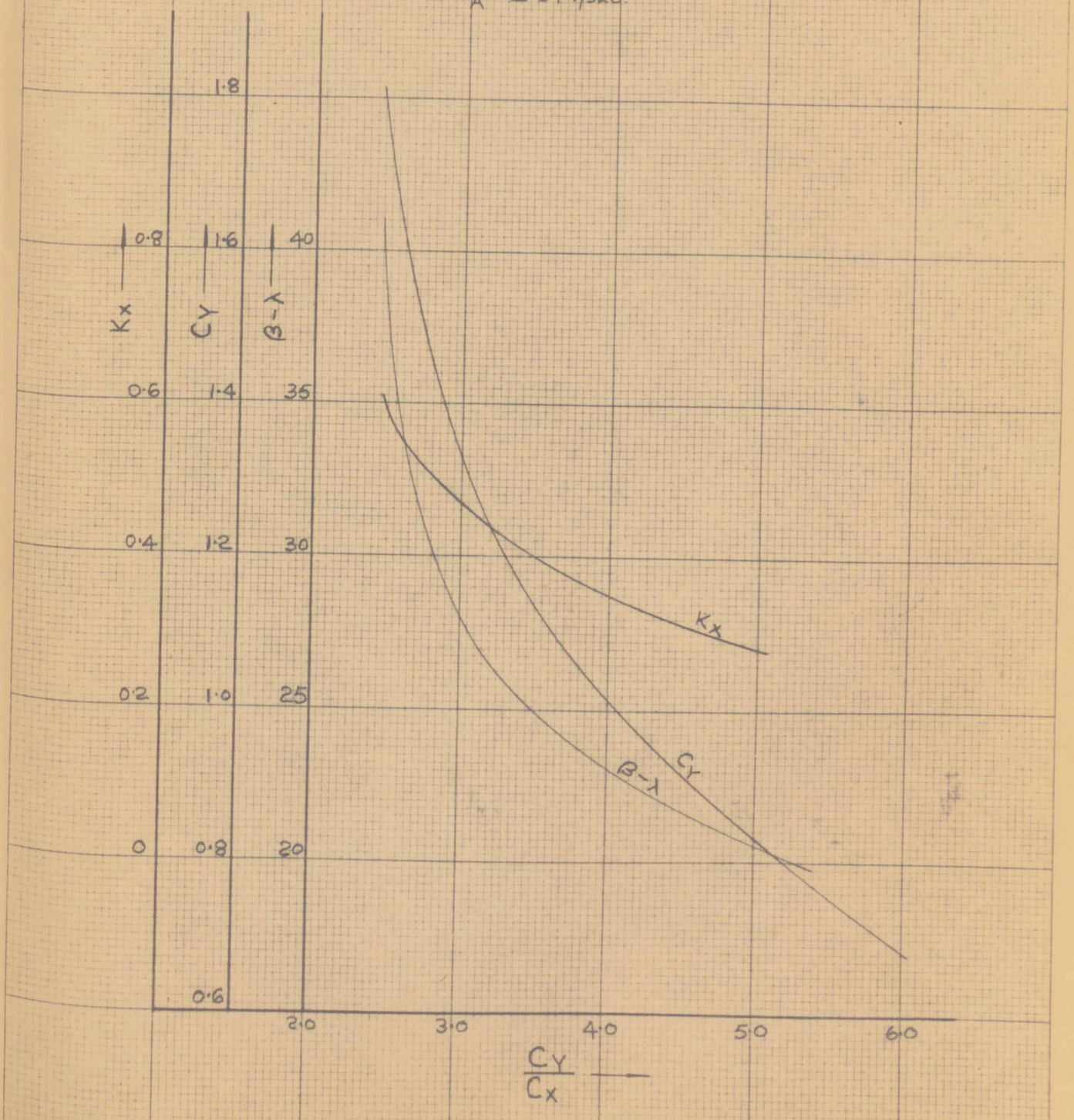

fig 29 sail coefficients at 7½° heel.

$\delta_M = 5°$, $\delta_F = 20°$

$V_A = 20$ FT/SEC.

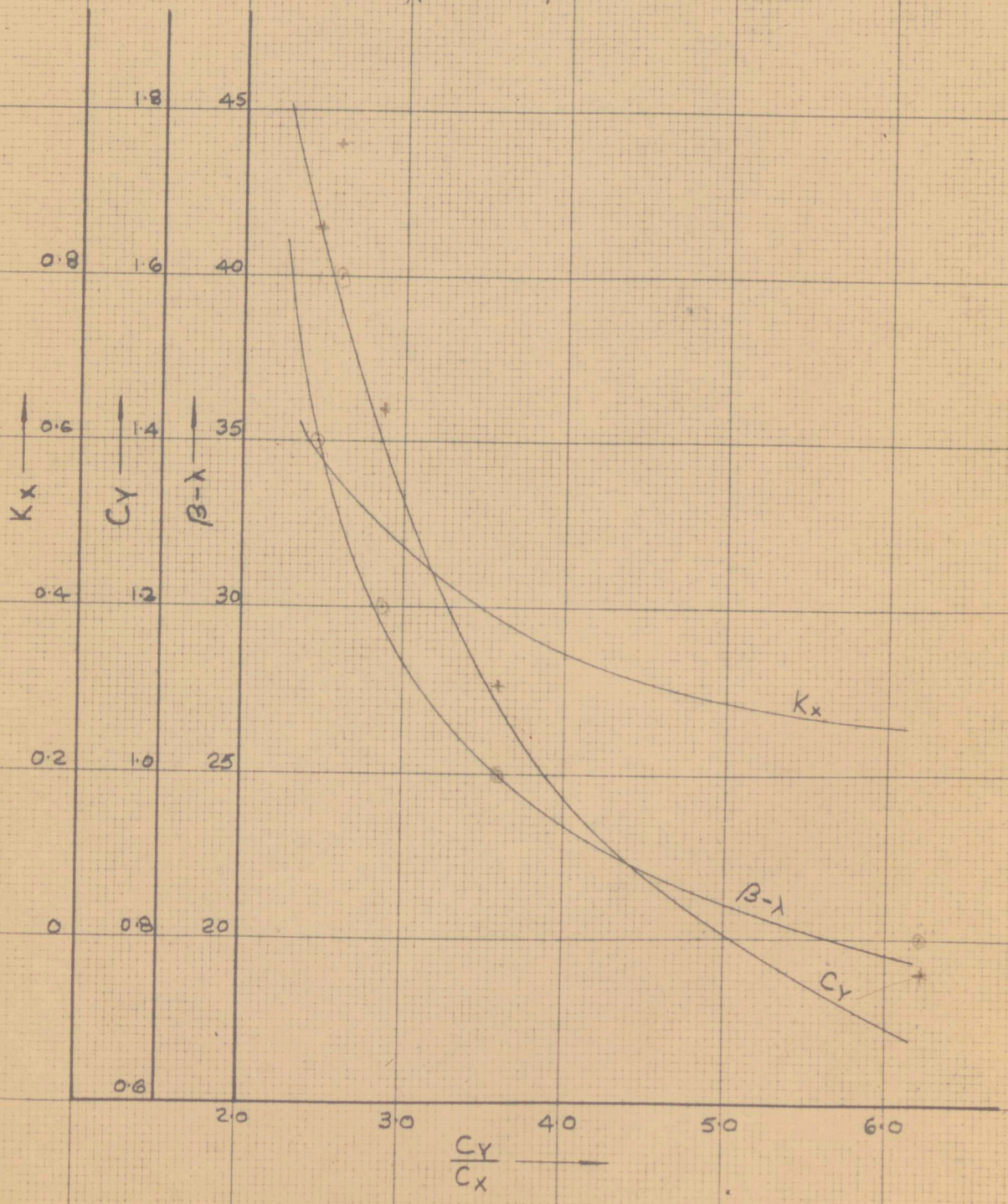

fig 30 sail coefficients at 7½° heel

$\delta_M = 5°$, $\delta_F = 17½°$

$V_A = 20$ FT/SEC.

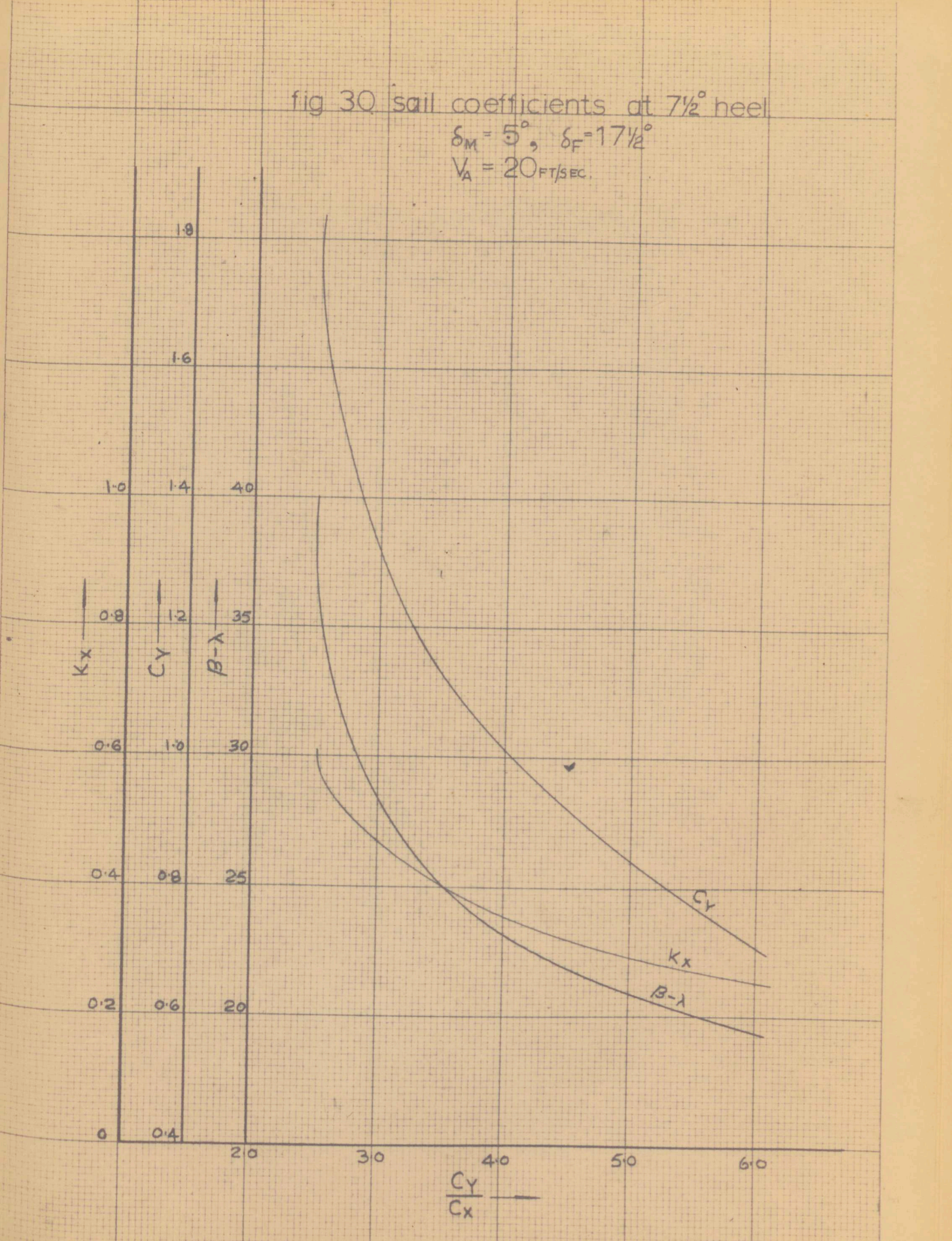

fig 31 sail coefficients at 7½° heel

$\delta_M = 10°$, $\delta_F = 17\frac{1}{2}°$

$V_A = 20$ FT/SEC.

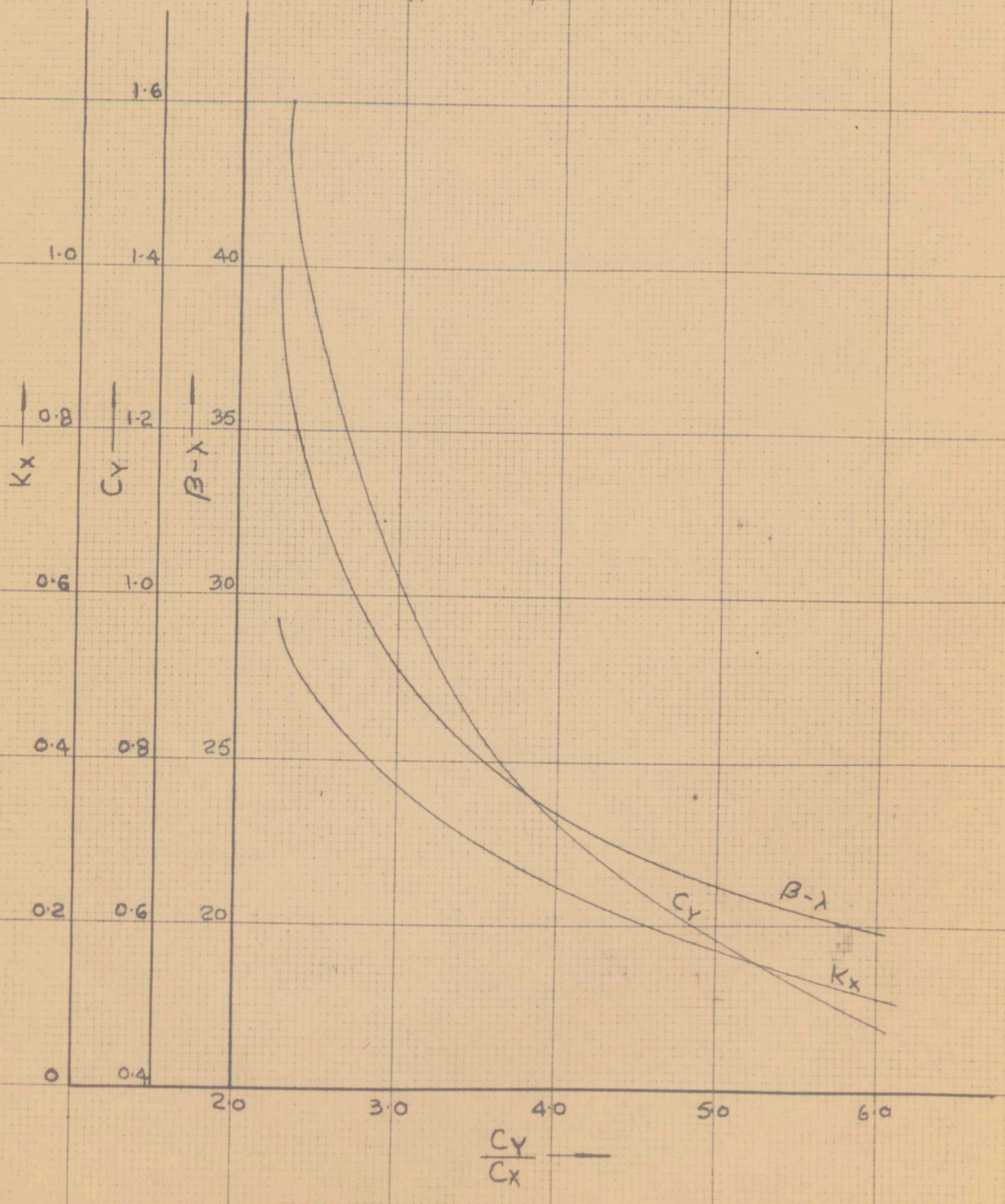

fig 32 sail coefficients at 7½° heel.
$\delta_M = 15°$, $\delta_F = 17\frac{1}{2}°$.
$V_A = 20$ FT/SEC.

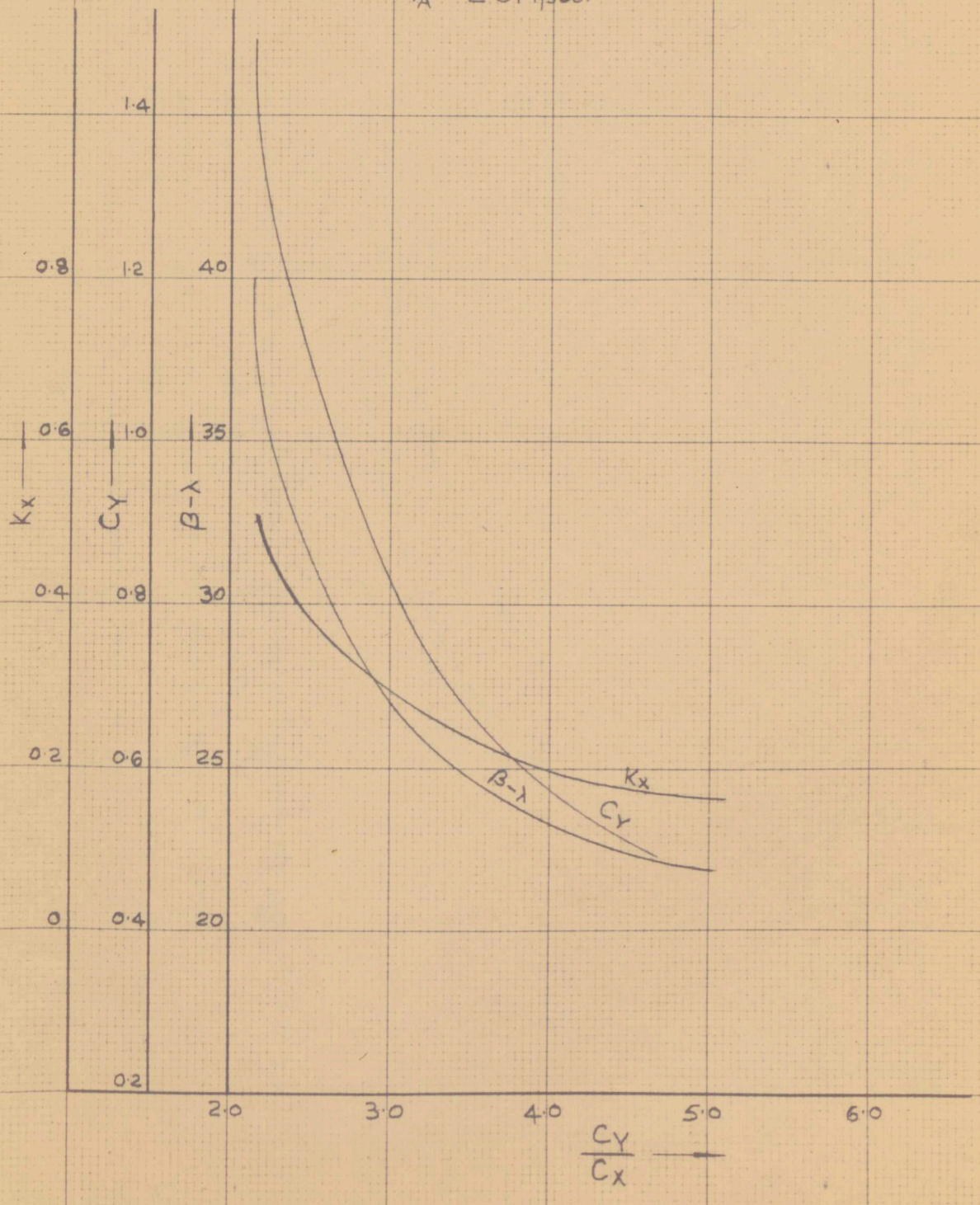

fig 33 sail coefficients at 7½° heel

$\delta_M = 5°$, $\delta_F = 20°$

$V_A = 17{\cdot}1$ FT/SEC.

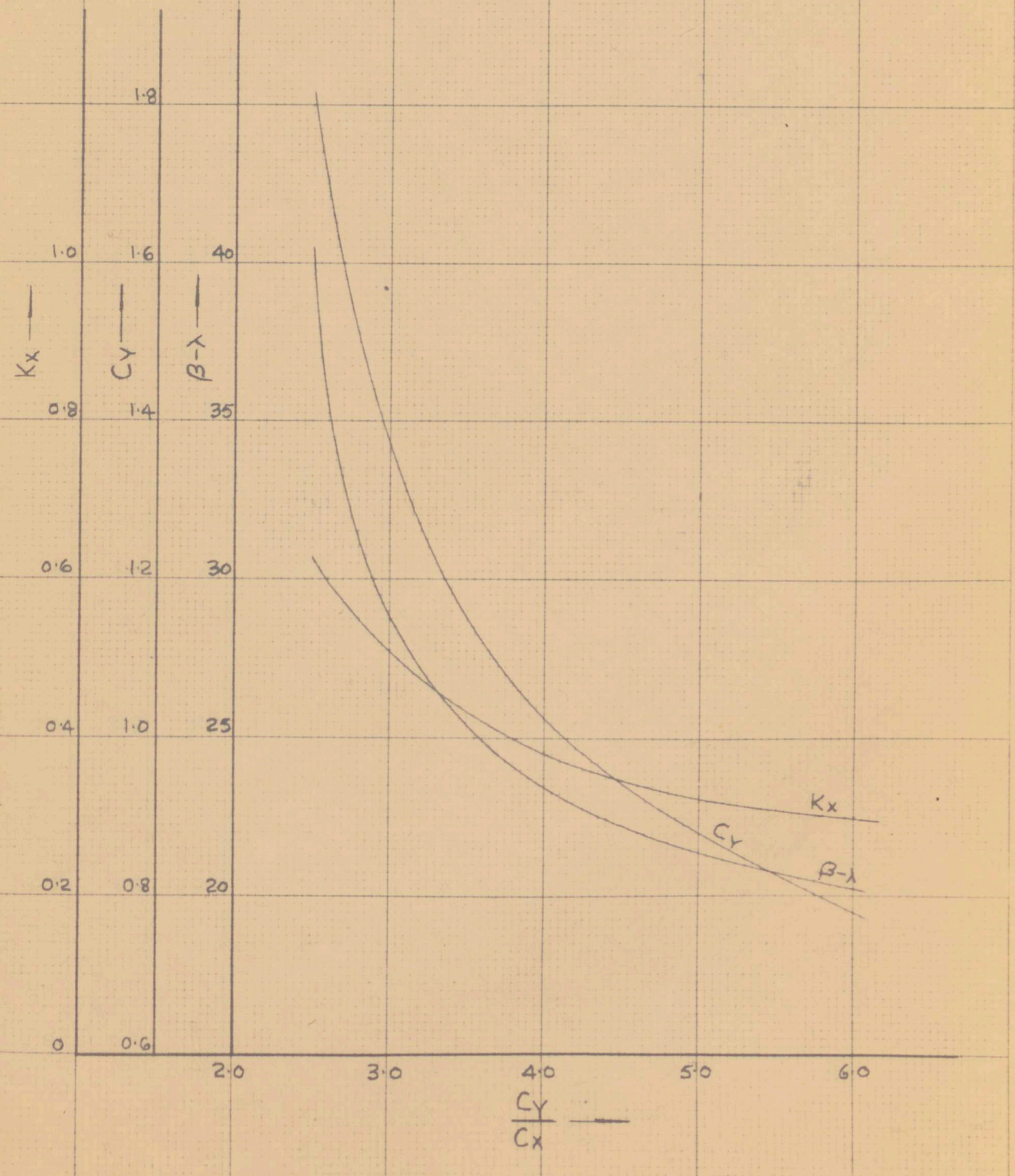

fig 34 sail coefficients at 7½° heel.
$\delta_M = 5°$, $\delta_F = 20°$
$V_A = 30$ FT/SEC.

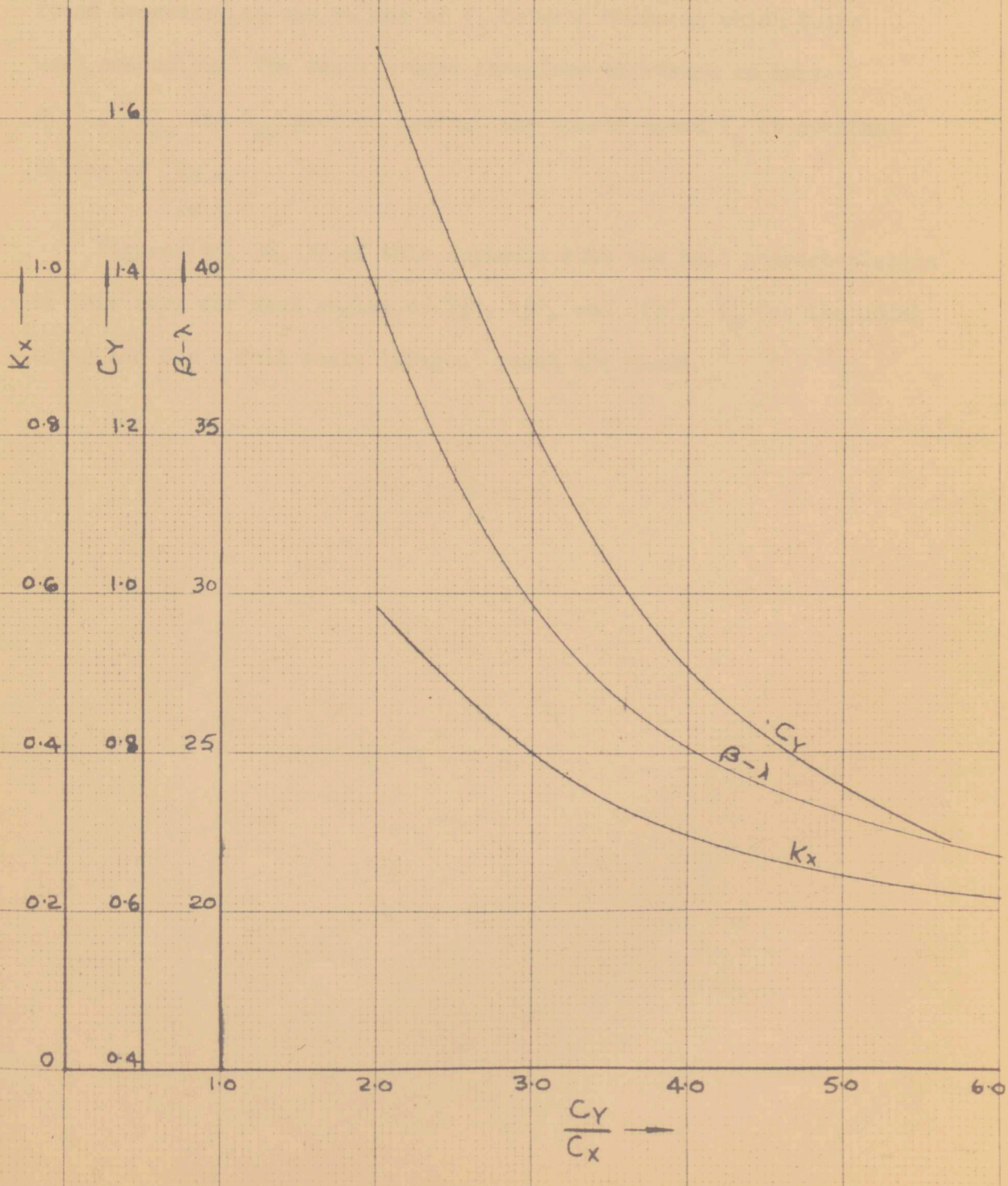

APPENDIX NO. 2: HULL DATA FOR USE IN THE PERFORMANCE ANALYSIS

During the application of the results of model test work described in Part 3, in the performance prediction of Part 1, it was found necessary to use values of V_S between those at which tests were conducted. The results were therefore expressed as curves of λ, C_{Yw} and K_{Xw} plotted against the course speed V_S at constant values of $\frac{C_{Yw}}{C_{Xw}}$.

Figures 35, 36, 37 of this appendix show the hull characteristics in this form for heel angles of $7\frac{1}{2}°$, 15°, and $21\frac{1}{2}°$. V_S for the model tests and for a full scale 'Dragon' yacht are shown.

fig 35 'dragon' hull characteristics at 7½° heel.

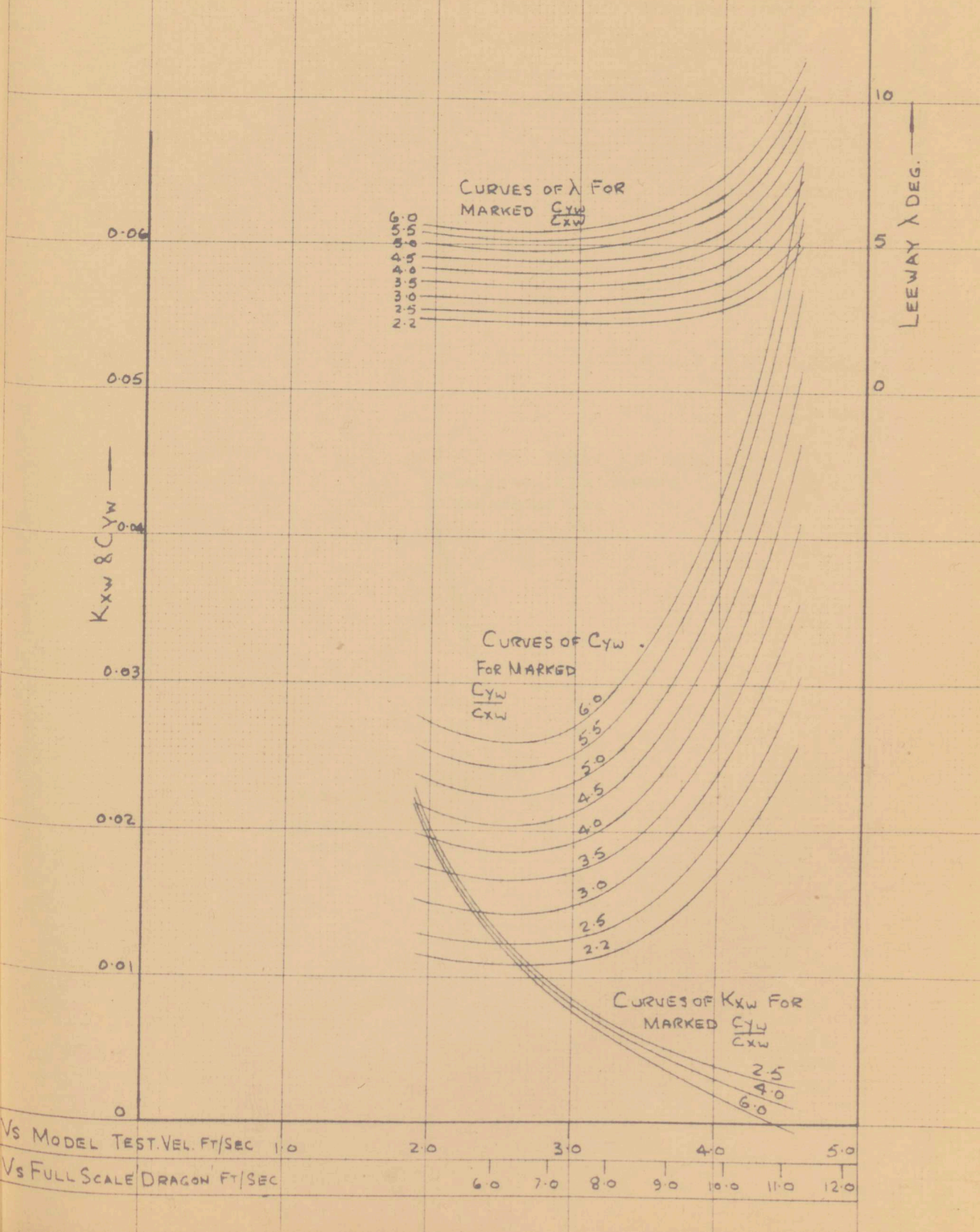

fig 36 dragon hull characteristics at 15 heel.

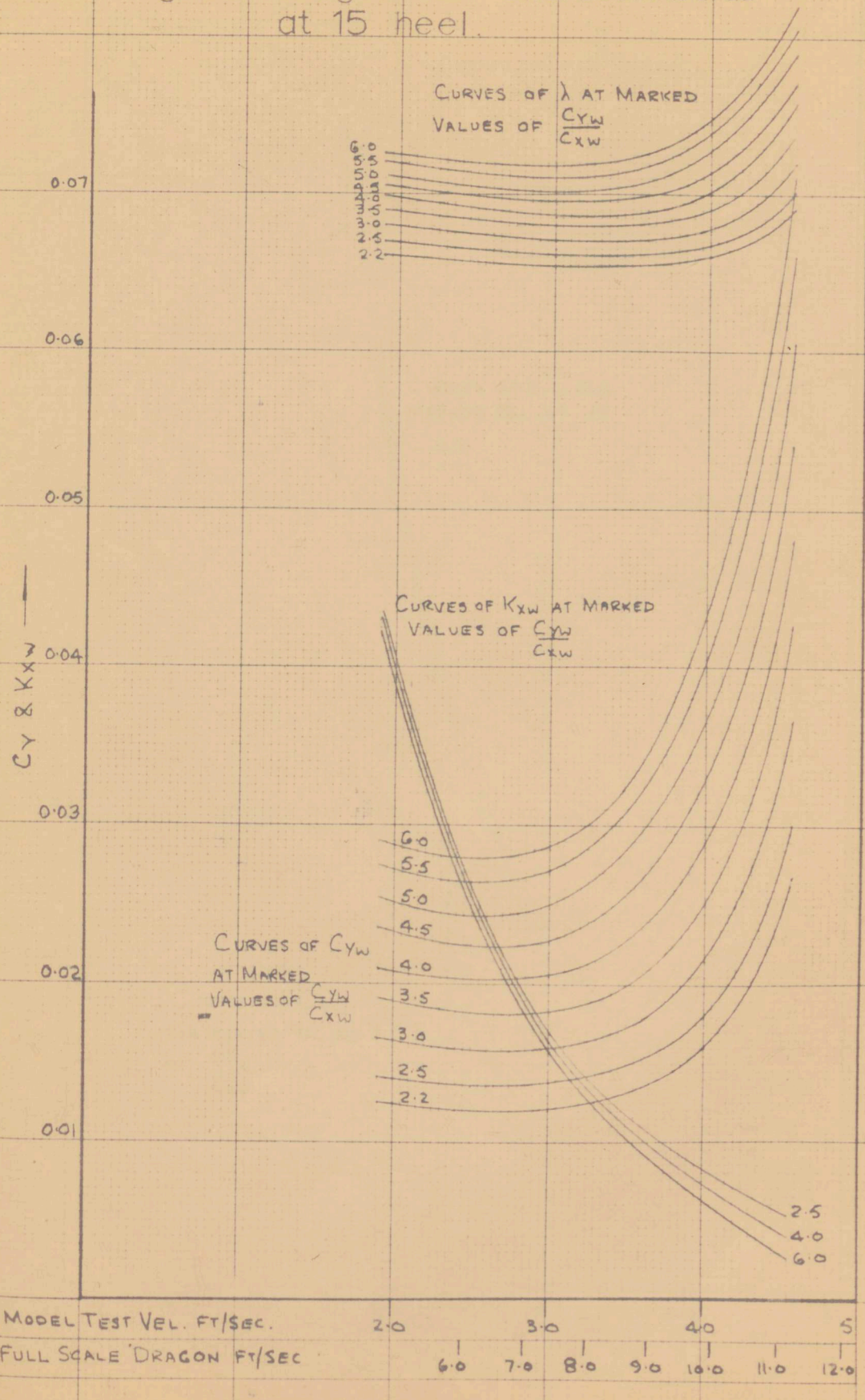

fig 37 dragon hull characteristics at 21½° heel.

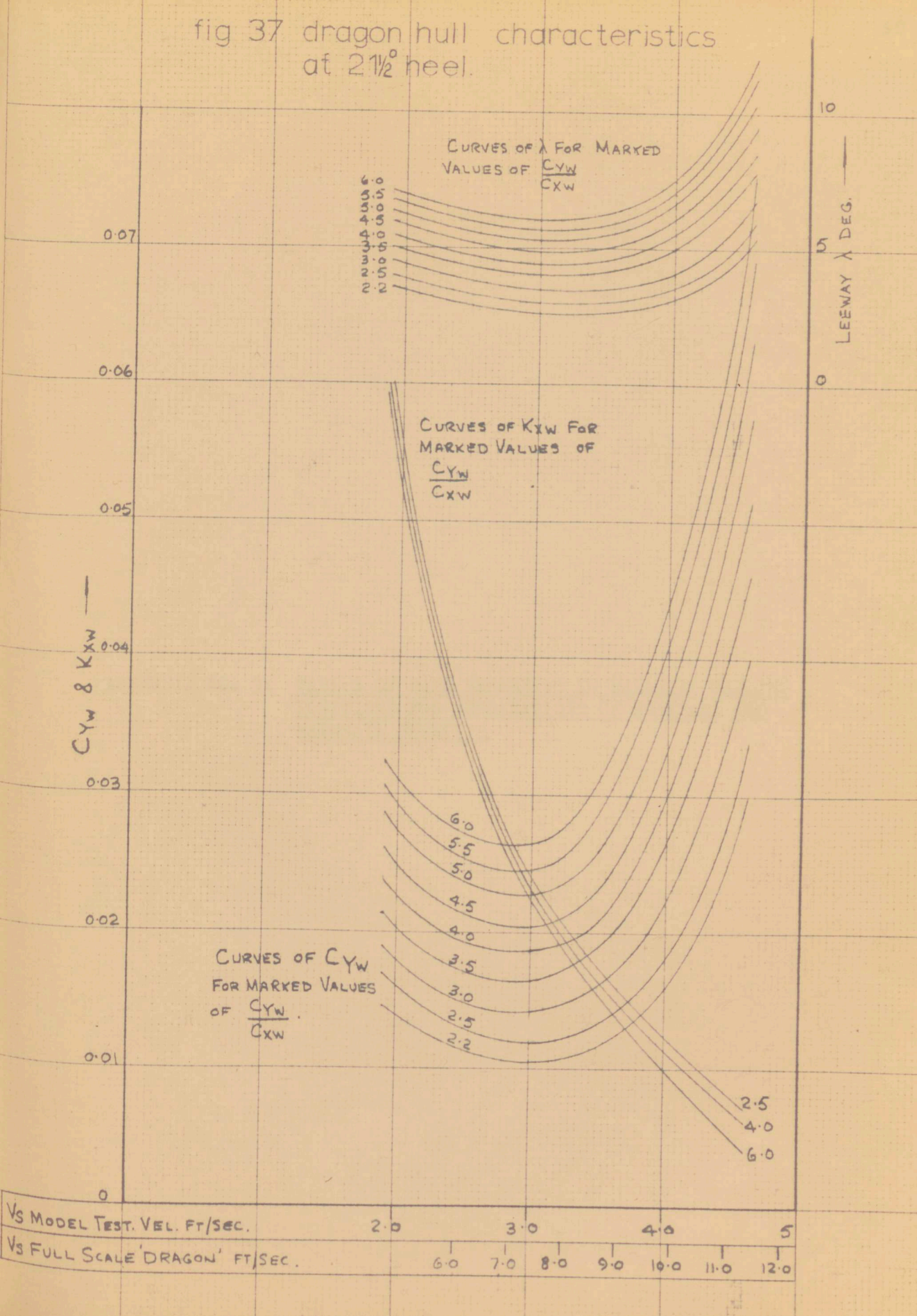

APPENDIX NO. 3: TABLES OF DATA REFERRING TO BALANCED SAILING POSITIONS FOR COMBINATIONS OF FORESAIL AND MAINSAIL SHEETING

TABLE 3. DATA FOR BALANCED SAILING POSITIONS.

$\theta°$	V_A FT/SEC	V_S FT/SEC	β	γ	V_{MG} FT/SEC	V_T FT/SEC	$\beta-\lambda$	λ	V_A FT/SEC	V_S FT/SEC	β	γ	V_{MG} FT/SEC	V_T FT/SEC	$\beta-\lambda$	λ
	SAIL SETTING: $\delta_M = 5°$, $\delta_F = 17\frac{1}{2}°$								SAIL SETTING: $\delta_M = 15°$, $\delta_F = 17\frac{1}{2}°$							
$7\frac{1}{2}$	21.95	6.13	25.6	34.8	5.03	16.63	20.7	4.9	25.9	6.79	27.5	36.6	5.45	20.1	23.7	3.8
$7\frac{1}{2}$	19.23	6.74	27.6	40.8	5.1	13.62	23.7	3.9	22.55	7.29	29.4	41.9	5.42	16.6	26.2	3.2
$7\frac{1}{2}$	17.15	7.28	29.7	47.3	4.94	11.95	26.3	3.4	20.45	7.6	31.6	47.7	5.11	14.5	28.7	2.9
$7\frac{1}{2}$	16.18	7.6	33.0	56.1	4.23	10.6	30.0	3.0	18.55	7.85	34.4	54.8	4.52	12.81	31.7	2.7
15	28.7	8.1	26.8	36.5	6.51	21.9	22.1	4.7	31.65	8.83	29.8	40.9	6.67	24.05	25.8	4.0
15	24.75	8.83	30.0	44.5	6.30	17.65	26.0	4.0	26.85	9.46	34.1	49.1	6.19	19.6	30.8	3.3
15	21.7	9.46	36.3	58.0	5.02	15.15	33.0	3.3	24.0	9.8	38.7	59.1	5.03	17.5	35.6	3.1
$21\frac{1}{2}$	34.9	8.1	26.2	33.7	6.74	27.85	20.9	5.3	42.5	9.46	29.4	37.1	7.54	34.6	24.7	4.7
$21\frac{1}{2}$	32.9	9.47	29.7	40.5	7.20	25.1	25.0	4.7	38.8	9.8	30.9	40.4	7.46	30.8	26.8	4.1
$21\frac{1}{2}$	30.5	9.81	31.8	45.0	6.93	22.7	27.5	4.3	30.45	10.3	38.7	54.9	5.93	25.25	35.0	3.7
$21\frac{1}{2}$									35.6	10.02	33.2	44.8	7.12	27.7	29.2	4.0
	SAIL SETTING: $\delta_M = 5°$, $\delta_F = 7\frac{1}{2}°$								SAIL SETTING: $\delta_M = 5°$, $\delta_F = 10°$							
$7\frac{1}{2}$	21.65	5.65	24.9	33.2	4.72	16.67	19.5	5.4	21.9	6.13	24.8	33.7	5.09	16.58	19.8	5.0
$7\frac{1}{2}$	20.35	6.13	26.0	36.4	4.94	15.05	21.3	4.7	18.66	6.75	27.5	41.3	5.07	13.07	23.7	3.8
$7\frac{1}{2}$	17.65	6.74	29.4	45.2	4.75	12.22	25.7	3.7	15.8	7.29	33.1	55.6	4.11	10.45	30.0	3.1
15	29.9	7.35	25.3	33.0	6.16	23.5	19.7	5.6	31.2	7.6	24.6	32.1	6.43	24.4	19.1	5.5
15	28.9	7.6	25.8	34.4	6.27	22.25	20.6	5.2	28.4	8.1	26.1	35.8	6.56	21.35	21.3	4.8
15	26.35	8.1	26.8	37.7	6.4	19.45	23.3	3.5	22.5	8.83	32.2	49.1	5.78	15.86	28.4	3.8
15	30.3	7.11	25.1	32.6	5.98	23.9	19.3	5.8								
15	23.4	8.57	31.4	47.1	5.84	16.65	27.3	4.1								
$21\frac{1}{2}$	32.6	9.2	28.8	38.8	7.06	24.55	24.2	4.6	38.0	8.83	26.8	35.0	7.23	29.9	21.2	5.6
$21\frac{1}{2}$	35.2	8.83	26.6	34.9	7.24	27.6	21.3	5.3	35.5	9.2	27.3	36.2	7.41	27.5	22.0	5.3
$21\frac{1}{2}$	38.3	8.33	26.1	33.0	6.98	30.95	19.9	6.2	31.3	9.46	30.0	41.3	7.1	23.75	25.5	4.5

TABLE 3. DATA FOR BALANCED SAILING POSITIONS.

θ°	V_A Ft/sec	V_S Ft/sec	β	γ	V_{MG} Ft/sec	V_T Ft/sec	$\beta-\lambda$	λ
SAIL SETTING: $\delta_M = 5^\circ$, $\delta_F = 15^\circ$								
7½	22.3	6.13	25.1	33.9	5.08	16.93	20.2	4.9
7½	19.5	6.74	27.3	40.3	5.15	13.82	23.3	4.0
7½	17.68	7.29	29.7	47.3	4.94	11.9	26.4	3.3
15	27.95	7.85	26.5	36.1	6.35	21.2	21.7	4.8
15	24.4	8.84	30.2	45.2	6.25	17.3	26.3	3.9
15	21.15	9.46	37.9	61.0	4.59	14.85	34.7	3.2
21½	38.8	8.83	26.0	33.2	7.39	31.1	20.5	5.5
21½	29.8	9.82	32.3	46.0	6.82	22.2	28.0	4.3
21½	33.3	9.46	29.5	44.5	7.24	25.4	24.7	4.8
SAIL SETTING: $\delta_M = 10^\circ$, $\delta_F = 17\frac{1}{2}^\circ$								
7½	27.4	6.5	26.0	33.5	5.42	21.75	21.2	4.8
7½	23.0	6.74	27.4	37.8	5.33	17.35	23.5	3.9
7½	19.6	7.28	30.4	46.0	5.05	13.8	27.2	3.2
7½	17.73	7.6	33.2	53.2	4.55	12.13	30.3	2.9
15	33.9	8.33	27.2	35.4	6.79	26.8	22.6	4.6
15	27.55	8.82	30.7	43.5	6.39	20.45	26.8	3.9
15	23.95	9.47	35.2	53.7	5.6	17.1	31.9	3.3
21½	52.2	9.07	26.5	31.8	7.7	43.2	20.2	6.3
21½	37.85	9.47	29.7	38.7	7.38	30.0	25.0	4.7
21½	33.4	9.81	32.1	43.9	7.06	25.6	28.1	4.0
21½	31.1	10.02	34.7	49.0	6.57	23.6	30.8	3.9

θ°	V_A Ft/sec	V_S Ft/sec	β	γ	V_{MG} Ft/sec	V_T Ft/sec	$\beta-\lambda$	λ
SAIL SETTING: $\delta_M = 5^\circ$, $\delta_F = 20^\circ$								
7½	23.6	4.65	24.9	30.7	3.99	10.5	18.3	6.6
7½	17.30	7.28	30.6	48.9	4.78	11.75	27.3	3.3
7½	14.9	7.84	37.8	67.2	3.04	9.9	35.2	2.58
7½	21.95	6.12	25.81	35.0	5.0	16.65	21.0	4.81
7½	19.24	6.74	27.9	41.3	5.06	13.63	24.1	3.8
15	31.4	7.29	25.4	34.5	6.0	23.8	19.8	5.6
15	28.9	8.1	30.9	41.7	6.05	22.3	26.3	4.6
15	24.1	8.83	30.9	46.4	6.09	17.1	27.0	3.9
15	21.3	9.44	37.6	59.2	4.83	15.12	34.4	3.2
15	23.3	9.07	32.1	49.9	5.84	16.2	28.4	3.7
15	26.1	8.58	29.5	42.2	6.35	19.1	24.8	4.3
21½	40.6	8.09	25.6	31.6	6.88	33.5	19.3	6.3
21½	38.0	8.82	26.8	34.4	7.28	30.4	21.3	5.5
21½	32.4	9.45	30.2	41.2	7.1	24.7	25.6	4.6
21½	29.25	9.80	33.5	47.8	6.58	21.8	29.0	4.5

PART 2. THE AUSTIN LAMONT YACHT TEST TANK

Design, Construction and Assessment

CHAPTER 9: INTRODUCTION TO PART 2

While evidence exists that experiments were undertaken to assess the resistance of sailing ship models during the middle of the eighteenth Century, the application of these results in order to determine the resistance of a full size ship was not understood, and due to their apparent inconsistency, such tests came into disrepute as a method of determining the capabilities of ships while at sea. It was not until around 1872 that William Froude working for the Admiralty at his tank in Torquay showed that the total resistance could be divided into two parts, and followed this by achieving remarkable agreement between his predictions and resistances measured during towing trials at sea.

Although Froude established a workable method of exprapolating model results, he was troubled during his work on friction by "perplexing anomalies"; Lackenby has since provided, in a paper read before the I$_n$stitution of Naval Architects in 1937, convincing evidence that in fact these "anomalies" were due to the presence of laminar flow.

Froude's original hypothesis showed that reasonable predictions could be made from small models, but in later years it was found increasingly impossible to obtain repeatable results at low Reynolds Numbers, and it became usual to adopt relatively large models, compared with Froude's which did not exceed about 12 ft. in length. The apparent unreliability of small models was later realised as being due to the persistence of laminar flow, which gave a decreasing discrepancy as model size and hence Reynolds No. was increased.

Davidson, around 1933, (Ref. 9) showed that reliable and repeatable measurements could be made using small models at low speeds, if a means was provided to stimulate the boundary layer into turbulance over the model hull; his work is notable because it led to the first use of a tank to measure the forces on small models of sailing yachts (some 3 to 3.5 ft. in length) under conditions of leeway and heel.

With the pioneer work of Davidson at the Stevens Institute in the testing of yacht models, following Davidson's breakthrough, which must have given American designers considerable assistance in their work for International Regattas, no parallel investigations were undertaken in Great Britain until the formation of the Yacht Research Council which instigated tests at both the National Physical Laboratory during the early 1950's, and at Saunders Roe Ltd. in 1955 to 1956. Work at both institutions was undertaken using small models (W.L. lengths of 5 ft. and 3½ ft. respectively.)

The approach and philosophy of experimenters on both sides of the Atlantic was essentially similar, the aim being to deduce the full-scale close-hauled performance of different sailing yachts, and tests were therefore made under conditions of speed, leeway and heel likely to be appropriate for the full-size yacht sailing over a wide range of true wind conditions.

Some attempt was made to analyse the results further, but the spread of the various parameters was too great to permit any notable success.

It became apparent in 1959 that tests on a hull covering in detail a very wide range both of speed and model attitude within and outside any presumed sailing values were desirable both in order to allow analysis in terms of aerodynamic knowledge and in order to provide a more general analysis of sailing yacht performance on all points of sailing; with reference to the former use, it is worth noting that in his paper (Ref. 9) Davidson and several contributors to the discussion had established some relationship between a yacht's hull and the aeroplane's wing, but no work of any consequence had been made generally available on this correlation since that of reference 9.

When funds became available, the University of Southampton, in 1959, put in hand at Saunders Roe Ltd. some experimental work on a

model of a 50 ft. waterline ketch using various appendages as 'Lift' producing devices. The work was primarily concerned with evaluating the relative efficiency of the various appendages for windward sailing using the established 'Gimcrack' technique propounded by Davidson, and at that stage there was no intention of using the results for more general study. When later in that year it became apparent that the wider approach was essential, it was also clear that the cost of such work in a Commercial Tank was prohibitive when account was taken of the funds then available, and likely to be available in the future, for research work on yachts.

Some additional work with the model at Saunders Roe Ltd. was instigated as a first step, but it was felt that much more could be achieved from a Tank at the University; accordingly a preliminary design study was undertaken in order to assess whether such an undertaking was a financial and practical possibility.

Once it was established that a facility sufficiently sophisiticated for the work required was possible, approval was given to the project and a suitable site chosen. Planning approval was obtained at the end of 1960 and the construction of both the enclosing building and tank structure proceeded during the Winter of 1960-61 under difficult conditions. The Waterway was filled in the Summer of 1961 and the various systems i.e. carriage, drive gear, balance and associated arrangements etc. were in position by the end of that year.

Development and preliminary evaluation of the tank and equipment proceeded during the last months of 1961, and the early months of 1962. The facility was, in reasonable working order by March 1962 and was officially opened by Dr. W. Cawood and named the Austin Lamont Yacht Test Tank on March 30, 1962 during the Conference on Yacht Design and Research then in progress at the University.

The preliminary evaluation was complete by early June, 1962, and the first item of Research work, the measurement of hull characteristics (described in Part 3) was undertaken during the period June to August that year.

CHAPTER 10: PRELIMINARY DESIGN STUDY

The majority of Towing Tanks are used both for Commercial work, e.g. the routine prediction of full scale performance of ships, together with a certain amount of basic research when time and facilities allow. In recent years, research on sea-keeping and ship motion has resulted in the construction of large manoevering basins and whirling arm installations.

Routine work includes resistance measurement, power experiments, and self-propulsion tests, for which the size of model required is governed more by the desirability of avoiding excessive scale effect from propellers and appendages, than from the question of Reynolds Number and laminar flow; hence models used in such tests must be of sufficient size, especially in the case of multi-screw ships, to avoid this trouble. The large model length leads to greater velocities being required and a considerable length of tank to allow for acceleration, a reasonable length and duration of steady run, and stopping; the large model section area entails a considerable water depth and cross section area to avoid excessive depth and blockage effect.

Such facilities are extremely expensive to provide and run; Ref. 17 gives the cost of the new Ship Hydrodynamics Laboratory of the National Physical Laboratory at Feltham, with a length of 1300 ft., as some £ 2M, and the cost per day to a user as approximately £ 300. (The initial cost includes all ancillary services, manoevering basin and water tunnel, although the cost per day is for the actual

tank alone).

These figures may be compared with the No. 2 tank at Saunders Roe Division of Westland Aircraft Ltd., 300 ft. in length, for which a daily charge for use of around £200 has been mentioned; the figure for the original cost is not available.

At this very early stage in the study, it was anticipated that a sum of about £4,500 might be available for construction of a tank at the University, (this was later reduced to £3,500) so that it was apparent that if such a facility was to be a practical possibility, the physical size of the tank must be kept as small as practicable commensurate with providing equipment which would allow useful work to be undertaken; this conclusion was strengthened by the lack of space available.

Model Size

The dependence of waterway dimensions on model size has already been mentioned. Both Davidson (Ref. 9) and Saunders Roe Division (ref. 1) used small models of between 3 ft. and 3½ ft. waterline length in their early work, from which it has been possible to obtain much reliable and useful information. Ref. 4 indicates that Saunders Roe Div'n now use slightly larger models of between 5 ft. and 6 ft. W. L. length while Ref. 18 gives lengths of 3 ft. to 3½ ft. as still being in use at the Davidson Laboratory.

Even with models of this size, effective stimulation of turbulance is difficult at low speeds, and the adoption of smaller models would exaggerate the problem and also lead to difficulty with wavemaking; at the lower speeds the wavemaking resistance of the model may not be proportional to that of the full size vessel due to ripples, dependent on surface tension, becoming important; according to Ref. 19, the lower limit of velocity to contain any error due to this within 1% has been set by Peabody at approx. 1.3 ft/sec.

As the tank cross section area required depends largely on consideration of blockage and depth, if the waterway were designed to accommodate full vessels of 3 ft. waterline length, it would be possible to run larger models or yachts having finer form without any increase in blockage; this led to the range of waterline length for normal models being taken as between 3 ft. and 4 ft.

In addition to reducing the first cost and space taken up, the adoption of the smallest possible model has the advantage of keeping manufacturing and modification costs for models to a minimum, and allowing their easy handling, although considerably more precise measurements are required from the balance arrangements than would be the case with larger models.

Waterway Length

The effective length of waterway must be sufficient to allow a reasonable duration of steady run in order to permit measurements to be taken, once the model has been accelerated from rest and achieved a steady state; at the far end of the run, the decelerating length must be such that the model comes to rest well before there is any likelihood of fouling any part of the tank or equipment. The minimum length to fulfil all these requirements will be related to the maximum model velocity available.

While the maximum speed of a displacement yacht is probably equivalent to a speed/length ratio ($V/\sqrt{L}$) of 1.4, the upper limit was set at $V/\sqrt{L} = 1.5$ to allow behavior at speeds normally above the maximum to be studied. With a 4 ft. model the maximum speed equivalent to this latter speed/length ratio is approximately 5 ft/sec.

Ref. 17 enabled a reasonable duration of steady run to be assessed; in the design of the new Ship Hydrodynamics Laboratory, a minimum steady run at the maximum carriage speed was accepted at 7 secs; on applying this to the proposal, using maximum possible carriage speed of 5 ft/sec., then a minimum length of steady run required is 35 ft. At more normal speeds and for models having a lower waterline length, the available run would of course be increased.

The acceleration available and possible is controlled by the carriage and propulsion system adopted. The maximum with a heavy manned carriage self-driven from on board appears from Ref. 17 and various papers in Ref. 20, to be about 3.5 ft/sec^2, while for an unmanned carriage using a towrope drive, it may be increased to 7 ft/sec.^{2}, or even more (these latter figures are given as referring to the Saunders Roe Tanks). It also appears during various discussions contained in Ref. 20 that some difficulty could arise with the balance and associated arrangements if the acceleration was too rapid At this stage of the study an acceleration length of 10 ft. was allowed; requiring a steady acceleration from rest of 1.25 ft/sec^2 which was, therefore, seemingly well within the usual figures.

If a length of 10 ft. is allowed for stopping, and a further 10 ft. for obtaining steady conditions following the acceleration period, then the minimum length of waterway required may be computed:

Length for 7 secs. steady run at 5 ft/sec.	35 ft.
Acceleration distance at 1.25 ft/sec.^{2}	10 ft.
Length of run to achieve steady state	10 ft.
Stopping Distance	10 ft.
TOTAL	65 ft.

If the top speed and model length were reduced to give a $V/\sqrt{L}$ of 1.4 for a 3 ft. waterline, with 10 secs. steady run, then the distances required for acceleration and stopping would be reduced, (assuming the acceleration remained 1.25 ft/sec^2) leading to approximately the same distance as the minimum requirement for waterway length. 10 secs. has been taken for the minimum time required for measurement in more usual tests, the 7 secs only being applicable to the highest speed runs.

Waterway Cross Section Area

A typical model which might be run in the tank is that of a 'Dragon' Class yacht used for experiments described in Ref. 1, with a waterline length of approx. 3.5 ft, and a maximum cross-section area of some 20 sq. in.

In Ref. 17, Allen gives the criterion, developed from work by Hughes, that in order to gain freedom from blockage effects, the tank cross-section area should be 250 times the maximum model cross-section. This leads to a cross section area of some 34.7 sq. ft. being desirable for the proposal.

It is often assumed that shallow water wavemaking effects may be neglected below a Froude Number (based on the water depth) of $F_D = V/\sqrt{gD} = 0.5$ (D is tank water depth), (Ref. 21). This criterion gives a minimum depth of approximately 3.2 ft. as being desirable.

The minimum over-all breadth and depth to fulfil these requirements will be gained using a rectangular tank cross-section.

Carriage, Rails and Drive System

In general, two types of carriage are in use with towing tanks, manned and un-manned; the former is often employed with tanks, having large dimensions, when it would be impossible to assess the model behavior from alongside the waterway; the manned carriage also has the advantage that a simplified balance and recording system may be practicable as operators are available on the carriage to make small adjustments during the run and to take readings from on board.

The unmanned carriage has the advantage of lighter weight, requiring less power from the drive gear, but although model behavior can be assessed adequately from alongside the waterway, all readings from the instrumentation must be recorded on the carriage or transmitted to recording units at the control position.

Power for towing the model and carriage may be provided by motors driving the main wheels, or through a tow-rope driven by motors alongside the waterway. The two systems lead to the use of heavy and light carriages respectively, and in either case acceleration rates above those considered desirable have been achieved (Refs. 17 & 20), and it is possible to arrange for control to be in the hands of operators on board.

In addition, a system where the model is towed with a falling weight through a tow-rope is used in several small tanks, e.g. Fort Steyne (Ref. 19); this appears to be an effective and simple method where models are run in the 'straight' condition and have reasonable directional stability, but would be impracticable in the case of a yacht model running with heel and leeway, where it is necessary to support and measure side-force.

A manned carriage must be heavier and stronger, so requiring greater power and heavier supporting arrangements than the un-manned, considerations which lead to considerably greater initial and running costs.

As the model behavior and carriage operation can be controlled adequately by an operator at a control position in the tank length, there was no reason to provide a manned carriage for the proposed facility.

Either drive system is suitable for use with an un-manned carriage, but in order to keep down weight (so assisting rapid acceleration and deceleration together with less liklihood of damage if the braking system should fail), and obviate any possible danger due to transmitting large voltages and powers in the presence of water, it was considered that a tow-rope system appeared the more suitable.

A common means of accomplishing steady controlled carriage speed is to use a winch driven by the output from a D.C. motor-generator set, or other voltage controlled D.C. system. An alternative, used

successfully for a number of years by the Saunders Roe Division of Westland Aircraft Ltd., for low speed work in their No. 2 Tank, is to take the output from an A.C. synchronous motor through a number of gears giving pre-set ratios, to the towing winch. The winch R.P.M. and hence carriage speed depends on the gear ratio selected and fluctuates only with the mains frequency, although a disadvantage is that only the set gears and speeds are available, there being no means of achieving an infinite variation.

The low cost and success of this arrangement at the Saunders Roe No. 2 Tank encouraged its use for the present project.

With light carriages of the type considered, it is usual to adopt a mono-rail to support and guide the moving vehicle, while heavy manned carriages use a two rail system. The more usual work undertaken by towing tanks does not necessitate the support and measurement of side-forde, and hence the lateral and rolling stability provided by a mono-rail is sufficient.

Although a twin rail arrangement requires greater accuracy in setting and lining up, it provides the considerable restraint against instability due to side force and roll, which appears desirable when working with yacht models; (this is confirmed from conversations with representatives of both the Davidson Laboratory and Saunders Roe Div., both of which use a mono-rail).

Consideration of the foregoing together with the available funds, led to the conclusion that a light, unmanned, carriage, carried by a twin rail system and driven by a synchronous motor via winch and tow-rope was the most suitable for the proposed tank facility.

Measurements Required

Mention has been made previously of the need to establish the full range of characteristics for yacht hulls in order to carry further the work on performance introduced in Part 1.

In the early stages of the work in Part 1, it appeared necessary to measure the side force, resistance and heeling or stability moment at various course speeds and hull inclinations (heel and leeway), these being the principal characteristics affecting the performance. Other quantities of direct interest appeared to be the yawing and trimming moments and vertical force component at the various speeds and inclinations.

Due to the expense of providing balance arrangements to measure all these quantities and the consideration in Part 1 of side force, resistance and stability or heeling moment only, it was felt desirable to concentrate at first on measuring these, adding to the equipment later when more advanced work was contemplated.

Other Requirements

The number of staff likely to be available for operating the tank and conducting experiments was likely to be limited, and it was therefore felt desirable to construct the facility for single-handed working if possible.

The minimum height, floor to ceiling, was set at approx. 10 ft. in order to allow construction of the tank, rails and carriage structure above floor level.

Adequate access to one side of the waterway was considered essential to permit model handling, alteration to the apparatus, and observation or photography of models while running.

It was assumed during this preliminary study that work in the tank would only concern displacement vessels; any other requirement e.g. fast planning sail or powered hulls, would lead to greater dimensions, particularly length. The tank would therefore have limitations as to the type of work for which it was suited.

CHAPTER 11: THE SITE AND TANK BUILDING

A plan of the site is shown in Fig. 38 together with a typical section. It will be seen that the actual floor area available for the waterway depended on the width between the existing reinforced concrete retaining wall for the earth bank behind the tunnel, and the concrete wind tunnel raft. Space above ground level was governed by the section shape of the wind tunnel casing which varies between circular and that shown.

Fig. 39 shows the construction adopted which is a combination of brickwork, asbestos sheeting and wood cladding, with aluminum roofing.

Although sunlight promotes unwanted growth in the water, and as a result is not usually encouraged in tank buildings, the cramped passageway and wind tunnel supports which encroach on the available space made adequate lighting essential if movement was not to be dangerous. Natural lighting is by transparent roof lights and windows in the North wall, while artificial lighting is provided from fluorescent tubes spaced along the length, with additional lighting above the control and working positions. Additional artificial lighting is provided for the drive gear and by wandering leads in conjunction with plug boards. A 240 volt power supply is available from points at each end of the waterway and adjacent to the control position.

Heating was considered essential to keep the building at a reasonable temperature, controllable, and constant within fine limits; (a) to maintain the water at a sensibly constant temperature while force measurements are being made, (b) to ensure that the rails and supporting structure and balance arrangements do not change their calibration with temperature, (c) to avoid damp and condensation in the electronic equipment, and on the rails (to prevent rusting). By a suitable disposition of heaters, the nominal temperature in the building may be maintained at within 1° of 60° F.

fig 38 site plan

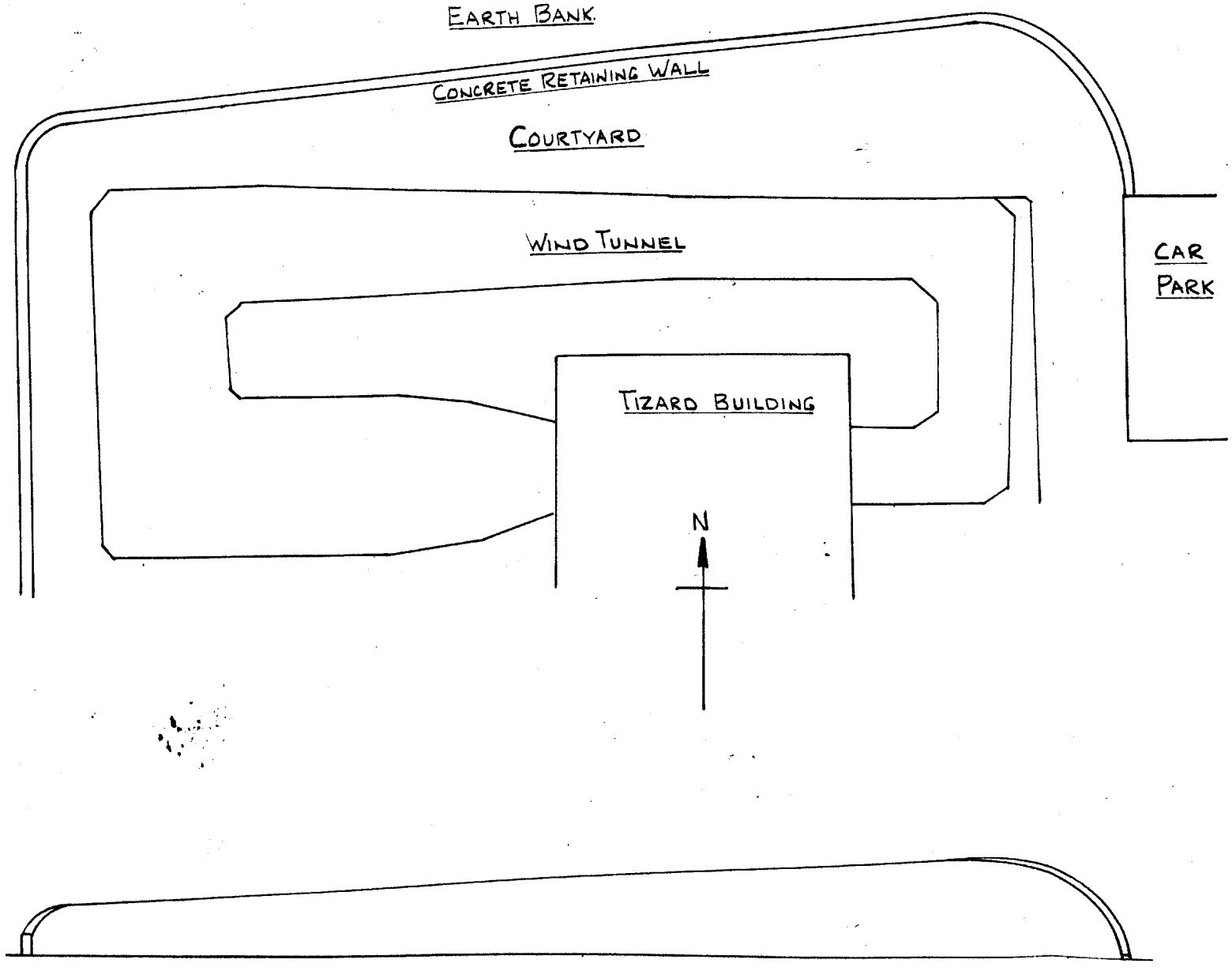

ELEVATION OF RETAINING WALL. LOOKING NORTH.

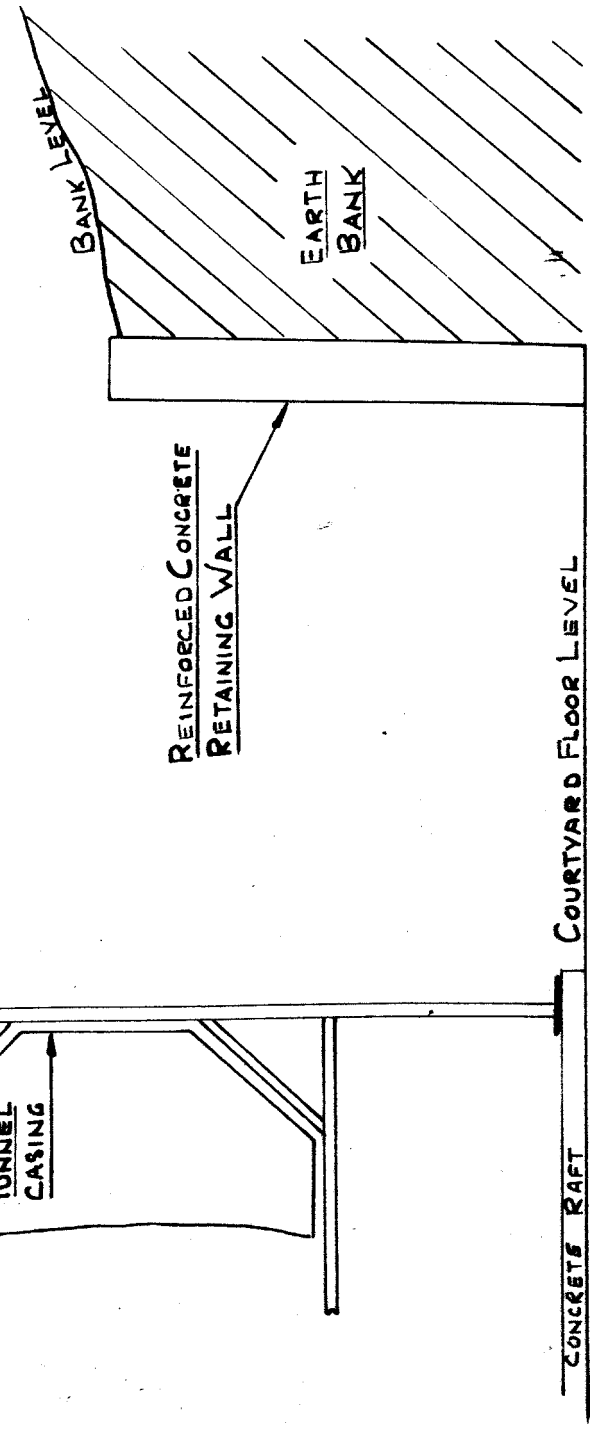

fig 39 towing tank building.

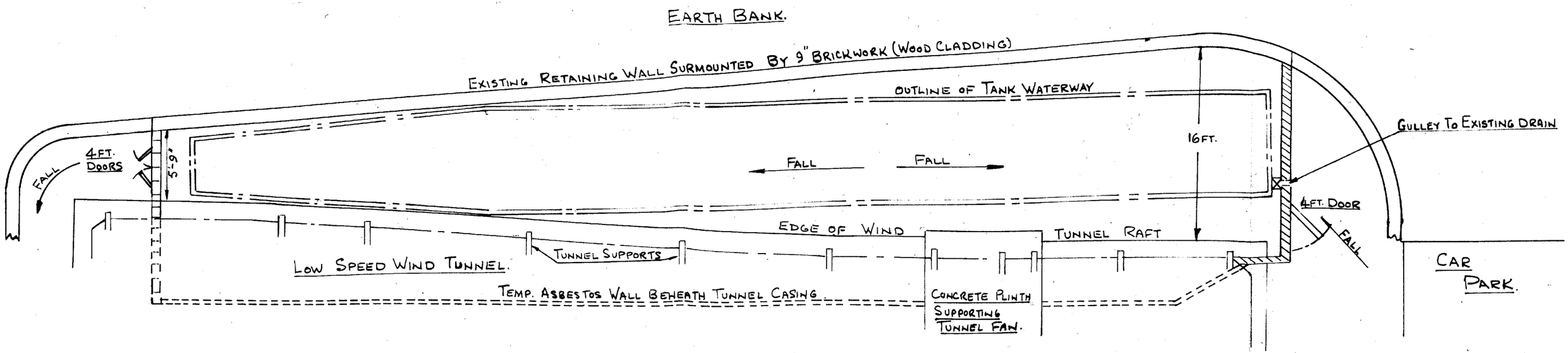

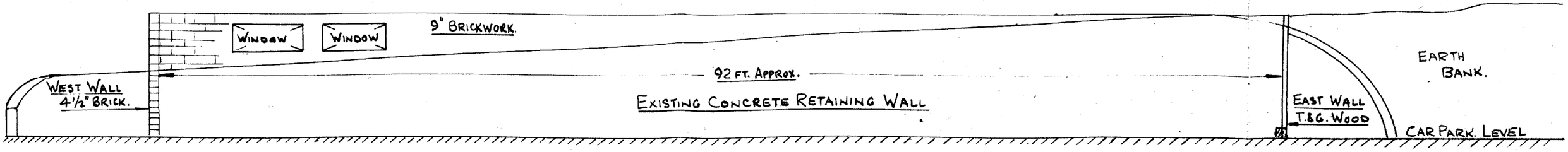

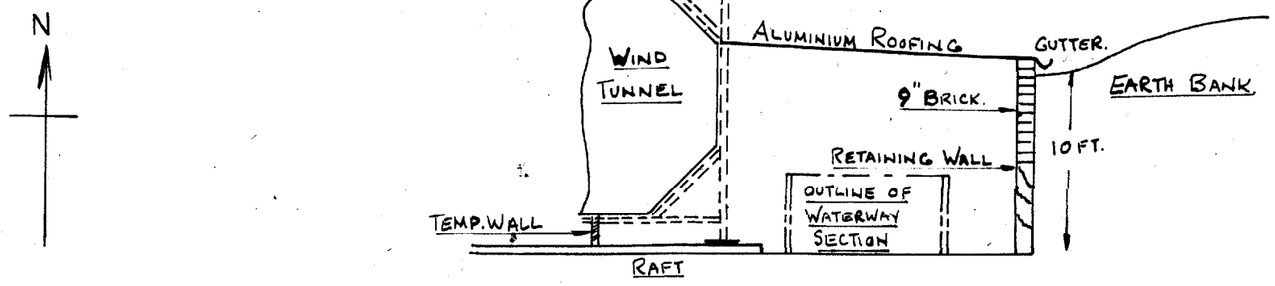

CHAPTER 12: GENERAL ARRANGEMENT OF THE TANK FACILITY

Design of the layout and construction for the tank structure and systems (see Fig. 40) was controlled largely by:

(a) Shape and cramped confines imposed by the courtyard and wind tunnel supporting structure.

(b) Need for the Eastern half of the structure to be easily dismantleable in case of wind tunnel fan damage.

(c) Cost.

The effect of these considerations on the design and construction of individual structures and systems will be discussed in later chapters; it will, however, be useful at this stage, to describe briefly and in general terms, the general arrangement of the facility as shown in Fig. 40.

By suitable positioning, it was possible to fit a waterway having a water cross section 8 ft. by 4 ft. with a parallel length of 64 ft. into the floor area; a further 24 ft. tapered length is available at the Western end.

At early stages during the design and construction it was intended that the tapered section of the waterway should be used for model handling and acceleration, but due to difficulties discussed in Chapter 15 the direction of run was later changed to East-West, with the tapered portion used for deceleration and stopping.

Beaches are provided along the Northern side and at each end of the waterway.

The method of construction adopted for the waterway, described in Chapter 13, precluded use of rails mounted on the sides, and these are, therefore, carried on longitudinals beneath gantries spaced at intervals along the waterway. The carriage, a simple structure using four main wheels, carries the balance and instrumentation and is driven from the drive gear through a winch drum and tow rope.

Model handling and control is from the stage and control positions near the Eastern end of the waterway.

The Control Position from which the model and carriage is managed and measurements recorded during runs is mounted on a platform above floor level to provide adequate view of the whole waterway.

Models may be handled and adjustments made to carriage, balance and model between runs, from the stage built over the waterway at the East end, and reached by ladder from the floor.

Drive gear is situated beneath the control platform, access to it being gained through a removable panel in the platform floor, so obviating any danger to personnel from the winch drum and chains; the

tow rope is taken from the winch drum of the drive gear, see Chapter 14.

A work bench and equipment storage cupboard is arranged to the west of the concrete plinth supporting the wind tunnel fan, and further storage is available inside and to the South of the main entrance, and adjacent to the South wall beyond the cupboard.

Adequate space alongside the waterway is available from the main entrance to beyond the cupboard but further access is restricted by the wind tunnel supporting structure (see Fig. 59, app. 4). A dry walkway is available in the event of water leakage, from duck boards on the concrete floor.

fig 40 general arrangement of tank facility.

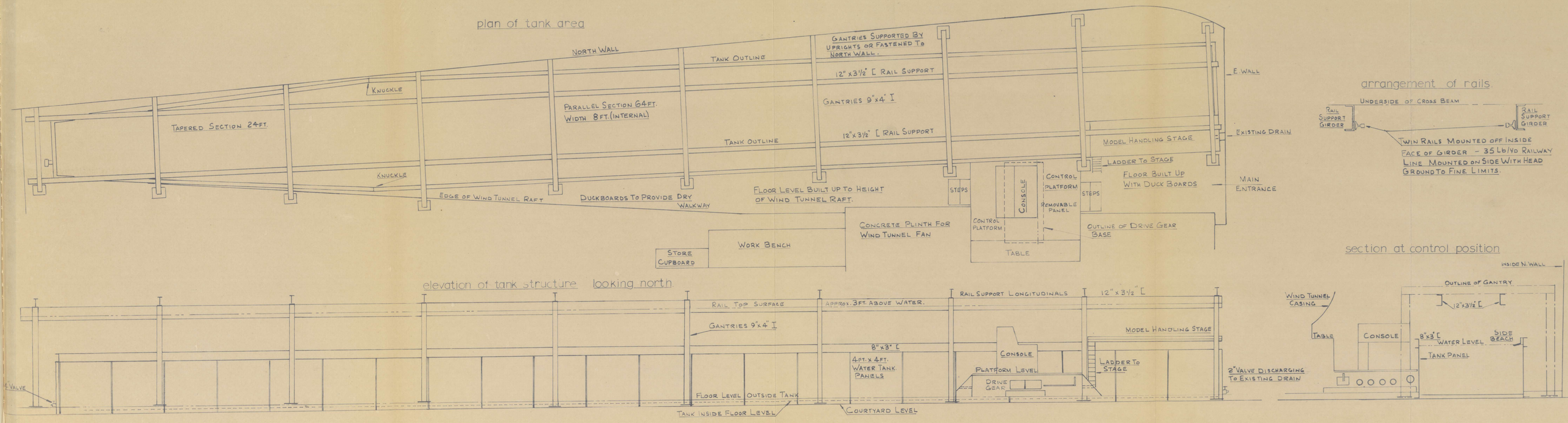

CHAPTER 13: THE WATERWAY & ASSOCIATED STRUCTURE

The Waterway

The necessity for providing a waterway which could easily be dismantled in the event of damage to the wind tunnel fan precluded use of the usual concrete or brick structure. An obvious alternative was to fabricate the structure from static water tank panels bolted together with sealant in the joints. These panels are manufactured in sections 4 ft. by 4 ft., so that the length and breadth of the tank was restricted to multiples of 4 ft.

It was not possible to obtain a reasonable length of waterway 12 ft. wide, but by reducing this dimension to 8 ft. i.e. two panels, a parallel run of 64 ft. was available, together with a further tapered length of 24 ft.

With a tank depth of some 4 ft., the actual water depth available would be about 3 ft.-6in., which although sufficient to prevent the presence of the bottom influencing measurements to any great extent, would provide a cross section of some 28 sq.ft., which was likely to be insufficient to prevent blockage effects becoming important especially at the higher model speeds, (see Chapter 10). If the water depth was increased to 4 ft., then the section becomes 32 sq. ft. giving the ratio of $\frac{\text{model section area}}{\text{tank section area}}$ as 231, slightly less than that suggested as desirable from Ref. 17

Having accepted that the water depth would be 4 ft. and the breadth 8 ft., it was possible to assess the effect of blockage on measured forces during experimental runs, on the basis that if the hull moving in the tank is compared with the model moving at the same speed in unrestricted water, then at any transverse plane in the length, there will be increased relative velocities because the water section area (A) will be reduced by the cross section of the model at that point. For small blockage the mean increase in velocity, dv, is given by: (from Ref. 6)

$$\frac{dv}{v} = \frac{a}{A - a - b.v^2}$$

where a is the model cross sect. area.
b is the tank breadth
v is the nominal model velocity.

and Emerson (Ref. 21) has shown that this may be applied to give the effective velocity increase over the complete hull if the area 'a' is now taken as the average of the maximum and prismatic areas for the model.

In the case of the 'Dragon' model used to illustrate Chapter 10, this area amounted to some 16.5 sq. in. (0.115 sq. ft.), so that with the hull running at a course velocity of 4.6 ft/sec. equivalent to a $V/\sqrt{L}$ of about 1.25,

$$dv = \frac{0.115}{32 - 0.115 - \frac{8 \times 21.2}{32.2}} = 0.0043$$

Reference 1 indicates that at this value of $V/\sqrt{L}$, the resistance coefficient C_{Xw} varies approximately as Vel.^{3}, so that measured values for C_{Xw} at this speed will be some 1% too great.

From Ref. 9, side force varies approximately as Vel.^{2} so that the error here will be below 1%.

Errors due to blockage will be considerably less at the lower model velocities used for much of the likely experimental work, so that the water section appeared sufficient to allow reasonable results being obtained, which could be corrected later if necessary; further, due to the assumptions involved if results are to be applied to full size vessels, (see Chapter 20), the error appeared reasonable.

The figures given here apply to a yacht model having a relatively large beam/length ratio; in the case of finer yacht hulls and ship models having lower beam/length ratios, the effect of blockage will be reduced considerably.

Details of the run length and times available for measurement at the various model velocities are included in the description of the driving gear and towing arrangments (Chapter 14).

Modern techniques in the construction of static water tanks involve the use of plastic panels, and the original intention was to take advantage of the negligible maintenance costs and simpler

erection procedure of such material. When the available funds were reduced however, this became impossible and an alternative was found in the use of secondhand steel panels.

The general arrangement of these and other waterway structure may be seen from Fig. 40, while the construction techniques involved in erection, fairing and making watertight are outlined in Appendix 4 to this part.

Arrangements were made to empty the waterway by means of two valves; at the East end a two inch screw down valve discharges into an existing drain which also takes the drainage from the immediate ground area outside the building; four inch valve at the West end is for use when rapid removal of the water is necessary; and discharges to the courtyard outside the West doors from where a natural fall takes water to a drain. In use, some flooding of the concrete area surrounding the wind tunnel occurs, and use of this valve should be restricted to emergencies.

The Rails and Supporting Structure

The importance of maintaining the carriage and balance in a steady state during its travel down the tank is emphasised in all references dealing with the construction of towing tank facilities (e.g. Refs. 4, 17, 20).

Any departure of the rails from the horizontal, or from directional linearity, may promote variations in carriage speed,

changes in the balance geometry, zero errors, and also introduce dynamic components into the force measurements. It was therefore important that the rail supporting structure should be stiff and that the rails be set accurately in both the vertical and horizontal planes.

A normally accepted variation in vertical and horizontal rail setting appeared from the references to be some ± 0.002 in., although in some cases care had been taken to achieve greater setting accuracy.

Usually, with a twin rail carriage mounting system, the rails are carried on top of the reinforced concrete waterway sides, the carriage running in a similar fashion to a railway truck, while monorails are supported from overhead with the carriage suspended beneath from wheels running on the top surface of the rail.

In the present case the construction and flexibility of the waterway made the usual arrangement impracticable, and overhead support of the rails was necessary; this had the advantage that a clearer view of the model and balance was possible than would otherwise have been the case.

The construction of the carriage and its support by the rails, discussed in detail in Chapter 14, involved the use of 35 lb/yard railway line mounted on its side; this was achieved by supporting the line from deep longitudinal girders running beneath transverse beams

spaced at intervals along the waterway as shown in Fig. 40. In order to allow the main carriage rails to be of reasonable diameter, and pass beneath the cross beams, it was necessary to make the girders twelve inches deep. Spacing of the cross beams was controlled by the necessity of keeping the movement of the carriage in vertical and horizontal directions to a minimum during its travel, and hence by the flexibility of the structure; the spacing of the beams had also to be sufficient for adequate visibility of and access to, the carriage and model.

Although desirable to separate the support of rails from any contact with the building structure, in case of movement in the latter, it was impracticable to support all the beams at their North end by uprights, because of the lack of space between the wall and waterway structure, so that the necessity of fixing them to the wall was accepted. At their South end, beams were supported easily by uprights adjacent to the waterway sides.

The width apart of the rail mounting girders was controlled by the width of the carriage which had been set at 4 ft. (see next chapter) so that the layout of the rail structure was now established.

A simplified calculation gave the minimum modulus required for the beams and uprights in order to allow a maximum of 0.0005 in. deflection in the longitudinal girders at any point of travel for the

carriage. For this calculation, it was assumed that the uprights and beams were freely pin-jointed at their ends, but held rigidly (welded) at their joints; joints between girders and beams were assumed pinned.

In fact, cost and delivery problems precluded the use of new steel of the sizes resulting from the calculations, so that the final scantlings of uprights, beams and girders were governed by the size of second hand material available, and the actual modulus of the structure was far in excess of the calculated valves.

The construction of the gantries from 9 in. by 4 in. I section steel, together with the erection and fairing of the 12 in. by 8 in. channel girders is described in Appendix 5 to this part.

Rails are of 35 lb/yard railway line mounted on its side with the head machined on all three faces to give smooth surfaces as may be seen in Fig. 40. The machining, mounting and alignment of the rails is described in detail in Appendix 5 to this part.

CHAPTER 14: THE CARRIAGE AND TOWING ARRANGEMENTS

Reasons leading to the choice of an un-manned carriage supported by twin rails and driven by a winch and towline have been outlined in Chapter 10.

The Carriage

The short length available for acceleration and stopping meant that the carriage should be light, yet strong enough to provide a steady platform for the carriage of any desired equipment; in particular it was imperative that the carriage provide a stable platform for a balance during its run down the waterway.

On the advice of Dr. Todd, at that time Superintendent of Ship Division at the N.P.L., the lengthwise wheelbase was determined by the distance between rail joints; Ref. 17, based on work for the design of the Ship Hydrodynamics Laboratory at Feltham, showed that wheels should be spaced approximately 4/3 the length of each rail section, in order that any disturbance at the joint should have the least effect on the centre of the length, at which balances were likely to be placed.

The breadth over running wheels had to be sufficient that the possible roll angle due to clearance between roll-steadying wheels and rail did not affect the balance geometry, or give zero errors; at the same time, the carriage structure should not foul any part

of the model handling or other arrangements.

These requirements led to the construction of a permanent skeleton carriage with main running and stabilising wheels on which some 250 lb. of equipment could be carried. Dimensions between the four main running wheels are approximately 6 ft. by 4 ft. and the main structure is composed of four lengths of 3 in. by 1½ in. Duralumin channel section bracketed at the corners as shown in Fig. 41. In addition, two intermediate transverse sections of the same size can be moved to the most convenient positions for the carriage of equipment. As set up for supporting the two component yacht balance and associated arrangements, the beams and longitudinals are positioned as shown in Fig. 41. A wheel assembly, consisting of running wheels and steadying wheels to prevent skew, pitch and roll is mounted on each corner, the total depth of the carriage being contained within the height of the rail supporting girders, and the pull from the tow rope is taken by a towing post carried on one of the transverse beams stiffened by a part beam between the inner longitudinals.

Satisfactory diameter and concentricity of the main running wheels, and a restriction of pitch, skew and roll is essential in order to prevent changes in the balance and model attitude while running, and the following figures were set as being reasonable: skew 0.005 deg., pitch 0.005 deg., roll 0.005 deg.; in fact it was found possible to better these in practice.

Appendix 6 to this part describes the arrangement of the running and steadying wheels, and details the method adopted for setting up and aligning the carriage on the rails.

Towing Arrangements

Design of the Drive Gear was based on that which had proved reliable, despite its simplicity and low cost, for low speed work in the No.2 Tank of the Saunders Roe Division. The system is based on the use of a standard ½ H.P. synchronous motor together with standard 4 speed motor-cycle and three cycle, 3 speed gearboxes to provide a series of fixed gear ratios between the motor and winch drums from which an endless towing cable drives the carriage.

As the synchronous motor runs at a constant 3000 R.P.M., it was necessary to provide a clutch in the system for smooth and controlled acceleration of the model; a motor-cycle gearbox was particularly useful therefore as part of the gearing arrangements since it incorporates a clutch assembly.

By suitable arrangement of the available gearboxes, together with the chain drives and sprocket sizes, it was possible to obtain a total of fourty constant gear ratios to the winch drum, covering the desired speed range of approximately 0.8 to 5.0 ft/sec.

The endless cable is arranged so that the carriage can be clamped at the desired position in its length and the model moved in

either direction by the cable unwinding from one drum while winding onto the other, the model direction depending on the direction of rotation for the motor.

To tension the wire and provide damping against the carriage's tendency to surge, especially when accelerating through the clutch or when stopping, the wire is looped through a pulley carrying a 15 lb. dead weight each side of the drive gear.

The towing cable is 22g. piano wire, which while having sufficient strength to accommodate normal acceleration, running and stopping loads, acts as a safety precaution in that if the carriage should become fouled during a run the cable breaks and so averts serious damage.

A detailed description of the arrangement of the drive gear and cable will be found in Appendix 6 to this part.

The drive gear assembly itself is mounted beneath the control platform which is some 18 ins. above floor level near the East end of the waterway as shown in Fig. 40, and access to the gear is through a removable panel in the platform floor.

All controls except the gear lever for the 4-speed gearbox are taken to a console mounted on the control platform, and their layout can be seen from Fig. 42.

The gearchange lever for the 4-speed motor-cycle gearbox is located beneath the steps to the control platform.

Smooth clutch application is obtained by replacement of the usual clutch lever found on motor cycles by a screw thread device which provides a gradual pull or release to the clutch cable when turned by means of a handle; in Fig. 42, the operator has his hand on the clutch operating mechanism; clockwise motion disengages and anti-clockwise motion engages the clutch.

FORWARD, REVERSE and STOP buttons to control the synchronous motor are mounted along the front edge of the left hand side of the console table, the STOP button lying proud of the surface for rapid identification in the event of emergency.

Changing gear on the cycle gearboxes is effected by the usual 'cycle' method of lever and cable, the levers being mounted on brackets situated at the front of the console table below the motor controls. It is important that the end fastenings of the cables are firmly located, and some difficulty was experienced in achieving this with the complicated cable runs through the platform floor; special stiffening to part of the floor and console structure was found necessary.

Carriage Speed: Stability and Measurement

Fluctuations of, and inaccuracies in measuring the models speed during its run down the tank could lead to considerable error in the measurement of forces.

If the measured speed is in error by a small amount dv from the

nominal speed v, then the force associated with the nominal speed (F) will be in error by dF; if the force varies as (Velocity)^n then

$$\frac{F + dF}{F} = \frac{(v + dv)^n}{v^n} \quad \text{i.e.} \quad dF = n.dv \quad \text{(approximately)}$$

As the resistance may vary as (Velocity)^5 or even higher, accurate measurement and stability of speed during a run is extremely important. Ref. 17 and 20 indicate that the order of repeatability and accuracy of speed lies between 0.1% and 0.25% for the various tanks concerned, Ref. 25 gave a uniformity of speed ± ¼% during the work at N.P.L. in the No. 2 Tank.

Although the speed of the synchronous motor is likely to vary only with the mains supply frequency, the remainder of the system is such that backlash and built in slackness could lead to considerable surging. In particular, a poor manipulation of the clutch is likely to promote large fluctuations which could persist during part of the model run. A considerable effort was made therefore, to detect and eliminate large speed fluctuations during the run and also to ensure that the repeatability was brought to an acceptable level.

The drive gear with its chain drives was found to require careful setting to avoid fluctuations in the drum revolutions. The revolutions were checked for stability by means of a stroboscope when in position, the necessary tightening of chains being achieved by adjusting the mounting plates of the various components (Appendix 6).

To achieve uniformity of drum revolutions, it was found necessary to have the chains tight, any slackness resulting immediately in variable drum R.P.M.

The method of operating the clutch was found to have a direct significance on the fluctuation of carriage speed; as the magnitude of the vertical movement of the damping weights on the wire gives a good guide to whether the clutch is being engaged smoothly, after considerable practice, it was found possible to operate the clutch so that only a comparatively small movement of the weights occurred.

In order to study the uniformity of speed during the run, one of the carriages main running wheels was arranged as shown in Fig. 43. Circular brass contact plates were let into the surface near the circumference at 15° intervals, and an annular ring let in nearer the hub. Each circular plate was joined electrically to the ring by wire recessed into the wheel surface; two spring loaded contacts were arranged, one to make contact with the various circular plates as the wheel was turned, the other bearing on the annular ring, and these contacts were joined through an 'Oscillomink' recorder and a 9 volt dry battery. When the wheel was turned, and the recorder operating, pulses were recorded as the spring loaded contact passed over each plate in turn. By choosing the relevant paper speed on the recorder, the time taken for one revolution or part of a revolution could be ascertained. The top record in Fig. 44 shows a typical length of trace as the wheel was turned through three revolutions.

The carriage was now taken down the tank over a range of gear ratios between the minimum and maximum, so that the uniformity of run speed could be assessed. By taking the time for each revolution (every 24 pulses on the trace) of the wheel, the graph of speed variation during the run, the distance required to achieve steady conditions, and the stopping distance could be obtained.

Before the check on drum revolutions, described previously, was carried out, fluctuations of over ½% from a nominal speed were found, but afterwards, these were brought within ¼% of the nominal over the complete speed range, a typical length of trace at uniform carriage velocity being shown in Fig. 44. This could be read to within ¼%, which was the quoted accuracy in paper speed on the recorder. The uniformity was found to exist if any of the pulses was taken as starting point to measure the time for each revolution.

By obtaining the time for each revolution of the wheel during its passage down the rails, it was possible to build up a graph showing the variation in speed from start to stop. A typical variation is shown in Fig. 45 as the time per rev. against the number of revolutions completed, and the approximate corresponding run length. In this particular case, the clutch operation was moderately smooth only and the resulting speed fluctuations can be seen at the beginning of the run. These were soon damped however, to give a smooth run before the motor was cut at rev. 37.

The inset graph shows a magnified view of the uniform speed part of the run from rev. 8 to rev. 38; it may be seen that the speed variation is within ¼% from a nominal value except at two points; similar jumps occurred at the majority of speeds, and were found to be due to slight misalignment of two rail lengths; the rails were realigned and checked (see Appendix 5) and in runs which followed, the variation was well within the ± ¼% limit over the whole length. In the case shown, the length of uniform run is 43.5 ft. (see Fig. 45) and this was found to be maintained even at very high carriage speeds.

Typical values of length required from start to steady run conditions are given in table 4 for various speeds within the range.

Stopping distances required by the carriage after the motor was cut were also determined from the recorded traces by measuring the number of wheel revolutions from power removal to rest. (see Fig. 44) and typical results are given in table 4.

The high cost of recording equipment precluded its purchase for use with the facility at that time, so that measurement of carriage speed during "production Runs" was not possible by the procedure described above.

A system basically similar to that used in a number of establishments was developed, by which the time taken by the carriage to complete a known length of steady run is measured accurately. The run was set at 42.5 ft. from the results of the experiments described previously, and the time measured by means of a crystal

oscillator driving a Dekatron counter which read to six figures. This may be seen in Fig. 42 level with the operators left hand. This clock is started by a horizontal plate mounted on the c rriage which breaks a photo-electric relay, and stopped in a similar manner after the 42.5 ft. run. The second relay also cuts the power to the synchronous motor, and stops the carriage; if it should fail to operate, a further relay some three feet further on, will stop both the clock and the motor, but in this case the time will refer to a greater distance. To achieve a time over the normal 42.5 ft. run, which was within $\frac{1}{4}\%$ of the nominal, it was necessary for the maximum error in the placing of relays to be within $1\frac{1}{2}$ in. As the relays were placed by means of a steel cored tape, it may be assumed that they are correct to within 1/8 in.

The counter is fed from a constant voltage transformer to obviate the effects of fluctuations in the mains voltage; however, if this voltage should fall appreciably, the counter will fail to operate correctly and adjustment must be made to the input setting to overcome this.

In order that the elapsed time for a run may remain on display for recording during the return run, and to ensure that the carriage does not operate the clock during this time, a button switch is so arranged that the clock is only actuated by the carriage after it has been operated. It was found during the early runs using the

system, that the photo-electric relays sometimes failed to operate, due to bulb failure or mis-alignment between bulb and element. The button switch is, therefore, connected into the motor circuit and the motor fails to operate for forward run if it is not depressed or if a relay is faulty, so acting as a direct safety aid which assists in fault tracing. This "READY BUTTON" is situated on the console, above the FORWARD motor start button and may be seen in Fig. 42.

The above procedure does not affect the return run so that the safety precaution is inoperative and although there is a photo-electric relay to stop the carriage on its return run, care is necessary in case of malfunctioning.

Comparison of the nominal mean speeds obtained using the timed run of 42.5 ft., with the actual means from the recorded traces, showed agreement within about 0.1% over the whole range tested.

The synchronous motor is liable to speed variation due to changes in the mains frequency and test runs were made under various conditions of mains loading to ascertain the effect on frequency and hence carriage speed. Over a number of days the mains frequency and carriage speed for the timed run were measured and a fluctuation of 0.15% in the latter; these measurements indicated that under normal conditions the likely error from nominal is likely to be within the limit.

At this stage a number of runs were made to assess the effect of the smoothness of clutch operation on the average speed as timed over 42.5 ft., and so check that a sufficient distance had been allowed for the speed to settle down before the clock was started. These tests showed that a variation of some 0.1% could result in the run time if the clutch was abused badly.

The results of the experiments described above indicated that the measured carriage speed could be considered as within the limit of $\pm \frac{1}{4}\%$ from a nominal value, and that variations in speed along the run were within the same limit. All these tests were made without a model in position, and several runs using the 'Oscillomink' recorder with a model, showed that the measured fluctuations were lower, presumably due to the damping effect of the models resistance on the carriage movement; there was no indication that the resistance of the model affected the carriage speed. It should be noted here that the fluctuations recorded were often below the limit of accuracy quoted for the recorders paper speed.

During "production" runs it is therefore only necessary to ensure that the time recorded by the Dekatron counter is within the limit of accuracy for the nominal speed at the selected gear ratio. Approximate speeds for the range of gear ratios are given in Table 5.

Stopping the Carriage

The available stopping distances with a run length of 42.5 ft. are adequate to allow the carriage to come to a halt naturally, when the motor is cut, from all speeds; if the first stopping relay fails to operate, then the second will normally cut the power, but at top speed, great care was found to be necessary, and if the first relay should fail to operate, use of the manual stop button is advisable.

In the event of the tow rope breaking behind the carriage during a run, cutting the motor would have little effect, and an accident could occur. During six months frequent running, several wire breakages occurred for different reasons, but all in front of the carriage; no emergency stopping system was developed at that time.

Available Time of Constant Speed Run

The length of 42.5 ft. allows a recording time during the run in excess of that considered desirable from Chapter 10, over most of the speed range, typical figures being given in Table 6.

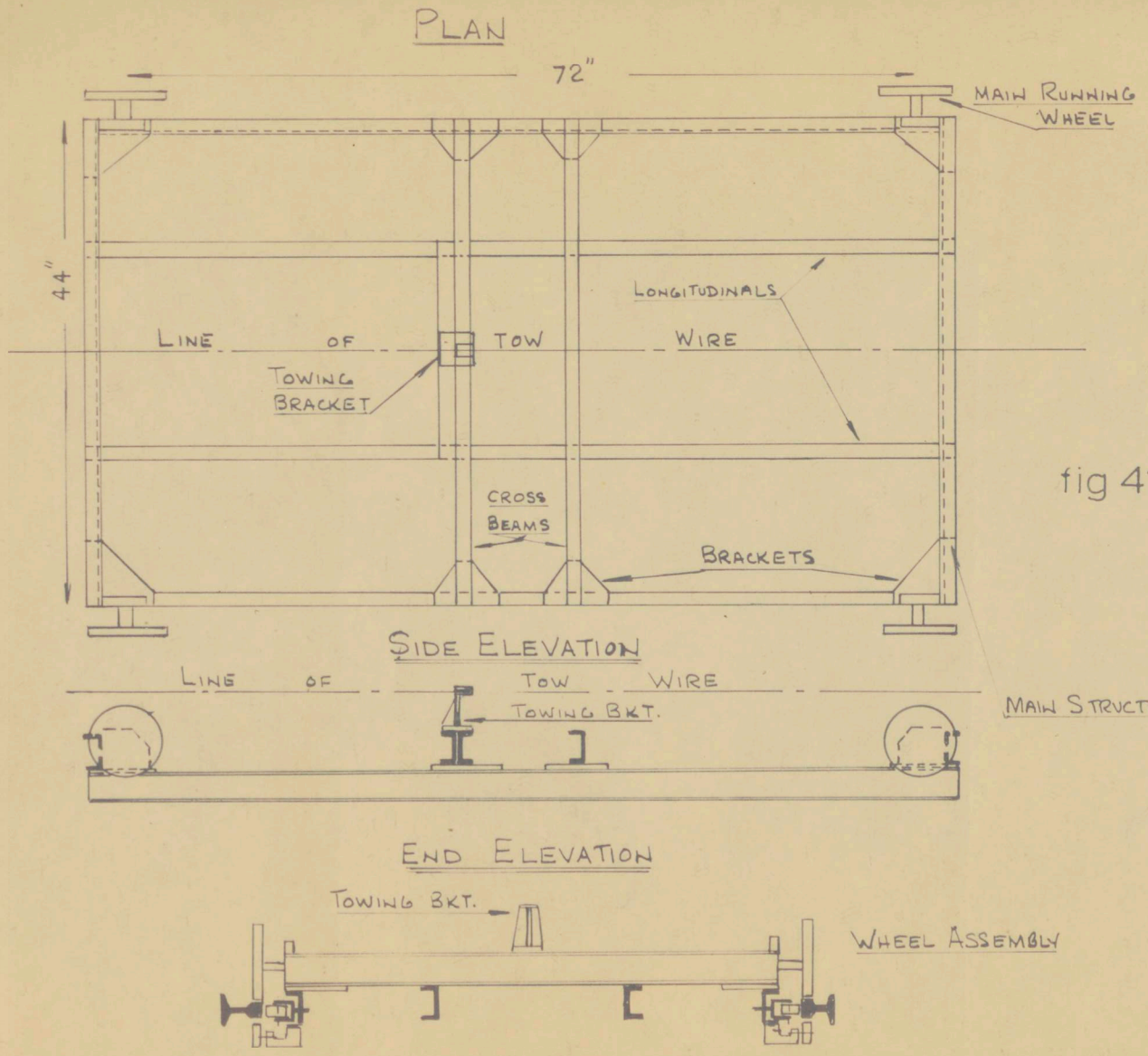

fig 41 arrangement of carriage structure.

INTERMEDIATE LONGITUDINAL AND TRANSVER
CHANNELS MAY BE PLACED TO SUIT
EQUIPMENT CARRIED.

MAIN STRUCTURE 3"x1½" [. DURAL. BRACKETED.

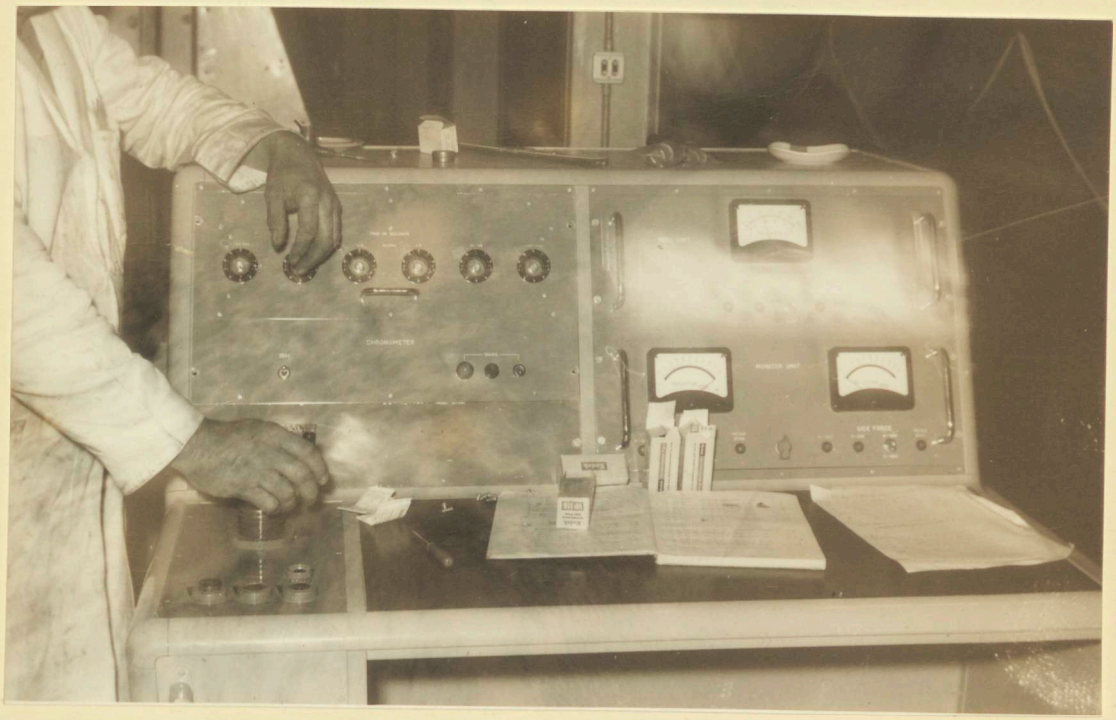

Fig.42. Towing Tank control console.

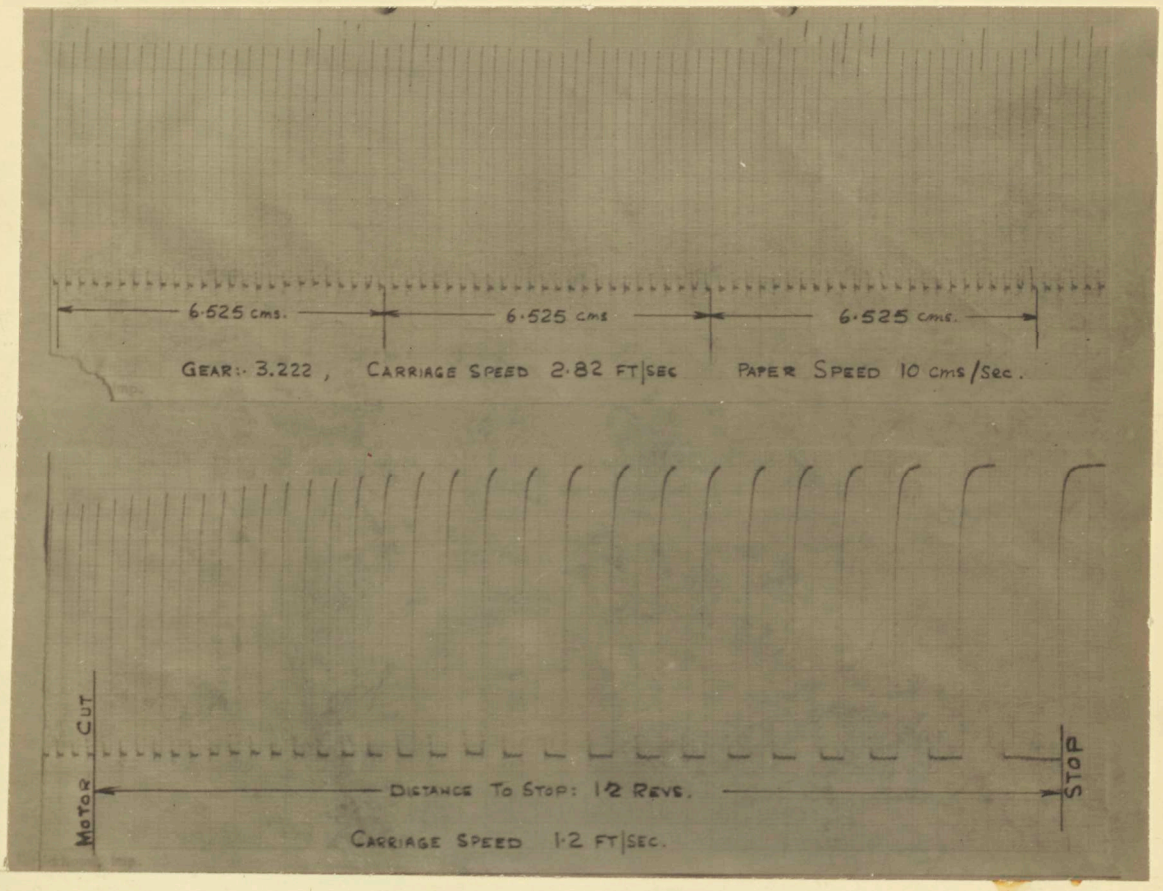

Fig.44. Portion of record from Oscillomink recorder, taken during tests to determine fluctuations in carriage speed.

TABLE 4. DISTANCE REQUIRED BY CARRIAGE TO ACHIEVE STEADY RUN AND TO STOP.

GEAR RATIO	CARRIAGE SPEED FT/SEC	DISTANCE REQD. TO ACHIEVE UNIFORM SPEED FT.	DISTANCE REQD. TO STOP FT.
1.222	1.38	12	2.4
1.333	1.90	12	2.5
2.333	2.975	16	3.2
3.332	3.48	19	3.8
4.332	4.08	22	4.25

TABLE 5. APPROXIMATE CARRIAGE SPEED FOR GEAR SETTING.

FIRST NUMBER GIVES GEAR SELECTED ON M/C BOX. THREE NUMBERS FOLLOWING POINT GIVE GEARS ON CYCLE BOXES.
e.g. 1.111 MEANS M/C BOX IN LOWEST GEAR, ALL CYCLE BOXES IN LOWEST GEAR.

GEAR SETTING	CARRIAGE SPEED FT/SEC	GEAR SETTING	CARRIAGE SPEED FT/SEC	GEAR SETTING	CARRIAGE SPEED FT/SEC.
1.111	0·803	2.132	2.010	3.332	3.480
1.112	0·961	2.222	2.161	3.333	3.860
1.113	1·102	2.133	2.230	4.111	2.130
1.122	1·181	2.322	2.404	4·112	2·780
1.132	1.283	2.332	2·675	4.113	2·845
1.222	1.382	2.333	2.975	4.122	3·065
1.133	1.429	3.111	1·631	4·132	3·415
1.322	1.540	3.112	1·956	4.222	3·680
1.323	1.710	3.113	2·175	4·133	3·800
1.333	1.901	3.122	2.350	4.322	4.090
2.111	1.250	3.132	2.605	4.332	4·550
2.112	1.500	3.222	2.820	4.333	5,070
2.113	1.668	3.133	2·900		
2.122	1.800	3·322	3·140		

TABLE 6. RECORDING TIME AVAILABLE DURING RUN. - TYPICAL SPEEDS IN RANGE.

GEAR SELECTED	SPEED FT/SEC.	TIME FOR 42.5' RUN SECS.
1.111	0.803	53
1.322	1.54	27.6
2.132	2.010	21.2
2.332	2.675	15.9
3.322	3.14	13.5
3.333	3.86	11.0
4.332	4.55	9.4
4.333	5.07	8.5

balance specification was drawn up using the established quantities.

Very little published information was available to give the range of forces and moments which might be expected on models of various types. Ref. 1 gave some guide, although the magnitude of leeway and hence maximum forces achieved were less than was desirable if the design was to provide characteristics both within and outside the sailing range (i.e. up to some 12° leeway).

The figures of Ref. 1 had been re-analysed by Crago (Ref. 12) in a form from which the maximum forces to be expected could be read off immediately.

Side-Force

For the 'Dragon' model at 10° leeway (the maximum used), the Lift coefficient, C_L was seen to be 0.15, so that at the maximum tank model speed of 5 ft/sec. with a 4 ft. waterline model, the sideforce was likely to be some 8.2 lb., while on a 3 ft. model it would be approximately 6 lb. As the range of leeway was likely to be higher (0° to 12°), for the design, it was concluded that the arrangement should be made to measure side force up to 10 lb. maximum, (for a 4 ft. model at maximum speed and 10° leeway), with a more normal range of 0 to 6 lb. to cover smaller models with a lower top speed.

Ref. 1 showed that previous measurements have been quoted as within 0.005 lb., and this was set as the desirable accuracy for side force.

Resistance

Again from Ref. 12, it appeared that the maximum Drag Coefficient for the 'Dragon' model had been approximately 0.07, about half the maximum Lift coefficient; it was, therefore, desirable to allow for measurement up to 5 lb. maximum (for 4 ft. model at top speed and 10° leeway) with normal use up to approximately 3 lb. Again, the accuracy in previous experiments was quoted as 0.005 lb. (Ref. 1).

Stability Moment

Due to the requirements of Part 1, it was desirable to measure the hull's available stability moment to oppose the over-turning moment from the sails while under way. This moment is equivalent to the actual hull stability while at speed, less the over-turning moment from the hull side force. It was necessary to set an axis about which to work, and following the line of Part 1, this longitudinal axis was to be arranged as desired in any particular case.

No information was available to give the stability of a hull under way, and an attempt was made to approximate the moment by consideration of likely over-turning moment on a scale model of the sails.

Reference 24 was the only information available giving any reliable information about sail forces, and this indicated that the maximum side force coefficient likely from the sails was in the region of 1.5. This was applied to a 4 ft. Dragon model, assuming an axis passing through the intersection of mast and deck, and with relative wind scale velocity of 15 ft/sec; the centre of effort height was taken as one third the mast height (2 ft.), so that with a sail area of 9.9 sq.ft., the moment was some 8 lb. ft. On a 3 ft. model this would be reduced to some 5 lb. ft.

Heel Angle

From experience, it was known that usual heel angles for yachts lie between 0° to 30°, figures which were confirmed by Ref. 13. In case of requirements for greater transverse model inclinations, the range was set as 0° to 45°. From the little information available, (Ref.1 and 9) it appeared that the hull forces are relatively insensitive to changes in heel, so that an accuracy of ± 0.5 ° was likely to be sufficient.

Ref. 9 showed that sideforce, and at large leeways, resistance is extremely sensitive to leeway, so that it was considered important to set and measure leeway to the maximum possible accuracy. Ref. 1 indicated that with the Dragon model, it had been possible to measure to within ± 0.1°, so that this was set as a minimum requirement.

Displacement and Model Weight

The weight of the 3.5 ft. Dragon model was, from Ref. 1, a maximum of 22 lb. which would be increased in the case of a 4 ft. model to around 35 lb. Allowing for models of heavier displacement gave an upper limit for model weight of 50 lb.

Choice of Configuration

The requirements outlined above were similar, largely, to those from which previous dynamometers at the Davidson Laboratory, National Physical Laboratory, and Saunders Roe Division had been developed, except that in all previous work, it had been considered necessary to measure the yawing moment, and to simulate the vertical component of sail force. Each dynamometer used previously in work with yachts had been designed in connection with the direct calculation of comparative close-hauled performance using the Gimcrack or similar coefficients, and involved applying a known side force and vertical force to the model at a simulated centre of effort position, and hence determining the resulting angles of heel and leeway.

Two different dynamometer configurations appeared, both fulfilling these requirements.

Dynamometer Configuration used in early work at N.P.L.

The model is towed from the top of a dummy mast at the assumed height for the designers centre of effort position, the mast being

attached by a universal joint to a vertical post which is free in vertical float and may be adjusted in yaw. Measurements of the resistance, side force and yawing moment are taken from the post. In use, a component of force (from the Gimcrack assumptions), perpendicular to the mast is chosen, and the corresponding vertical component applied by loading the post; the model is now run up to speed and leeway adjusted until the correct side force corresponding to the chosen vertical component is measured; the hull is now in a stable, simulated sailing position, so that the resistance, leeway, heel angle, and yawing moment may be recorded.

A full description of the construction and operation of this dynamometer will be found in Ref. 25.

Dynamometer in use at the Davidson Laboratory

The lateral dynamometers near each end of the hull are used to provide a known side force equivalent ot a chosen sail force at right angles to the mast, while the vertical component is applied by ballast at the correct fore and aft position. The relative loads on each lateral dynamometer are used to determine the yawing moment, and resistance is measured on a separate dynmaometer. As the side force is applied well below the assumed centre of effort for the sails, a weight is arranged to have lateral travel across the hull for setting the angle of heel required.

In use, the chosen side force and vertical force are applied, the angle of leeway adjusted until the sideforce produced by the hull balances that applied by the lateral dynamometers, and the transverse sliding weight positoned to give the required heel angle. Leeway, heel, resistance, and yawing moment may now be recorded. As the carriage at the Davidson Laboratory is un-manned, several runs are usually necessary before correct adjustment of heel and leeway is obtained.

Ref.9 gives a description and photograph of the system.

Dynamometers in Use at the Saunders Roe Division

It is interesting to note that the N.P.L. dynamometer is used on a manned carriage, so that operators are available to make the necessary adjustments and readings, while the Davidson Laboratory used an un-manned mono-rail system.

The two dynamometers in current use at Saunders Roe Division are on a manned carriage in No. 1 Tank and on an un-manned carriage in No. 2 Tank.

Early work at Saunders Roe was carried out in the No. 1 Tank, following on that at N.P.L., so that the dynamometer is a slightly modified version of that described previously. A full description of its construction and use will be found in Ref. 1

The dynamometer used in the No. 2 Tank was developed to undertake work for the Red Duster Syndicate, and follows, basically, the principles of that at the Davidson Laboratory. In detail, however, it is considerably improved, the balancing of side force from leeway with that applied, and the setting of heel, being achieved by self-setting servo motor systems using jockey weights.

A full description will be found in Ref. 4 & 8.

Other Previous Arrangements

Reference 25 notes a balance constructed by a "Mr. Marshall of North Hayling". This was a five component balance to which the model was rigidly attached.

Work by Kempf is mentioned in both Ref. 9 and 25; where the effect of wind force on the yacht was simulated by applying forces at a centre of effort position by falling weights and pulleys.

Work with the dynamometers described in detail has been commercial in character, so that use of the Gimcrack analysis was implicit since this was the only method available for applying model test results to the full scale yacht. Acceptance of this, in turn, meant that for such work to be a feasible proposition economically, the number of runs had to be kept to a minimum and the dynamometer systems ensure that the model was run near practical sailing or

self-propelled conditions in every run.

In the case of the University Tank, exactly the opposite aims were proposed, so that rather than pre-selecting a sailing condition and then determining the yachts attitude and resistance, it was desirable to pre-set the attitude and measure directly the resulting forces and moments.

Using the N.P.L. type of balance whether in its original or modified form, it would be impossible to obtain measurements of the type required although it could be set, after some modification, to measure under either system of axes.

Again, while the Davidson Laboratory/Saunders Roe No. 2 configuration might be used to give the necessary measurements over wide ranges of heel and leeway, by its very layout and use of separate resistance and lateral dynamometers, it would be possible to measure quantities only with the Sea axes.

In wind tunnel work, it is usual to keep the model rigidly attached to the balance, and measure the required quantities resulting from changes in attitude or shape, in a manner similar to that proposed by the "Mr. Marshall of North Hayling". In the case of a yacht, or any other model in a towing tank, this would result in a set depth of immersion for the hull rather than constant displacement; while running, the model if free to move will usually change both its

attitude longitudinally and depth of immersion, so that additional variables would be introduced requiring further measurements and making the interpretation of results difficult. An additional complication is likely to arise from the possibility of the model being swamped, the imposed forces causing it to break up and perhaps damage the dynamometer. In an answer to a question during the preliminary discussion to Ref. 8, Crago intimated that from his experience this was a likely possibility.

If the model were free in heave and pitch however, then a three component balance having the model tied in heel and leeway would allow systematic variation of parameters and measurement of all the desired quantities.

An outline specification based on this last arrangement was now drawn up for the dynamometry:

Summary of outline specifications

1. A three component balance is to be used, with the model constrained in heel and leeway, but free in pitch and heave. Quantities to be measured are ; Side force and Resistance (components at right angles) and Stability (righting) Moment about a convenient axis. Arrangements to be such that eigher Course/Sea or Body/Sea axes may be used.

2. Range and accuracy of various quantities to be:

Side Force: 0 to 6 lb. normal use, 0 to 10 lb. maximum, within 0.005 lb.

Resistance: 0 to 3 lb. normal use, 0 to 5 lb. maximum, within 0.005 lb.

Stability (Righting) Moment: 0 to 5 lb. ft. normal use, 0 to 8 lb. ft. maximum, to within 0.01 lb. ft.

Heel angle: 0 to 30° normal, 0 to 45° maximum, in either direction to within 0.5°.

Leeway: Range 0 to 15° in either direction, preferably to greater sensitivity than 0.1°.

3. Maximum model weight: 50 lb.

4. System must withstand the acceleration and deceleration imposed, and give stable readings some 3 sec. after steady run speed is reached.

5. Measurements may be recorded on board the carriage for analysis between runs, or be transmitted to recording apparatus at the control position.

The Balance Design

The outline specification was submitted to several firms specialising in the manufacture of similar equipment. The only firm tender was from Saunders Roe Ltd., who submitted a scheme using a two

component balance to measure Side Force and Resistance, while the stability moment was ascertained by giving a known movement to a transverse sliding weight, and measuring the resultant heel when the hull was towed at the desired leeway.

A diagrammatic outline of their proposal for the two component balance is contained in Fig. 46. It was proposed that force in the horizontal plane should be transferred to the dynamometer through a central tubular post which had freedom to rise and fall, but was restricted in all other movement by rollers and guides. The force on this post was to be separated into the two desired components by two systems of swinging gates and trays which had freedom of motion only in directions normal to one another. Movement of each force tray would have been restricted by a bell crank mechanism using dead weights to counteract the major proportion of the forces, the remaining load being allowed to displace the tray, the movement of which was recorded by electrical means. Damping was to be provided for both components and the model held fixed in yaw.

The proposal was an extension of a standard type of dynamometer used for measuring ship model resistance. In this form, however, its complexity, large number of flexures, and size, was likely to provide problems in altering the system of axes used, and in maintaining and checking alignment and calibration especially as it was

likely to be treated harshly during the acceleration period with carriage speed oscillating considerably. There was also a liklihood of some interaction between components.

The type of equipment had been in use, albeit in a simplified form, in a number of establishments as a single component dynamometer, so that there was a good possibility that it could have been brought into use quickly; however, the cost of some £1200 made its further consideration impossible.

None of the other firms approached would undertake to offer a design at a price near that of Saunders Roe, so that it was decided to design and construct a dyhamometer to the requirements in the University workshops.

To reduce the complexity and cost involved in designing and building a three component balance, the use of a sliding weight to provide heeling moment to the hull so that the resulting heel could be measured was accepted; this had the additional advantage that the moment was always applied, and heel measured, in the athwartships plane of the model which might not have been possible with a full three component balance system.

It remained, therefore, to provide a two component balance measuring two force components at right angles with either axis system. The latter requirement meant that the system had to be

capable of arrangement in two ways: (a) the balance axes corresponding to the carriage longitudinal and transverse axes, while model leeway was adjusted relative to the balance; (b) the balance rotated to the required leeway in relation to the carriage axes, while the model centreline was held along the balance longitudinal axis.

It was obviously desirable for the actual force translating mechanism to be compact and simple so that these requirements could be satisfied.

At that time the N.P.L. had been using, for both steady state and oscillatory measurements, a simple balance, extremely compact, in which the small relative movement of two horizontal plates held apart by stiff flexures was measured.

Due to a resurgence of interest in yacht testing with the interest in the America's Cup by various syndicates, the Ship Hydrodynamics Laboratory had made a preliminary investigation into the use of such a system for a yacht dynamometer.

The elegant simplicity of the system encouraged its use for the dynamometer for the University Tank, and a study was made leading to the construction of the balance arrangements shown in Fig. 47, 48, & 49, and described below.

General Arrangement of Balance

A vertical post is attached to the model at the desired towing point by a universal joint allowing freedom in pitch and roll, but not in yaw. The axis of the portion of the universal joint allowing freedom in roll may be arranged to coincide with that about which the righting moment is to be measured.

The post, the lower part of which is cylindrical and the upper part square in section, is located with respect to the lower force plate by two sets of bearings; the lower bearing is a linear ball bushing for vertical motion located by four webs from the underside of the lower force plate. The upper bearing consists of six $\frac{1}{2}$ inch ball races locating the square section of the post in yaw, but allowing it to move vertically. These bearings are carried on webs attached to a plate which may rotate relative to the lower force plate to set the model leeway when Sea axes are used. This circular plate is graduated, and may be clamped within 0.1° with the aid of a vernier.

The lower force plate is suspended and located relative to the intermediate force plate by four flexures having a substantial ratio of major to minor stiffness and with their major axes set in a transverse direction.

A further four similar flexures, set with their major axes longitudinally, position the intermediate force plate from the mounting plate.

To allow the whole balance arrangement to be pivoted with respect to the carriage and allow Body/Sea axes to be used, the mounting plate is carried on a rigid turntable from the carriage structure: its alignment may be set to within 0.1° by use of a scale and vernier on the turntable.

Thus, resistance using either axis system is measured by the movement of the lower force plate relative to the intermediate force plate and side force by the relative movement of the intermediate force plate and mounting plate.

In both cases, this displacement of some 0.020 in. maximum is measured by differential transformer linear pick-offs energised by a 400 c/s oscillator. The pick-offs are set to measure the direct displacement between plates, and are positioned to minimise any effects resulting from rotation of the plates relative to one another due to yawing moment from the model. This, together with the substantial ratio of major to minor stiffness for the flexures, virtually eliminates any mutual interference mechanically between the components.

Measurement of heel angle due to the running speed and leeway, together with the movement of the sliding weight athwartships, is arranged by a rotary differential transformer pick-off energised by

a 400 c/s supply and mounted on the end of the roll shaft in the Universal joint connecting model to post.

The maximum transverse movement of the sliding weight is restricted, if the weight is not to enter the water at large heel angles, to about 6 in., so that in order to obtain a transverse moment of 5 lb. ft., a weight of 10 lb. would be required, while to give an accuracy of 0.01 lb. ft., its movement must be measured to within approximately 0.015 in. which is just possible with a normal scale rule. In practice a suitable weight is chosen to provide the range of heel angle required.

Flexures

Arrangement of the flexures and their end fastenings is shown in Fig. 47. It was important that the end fastenings be made effectively encastre to avoid sloppiness of the balance around the zero position, as only very small displacements between the force plates were being measured.

The flexures, of E.N. 27 steel (on advice from the National Physical Laboratory), were designed to give deflections between the respective force plates of approx. 0.01 ins. under the loads designated as 'normal' in the specification, and manufactured from 5/8 in. hexagon bar.

To obtain effective encastre end fastenings, the shanks were made a very tight push fit into holes drilled in the force plates and nuts arranged to pull the shoulders hard against the force plate surface.

The design and manufacture of the flexures is described in detail in Appendix 7.

To avoid interaction between components it is essential that the major axes of each flexure set should be exactly square to the line of action for the force component being measured. It was found convenient to set the flexures square by laying a short straight edge across each pair in turn, parallel to the major axes, and to adjust the flexures until the faces married up with the straight edge. By use of two spanners, on the hexagon body and on the nut, the flexure could be adjusted and pulled down tight. Tightness was found to be extremely important if sloppiness about the zero is to be avoided.

The Linear Pick-Offs

These are Speery type 11LPO/30 and their output characteristic is shown in Fig. 50. Output is linear up to a core displacement of 0.020 in. from the null position, with a phase change of 180° at the null point which is with the core displaced some 0.030 in. from its mechanically full out position; the core is normally spring loaded to the fully out position, and on the balance adjustment may be made to obtain the null by means of a screw on the abutting plate shown in Fig. 47. The electrical arrangements are discussed in the following section.

Electronics

In the early stages of the design, it was considered impracticable to feed a mains supply along the tank to the carriage, due to the presence of water; hence, the original conception was to use transistorised circuits supplied from batteries carried on the carriage, and to take all readings from the pick-offs to a battery operated pen recorder also carried on the carriage, the records being removed after each run.

However, it proved impracticable to obtain a suitable battery operated pen recorder, and although it was practicable to use a transistorised converter from the battery at 12 volts d.c. to supply 240 volt at 50c/ a.c. and operate a mains recorder, the additional weight of such a recorder (60 lb Minimum) together with that of the batteries and balance, brought the total load in excess of the design figures for the carriage.

The alternative was now to use mains operated equipment at the console, and relay both the energising power and output from the transducers down a cable to and from the carriage. Three possible configurations emerged:

1. To use mains operated equipment on the console and 'pipe' it to and from the carriage. This was a convenient method using established techniques, but involved the use of mains voltages in the

cable carried above water.

2. To use a mains operated transistor power supply with transistorised units at the console. This, again, was very convenient and obviated the supply of mains via the cable, but involved unproved transistor techniques.

3. To use a battery on the carriage, as originally intended, with some transistorised units, feeding only results back to the console via the cable. The battery weight could be accommodated on the carriage and this was the nearest configuration to that first envisaged, but as it was necessary to rig the cable arrangement to the carriage, there seemed no point in having the inherent dependence on battery charging with the attendant frequent removal and replacement of batteries.

The use of alternative 2, meant that the danger of handling mains in the cable above water was eliminated without the disadvantages of method 3, so that this was the arrangement finally adopted.

The electronic arrangements involved are shown schematically in Fig. 51. At this stage of construction the cost of a mains recorder (approximately £300) was unacceptable and as an alternative it was decided to experiment with the use of dials to record the output from the pick offs, and hence the measured results.

A stabilised power supply is taken to a transistorised oscillator unit from which 6.3 volts at 400c/s, stabilised within 5% both in amplitude and frequency, is taken via the cable to the carriage for energising the differential transformers. Outputs from the transducers are returned via the cable to amplifiers matched with the recording dials on which the measurements are displayed at the console. In each case, arrangements are made to adjust the zero and full scale setting of these dials. The three display units may be seen in Fig. 42 on the right hand side of the console face. Heel is shown by the single dial at the top, resistance at bottom left, and side force at bottom right; each unit may be switched and controlled separately.

Due to spring loading of the pick off cores, it was possible to arrange for the movement between force plates to displace them in either direction about the null. In practice, it was found most suitable to arrange for the relative plate movement to act against the spring to avoid any slight hesitance in the measurements. In order to use the complete dial face, and so gain maximum sensitivity in reading, the electronics were arranged to be non-phase sensitive, and produce a positive dial deflection for movement of the core in either direction from the null. Arrangement of the electronics in this manner had the additional advantage of reducing their complexity

and cost, an extremely important consideration at this stage in the construction. If at any time it were desired to carry out oscillating force measurement, e.g. models in waves, then phase sensitivity would be essential, and could be arranged by the addition of a further electronic unit.

In practice, some trouble due to the small maximum deflection of flexures was experienced in the measurement of resistance, as the maximum deflection of these had been reduced to some 0.005 in. under maximum load, and it was found necessary to set the core some 0.005 in from the null in the direction of movement; this is discussed in more detail in the following chapter and in Ref. 26.

Side force and resistance display dials were arranged to give full scale deflection for either 0.010 in. or 0.020 in. relative movement between force plates, depending on amplification, the required range being selected by switches beneath each dial.

The heel unit was arranged to read from 0° to 30° over the dial length, this being the range within which the practical values of heel might be expected to lie.

A twelve channel cable was arranged to run on a standard steel cored nylon curtain rail suspended by its usual household fittings below the Southern rail supporting girder; it was erected in 12 ft. lengths, adequate alignment of butts being obtained by using support

fittings at the extreme ends of each length. The cable was loosely lashed to standard nylon runners, and at the start of a run is looped closely at the Eastern end of the rail; during the run, the cable is towed from a post on the carriage and carried on the runners. Junction boxes were arranged at the console and on the carriage as terminal points.

At first, some interference between components was experienced, but by the use of appropriately shielded cable, all electrical interference was eliminated.

Calibration

Calibration of the balance for side force and resistance implied the application of known loads along, and perpendicular to, the centre-line between rails at the model attachment post.

It had been intended that the run direction should be from West to East, so allowing the tapered portion of the waterway to be used in running up to speed and obtaining stable model conditions; however, due to the cramped nonfines and difficult access to the Western end of the tank, it proved impossible to arrange for convenient calibration of the balance at the beginning of a run. An attempt was made to calibrate at the Eastern end before the model was run back to its starting position, but this resulted both in a doubling of time between runs to allow for wave dissipation, and in a likli-hood of difficulties in being sure of the calibration for the actual run.

Resistance

As the towing wire had been arranged directly along the centre-line between rails, this gave a reference line for the application of resistance calibration. A pulley was fixed at the centreline of the waterways Eastern end, and arranged to have transverse adjustment, facilitating accurate alignment of a cord from the model attachment post at the balance and passing over the pulley to a freely hanging weight. After releasing the tow wire from the carriage post, plumb bobs may be used to align the cord longitudinally, the distance between model attachment post and pulley being sufficient to allow adequate longitudinal separation of the plumb bobs for alignment of the cord. In this manner, it was found possible to align the cord within 1/32 in. from the bob support wires, so that the bobs should be at least 3 ft. apart in order to align the cord within 0.05°. In practice, it was found possible to make adjustments at the carriage with it some ten feet from the Eastern end of the water-way, so that the accuracy is considerably greater.

With the calibration cord attached to the balance, the latter may now be turned using the top turntable so that the major axes of the resistance flexures are exactly perpendicular to the longitudinal tank axis, as indicated by lack of movement on the side force dial indicator at the console on application of load. A check on this method of alignment using a 6 ft. straight edge clamped along the balance centreline showed complete agreement.

Side Force

Arrangements were made to apply a load at right angles to the rail centreline by means of a pulley attached to the waterway top at the model handling platform, some 6 ft. from the Eastern end. A cord, passing over this pulley applies a load from a freely suspended weight to the model attachment post. The longitudinal position of the carriage may be arranged so that no movement of the resistance dial unit occurs when side force is applied, the carriage being clamped in this position while calibration is effected.

It was found necessary to ensure that the pulleys ran freely before undertaking calibration, achieved by frequent washing out and a very sparing application of light oil.

Owing to the electronic adjustment available for the meter, full scale readings could be employed down to a load of 1.15 lb.

For both side force and resistance, the meters were found to be non-linear, and typical calibrations are given in Figs. 52 & 53. In each case, the repeatability of readings were within a range of 0.5% of full scale despite the small deflections of the resistance flexures.

The calibration and sensitivity under running conditions is discussed further in the following chapter.

Heel

This unit was calibrated by use of an accurate clinometer laid on the partial deck of the model, it being assumed that initially the model floated upright in the water. The meter is marked in degrees from 0° to 30° and again, non-linearity is evident as shown in Fig. 54. Repeatability was found to be within 0.1° and governed by the accuracy of reading for the clinometer.

Setting of model in yaw and vertical freedom

The model attachment post, and hence the hull, is held from movement in yaw by the top bearing arrangement of ball races as shown in Fig. 47. Originally, on advice from N.P.L., nylon rollers were used, but tests with a stiff plate fastened in place of a hull, showed that considerable movement in yaw was likely despite the rollers being adjusted so hard against the shaft that vertical movement was also resisted. The nylon rollers were replaced by $\frac{1}{8}$ in. ball races, and with these suitably adjusted, angular movement, as shown by the board, was restricted to 0.05° without undue restriction on vertical movement.

The attachment post and hence the model, is restricted in vertical movement only by friction in the linear ball bushing and the top bearing. It was found essential to keep these bearings dry and reasonably free from lubricant in order to give minimum friction; the post included in the model weight, was found to be free under a force of some 0.1 lb.

Measurement of Model L.C.G. and V.C.G.

A common method of setting the L.C.G. and V.C.G. to the desired position in a model is to support it by a rod passing laterally through the hull at the C.G. location; weight is then distributed to give the correct all up weight and C.G. location as indicated by the hull's balancing perfectly about the rod when the latter is supported in bearings.

An alternative method, which enabled the measurement of V.C.G. position of an existing hull while also allowing its correct setting if desired, was evolved, based on the simple balance principle as shown in Fig. 55.

The model is clamped to the supporting plate at one end of the balance arm, which may be pivoted in several position over a length of some four inches. A pointer is fixed at the other end of this arm, reading against a scale, which allows the weight of the model to be balanced by weights added to a hangar.

Using this arrangement, it was found possible to measure the V.C.G. to within 0.05 in., a value which could be checked by using alternative support positions for the balance arm.

The L.C.G. was obtained by measuring the proportion of weight at bow and stern in turn, on an ordinary balance while the other end was freely supported.

fig 46 two components balance proposed by saunders roe division. method of measuring resistance shown. sideforce measurement similar.

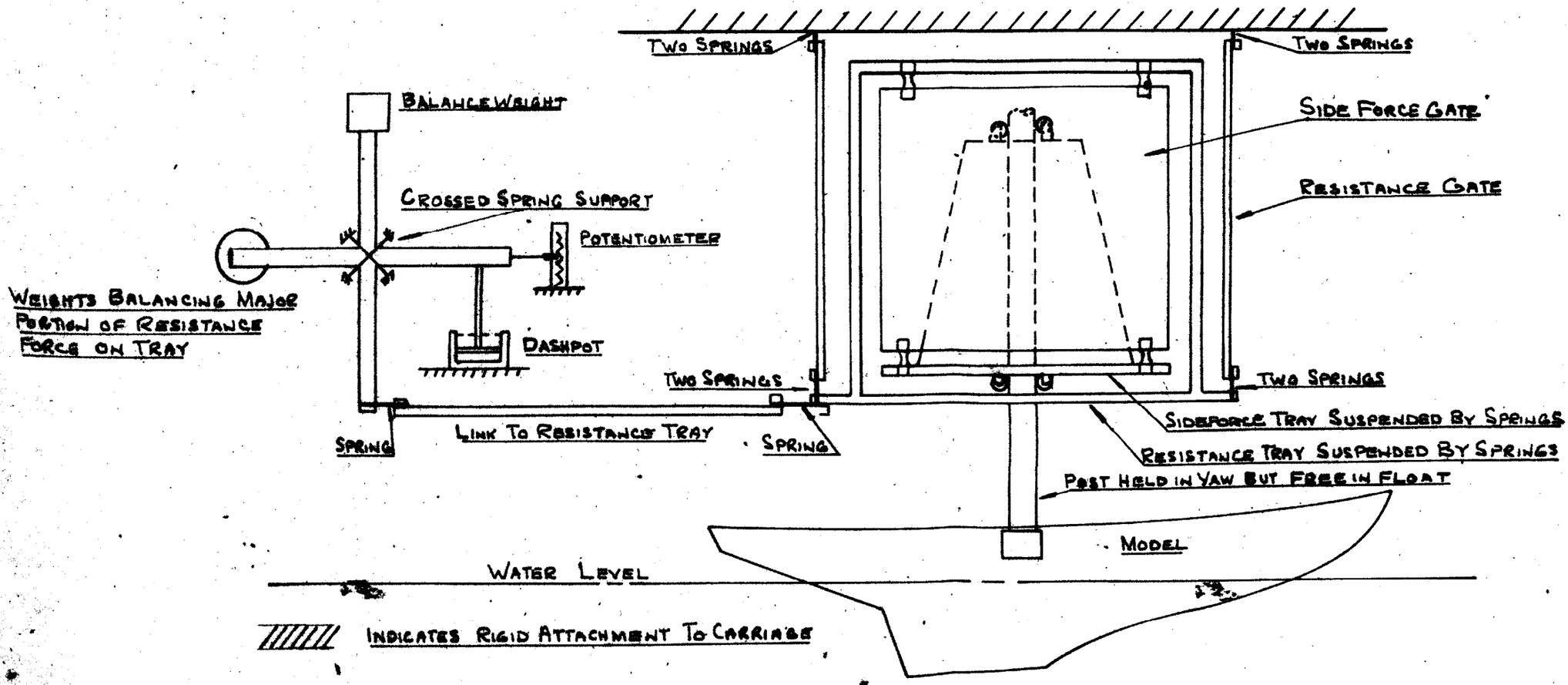

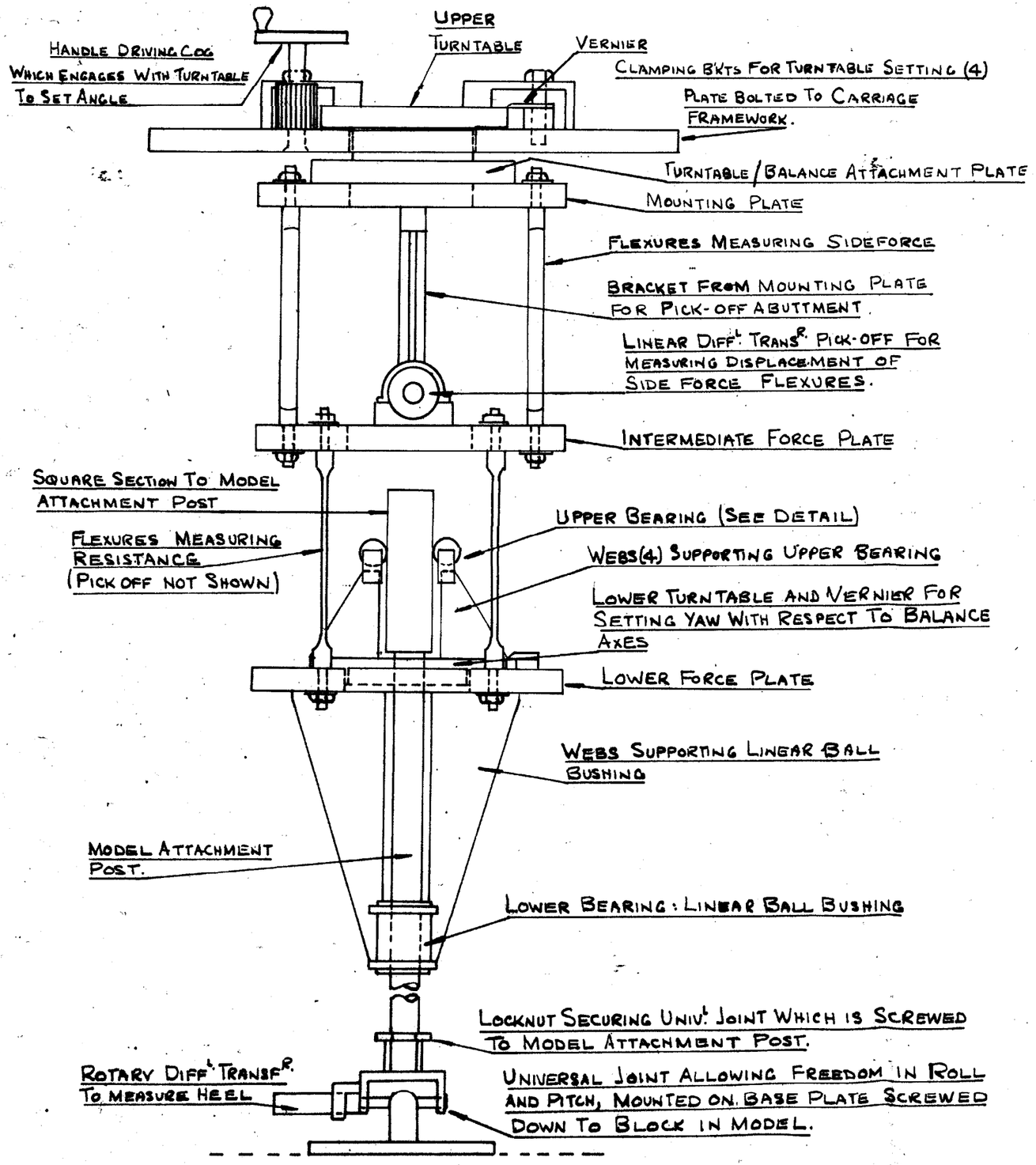

ARRANGEMENT OF UPPER POST BEARING TO HOLD MODEL IN YAW

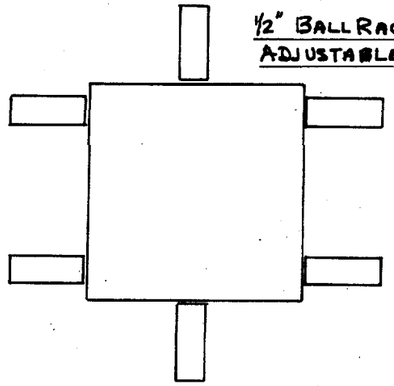

DETAIL OF PICK OFF ABUTTMENT

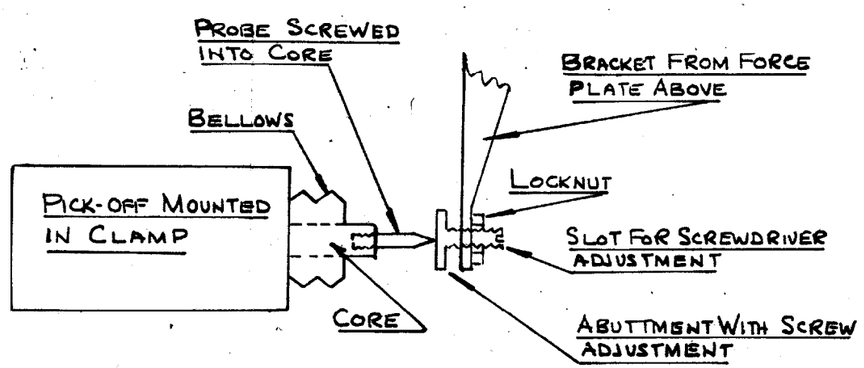

fig 47 two component balance allowing measurement of sideforce and resistance using course/sea or body/sea axes.

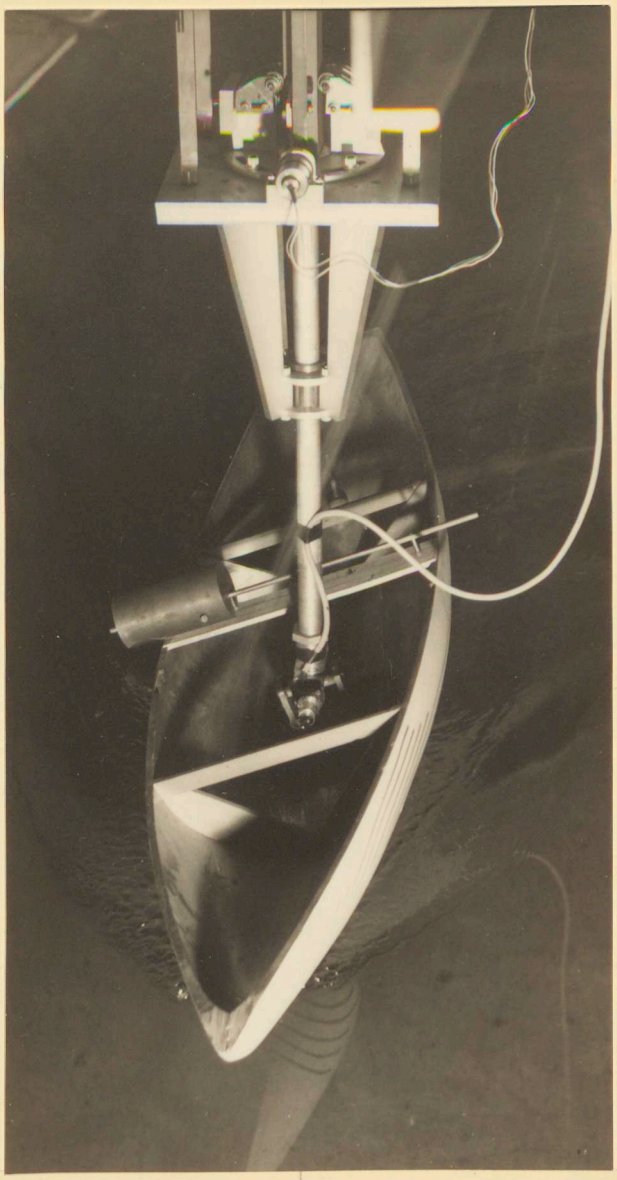

Fig.48. View of bottom force plate of balance, and turntable allowing adjustment to leeway when course/sea axes are used.

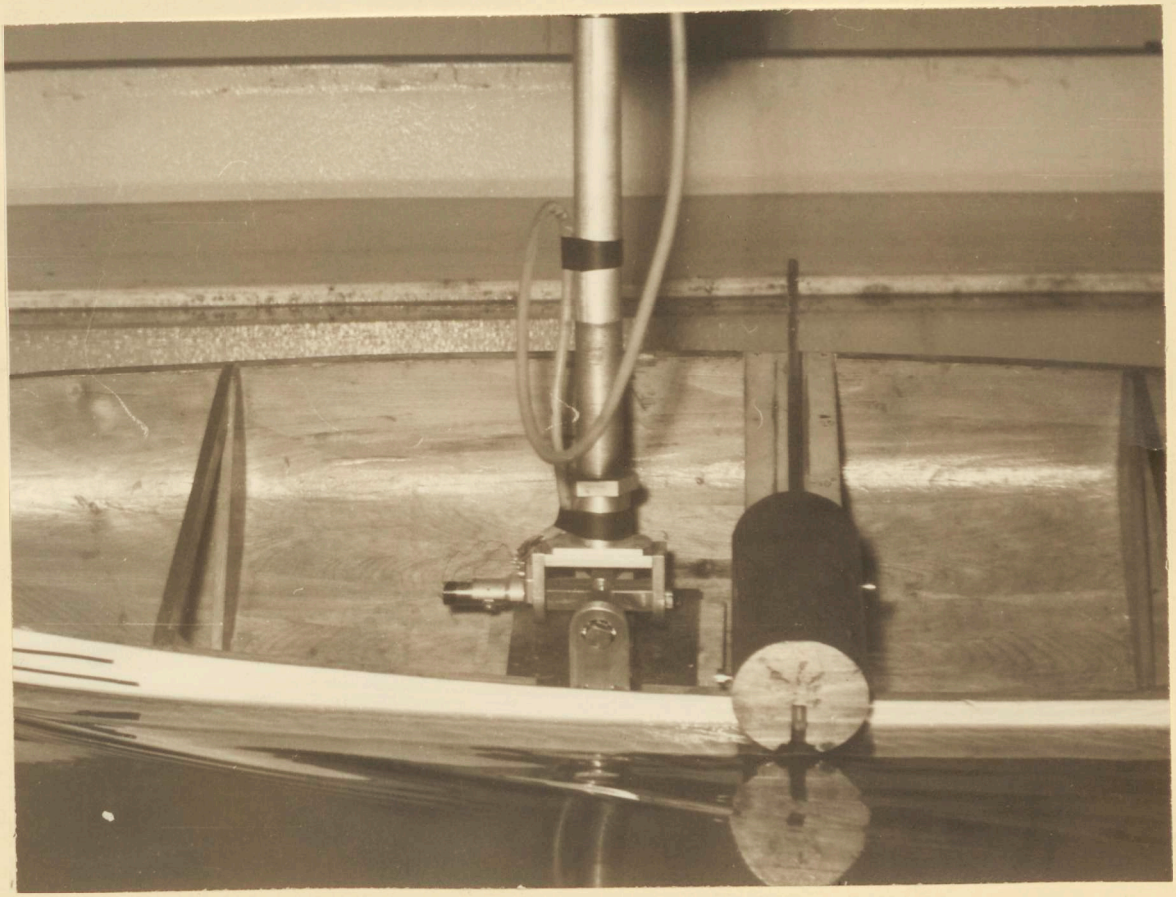

Fig.49. Arrangements for measuring transverse stability moment.

fig 50 characteristic of linear pick-off.
core displacement-output.

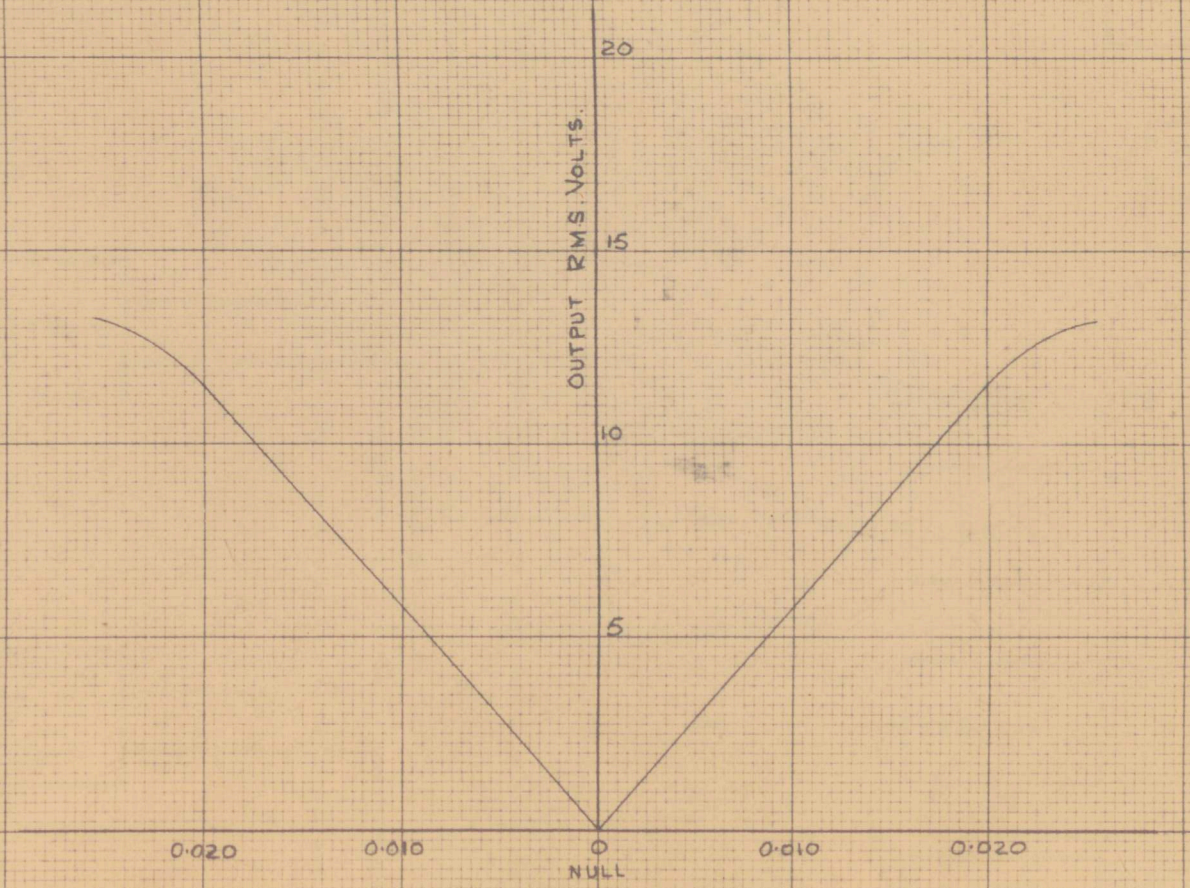

fig 52 calibration for sideforce measurement.
full scale reading 5·25 lb

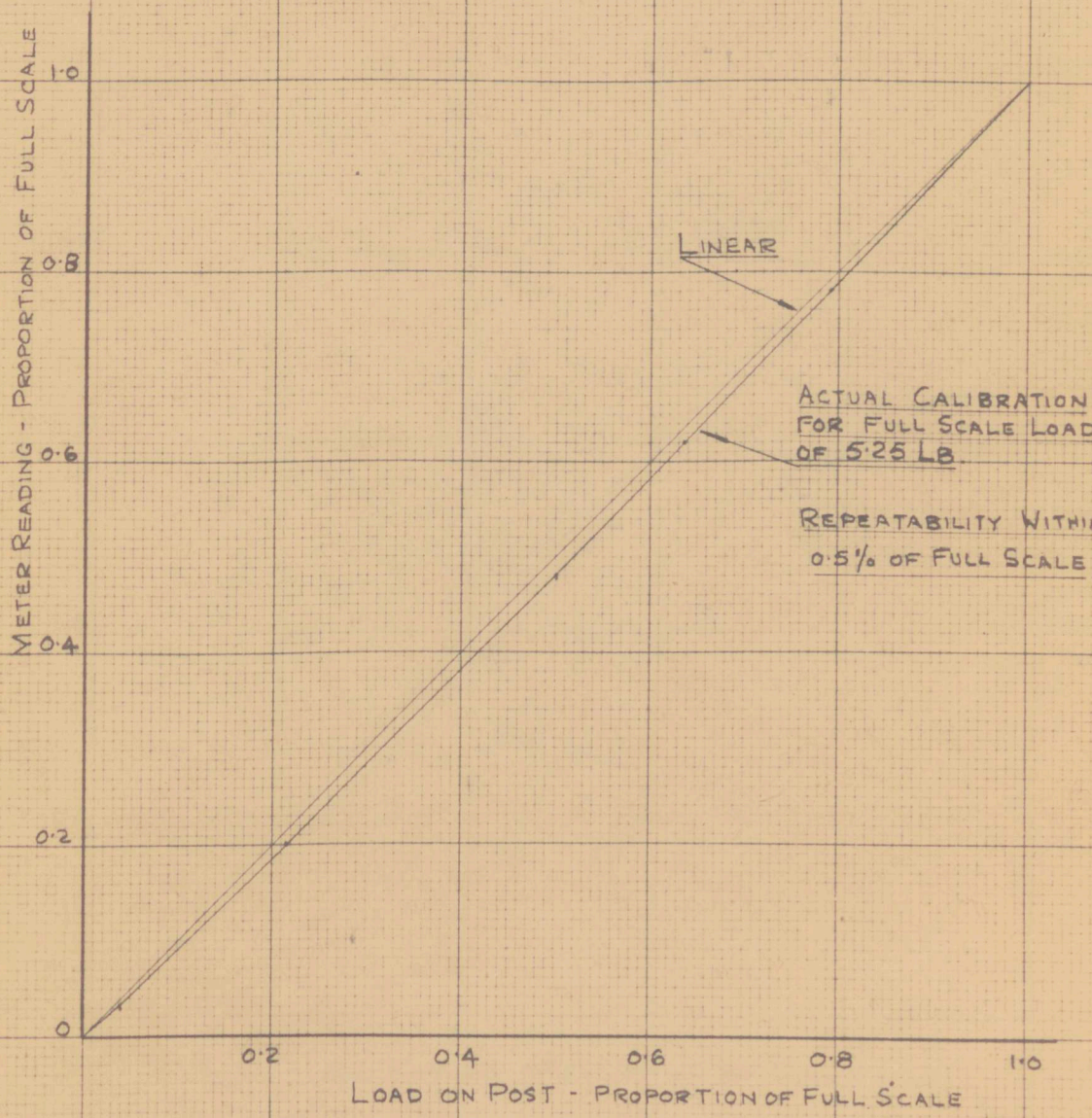

fig 53 calibration for resistance measurement.
full scale reading 1·16 lb.

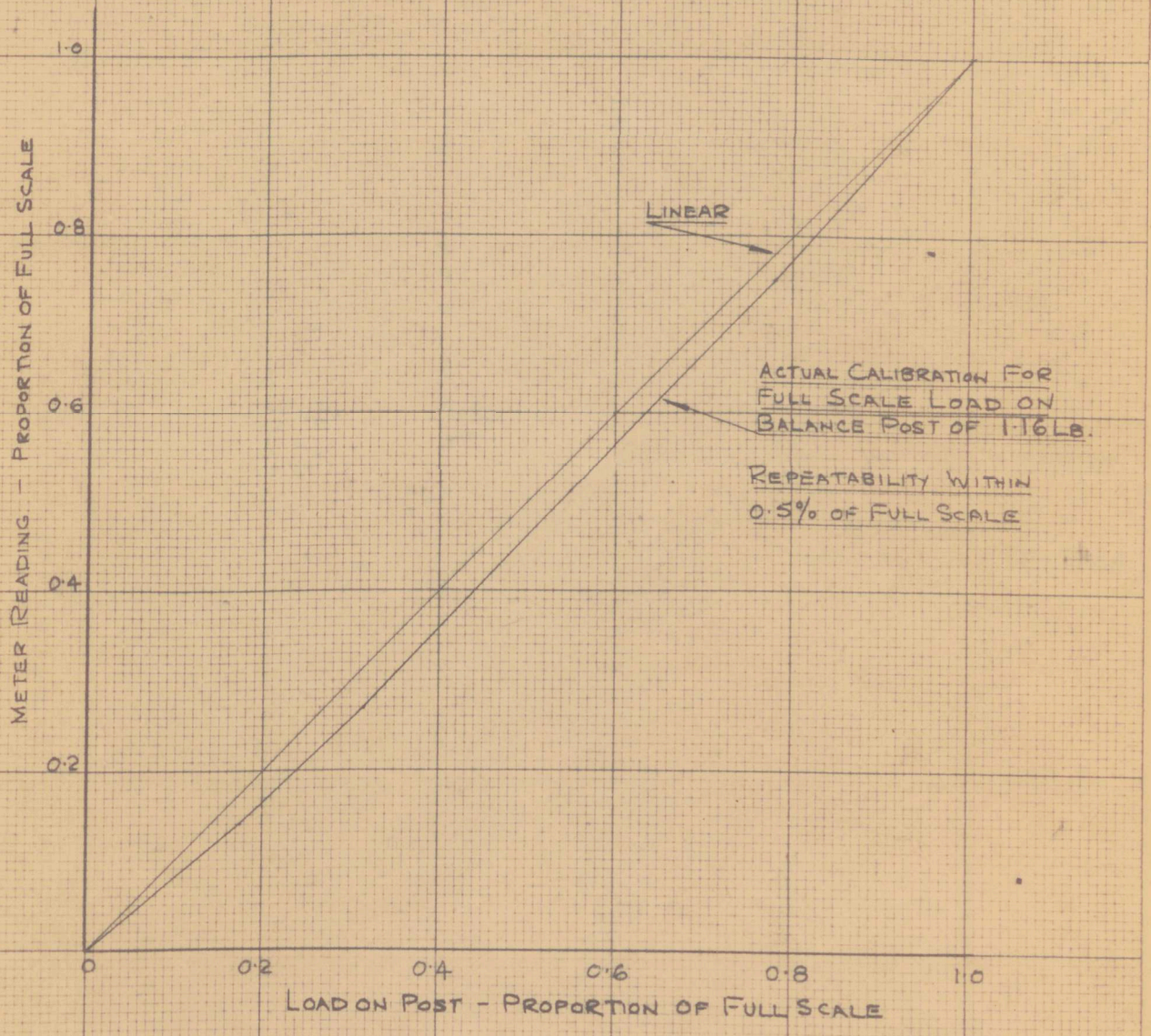

fig 54 calibration for measurement of heel.

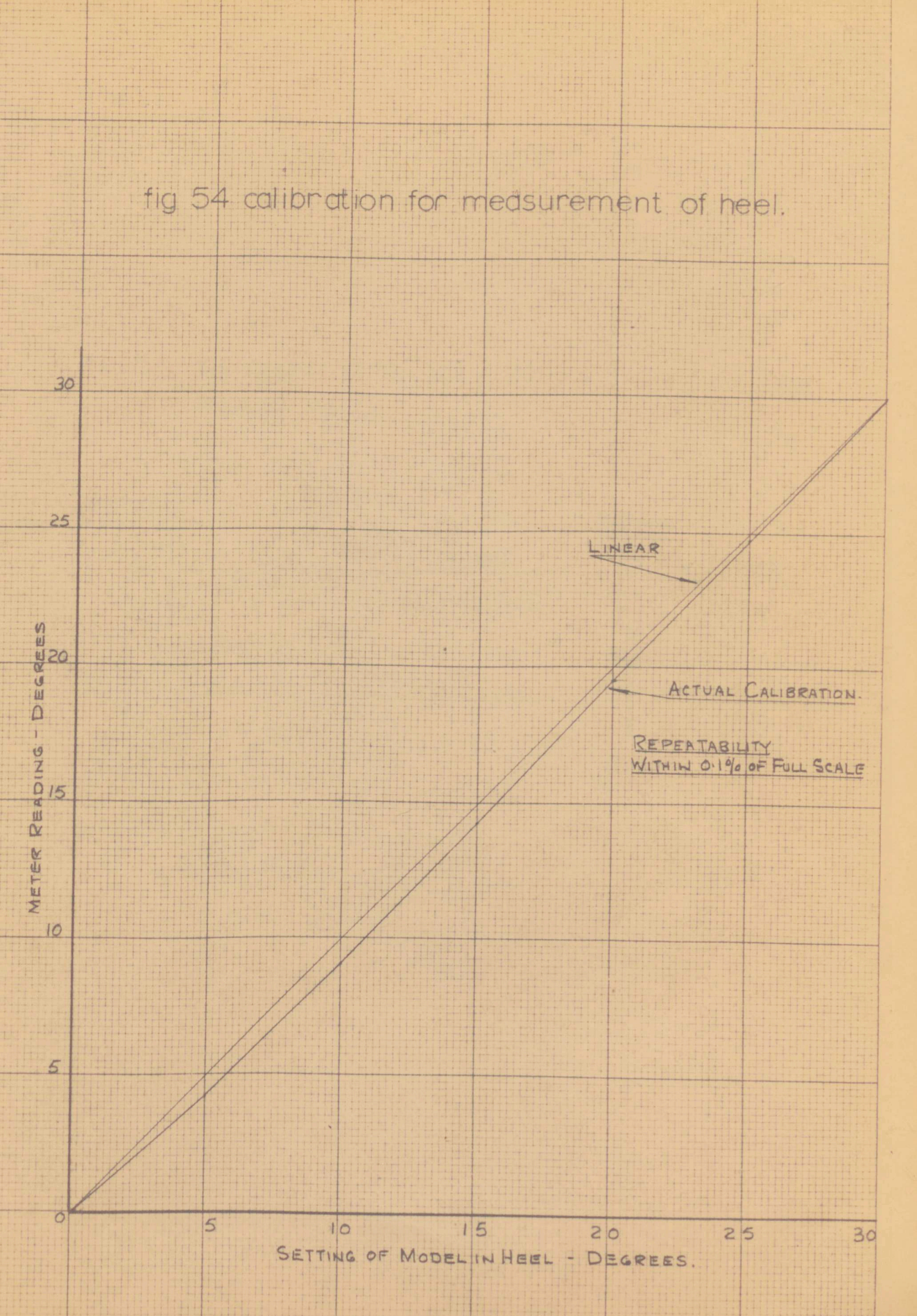

fig 55 arrangements for measuring model V.C.G.

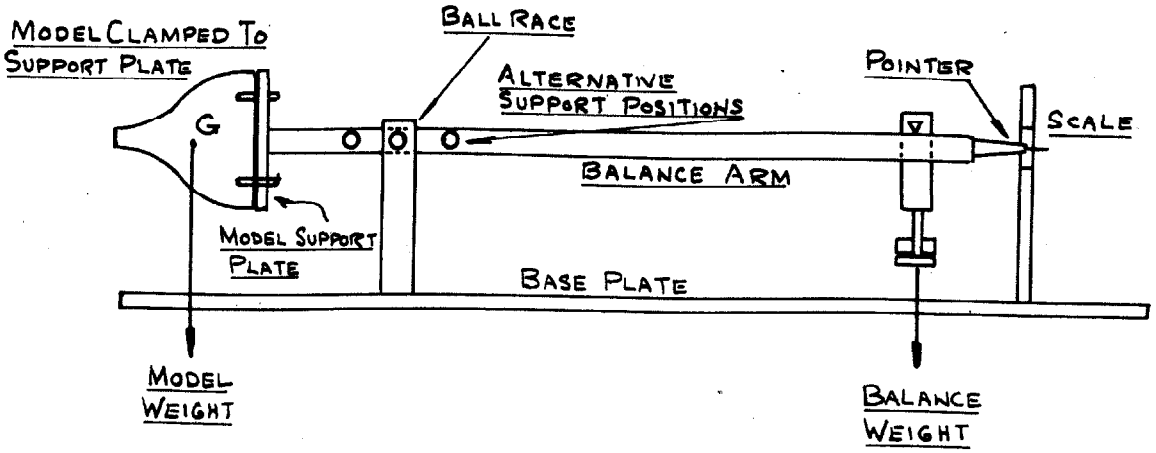

CHAPTER 16: EVALUATION OF TANK FACILITY

Evaluation of the facility was undertaken over a period of some three months constant working, the principle objects being to determine the order of accuracy which might be expected in the various measurements, and to derive the most suitable methods of working and use of the equipment in order to obtain this accuracy while allowing a reasonable rapidity of working.

The model used for this work was that of a Dragon class yacht, constructed by Saunders Roe Ltd. for work reported in Ref.1. It had been presented to the University and used for several series of experiments in the Wind Tunnels, with the result that some mishandling, damage, and modification had taken place; this is considered more fully in Chapter 19 of Part 3; for the present purpose it had the original varnish finish.

The waterway and water

The amplitude of travelling waves caused by the passage of the model down the waterway varies with speed, and while they were found to decay within some five to six minutes after a run at low speed, their decay time after runs near the maximum velocity could last up to twenty minutes. In each case the decay times were assessed at first by observation of a small float on the water surface, it being assumed that the decay was complete when the float ceased to move due to the passage of waves. After some practice it was found this

procedure was not imperative, as an extremely good guide to the presence of even very small wavelets was given by the reflection of overhead lights in the water.

The installation of beaches brought wave decay times from the highest model speeds down to approximately five minutes.

The design of side beaches was based on those in the Saunders Roe No. 2 Tank, which had proved satisfactory. One inch thick wood planks were arranged to be held at each end, and at their centres, by supports from the top of the Northern side of the waterway, allowing adjustment in inclination to the water surface. The most suitable inclination was found to be some 10° with the static waterline just above the lower dege of the beach; following Saunders Roe practice, the beaches were placed along one side of the waterway only, waves reflecting from the Southern side being damped adequately due to the narrow waterway width.

The necessity of providing end beaches was accepted, despite a slight reduction in run length of some 4 ft.; two inch slats were screwed across supporting members, a vee being worked to give additional model clearance at each end of the run. The structure is hinged on the waterway ends and arrangements made to fix the beaches over a wide range of angle if necessary; an angle of between

$12\frac{1}{2}°$ and $17\frac{1}{2}°$ was found effective over the whole range of model speeds.

The hull's passage produces currents and circulation which appear in the surface as drift and a vortex. These were found to amount to some 2% of the nominal velocity at high model speeds, but to decay within approximately five minutes. As the decay time was similar to that for the waves, the complication of using screens to assist decay was thought unnecessary.

A fairly constant level of turbulence in the tank water was found to be desirable in order to assist stimulation and gain repeatable results; for this reason a constant time interval between runs is often used in model tanks and Ref.18 indicates that at the Davidson Laboratory, each day begins with several high speed runs before readings are taken, and a time interval of two minutes is used between runs; also, results are only acceptable if at least three runs at two minute intervals have been made.

Experience with the University tank showed that such a rigid discipline is unnecessary, and that it is sufficient to disregard the first run each day, or after a time interval of half an hour or more, and use an interval between runs of six to seven minutes. In addition to providing ample time for wave and current decay, this interval allows anlaysis and plotting of results between each run. In

practice, it was found that this time interval also allowed sufficient time for the required analysis and plotting of results between runs.

Growth of weed in the tank water, and accumulation of dust on the surface did not appear to be reflected in the measurements, until the latter had accumulated considerable. The introduction of Sodium Hypochlorite to a proportion of 1 in 12000 by volume at intervals of approximately one month was found adequate to keep down the weed growth. A length of sacking or wood pulled along the surface from each side of the waterway once a week was found adequate to deal with dust and other accumulated debris on the surface, providing the tank was in fairly constant use during that time.

A reasonably uniform temperature of the water was considered desirable so that excessive changes of kinetic viscosity did not give rise to large corrections in the measured resistance. It was found, using an ordinary laboratory theromemeter lowered into the tank water at a number of stations and depths, that providing the tank was in reasonably constant use, the drift and circulation appeared advantageous in maintaining a uniform temperature over the volume.

The Rails

Although, no great difficulty was found in setting the milled rail butts fair, and later when running, the carriage wheels did not appear to be affected by passing over the butts, the arrangement could tend to promote vibration in the balance especially as the

longitudinal positions of joints correspond closely in both rails; the possibility could have been avoided by using angled butts between rail lengths, so allowing easier fairing of the joints and a more gradual transfer of wheels between lengths.

Under the humid conditions present in the tank building, the rails were found prone to some furface rusting, sufficient to affect the measurements slightly; this was cured by a thorough wire brushing and sparing application of a very light oil. No further trouble was experienced during the evaluation period or the time spent on the experimental work described in Part 3.

In many tanks, it is the practice to carry wire brushes on the carriage to clean rails each day before making test runs (Ref. 20); this did not appear necessary, although a close watch should be kept on the rail surfaces.

The methods of aligning the carriage longitudinally, described in Chapter 14, could lead to errors in the order of $\frac{1}{4}^{o}$. If more accurate alignment is required, this could well be achieved by use of a spacing bar between rails, using a central head to position the carriage centreline as marked on its end cross beams.

As originally constructed, the carriage's main running wheels were fitted with self-aligning ball races. When setting up the arrangements to assess speed fluctuations during a run, it was found necessary to replace the ball race of that wheel with a normal fixed race so that

the spring contact did not force the wheel off the rail. The self-aligning ball races allow wheels to turn about a vertical axis; while small discrepancies in wheel alignment are corrected by the carriage weight at a very early stage in the run, if a wheel was accidentally knocked some way out of alignment, it would become derailed. This occurred on several occasions during the evaluation period, resulting in a tow rope breakage on each occasion, so that it became standard practice to check wheel alignment after any adjustments or work carried out where the wheels might have been moved accidentally. It could prove useful to replace the self-aligning races by normal races, providing this did not lead to any problems arising from slight inaccuracies in rail angular alignment.

Although the speed variation during a run is within $\pm \frac{1}{4}\%$ of the nominal, it may be observed that the tension/damping weights in the drive system are always in motion. It is also noticeable that the unsupported length of wire over the water oscillates transversely during a run, so indicating that there are oscillatory forces present at the carriage of a higher frequency than those measured by the wheel revolutions. It would also be desirable to damp out as far as possible the large oscillations in speed due to clutch application at the start of a run, and so obtain a greater length of steady run

and reduce the promotion of longitudinal oscillations in the resistance flexures. Such damping could be applied either to the tension/damping weights or by a viscous piston/spring damper incorporated in the tow wire adjacent to and in front of the carriage.

With the arrangement described in Chapter 14 if the second stopping relay fails to cut power from the motor, then only manual operation of the console STOP button will bring the carriage to a halt. Time for the run is known accurately from the gear and speed selected, so that a careful watch on the Dekatron counter could allow the operator to depress the emergency button in time. At low carriage speeds this may be satisfactory, as the operator has time to judge whether or not the photo-electric relay has functioned, either by direct observation or by reference to the counter; at high carriage speeds, however, the operator's reaction time would be too great to allow a reasonable chance of cutting the motor before the model struck the waterway end. In practice, during a run the operator is watching and recording measurements on the meters and would not notice immediately if the carriage had over-run.

Further, if the tow rope should break behind the carriage during the deceleration sequence, then cutting the power would be ineffective and an accident is inevitable. There is, therefore, an

immediate need for both a system to warn the operator that the carriage has passed the first relay, and for an arrangement to provide emergency braking.

A warning system might take the form of a large flashing red light situated between the meters on the console face to gain immediate attention, and triggered by a trip switch situated just past the first stopping relay. It could then become habitual to depress the STOP button directly the light began to flash.

If this warning system were adopted, then an emergency braking arrangement would only be necessary due to failure on the part of an operator to depress the button, or if the tow wire broke behind the carriage. It would have to be gradual in operation to prevent balance damage, but firm in order to stop the carriage and break the tow line if the motor failed to stop. Hydraulic or spring loaded piston buffers would be suitable here, with perhaps the initial retardation being effected by bungee cord stretched between the rail supporting girders.

It was found that in order to prevent distrubance of the model setting, and possible damage which running astern into waves initiated previously during the forward run, that it was advisable to restrict the model speed for the return run to 1.9 ft/sec, setting 1.333

for the gears. The return stopping relay at the Eastern end of the tank was positioned to stop the model in a convenient position for adjustment and at the correct starting position when this gear setting is adopted. If the carriage is taken back at a higher speed, then use of the STOP button is essential to prevent over running.

The Balance and Associated Arrangements

Generally, the balance arrangements proved sufficiently robust to stand up to the rough handling which they might be expected to receive at times. During the evaluation period, the carriage was caught up and stopped violently on several occasions, usually because of a wheel jumping the rails, but the balance retained its geometry and calibration characteristics.

Applied Moment and Measurement of Heel

During a run, the model was found to take up an entirely stable running attitude, and heel could be read easily to within a quarter of a degree. Experiments were made to ascertain the limits of repeatability of heel angle when model sliding weight and meter setting were distrubed and then re-set; it was found that providing the meter was calibrated and set correctly, the measurements were repeatable within 0.25°. This is some 0.08° of the maximum and was considered adequate from the results of Part 3.

Preparation of hull characteristics as described in Part 3, required the model to be run at pre-set angles of leeway and heel, so that the appropriate force components could be measured. This in turn meant that the transverse location of the sliding weight, which varies according to heel and leeway, must be set correctly before each run.

Rather than use the method of 'trial and error' which appears to be adopted at the Davidson Laboratory, (Ref. 22) it was found preferable to undertake a short series of runs in which the sliding weight was moved progressively, and the resulting heel angle measured at each speed and leeway. A typical set of results is shown in Fig.56. The necessary displacement of the sliding weight from the centreline may then be read off to give the required heel at the speed and leeway under consideration. During these runs, it was found that the usual five or six minute interval could be halved without introduction of unacceptable inaccuracies in measurement of heel.

Measurement of Resistance

The flexures measuring this component were somewhat thicker than originally intended, due to machining difficulties, so that their deflection under maximum load was much lower than originally intended.

The design loads had been estimated by reference to results from previous tests using Sea ases; it had been intended to undertake the

extensive series of experiments discussed in Part 3, using sea axes, and it had not been appreciated that the maximum likely force would be so much lower than the original design loads. As a result, the maximum deflection of the flexures was around 0.004 in.

The electronics had been designed to measure the deflection of the differential transformer core from its null position, due to the application of forces; under these conditions, the zero of the meter at the console would be adjusted to coincide with the transducer null, and the meter maximum be adjusted to suit the desired range for calibration.

In practice, it was found difficult to ensure the exact setting of the transducer null to the meter zero, and any slight inaccuracy was exaggerated by the small range of movement for the transducer core, which used only a small section of its linear out put range. By off-setting the core in the direction of movement due to applied force, the trouble was cured; an off-set between 0.004 in. and 0.005 in. was adopted as standard practice, any slight difference in initial offset appearing to have no effect on the calibration.

The arrangement to off-set the transducer core did, however, affect the electronic arrangements for setting the zero and scale maximum, as adjustments to one affected the other. In practice, it soon became simple to make the necessary adjustments more quickly than it was possible to adjust the core null with meter zero. If the

electronics had been made phase sensitive, this procedure would not have been necessary.

At the beginning of a run, the resistance meter was found to fluctuate considerably, due to the carriage oscillations during clutch engagement; the measurement settled down in the last twenty feet of tied run, although a certain amount of long-term change in reading was apparent. This is a common occurrence in tank work, where the resistance is usually measured on a recorder, the trace oscillating in vertical position on the paper during a run. When measuring in this manner, it is a simple matter to obtain an accurate mean, but when using the meter, it became essential to take the reading at around the same carriage position for every run. In practice little difficulty was encountered due to this.

During work immediately following that described in Part 3, Chapleo (Ref. 24) experienced difficulties from vibrations apparently due to the small deflections of the resistance flexures, coupled with the non-phase sensitive electronics. He at first used the transducers with the null corresponding to meter zero, but found the the inaccuracies disappeared when the transducer core was offset some 0.004 in. In the evaluation work and experiments of Part 3, no trouble of this nature was experienced, presumably due to the transducer core always being off-set between 0.004 and 0.005 in.

The need for turbulence stimulation of the model boundary layer, and a further investigation into the most suitable method is discussed in Part 3. The model, having previously been used in the

Saunders Roe tank, was equipped with stud stimulators, forty four of which were employed projecting 1/16 in. from the hull and spaced some 2 in. apart in two lines a mean distance of 3.2 in. abaft the hull leading edge. This arrangement had been decided in consultation with the N.P.L., and its effectiveness examined by use of ink bleads (Ref.1), it being concluded that they functioned satisfactorily above a model velocity of approximately 1.4 ft/sec.

As stimulation had appeared satisfactory, the existing arrangement was used during both the evaluation and experimental work of Part 3, where the model velocity was never below 1.4 ft/sec.

With the wind tunnel in operation, it was observed that the tank water was in a state of constant agitation due to the vibration, but this was not found to affect either magintude or repeatability of the resistance measurements.

It was found that for the majority of model speeds, meter calibration using a range of 1.16 lb. was suitable, and that with practice, the meter could be read to within 1% of the maximum. With speeds up to about 3 ft/sec. an attempt could be made to read within 0.5% of the maximum, but above this velocity the meter fluctuations made such accuracy impossible. 1% of the maximum represents a sensitivity of approximately 0.01 lb. which was considered acceptable for an over-all study similar to that proposed and

discussed in Part 3, especially when allowing for the very small deflections of the balance flexures at low speeds. For meter full scale readings representing loads above 1.16 lb., sensitivity was reduced proportionally.

To avoid sloppiness about the zero, it was found essential that the flexure securing nuts were pulled hard down, any slackness resulting immediately in small changes of zero between runs; which again, were exaggerated by the very low mean deflections being used.

Experiments were undertaken to establish the order of repeatability attainable when the model was removed and replaced, a typical set of results for three runs being shown in Fig. 57. Providing the model was very carefully re-aligned using plumb bobs from the wire to its centreline at bow and stern, it appeared that the measurements could be repeated within the limits to which it was possible to read the meter; at this speed within some 0.005 lb.

As a check on the measurement of resistance, a full curve of upright resistance at zero leeway was obtained over a wide range in speed and compared with the results obtained on the same model during previous work by Saunders Roe Division. This comparison is shown in Fig. 58. The test results were put in the form of total resistance coefficients scaled up to full scale using the method detailed in Chapter 22, as results from the previous work were only available in

this form (from Ref. 1).

The vertical separation of the curves is discussed in Part 3, but it may be seen that they follow essentially the same form, and that before wave making becomes noticeable, the results from the University tank follow the approximate curve of skin friction coefficient, indicating that they take the usual form and that turbulence stimulation was effective.

It was concluded from this work, that the measured values of resistance were satisfactory over the range of speed considered.

While for a general investigation, similar to that proposed and described in Part 3, the order of accuracy obtained is sufficient, for more detailed work where the mean level of resistance is required with great accuracy, the meter fluctuation during a run, amounting in some cases to 2% of the maximum, and the necessity for making recordings at the same carriage position in every run could not be tolerated, and it appears necessary that a recorder be provided for measurement of resistance.

Meter vibration as distinct from the long term fluctuations mentioned above, was found generally to be some 2% of the meter maximum except at low speeds when it was much less. It was, however, necessary to provide electrical damping in order to achieve this, and and in the light of difficulties found by Chaleo (Ref. 26), there is

an obvious necessity to suppress the promotion of balance vibrations at their source where possible.

The possible damping of tow rope oscillations has been mentioned previously. In addition, the acceleration phase of the run with its associated surging may be seen to promote violent oscillation of the resistance flexures, so that immediate gain would result here if the lower force plate were clamped securely during this part of the run, possibly by an electro magnetic head released automatically by the photo-electric cell which is used to start the timing counter.

The effect of these flexure oscillations at the meter could be lessened by decreasing their stiffness to allow a maximum deflection nearer the original design figure of 0.010 in. although difficulty is likely to arise here due to machining problems. It might be possible to manufacture flexures from EN27 steel in thin plate form, but problems are likely to arise in obtaining the true encastre end fixing which is essential if the zero is not to wander. Possible end fixings here would be either fitting the flexure into fork ends with a similar clamping arrangement to that existing, or to clamp each end of the flexure against a ground portion of the force plate edges.

Side-Force

With practice, it was found possible to read the side force to within 1% of the full scale meter deflection at all speeds, while

at the lower speeds this could be reduced to 0.5%. Using a full scale deflection equivalent to 5.25 lb., which was adequate for all except very high model velocities, this resulted in a sensitivity in force determination of approximately 0.005 lb., reducing to 0.0025 lb. at the lower speeds (up to 3 ft./sec.)

The results of experiments to assess the repeatability after disturbance of the model setting are shown in Fig. 57, which indicates that it is possible, providing the model is carefully aligned to bring repeatability to the same order as the meter readings.

Short term oscillations of the meter were found to be some 2% of full scale deflection generally, reducing to some 1% at speeds below approximately 3 ft./sec.

Any reduction in the promotion of balance vibrations both by damping in the towing system and by firmly clamping the balance during the acceleration phase of the run, would no doubt benefit the measurement of side force.

fig 56 typical set of curves for transverse stability under dynamic conditions. model velocity 2·97 FT/SEC

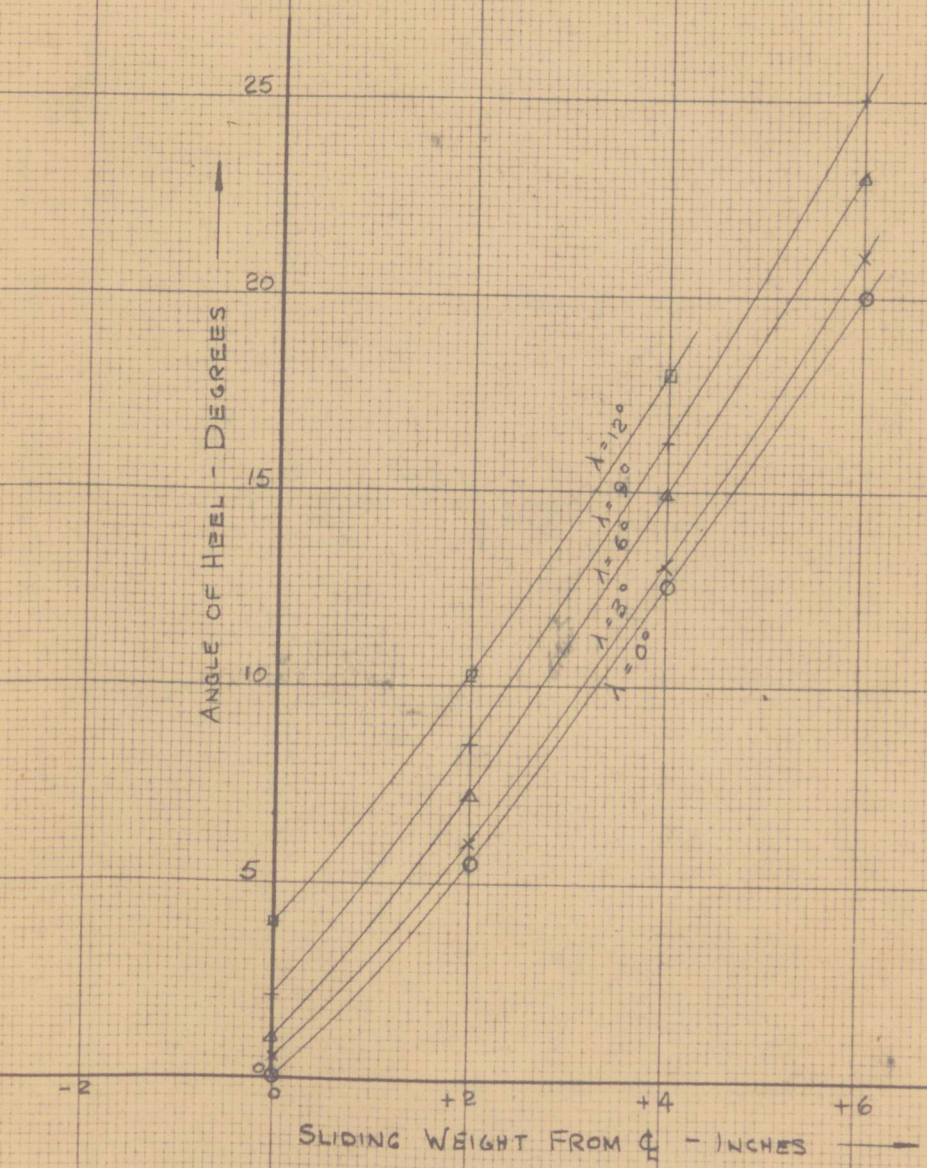

fig 57 repeatability of sideforce and resistance measurements. model vel. 2·97 FT/SEC. heel 7½° body-sea axes

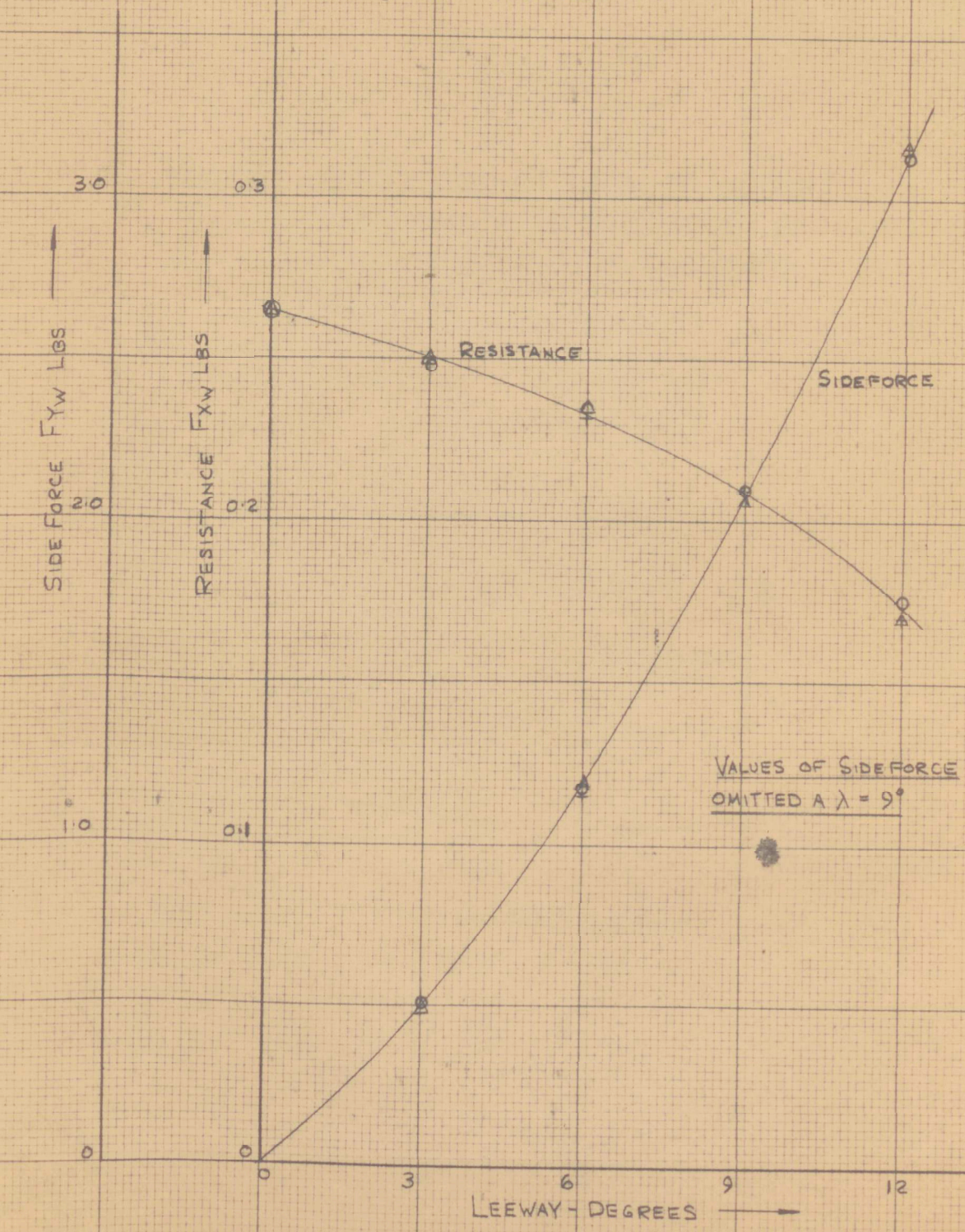

CHAPTER 17: GENERAL CONCLUSIONS AND RECOMMENDATIONS

It appears from the evaluation work described previously that the facility is at present suitable for undertaking work of a general nature, similar to that of Part 3, but requires some development before being adequate for more specialised and localised studies.

In particular, damping must be provided to reduce the effect of drive gear vibration on the carriage and two component balance, and arrangements should be made to lock the balance and so prevent violent oscillations which may persist over part of the timed run, resulting from the acceleration phase.

A modification to the flexures measuring resistance is necessary to bring their maximum deflection under expected loads to the design figure of 0.010 in. although if Sea axes are to be used, as distinct from the Body/Sea system adopted for the work described, the maximum resistance is likely to twice the maximum found here.

It was found necessary and convenient to adopt a fairly rigid discipline in operating the facility in order to achieve the levels of accuracy and repeatability detailed previously, while allowing a reasonable rapidity of working. The procedure adopted is set out in Appendix 8.

For the model used in the present work, turbulence stimulation was by means of studs, a method which was apparently satisfactory from Ref. 1 and is adopted widely in Tank work. The Davidson Laboratory (Ref. 18) however, follow the procedure, originated by Davidson, of using sand strips near the models bow. Various methods, all of which require some correction for the additional resistance of the stimulators, are available and it would appear desirable to undertake a detailed investigation in order to determine the most suitable method for use with yacht models.

Appendix 4: Erection of Waterway Structure

The general arrangement of the waterway structure is shown in Fig. 40, while Figs. 59 and 60 illustrate the methods of building and fairing.

Static water tank panels were bolted together and stood on the existing concrete courtyard floor to form the sides and ends of the waterway; three inch angle bar was used to form the corners and channel beam of 8 ins. by 4 ins., bolted round the upper edge (Fig. 60) both to bring the available water depth up to 4 ft., and to aid in stiffening and fairing the upper edge of the structure. Watertightness was obtained by the use of yarn and butumastic sealant in all joints.

Due to the slight fall built into the floor for courtyard drainage, each end of the structure was lower than the centre, so that when filled with water, the freeboard at centre was some one to one and a half inches greater than at the ends.

Some difficulty was experienced in fairing the structure due to deformation in the flanges of each panel; at their base, panels forming the waterway sides were maintained the desired distance apart by tie bars at 4 ft. intervals pulling the panels onto wodd struts laid on the concrete floor. Sides were fairedlongitudinally by means of a piano wire stretched between the centre of each end, and

held in position by wood spacing pieces which butted against the wind tunnel raft and the retaining wall. At this stage, the upper edges of each side were kept at a constant spread by wood spacing pieces. The tie bars and struts can be seen in Fig. 59.

When the structure was properly aligned and positioned, alternate panels were dogged down by short lengths of angle and rag bolts; struts were now welded to panels and bolted into the floor or to the concrete retaining wall at algernate panels to stiffen the structure.

The tank was made watertight at the base after erection of the rail gantries in two stages as illustrated in Fig. 61; first, the panels were lifted approximately half an inch from the floor by easing the dogs, and a thin waterproof mixture of one part cement to four parts sand worked in beneath the bottom flanges and to a depth of about two inches between temporary boarding; the dogs were now tightened. Before this mixture was hard, the boarding was removed and a thick waterproofed mix of one part cement to two of sand and four of aggregate laid inside and outside the panels. Inside the waterway, the floor was levelled off above the tie bars and wood struts which remained in place; because of the fall in the floor, the depth of concrete was greatest at each end of the waterway.

Outside the waterway, the floor was laid level with the top of the wind tunnel raft to ensure a level floor area. It was accepted

that in the event of dismantling being necessary this floor would have to be chipped away to obtain access to the panel bases.

The existing water supply to the cooling system for the wind tunnel passed through the tank building, and although useful for general purposes, the supply was insufficient for filling the waterway within a reasonable time. A suitable alternative, which avoided the expense of providing a permanent line having only rare use, was found in the fire hose situated in the basement of the Tizard Building; when this was led through an office on this floor, it proved possible to provide a supply which would fill the tank in twelve hours.

Following a thorough treatment with a wire brush and rust remover, the steel surfaces of the waterway were given one coat of aluminum primer and two coats of white anti-corrosive paint.

Once valves for emptying the tank were installed, and the concrete hard, the waterway was slowly filled, any leaks at the joints being controlled by systematic tightening of the securing bolts. At first the water apparently found its way through the sealing at floor level and covered the floor outside the waterway to a depth of over ¼ inch; at the same time the level of water in the tank fell by approximately 3/4 inch per day. After ten days the joint tightened up and flooding gradually reduced in quantity until some eight weeks

after filling, the complete floor area was dry and the drop in water level reduced to about 1/8 inch per week, a value which remained nearly constant throughout the first year of operation, and it is assumed to be due largely to evaporation with some seepage through the concrete base.

Duckboards were constructed to provide a dry walkway over the concete floor of the main movement area, especially in case of water accumulation.

When the supporting struts were arranged at the waterway sides and the wooden spacing pieces removed, the centre of each side wall had been allowed to bow some 1/4 inch inwards so that when the tank filled the water pressure would push the structure back to its correct width. With 4 ft. water depth the sides moved outwards some 5/16 ins. so causing an outward set of 1/16 inch.

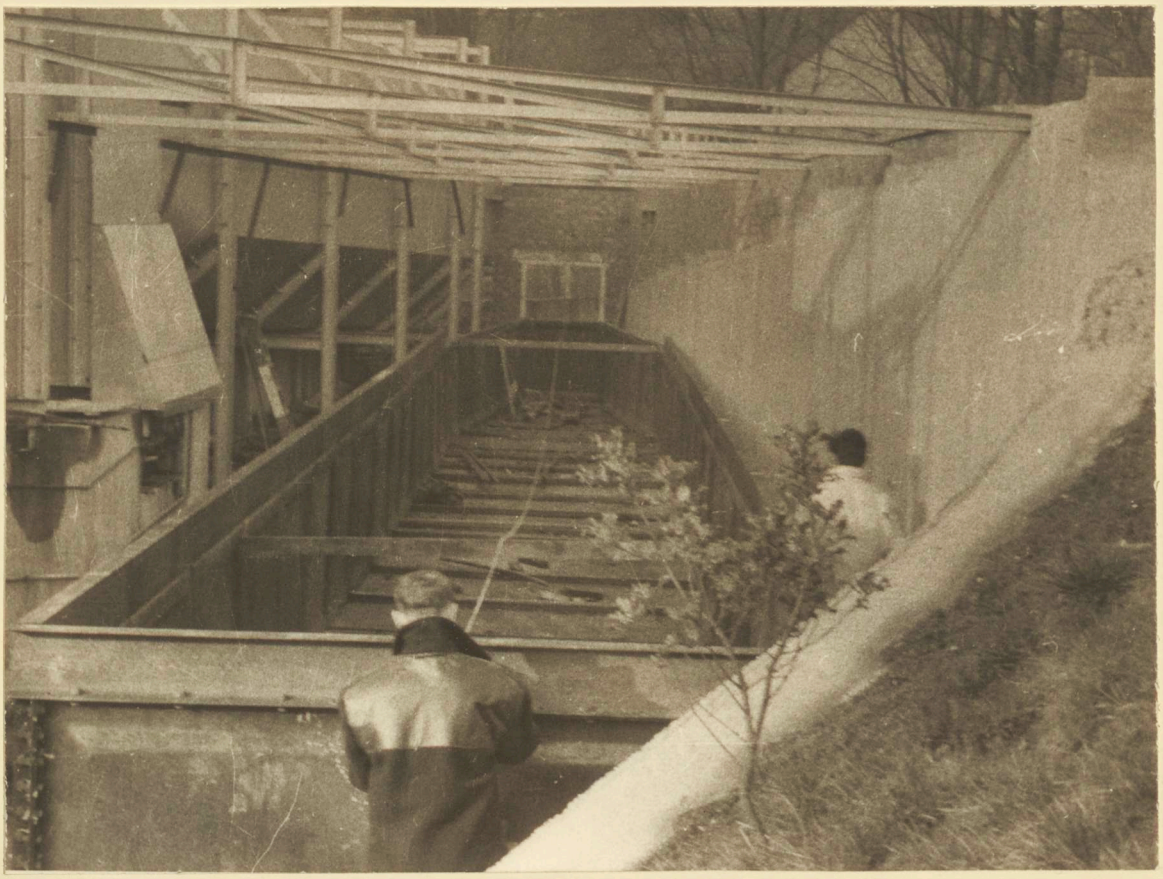

Fig.59. View of tank building looking West before East wall and roof were erected.

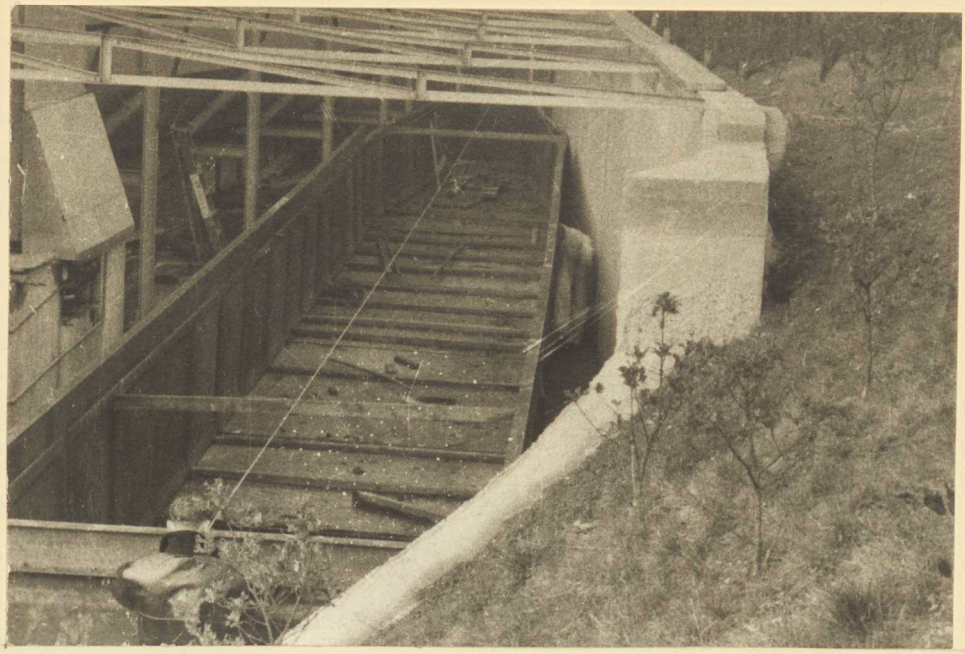

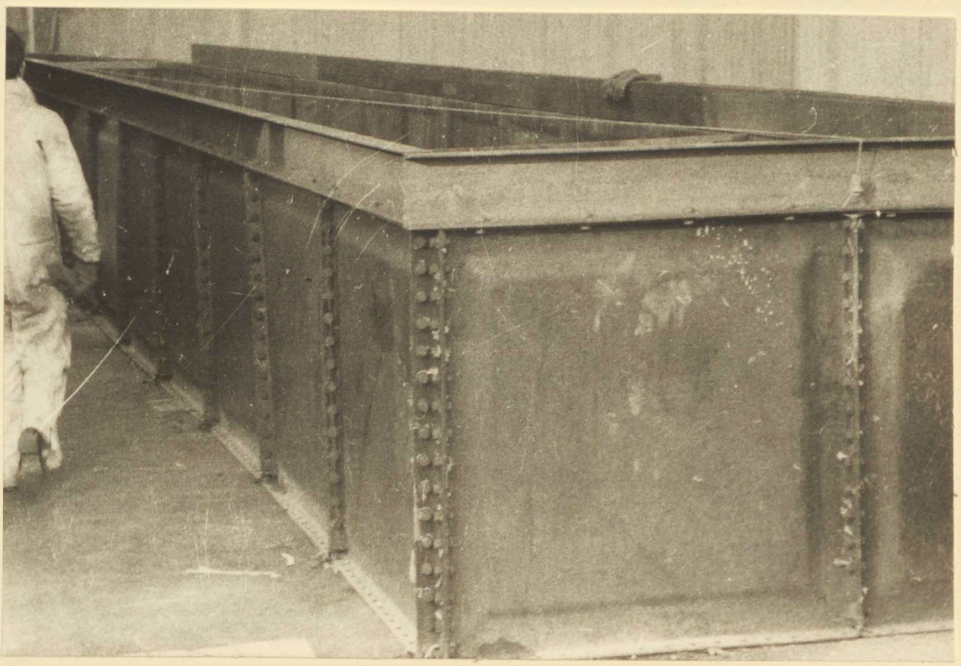

Fig.60. Illustrates the construction and fairing of waterway.

fig 61 watertight seal at base of panels.

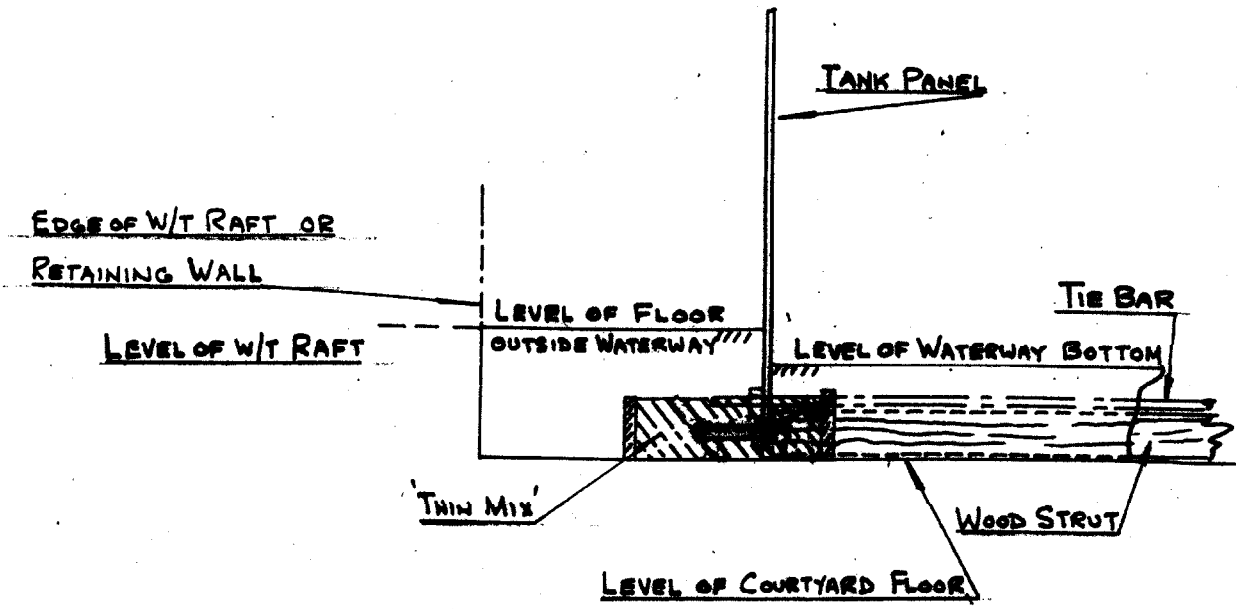

Appendix 5: Erection of the Rails and Supporting Structure.

The construction of the gantries from 9 inch. by 4 inch. 'I' section may be seen in Fig. 62; uprights were welded at their base to twelve inch square, 3/8 inch steel plates rag-bolted to the floor, plumbed vertical. Beams rested on, and were welded to, the top of the uprights and short lengths of angle rag-bolted to the retaining wall (in some cases, the cross beams were concreted into the 9 inch brickwork above the retaining wall). It had been intended to use fixing plates similar to those of the uprights with four bolts, but as the reinforcement was closely meshed and near the surface of the retaining wall, great difficulty was experienced in making the necessary holes for bolts and it was decided to use the alternative means of support. (Fig. 62 shows the arrangement.)

When the cross beams had been welded to the uprights, the structure was levelled with the aid of a 'dumpy' level, packing being inserted as necessary. Due to the difficulty of arranging holes in the concrete wall, a variation of $\frac{1}{4}$ inch was accepted in the heights of the cross beams along the waterway.

The longitudinal girders were erected in lengths of approximately 24 ft., joined when in position by butt straps; before being placed in position, the lengths were drilled as necessary to take the rail mounting and setting bolts.

Fairing longitudinally was from a piano wire stretched along the centreline between end gantries, and fairing vertically by 'dumpy' level, packing being placed where necessary between cross beams and girders when bolting. Bolts were used for all connections to facilitate dismantling and re-alignment if necessary. Although nominally, the girders were set 54 ins. apart, due to latent distortion it was possible to align each girder only to within ± ¼ inch from this. Vertical setting was within ± 1/32 inch. Both these values are within the range of adjustment allowed in the rail setting arrangements.

The Rails

Rails are of 35 lb/yard railway line mounted on its side with the head machined on all three faces to give smooth surfaces, as may be seen in Fig. 63.

To avoid vibration and heavy wheel wear, it was essential to obtain as true and smooth a running surface as possible and the rail head was machined carefully, first with a plane to remove the outer layers and give surfaces at right angles, then, after normalising, finely ground. Some difficulty was experienced in finding a firm willing to undertake and guarantee the result; finally a local firm agreed to do the work but could only handle the rail in lengths of 4 ft.-6 ins.

The problems involved in machining, mounting and aligning such short lengths had to be accepted, and it was hoped that the cross section shape and body of material would prevent excessive distortion while working, checks on random lengths of rail after delivery showed the 'spring' over each length had been kept well under 0.001 inch. in both horizontal and vertical directions. Butts were milled square.

The method of mounting and adjusting the rail lengths is shown in Fig. 63; each length is held by two short lengths of screwed rod, screwed into tapped holes in the vertical base and held by lock nuts, near each end and at mid-length. Horizontal and angular setting may be adjusted by the nuts where the screwed rod passes through the girder web. The holes in the girder web are over-size to allow the screwed rod an adjustment of ± 1/8 inch both vertically and longitudinally. Vertical adjustment is arranged at each setting position by bolts through the web of the rail section supported from angle brackets bolted to the girder; horizontal adjustment is allowed by the elongated hole in this bracket.

Alignment of the rails in the horizontal plane was achieved by use of two piano wires stretched lengthwise, from which the rail lengths were set by slip gauges. A hook gauge mounted on a specially designed clamp was used to set the height of each rail length above

the water, and angular alignment achieved by use of an accurate spirit level and straight edge.

The mounting of rails was commenced by setting one length horizontally and vertically by means of the slip and hook gauges, the top face being adjusted horizontally by use of the spirit level. The next length of rail was now butted against that already in place with surfaces fair, and the free end aligned with slip and hook gauges, together with the spirit level and straight edge. Both complete rails were erected in this manner, then checked for separation by a spacing bar and slip gauges and for horizontal upper surfaces by laying the straight edge transversly across both.

At the first attempt, when the rail lengths were being mounted and the Technicians inexperienced, the accuracy of alignment was about ± 0.004 to 0.005 ins., but this was considerably improved as the operators became used to the procedure.

Experiments indicated that experienced Technicians could align the lengths to within ± 0.001 ins. in the horizontal plane by using the slip gauges and piano wire and to within the same tolerance in the vertical plane using hook gauges.

Measurements on the rails some six months after the initial setting indicated misalignment of some lengths, the maximum being a of 0.003 ins. below the nominal level. There were no indications

whether the fall was due to movement of the supporting structure or the rail mounting arrangements; these faults were corrected and a check after a further three months indicated no further changes.

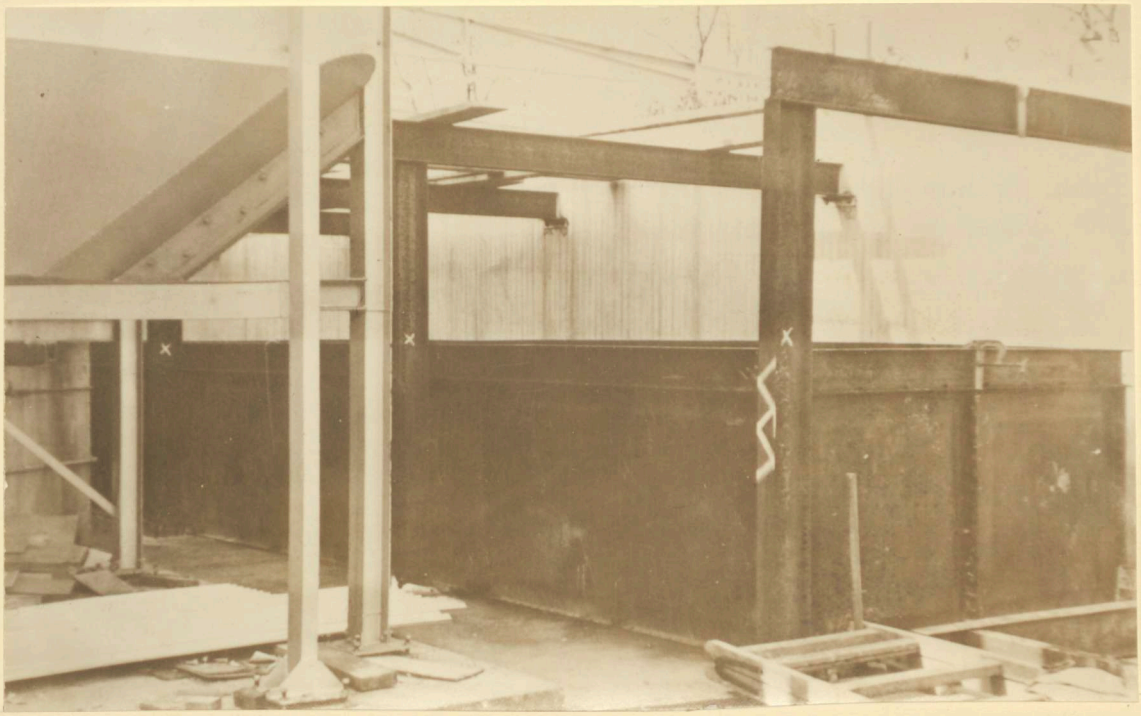

Fig.62. Arrangement of gantries for rail support.

fig 63 rail mounting and setting arr'g'ts

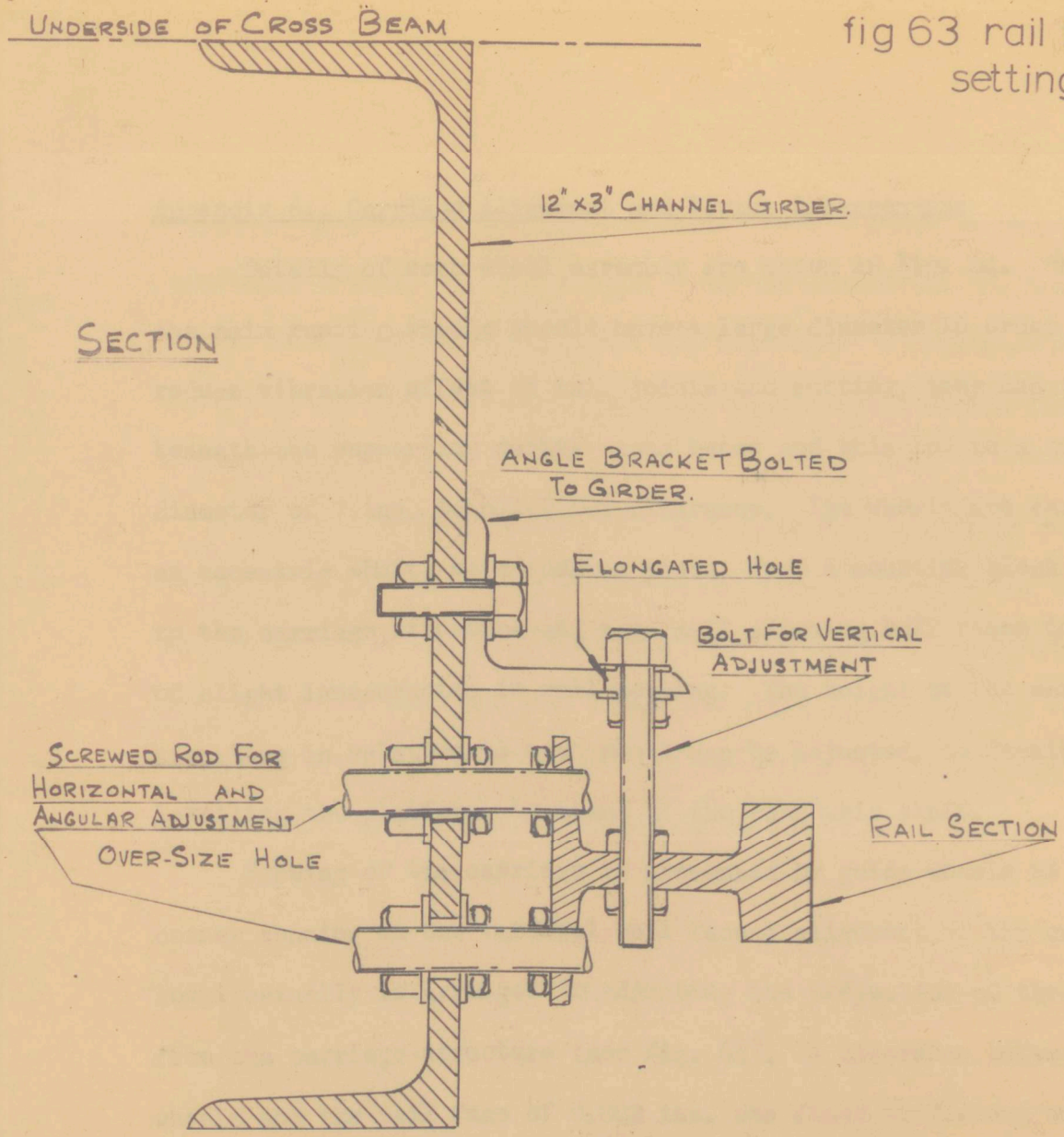

TION.

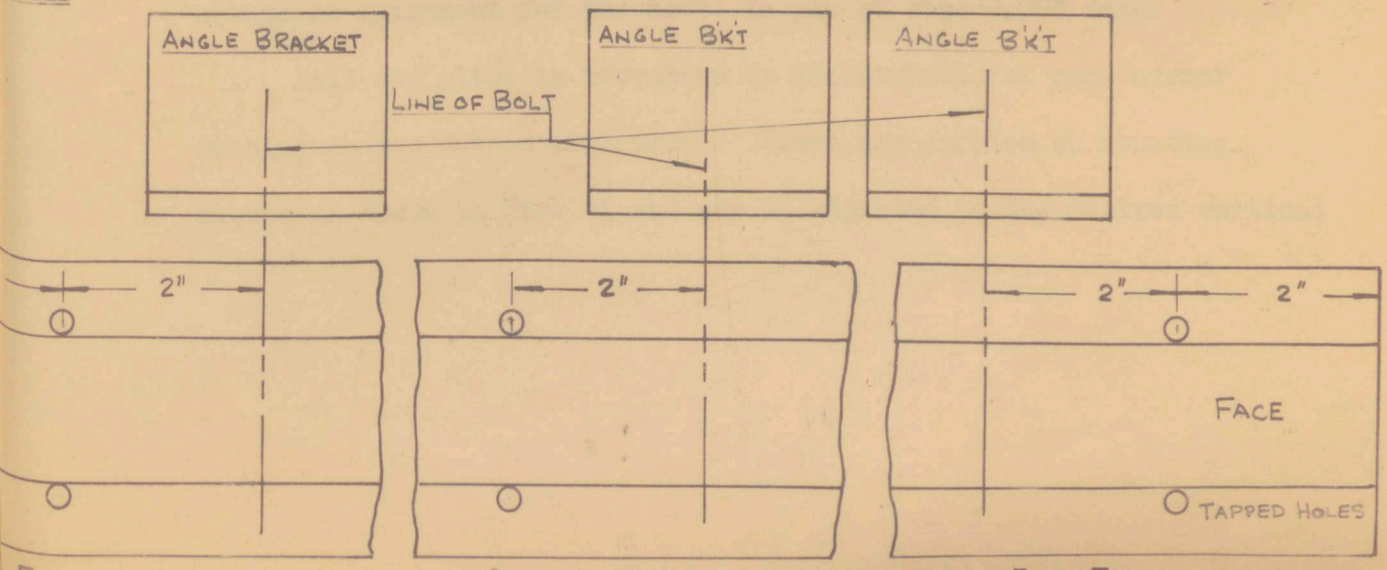

Appendix 6: Carriage Alignment and Towing Arrangements

Details of each wheel assembly are shown in Fig. 64. While the main running wheels should have a large diameter in order to reduce vibration effect of rail joints and rusting, they had to pass beneath the supporting gantry cross beams and this led to a maximum diameter of 7 ins. to allow for clearance. The wheels are carried on an eccentric shaft, by a spacing piece, from a mounting block attached to the carriage structure and have self aligning ball races in case of slight innacuracies in rail setting. The height of the carriage structure in relation to each wheel can be adjusted, to facilitate levelling the platform, by means of the eccentric shaft.

Skewing of the carriage is prevented by guide wheels at each corner running on the vertical rail faces; alignment of the carriage longitudinally is arranged by adjusting the projection of these wheels from the carriage structure (see Fig. 64). A clearance between the wheels and the rail face of 0.002 ins. was found sufficient to provide a free run without excessive skewing, so allowing a possible change in alignment for the model in yaw of some 0.003 degs.

Roll and pitch is prevented by guide wheels on each corner running on the bottom rail faces. These are carried on mounting blocks as shown in Fig. 64 and may be adjusted to the desired vertical

position by means of eccentric shafts. When placing or removing the carriage, the wheels may be swung clear by slackening the securing screw between the mounting block and carriage. A clearance of 0.002ins. between wheel and rail face was found desirable to obtain completely free running.

All wheels were constructed of Jabroc with a nominal concentricity of 0.005 ins; tests of the main running wheels after delivery showed that this had been obtained, and the running clearances detailed above indicate that under the worst combination of tolerances, the total errors of wheels and rail amount to less than 0.002 ins. between running and roll/pitch steadying wheels.

Arrangement of Drive Gear and Towing Cable

A Diagrammatic view of the Drive Gear layout is given in Fig. 65.

The output from the A.E.I. synchronous motor is taken via a reduction gear to the four speed motor-cycle gearbox/clutch assembly; the reduction gear is required here to bring the input R.P.M. at the clutch to near the usual value met with in motor cycles. This clutch/gearbox (a 1952 model manufactured by Associated Motor Cycles Ltd.) has input/output ratios between shafts of 2.65, 1.70, 1.308, 1.0. From its output spocket, the drive is led to three 3-speed cycle gearboxes (Sturmey Archer type A.S.C.) mounted in series, each having ratios of 0.75 0.9 and 1.0, output to input between shafts; and hence to the spocket on the winch drum shaft.

The two winch drums were manufactured from 6 in. diameter mild steel and keyed to a 2 inch diameter shaft carried in ball races. Each drum was designed to carry approximately 95 ft. of towing cable, more than sufficient for the travel of the carriage during each run. The arrangement is such that while the cable winds on to one drum, exerting a pull on the carriage, it unwinds from the other, the direction of motion of the carriage depending on the direction of rotation of the motor. A uniform feed of cable to and from the winch drums is obtained by the cable running in helical grooves cut into the drum surfaces.

From one drum, the cable is led, as shown diagrammatically in Fig. 66, over a 6 inch pulley mounted on a self-aligning ball race to allow correct feeding to and from the drum, along inside the channel section of the waterway top edge, and so over 2 inch diameter pulleys to the underside of the gantry cross beam at one end on the centre line of waterway, down the tank to a similar pulley on the other end cross beam, and so back over a second large pulley to the other drum. To tension the wire and provide damping against the tendency to surge, especially when accelerating through the clutch or stopping, on each side of the drive gear the wire is looped through a pulley which carries a freely hanging weight of fifteen pounds.

At the carriage, the cable passes through two clamping plates at the top of the towing post which enable rapid connection and disconnection.

When first erected, the cable of 22g piano wire was arranged in one continuous length between the winch drums, but in the event of breakage, replacement of the complete cable was necessary; in practice it was found to snap at or near its attachment to the towing post in nearly all cases of breakage, presumably due to the weakening effect of the clamping plate edges; to obviate the need to replace the complete length of cable, a short length of piano wire of smaller gauge was placed between the two lengths passing over the winch

From one drum, the cable is led, as shown diagrammatically in Fig. 66, over a 6 inch pulley mounted on a self-aligning ball race to allow correct feeding to and from the drum, along inside the channel section of the waterway top edge, and so over 2 inch diameter pulleys to the underside of the gantry cross beam at one end on the centre line of waterway, down the tank to a similar pulley on the other end cross beam, and so back over a second large pulley to the other drum. To tension the wire and provide damping against the tendency to surge, especially when accelerating through the clutch or stopping, on each side of the drive gear the wire is looped through a pulley which carries a freely hanging weight of fifteen pounds.

At the carriage, the cable passes through two clamping plates at the top of the towing post which enable rapid connection and disconnection.

When first erected, the cable of 22g piano wire was arranged in one continuous length between the winch drums, but in the event of breakage, replacement of the complete cable was necessary; in practice it was found to snap at or near its attachment to the towing post in nearly all cases of breakage, presumably due to the weakening effect of the clamping plate edges; to obviate the need to replace the complete length of cable, a short length of piano wire of smaller gauge was placed between the two lengths passing over the winch

drums, and connected to them by rigging screws. This arrangement has the additional advantages that cable tension can now be adjusted by the rigging screws, and that the position of the carriage on the towrope was immediately obvious after any period of separation.

To prevent injury from the wire while running, guard plates are fitted over all exposed parts of the wire in the main working areas.

Positioning and Aligning the Carriage

To place or remove the carriage, the four horizontal steadying wheels should be wound inward to give maximum clearance from the rails, and the four vertical steadying wheels swung inward by slackening the screws between their mounting blocks and the carriage. The carriage with the four main running wheels in position, may now be lifted slantwise to pass between the rails and then lowered down to its correct position. At this stage it is adviseable to align the carriage longitudinally, by adjusting the horizontal steadying wheels, to ensure that any travel does not cause the main wheels to jump the rails.

As the towing wire is set at the centre of the rail width within approximately 1/32 ins. at each end pulley, the carriage may be set along this axis by suspending plumb bobs from the two carriage end beams. It was found possible to align the carriage to within 1/64 ins. at each end by this method which could lead to a maximum error of 0.025°.

The height of the main running wheels may now be set to make the carriage platform level, or at any small angle required, by reference to an accurate spirit level or by use of the hook gauges set at each side and each end of the carriage structure in turn. The spirit level will give sufficient accuracy (1 min.) for normal work, but by use of hook gauges, the maximum difference in height of the sides could be set within 0.004 ins. (giving a maximum error in roll angle of 0.005°), and the maximum difference in height of the ends to the same accuracy, giving a possible error in pitch of 0.003°.

The vertical steadying wheels can now be set to the required clearance by use of the eccentric shafts and the carriage tow rope connected by means of the clamping plates on the tow post.

As a check on the accuracy of rail alignment and its effect on the stability of the carriage platform, the error in level, pitch and roll for 2 ft. intervals of travel down the waterway was assessed by mounting the hook gauges at each side and each end in turn. It was found that the maximum change in height at any gauge was within the limits of reading for the gauge i.e. 0.001 ins.

fig 64 detail of carriage wheel assembly

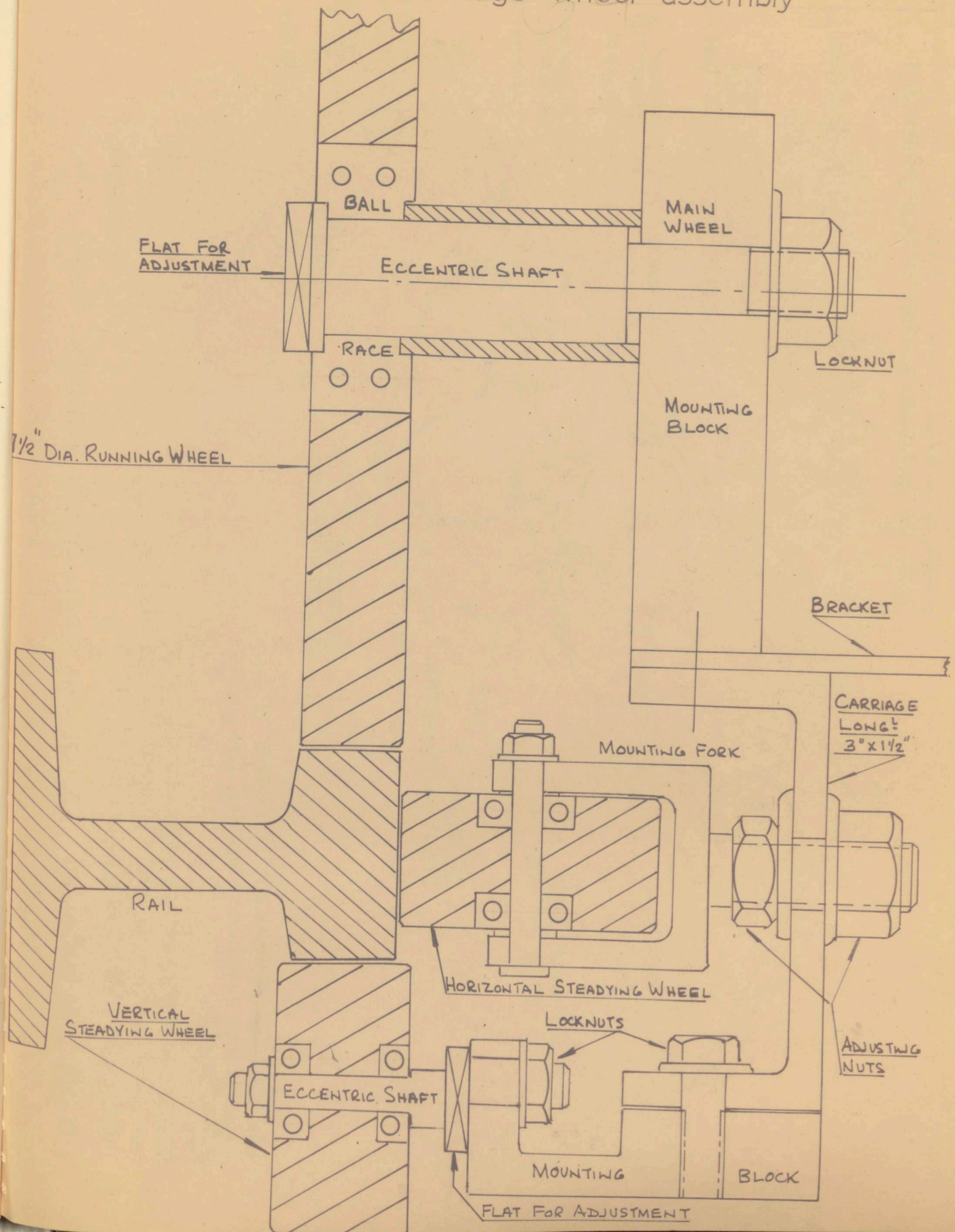

fig 65 arrangement of drive gear (diagrammatic only)

INPUT/OUTPUT RATIOS FOR GEARBOXES

1952 MODEL ASS. M/C. LTD CLUTCH/GEARBOX: 2·65, 1·70, 1·308, 1·0
STURMEY ARCHER 3-SPEED A.S.C. GEARBOX: 0·75, 0·9, 1·0

CHAIN DRIVES

MOTOR TO 4 SP. CLUTCH/G.B.: INPUT: STD. M/C. 3/8" PITCH.
4 SP. G/B TO WINCH SPROCKET: STD. CYCLE. 1/2" PITCH.

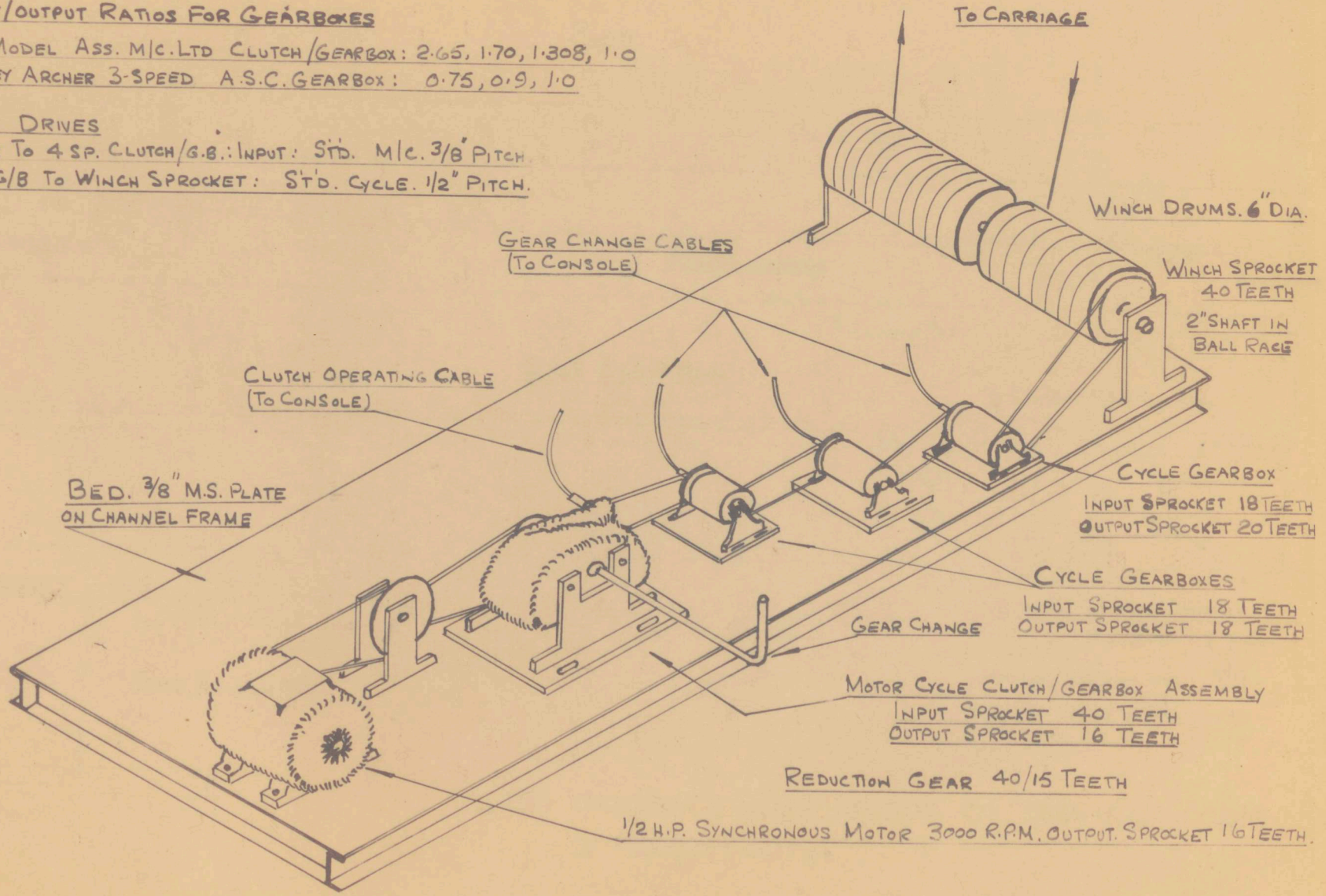

NOTE:- ALL GEARBOXES MOUNTED ON BASE PLATES WITH ELONGATED HOLES FOR HOLDING DOWN BOLTS, TO ALLOW ADJUSTMENT TO CHAIN TENSION.

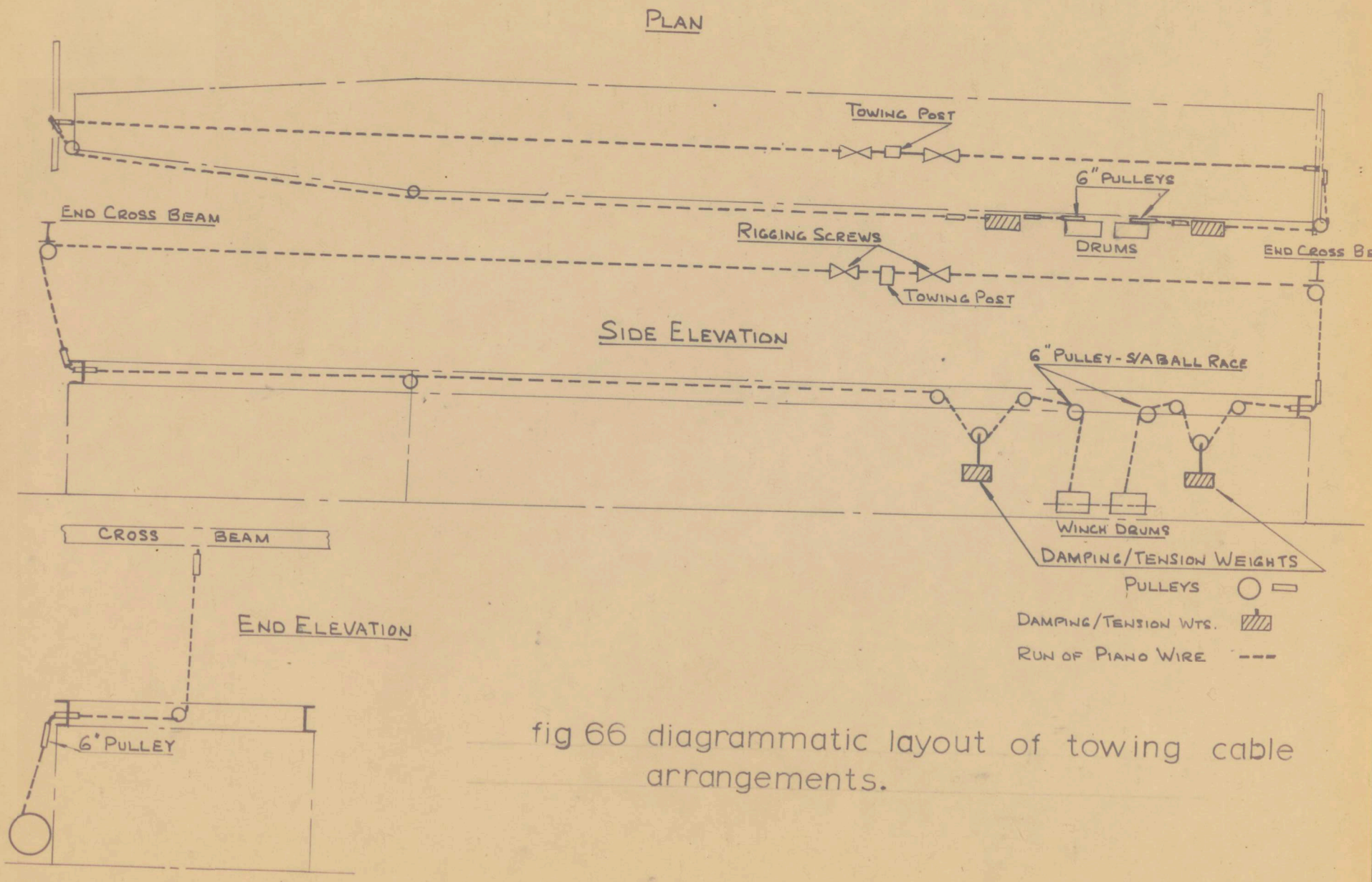

fig 66 diagrammatic layout of towing cable arrangements.

Appendix 7

Design and Manufacture of Balance Flexures

The arrangement of the balance flexures is shown in Fig. 47; each flexure was designed to be machined from solid bar steel with the end fastenings made encastre.

The design problem therefore became that shown in Fig. 67a, of a beam length 's', under a side force 'W' which displaces its ends a distance 'a' while under a tension 'P'.

The deflection 'a' is the relative movement of the two force plates considered, which is measured by the linear pick-offs, and the tension 'P' is due to the weight of that part of the balance below the flexure considered.

The problem amy be simplified to that in Fig. 67b, viz. two cantilevers having length $\ell = s/2$ under the loads W and P.

Using the usual methods, it can be shown that the deflection δ at the free end of each cantilever is given by:

$$\delta = \frac{W}{P}\left(\ell - \sqrt{\frac{EI}{P}}\tanh\sqrt{\frac{P}{EI}}\cdot\ell\right)$$

so that for the complete flexure,

$$a = \frac{W}{P}\left(s - 2\sqrt{\frac{EI}{P}}\tanh\sqrt{\frac{P}{EI}}\cdot\frac{s}{2}\right)$$

If the tension P is reduced to zero, then the expression for the

cantilever can be shown as reducing to

$$\delta = \frac{W\ell^3}{3EI}$$

the usual expression for a cantilever having a weight W at its free end; this will be seen to aid the calculation of flexure dimensions.

The required second moment of area for the flexure cross sections was calculated give deflections between respective force plates of 0.010 ins. under the loads designated as 'normal' in the specification. (6lbs. for side force and 3lbs. for resistance). The method of calculation is illustrated for the case of the Side force flexures.

These had to give a deflection (a in the expression) under a load (W) of 6 lbs. In their case the weight of the balance supported by the four flexures was approx. 50 lb., so that P = 50/4 lbs. 's' was set at 6 ins. to provide a convenient layout for the balance system, E being taken as 30×10^6 lb/sq. in.

Using the expression, it is difficult to obtain I the required second moment of area in terms of the remaining quantities, but reference to the simplified case of the cultilever without tension-load, indicates that a reasonable value for I is 0.003 in^4 (for four flexures.)

Using this value in the complete expression, gives a deflection of 0.0096 ins. so that for normal calculations, it would be sufficient

to consider the flexures as double cantilevers, giving the second moment of area $I = \frac{WS^3}{12Ea}$

This simplified expression was used to calculate the particulars for both side force and resistance flexures, and gave:

I, side force = 0.003 in^4 for a total of four flexures.

I, resistance = 0.00015 in^4 for a total of four flexures.

It was also necessary to choose the ratio of thickness to breadth for flexures to obviate any poisson ratio effect due to application of loads at right angles to those being measured, but as the linear pick-offs measure the actual deflection between plates, any cross coupling due to deflections about the minor axis is obviated.

With 5/8 ins. hexagonal bar, the thickness of each flexure to give a deflection of 0.010 ins. under normal loads was approx. 0.12ins. for side force, and 0.095 ins., for resistance.

Experience at the N.P.L. indicated the use of steel to B.S.S. EN27 (S96) for manufacture of flexures in order to gain repeatability and absence of hysterisis effects about the zero.

Considerable difficulty was experienced in obtaining steel to this specification; it was finally purchased from Folland Aircraft Ltd., first as half inch bar, and later as 5/8 inch hexagonal bar.

Due to its hardness, great difficulty was encountered in

machining the flexures from bar; it was found that normal mill tool cutting edges were not sufficiently strong and soon became chipped; problems also arose in preventing 'spring' while machining the long straight section, a situation exaggerated by the difficulty of holding round bar on the machine bed. The use of hexagonal bar obviated this last trouble, and from experience it was found that the machining process illustrated in Fig. 68 reduced 'spring' to a minimum.

Despite this approach, it was extremely difficult to machine the flexures below 0.12 ins., and after several attempts it was considered adviseable to accept resistance flexures having thickness of some 0.105 inches in order to achieve four of uniform dimensions. This reduced the maximum deflection between resistance force plates under normal loads. but was accepted for the preliminary model tests which were to follow.

fig 67 calculation of flexure size – assumptions and definitions.

FIG 67b HALF FLEXURE

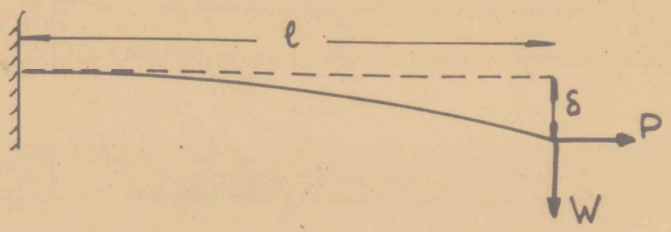

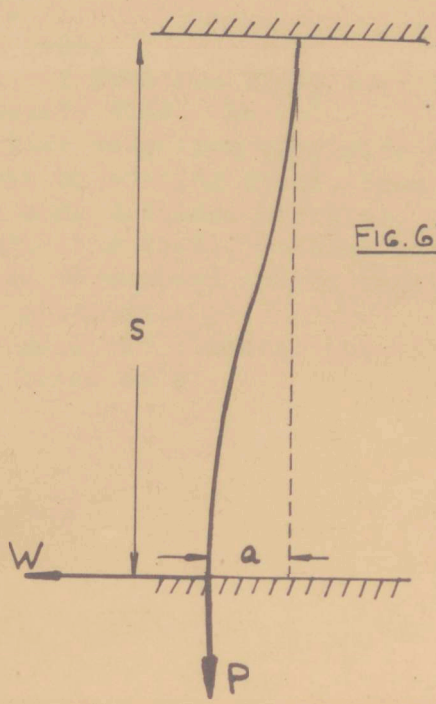

FIG. 67a COMPLETE FLEXURE

APPENDIX 8

Operating Procedure for Towing Tank

1. The following discipline should be observed regarding run timing:

(a) Ignore the first run of the day, which should be made at a speed of around 4 ft/sec.

(b) Allow six minutes between runs and keep to this frequency.

(c) If a time interval of over half an hour should occur between runs, the first run afterwaads hould be made at about 4 ft/sec. and the results ignored.

2. The heel unit and two dimensional balance should be calibrated before starting a series of runs as follows:

(a) Disconnect towing wire from the carriage clamp and ensure that it is free to lie centrally along the tank centre line. Move the carriage so that the model attachment post is some eight feet from the Eastern end of the Waterway, and secure by use of wedges beneath one wheel.

(b) Apply the resistance calibrating weight by hooking the cord round the post, ensuring the pulley runs freely. The cord may be checked for alignment by use of plumb bobs suspended from the tow wire; these should hang in the water to damp movement, and be spaced some 6 ft. apart. Cord level may be checked from the water

surface by use of a normal scale, ensure there is no movement of the Side force meter when the calibrating weight is applied. If movement occurs, then the balance must be rotated so that the resistance flexures are correctly aligned as shown by the side force meter remaining static when weight is applied.

(c) Remove calibrating weight, arrange the required offset for the resistance transducer core (0.004 to 0.005 ins.), and zero the meter.

(d) Set the meter maximum scale reading by applying the necessary calibrating weight. This is likely to alter the zero setting of the meter, but several adjustments of zero and full scale will bring both to their correct settings.

(e) Remove the resistance calibrating weight and run the carriage back so that the model attachment post is square to the pulley for side force calibration which is situated on the waterway side at the model handling platform.

(f) When the carriage is seen by eye to be nearly at its correct position, apply the side force calibrating weight by hooking the cord round the model attachment post. The carriage may now be positioned by means of wedges until the application of weight results in no movement of the resistance dial.

(g) Remove the weight and set the meter zero. Set the maximum

scale and zero as described for resistance.

(h) Remove all calibrating weights and wedges, reconnect towing wire to carriage and the model is ready for running.

NOTE: (1) It may be advisable to check model alignment periodically,

(2) Calibration should be checked roughly, to ensure its stability, after approximately every six runs. Providing sharp changes in temperature have not affected the electronics, no variation will be found. This rough check need not be so concise, it is usually sufficient to position the carriage opposite the side force pulley and apply resistance calibrating load there also. Indication that a check in calibration is needed will be found in small changes of meter zero that fail to disappear when a small displacement is given to the lower force plate and then removed.

(3) The electronics should be allowed at least ninety minutes to warm up and stabilise their temperature before use.

3. Run Procedure

(a) Check that the carriage is free from all wedges, clamps on rail, tools projecting from platform etc. and that all calibrating weights have been removed. Also check that travelling cable is free on its runners.

(b) Withdraw clutch approx $3\frac{1}{2}$ complete turns of the handle from its fully in position; on no account must it be wound out more than

4 turns as this may result in cable breakage or the clutch mechanism jamming inside the gearbox.

(c) Press 'READY' button, check operation (denoted by small click).

(d) Press 'FORWARD' motor start button; if the motor fails to start, this may be due to failure of the READY button to function, or because one of the photo-electric relays is not operating correctly. The latter are set to 'fail safe' and a bulb may have burnt out or be mis-aligned with respect to its light sensitive element.

(e) Select gear required; although it will be found possible to seledt the cycle gears without the motor running it is not adviseable and may cause mis-alignment of the gear wires. It is usually not possible to select the motor-cycle gears with motor stationary.

(f) Ensure the waterway is clear, then engage the clutch smoothly, allowing it to slip when the model first begins to move. It is essential that while achieving a rapid run-up to speed, the clutch is handled delicately and smoothly, as the quality of model measurements is dependent on this.

(g) When the carriage reaches the start of the timed run, the photo-electric relay switches on the Dekatron counter; at the end

of the timed run, the counter is switched off by a further relay; if this fails to operate, a second some three feet further on will shut off the counter and the motor. As the time for the run is known closely, indication of failure in the first end stop is given by the run time over-running on the counter; if this occurs, the console STOP button should be depressed immediately.

(h) When the run is completed, withdraw the clutch, press the motor REVERSE button, select gear 1.333 and engage the clutch smoothly to make the return run. An end stop relay at the Eastern end of the waterway will halt the carriage from this speed at the required position for adjustment and the following forward run.

If a model is connected to the carriage, it should normally not be run back at a speed in excess of the gear setting quoted, as the model leeway angle may change as it passes sternwards through waves. If at any time the carriage is run back at greater speed, then the console STOP button must be used as the end stop is positioned to cater for low speeds only.

(j) At the end of the return run, withdraw clutch and prepare for the following forward run. It will be found that the six minute interval is sufficient to allow the check calibration to be made if required.

(k) At the end of a period of running:

(a) Leave clutch wound in.

(b) Leave motor cycle gear box in neutral, cycle gear-boxes in top gear.

(c) Switch off electronics unless further work is contemplated. Adequate warming up time must be allowed for the electronics to avoid small changes in meter setting during early runs of a series.

(d) Switch off building lights but NOT heaters.

APPENDIX 9

List of Drawings giving Details of Towing Tank

Drawing Number	Title
AE/TT/1	Drive Unit for Towing Tank Winch Structure
2	General Arrangement of Tank Structure
3	Testing Tank Carriage (G.A.)
4	Carriage Bogie Unit
5	G.A. Two Component Balance
6	Balance Details (3 sheets)
7	Mounting Brackets for Drive Components (2 sheets)
8	Drive Components
9	Balance Flexure
10	Rail Support and Adjustment Arrangements
11	Rail Alignment Jig. (Rail Clamp)
12	Rail Alignment Unit (Hook Gauge)
13	Control Console
14	Turntable G.A. (Balance)
15	Turntable Top Plate
16	Turntable Backing Plate
17	Turntable Mounting Plate

18	Towing Bracket for Carriage
19	Universal Joint Details (Balance)
20	Mounting of Differential Transformer Pick-Offs.

PART 3. MODEL EXPERIMENTS

CHAPTER 18: INTRODUCTION

Since the early work of Davidson (Ref. 9) which established the basic concept of splitting the total hydrodynamic force on the yacht's hull into three components as an aid to study, very little published data has been made available from which the hydrodynamic characteristics of a hull could be established over a wide range of conditions, both within and outside the sailing envelope.

By far the most part of experimental work on hulls has been the result of routine commercial testing for various designers or for the Yacht Research Council, at the Davidson Laboratory, the National Physical Laboratory and the Saunders Roe Division of Westland Aircraft Ltd; the number of runs and coverage of conditions in each case has been too restricted to allow their use in more general work.

The surge back to popularity of Twelve Metre Yachts resulted in the Saunders Roe Division undertaking an extensive programme of tank tests on a variety of these models for the Red Duster Syndicate; unfortunately due to the cost and the heavy competition for the America's Cup, the results are unlikely to be made generally available in the near future, although some data believed to come from this work has been included by Crewe (Ref. 15) in a very recent paper read

before the Royal Institution of Naval Architects.

H.M. Barkla has recently undertaken a series of model experiments at the Davidson Laboratory, the results of which are not available although he is believed to have studied a series of models using the established Gimcrack Technique to establish their variation in performance with changes in hull proportion. It is not known whether the results give a sufficient coverage to enable more general characteristics to emerge.

The lack of information concerning the hydrodynamic characteristics of sailing yachts of normal size has hampered the development of a more generalised analysis of performance than that originally established by Davidson, and now used in a modified form during routine tank testing and comparative performance prediction.

CHAPTER 19: OBJECT AND LAYOUT OF EXPERIMENTS

19.1 Object of Experiments

Existing results of model tests are unsuitable for use in a general manner with the performance analysis of Part 1., and the primary purpose of the present work was to obtain a typical set of 'hull characteristics' in the form required for the analysis, by measurement of the relevant quantities.

In addition, further model tests were made to determine various properties of the model.

The object of the experiments may therefore be summarised as:

(1) To obtain and examine a set of hull characteristics as required for the performance analysis of Part 1, extrapolated to a full scale yacht at one A.U.W. and C.G. location.

(2) To study the upright, zero leeway, resistance and its variation with course velocity.

(3) To compare the measurements made during these experiments with those obtained during previous work with the same model.

(4) To study the hull's transverse stability under static and dynamic conditions.

(5) A brief series of experiments to determine the effect on the hull properties of changes in: All-Up-Weight (depth of hull immersion),

C.G. location, rudder application.

(6) To investigate the variation in hull wetted area with course velocity, leeway, and heel; the wetted surface of the model and full size yacht is of importance when determining the skin friction resistance during the scaling up process from model to ship, discussed in Chapter 20; with a yacht it might be expected to vary considerably with speed and hull attitude and this investigation was undertaken to provide a preliminary assessment of these changes.

19.2 Layout of Experimental Work

Range of variables

A yacht may work under conditions which vary widely in terms of true wind velocity and sea conditions, and any comprehensive series of model tests must cover as much of this range as practicable.

The course velocity may vary from practically zero to a maximum set only by the ability of the vessel to sail, and these two extremes are difficult to simulate in experimental work.

At the lower end of the velocity scale, the model used in a small tank is subject to an unknown flow state in the boundary layer as the stimulation of turbulence is usually ineffective at the low Reynolds Numbers involved; results are likely therefore to be meaningless and impossible to extrapolate to a full size vessel if

required. In the case of the model used in these tests it was found that the minimum course velocity to give repeatable results with effective turbulence stimulation was around 1.54 ft/sec. (see Chapter 16, Part 2, describing tank evaluation.)

At the higher speeds, an actual yacht is likely to be working in high and confused sea conditions, so that results from tests in smooth water are unlikely to apply. With the present state of knowledge, however, the understanding of smooth water preformance is far from complete, and work on this must be advanced before performance under more complicated circumstances is attempted.

In practice, the maximum speed-length ratio ($V/\sqrt{L}$) attained by displacement yachts is agreed to be around 1.4, and this set a nominal upper limit of course velocity for the runs.

The attitude adopted when sailing depends on a combination of the sailing geometry, hydrodynamic properties and aerodynamic properties of the yacht.

Leeway may vary from 0° when running to a maximum believed to be around 6° to 10° when close-hauled, depending on the type of yacht; Ref. 13 gives a maximum of about 6° obtained during full scale performance trials of the 5.5 metre yacht 'Yeoman IV'. A range of leeway between 0° and 12° was therefore adopted for the tests.

Heel while sailing may vary from zero while on the run or a broad reach to a maximum depending on the vessel's stability and the overturning couple from hull and sails. The maximum usually adopted in tank tests is 30°, but in the case of the model used in the experiments attainable heel was restricted to about 22°; above this angle, the deck edge became immersed and the model shipped water. Conversation with owners and experience while sailing the type of craft suggests that this is likely to be near the maximum heel in practice, while Refs. 1. & 12 indicate that the maximum heel angle achieved in previous work with the model in tests simulating actual sailing conditions was around 19°.

Details of the range of course velocities, A.U.W., C.G. location, model attitude, and measurements made will be found in the description of each series of experiments given in Chapters 21 to 26.

A description of the balance and associated arrangements for measuring the required quantities will be found in Part 2; they were developed in conjunction with the same model so that details of measurement, accuracy, and geometry apply to these experiments.

Flexibility of the balance design enabled measurement of the hydrodynamic force components using either 'Sea' axes or 'Body-Sea' axes; as the present work was designed to obtain information of use in the performance analysis and to establish the hull characteristics, force components were measured using the 'Body-Sea' system of axes.

Hull characteristics used in the work of Part 1 to evaluate the performance analysis were required in terms of the full scale yacht, and the expansion of results from model to full scale is discussed in Chapter 20. Applicable results from the experiments were scaled up in a simple manner to provide this data, an account of the scaling used in each case is given in Chapters 21 and 22.

19.3 The Model

Immediately available was the model used in work to evaluate the use and capabilities of the tank, described in Part 2.

Manufactured originally by the Saunders Roe Division of Westland Aircraft Ltd., and used by them in work for the Yacht Research Council, the model was nominally a one-sixth scale hull of a Dragon Class One Design yacht. Particulars of this hull and the previous series of tests will be found in Ref. 1. The model had been presented to the University by Saunders Roe Division for use during wind tunnel work, and some modification and damage had occurred. Due to its age, the various modifications, damage, poor storage, and use, some distortion was evident, so that doubt must exist whether in fact it represented the hull of a 'Dragon' during these experiments; Crago (Ref.4) gives a life of one year for a model before re-cutting

may be advisable, and this model was some seven years old at the time of use.

For the present experiments, the model should therefore be considered as merely a 'typical' hull for use in obtaining a 'typical' set of characteristics and their variation with the various parameters involved.

The original surface finish was varnish, but this had deteriorated badly, and the hull was re-finished in while enamel paint to give a good surface which would also provide a reasonable background for the photographic work required during the wetted surface investigation.

Details of the model mounting and arrangement will be found in Part 2.

19.4 Sequence of Experiments.

To satisfy the objects stated previously with a minimum number of test runs, the following sequence of experiments was adopted:

(1) Measurement of the hull's transverse stability under both static and dynamic conditions at one A.U.W. and C.G. location, designated the 'Standard' condition, and the effect on stability of changing the V.C.G.

(2) Measurement of the hydrodynamic force components F_X and F_Y

associated with the hull in the 'standard' condition over a wide range of course velocity and hull inclination.

(3) A study of the upright resistance.

(4) A brief series of experiments to study the effect of variation in A.U.W., L.C.G. location, and Rudder Application.

(5) A series of runs to determine the variation in wetted surface with model velocity, and hull inclination.

The results of these experiments have been used, as detailed below, to satisfy the objects of the work set out in section 19:

(a) Results from (1) & (2) were used to determine and examine the typical hull characteristics required for use with Part 1, see Chapter 21.

(b) Results from (3.) have been used in Chapter 22 to study the hull's upright resistance.

(c) Results from (2) and (3) have been used in Chapter 23 to compare the results of these experiments with those obtained during previous work with the model at Saunders Roe Division, and available data on other hull forms.

(d) A study of the hull's transverse stability is made in Chapter 24 using results from (1).

(e) The effect of L.C.G. position, and A.U.W. on the close hauled

performance and upright resistance is studied in Chapter 25 using results from (4).

(f) Rudder Application and its effect on the vessels performance is discussed in Chapter 25, using results from (4).

(g) The variation in wetted surface is studied in Chapter 26, using results from (5).

In all, these experiments occupied fourteen weeks, and a total of some three hundred and thirty six 'useful' runs were made (as distinct from runs made to set up the model, and check runs.) Check runs were made of approximately 25% of the points to ensure correct and repeatable results were obtained from the tank. In future work, these check runs would not be necessary as the agreement was found to be excellent; they were used here as a precaution during the first scale 'production' operation of the Facility.

CHAPTER 20: EXPANSION OF MODEL TEST RESULTS TO A FULL SCALE YACHT

It is often necessary, especially during the routine tank testing of yacht hulls for performance prediction, to scale up the results for applied moment and hydrodynamic force to a full size vessel.

Until the present series of tests, the force components have been measured using a system of 'Sea' axes, and were the quantities Side Force and Resistance, equivalent to aerodynamic Lift and Drag, required for the full scale performance prediction using established methods developed from the work of Davidson.

Fig. 69 shows the side force and resistance in plan view using the established Course/sea axes.

FIG. 69. HYDRODYNAMIC FORCE COMPONENTS IN HORIZONTAL (SEA) PLANE WITH 'SEA' AXES.

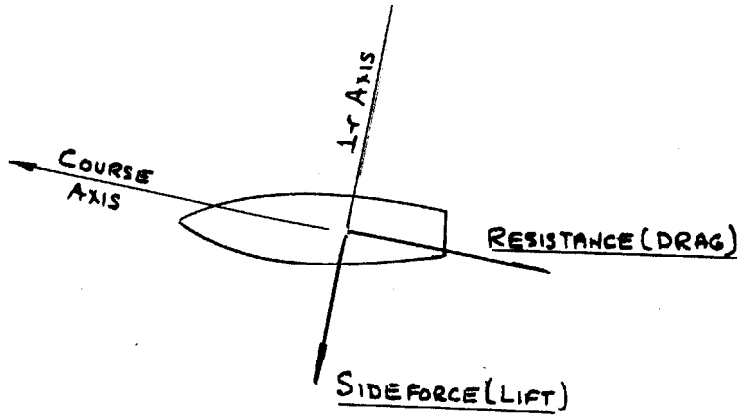

The scaling-up of these force components and moments has necessitated the usual assumptions and scaling methods used in the extrapolation of tank tests on ship models. In fact it is not yet established whether the traditional method of scaling up resistance is permissible with yacht forms.

Resistance

The most difficult component of force to expand is the resistance, and the usual techniques dictate the method of tank testing.

It is well known that the resistance of a ship is a function of Froude Number, Reynolds Number and Form.

$$\text{i.e.} \qquad R_{total} = F(Fr, Re, form)$$

The direct use of this in scaling up model results is impossible, however, as the full size Froude and Reynolds Numbers cannot both be satisfied at the same time on the model scale. In practice, the Froude Number is maintained constant, and the model run at the same $V/\sqrt{L}$ required for the ship; there are two main reasons for this: the correct Reynolds Number would lead to extremely large model velocities, impossible to attain, also the friction resistance due to Reynolds Number is more easily approximated than would be the portion of resistance controlled by Froude Number.

As originally proposed by William Froude, it is taken as a first

assumption that the total resistance can be split into two parts, one controlled by Reynolds No. (Friction Resistance), and one by Froude No. (Residuary resistance).

i.e. $R_{total} = R_F + R_R$. R_R is residuary resistance

R_F is friction resistance.

Where R_R for a ship is made up of both form and wave-making resistance.

In the case of a yacht, when the hull is making leeway and producing Lift, the induced resistance is considerable and must be included under the heading of form resistance, which will therefore change with leeway.

The friction resistance is approximated for both model and ship by the use of coefficients at the respective Reynolds No., taken for an equivalent flat plate.

When scaling up, the estimated friction coefficient of the model is subtracted from the total coefficient to give the residuary coefficient:

$$\text{i.e. } C_R = C_T - C_F \quad \text{(estimate for model)}$$

C_F for the ship is now estimated from the established data and added to C_R giving the total resistance coefficient for the full size ship. To this coefficient may be added a roughness allowance for the full size vessel, which varies according to the practice of the the establishment undertaking the tests, and according to the

friction data being used. The various formulations, each of which claim to give the true variation of friction coefficient with Reynolds No. give different values and much of the roughness coefficient may be used to 'iron out' the differences, according to the experience of each tank.

It has been recognised for many years that although model experiment tanks have a wealth of experience in applying this type of extrapolation, and much feed-back data from trials to assist in making a very close approximation, the method is not entirely satisfactory. Basically, the resistance should not be separated into the two components, but as this is necessary to permit scaling up, then there must be cross-coupling effects between the two parts; in particular the friction resistance is dependent of hull curvature as it acts tangentially at every point and also on the local velocities which are not constant over the surface due to the pressure field; similarly, the form resistance will be affected by the boundary layer and hence Reynolds No.

The difficulties of scaling up are multiplied in the case of a yacht because of its unsymmetrical travel along the course, the pressure distribution is complex and unsymmetrical, resulting in a non-uniform wave formation on each side of the hull, a large form or induced resistance, a wetted surface which may vary considerably, a variation

in the wetted length, and a considerable variation in local velocity over the hull surface. The position is further confused by part of the resistance acting along the centre-line (principally friction) and part along the course.

It would be fortunate therefore, if the same methods which have proved satisfactory for large-ship work could be applied unchanged for yachts.

Of great importance during the tests is the state of flow in the boundary layer. In order to gain repeatable results and to calculate the friction resistance for both model and ship, it is necessary to know the flow state in both their boundary layers.

On the model scale, it is usual to make the boundary layer fully turbulent by means of stimulators as it would be impracticable to maintain laminar flow over the whole wetted surface.

In the case of a ship, it is assumed that the boundary layer is fully turbulent, which must be a very close approximation to the truth, expecially under all but dead calm sea conditions.

Whereas the prime concern in ship testing will be to obtain accurate predictions around the upper region of speed, with a yacht whose speed range will vary from zero to a maximum controlled by the design and sailing conditions, the whole range is important.

A full size yacht is of a length and a form which could lead to the flow being largely laminar, especially on the pressure side when making leeway at low speeds when the water will be reasonably still. At high speeds it may be that the natural turbulence from the distrubed free-water conditions causes a completely turbulent boundary layer, but this is not confirmed as yet.

In addition therefore, to the other problems peculiar to yachts, the computation of full-scale friction resistance is complicated by this uncertainty; it must also be queried whether the separation points and forms are similar for model and yacht.

Although there are many problems in the use of established procedures with yachts, there is the advantage that for many craft, their length is such that it is only marginally greater than models used in the larger tanks. Correlation over the model range is well established, so that here is one factor supporting use of the method.

Despite the lack of understanding in the situation, the method is used by tanks when predicting full scale performance; unfortunately andy feed-back from full scale yacht trials to confirm this prediction is expensive, difficult and infrequent. The main claim th accuracy lies in the fact that yacht designers have found it pays them to have their designs tested, the resulting improvements being well worth while. (Ref. 4).

Side Force

The expansion to full-scale of side force measured perpendicular to the course is met with primarily in yachts, and no work on it is available.

As the skin friction on the hull acts along the body and not the course, and the full-scale coefficient is smaller than that on the model scale, the full-scale side force will be reduced by a small amount as shown in Fig. 70.

It appears to be assumed in commercial work that the effect of Reynolds No. is unimportant, and that the coefficients at comparable speeds are identical for model and yacht; (ref.5).

FIG.70. SCALE EFFECT ON LIFT (SIDE FORCE)

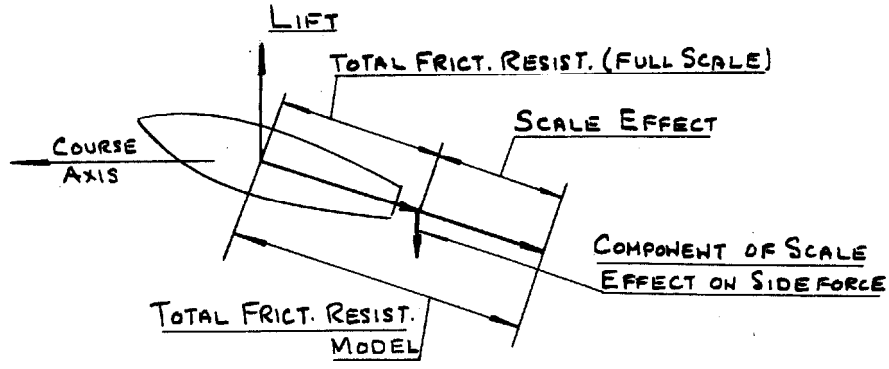

Body/Sea Axes

When using these axes, the two horizontal components of force are measured parallel and perpendicular to the yachts centre-line,

the X axis being the centre-line and the X-Y plane parallel to the sea (fig. 71)

Part of the force F_{X_W} (equivalent to friction resistance) acts along the axis (C.L.) and part along the course. The scaling position is no clearer than with the established axes, and there seems no reason to believe that the traditional method of extrapolation should prove any less reliable.

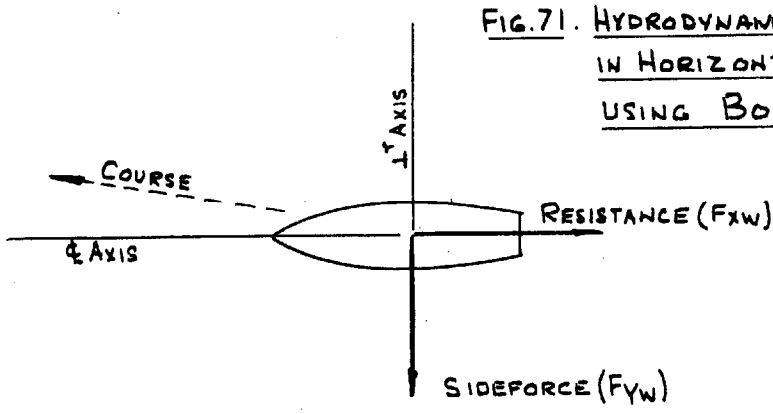

FIG. 71. HYDRODYNAMIC FORCE COMPONENTS IN HORIZONTAL (SEA) PLANE WHEN USING BODY/SEA AXES.

The expansion of F_{Y_W} to full scale is not complicated by skin friction scale effect, the component being largely due to the pressure distribution over the hull surface. Although it is unlikely that Reynolds No. effects are entirely missing, without further knowledge it appears necessary to assume that F_{Y_W} is independent of Reynolds No. for scaling purposes.

Stability Moment

The moment acutally required during experiments, for the purpose of Part 1, is that necessary to heel the yacht to a certain

angle. As such, it involves the movement of a weight through a known distance, so that no complications arise in the scaling to full size. The question of stability under dynamic conditions is considered at greater length in Chapter 24.

CHAPTER 21: HULL CHARACTERISTICS FOR USE WITH THE PERFORMANCE ANALYSIS OF PART 1

In its basic form, the analysis of Part 1 requires hull characteristics as curves of C_{Yw}, K_{Xw} and λ plotted against $\frac{C_{Yw}}{C_{Xw}}$ for a number of values of V_S at several angles of heel.

This called for F_{Yw}, F_{Xw} and M_{Xw} to be measured at a particular combination of θ, λ, and V_S. In practice, the model was set at the required heel angle with the model travelling at the particular course velocity V_S. F_{Xw} and F_{Yw} were measured directly and the position of the sliding weight gave the models restoring moment M_{Xw}. C_{Yw}, C_{Xw} and K_{Xw} could now be calculated and hence curves drawn of C_{Yw}, K_{Xw}, and λ against $\frac{C_{Yw}}{C_{Xw}}$ for various constant values of θ and V_S.

In these experiments the position of the sliding weight to give the desired heel angle a each combination of λ and V_S was interpolated from the results of runs to give the stability information required for Chapter 24 and which had been carried out previously, and rechecked.

During the experiments, F_{Xw} and F_{Yw} were measured at the following combinations of V_S: 1.90 ft/sec. ($V/\sqrt{L}$ = 0.602), 2.97 ft/sec ($V/\sqrt{L}$ = 0.904)

3.86 ft/sec. ($V/\sqrt{L} = 1.22$), 4.55 ft/sec. ($V/\sqrt{L} = 1.44$)

Heel, θ :0°, 7½°, 15°, 21½° (maximum restricted by immersion of deck edge)

Leeway: 0°, 3°, 6°, 9°, 12°.

The value of the sliding weight necessary to provide 21½° heel led to the model being over the scale A.U.W. for a 'Dragon' class yacht and the particulars of the model condition during test i.e. 'Standard Condition' were:

Standard Model Condition.

Model All Up Weight.	24.89 lb.

(equivalent to a full size displacement of 5380 lbs. i.e. approx. 48 cwts)

Sliding weight	6.33 lb.
V.C.G.	1.74 ins. below datum
L.C.G.	29.3 ins. forward of datum

(datum for C.G. location is height of deck at side amidships and extreme A/E. of Hull).

Freeboard	forward	3.5/8 ins.
	Aft.	2.5/8 ins.
Maximum draught, static		8.7/16 ins.

Pivot of Universal Joint 2 ins below datum

31.2 ins forward of datum.

The standard condition is illustrated in Fig. 72.

Experimental Results for F_{Xw} And F_{Yw} and scaling to Full Size.

The values of F_{Xw} and F_{Yw} are recorded in Table 7 and these were placed in coefficient form at the model scale from:

$$C_{Yw} = \frac{F_{Yw}}{\frac{1}{2}.\rho.A.V^2}$$

$$C_{Xw} = \frac{F_{Xw}}{\frac{1}{2}.\rho.A.V^2}$$

where ρ = water density at 60°F.

A = static upright wetted surface in ft.^{2}.

V = Model Course velocity in ft/sec.

In the light of discussion contained in Chapter 20, it was assumed that C_{Yw} for the model and full scale are identical and these are shown in Table 8.

The scaling of C_{Xw} from model to full size has been discussed in Chapter 20; due to the complexity of the problem and to the fact that the full scale values are required only for use in demonstrating the performance analysis of Part 1, rather than for the prediction of performance for an actual yacht, the following procedure and assumptions were adopted:

(a) The Schoenherr friction formulation has been used to determine model and yacht friction resistance coefficient, this data being that

used by the Davidson Laboratory; in the United Kingdom it is more usual to use the I.T.T.C. correlation line as the Schoenherr values are said to be somewhat low at Reynolds Numbers in the small model sphere. There is no reason why, for the present purpose, any one line should be preferred, and Schoenherr was used owing to the data being available immediately.

(b) In computing the friction resistance, the hull wetted surface area has been assumed constant, and equal to the upright static value of 4.43 ft^2 (see Chapter 26). This is the usual assumption made by Saunders Roe Divn. in their work with yachts (Refs. 4 & 5) and simplifies the scaling procedure considerably.

(c) The wetted length for computation of Reynolds Number has been taken as that in the static upright condition, equal to 3.48 ft. In fact the wetted length altered appreciably, being considerably increased at high speeds when the wave profile moved up the stern overhang. This assumption is used by Saunders Roe Division in the form of a mean chord; (Refs. 4 & 5).

(d) The laminar flow deficit from the smooth turbulent condition because of the area in front of the stud turbulence stimulators

has been assumed equal to the increase in resistance from the stimulators. This is not strictly correct, but satisfactory for the present purpose; according to Crago (Ref. 4) the "two practically cancel" and this assumption obviated a tedious calculation.

(e) Turbulent flow has been assumed to exist over the hull of the equivalent full size yacht, a normal assumption in this type of work.

The full scale C_{X_w} is therefore calculated from:

C_{X_w} (full scale) = C_{X_w} (model scale) - C_F (model) + C_F (full scale)

where C_F is the friction coefficient from the Schoenherr formulation at the respective Reynolds Number.

$(C_F$ (full scale) - C_F (model) $)$ is constant for one model velocity with the assumptions detailed above.

The calculation of C_{X_w} (full scale) is shown in Table 10, the values being given also in Table 8. Values of C_{X_w} on the model scale are given in Table 9.

Experimental Values of M_{X_w} and scaling to full size

The moment M_{X_w} required for the hull characteristics is equal to the applied moment due to transverse movement of the sliding weight from the hull centreline.

i.e. $M_{X_w} = W.x.\cos\theta$ lb.ft. where x is in feet and

is distance of sliding wt. from centreline.
W is sliding weight in lbs.
θ is angle of heel.

which reduces to $M_{X_W} = \frac{6.33}{12} . x . \cos\theta$ where x is in inches.

Values of M_{X_W} for the combinations of V_S, θ and λ are shown in Table 11, in every case at 0° leeway the sliding weight was found to be in the position required in the static condition to heel the model to the appropriate heel angle.

The applied moment coefficient K_{X_W} was calculated from:

$$K_{X_W} = \frac{M_{X_W}}{\frac{1}{2} . \rho . A . Q . V^2}$$

where: V is the model course vel. in ft/sec.
ρ is the density of tank water at 60°F
A is the static upright wetted surface area.
Q is the static upright waterline length.

The values of A and Q used were those suggested in Part 1.

K_{X_W} for the test points is shown in Table 11 at the model scale. The scaling of this coefficient to the full scale yacht has been discussed in Chapter 20. It is assumed here that K_{X_W} for model and yacht are identical at comparable speeds and therefore are those of Table 11.

The hull characteristics

Using the values of C_{Y_W}, C_{X_W} and K_{X_W} obtained for the various

combinations of θ, λ, and V_S, for a full scale yacht having the dimensions of a 'Dragon', it was possible to construct the hull characteristics in the form required by Part 1; i.e. as curves of C_{Yw}, λ, and K_{Xw} plotted against $\frac{C_{Yw}}{C_{Xw}}$ for each velocity and angle of heel.

Figures 73, 74, 75, show these for heel angles of $7\frac{1}{2}°$, 15° and $21\frac{1}{2}°$. The upright condition was not considered as it is not a true practical possibility for windward sailing.

When plotted to a base of $\frac{C_{Yw}}{C_{Xw}}$, the general layout of curves at each angle of heel is similar, although some vertical displacement on the plot is evident. Very noticeable in Figs. 73, 74, 75 is the linear variation of K_{Xw} with $\frac{C_{Yw}}{C_{Xw}}$ and the vertical separation of these curves with course velocity, which are evident at all angles of heel.

At a particular angle of heel and for a fixed value of $\frac{C_{Yw}}{C_{Xw}}$, C_{Yw} is seen to first fall and then increases so that when it is plotted to a base of velocity, a family of curves appears; Fig. 76 at $\theta = 15°$. The same arrangement occurs at other heel angles. On plotting the leeway and K_{Xw} in a similar manner, further families appear, see Fig. 76; it may be noted here than on using the data

from these experiments in the work of Part 1, hull characteristics charted in this manner were found to be desirable as they enable the calculations to be performed at velocities other than those used in the test work without interpolation. A full set of hull characteristics for the model as used in the performance analysis will be found in Appendix 2, Part 1.

The variation of the quantities C_{Yw}, λ, and K_{Xw} with heel angle at constant $\frac{C_{Yw}}{C_{Xw}}$ is shown in Figs. 77, 78, 79, for $\frac{C_{Yw}}{C_{Xw}} = 6.0$, a similar plot occurs at other values of $\frac{C_{Yw}}{C_{Xw}}$.

A study of the figures shows that the effect of heel is similar at each model velocity tested except at 2.97 ft/sec. model scale; this at first led to some doubt concerning the validity of the experimental results at that velocity, but check runs indicated the variation is correct so it may well be that a complicated pressure distribution exists around the hull at this speed, equivalent to $V/\sqrt{L} = 0.904$, with interaction between the wave formations.

It will be seen from Figs. 73, 74, 75, that the lines of λ have quite a small curvature so it might be expected that if the component quantities of the hull characteristics are plotted using λ as base, essentially the same variations will occur. Fig. 80 shows a typical set of C_{Yw} curves plotted in this manner for a model

velocity of 1.90 ft/sec. while the heel angle increases in stages from 0° to 21½°. Within the close hauled region of λ some reduction of C_{Y_w} occurs as heel is increased but this tendency was found to be reversed at the highest velocities. In all cases, C_{Y_w} was found to be zero at zero hull incidence, and its variation with C_{Y_w} to be non-linear, the curves showing increasing slope as leeway increases.

With the heel angle held constant while the course velocity varies, Fig. 81 shows some increase in C_{Y_w} as the speed increases; this was found to be more pronounced at the larger heel angles but no finite pattern emerged.

The variation of C_{X_w} with model incidence λ is seen from Fig. 82 to be complex in terms of velocity and heel; at the lower speeds, C_{X_w} falls as leeway is increased, probably due to the wave-making and from component of resistance acting along the course; this effect is reduced as the velocity increases until at the highest velocity C_{X_w} tends to rise as leeway is increased, falling off again around the usual maximum λ attained while sailing (7° to 8°), this might well be due to the greatly increased wetted surface and hence skin friction at the higher velocities.

When K_{X_w} is plotted against leeway, the variation again appears linear for constant V_S as shown in Fig. 83; apparrently the small

scatter in values permits this to appear when K_{X_w} is plotted against either $\frac{C_{Y_w}}{C_{X_w}}$ or λ as base despite the non-linear variation of λ with $\frac{C_{Y_w}}{C_{X_w}}$ noted previously.

A linear relationship independent of leeway appears between K_{X_w} and heel, the slope of which decreases markedly as speed increases (Fig. 84 shows this for $\lambda = 3°$), while the variation of K_{X_w} with model velocity is illustrated in Fig. 85.

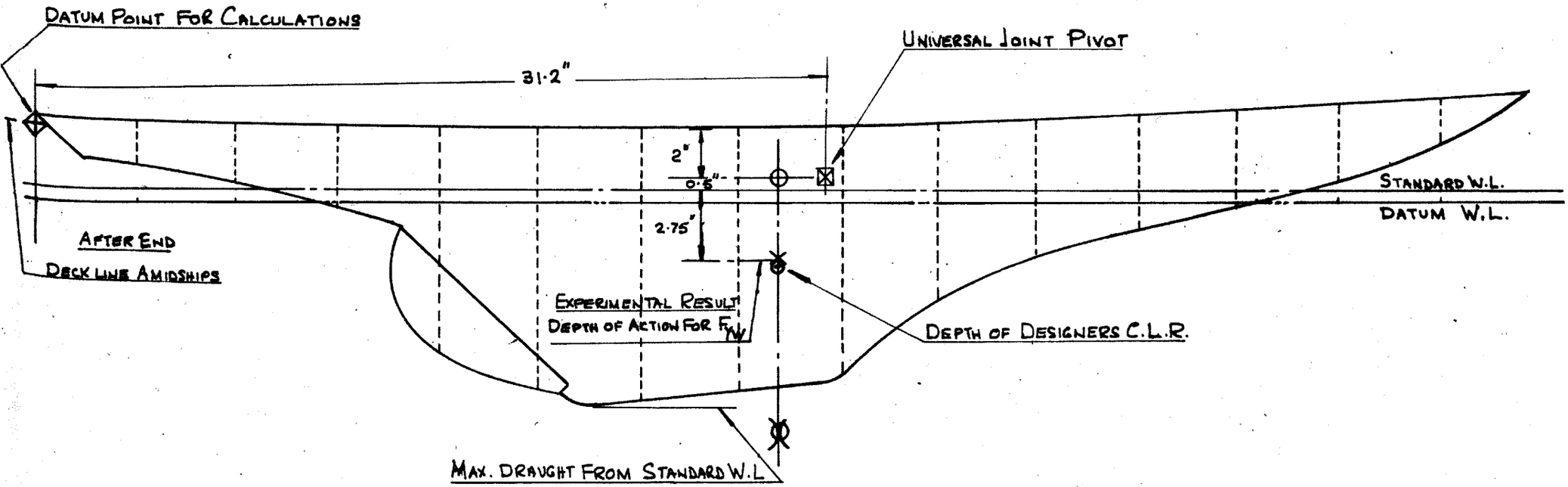

fig 72 geometry of the model.

fig 73 hull characteristics. dragon hull at 7½° heel.

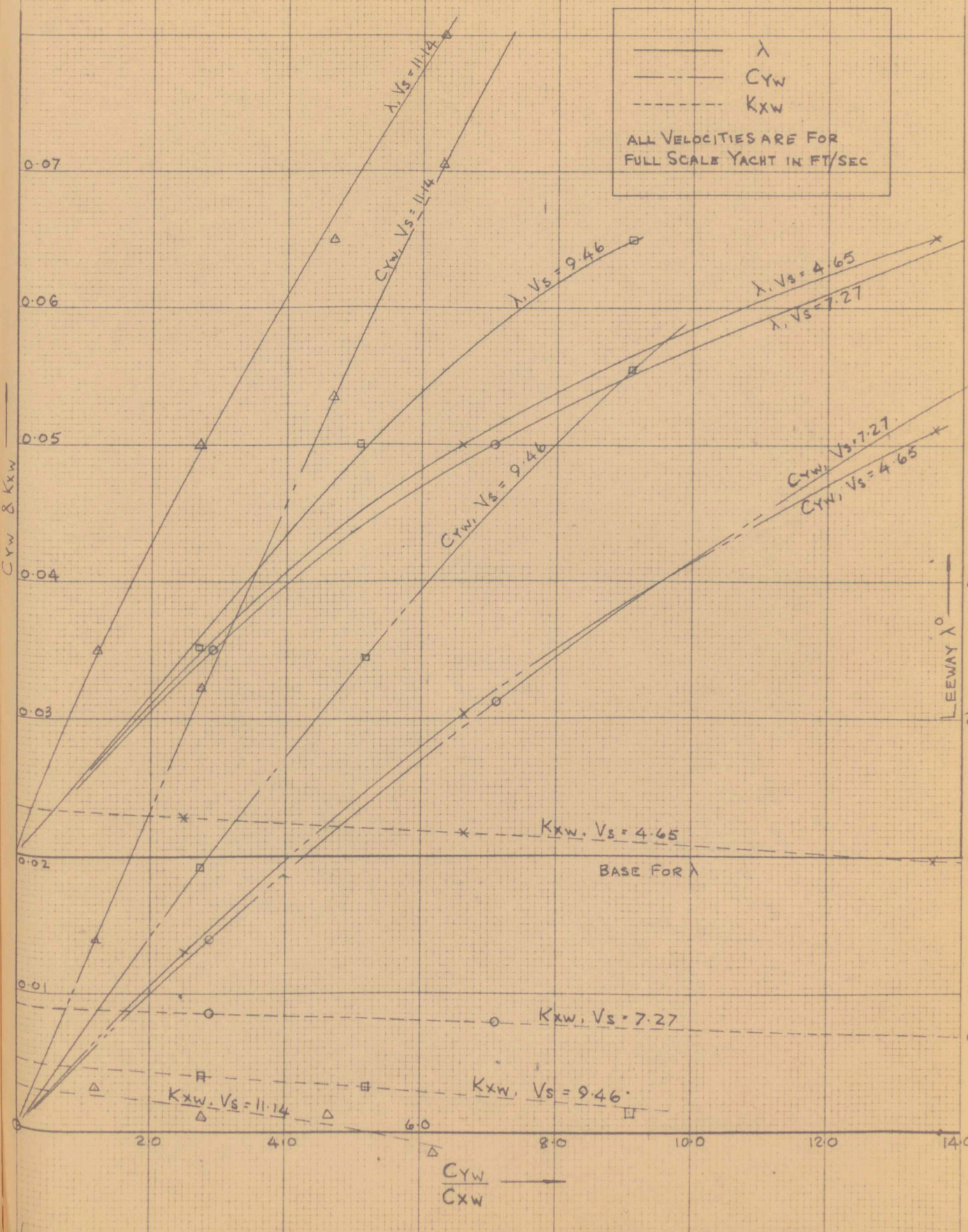

fig 74 typical hull characteristics
dragon hull at 15° heel.

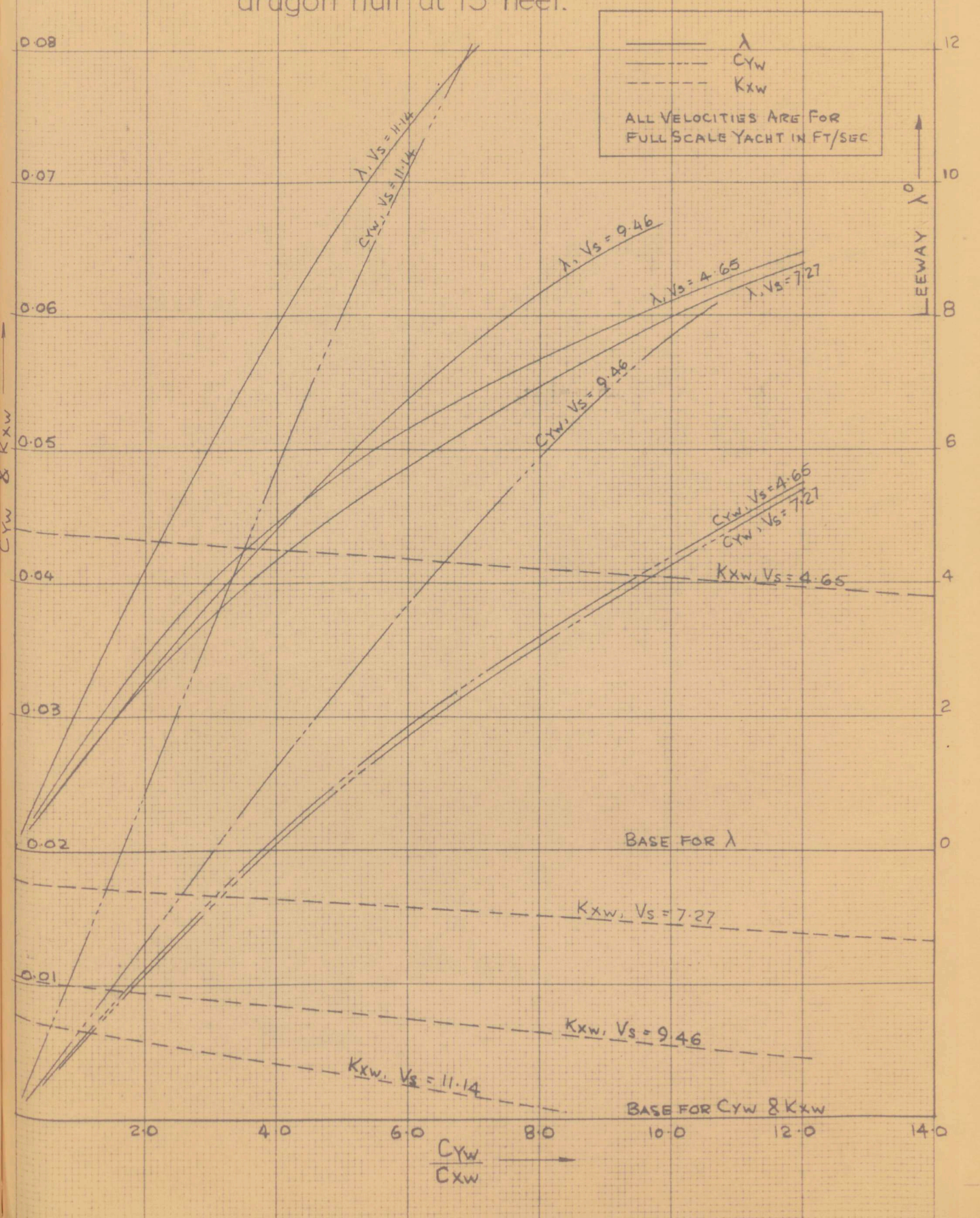

fig 75 hull characteristics. dragon hull at 21½° heel.

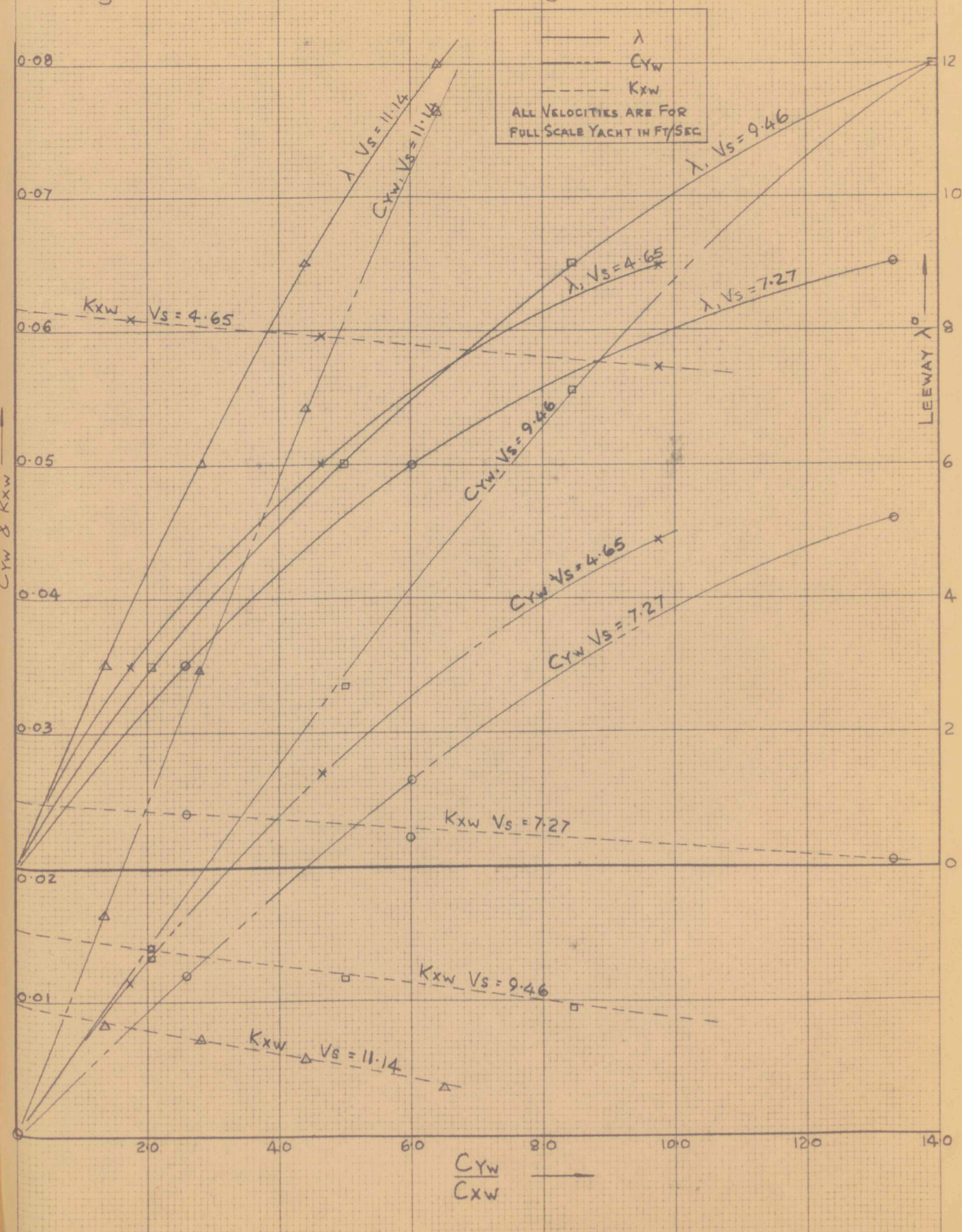

fig 76 dragon hull characteristics at 15 heel.

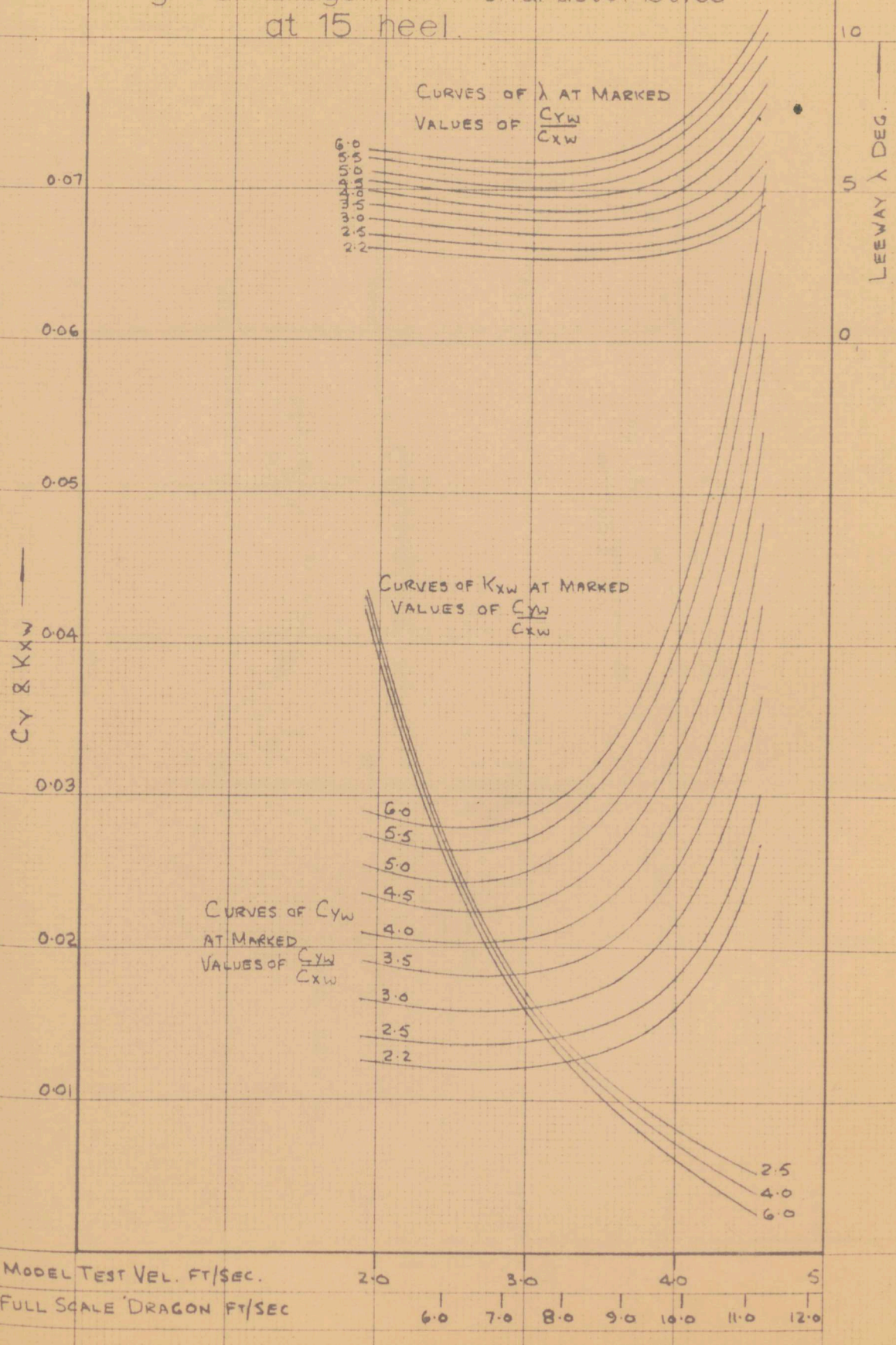

fig 77 variation in C_{Yw} with heel at $\frac{C_{Yw}}{C_{Xw}} = 6.0$

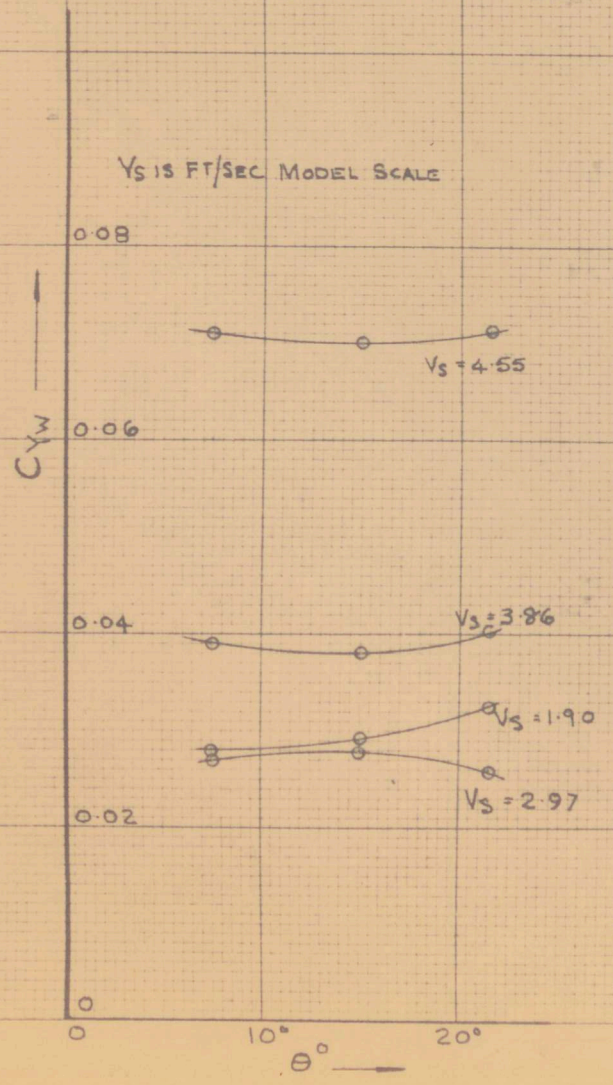

fig 78 variation in λ with heel at $\frac{C_{Yw}}{C_{Xw}} = 6.0$

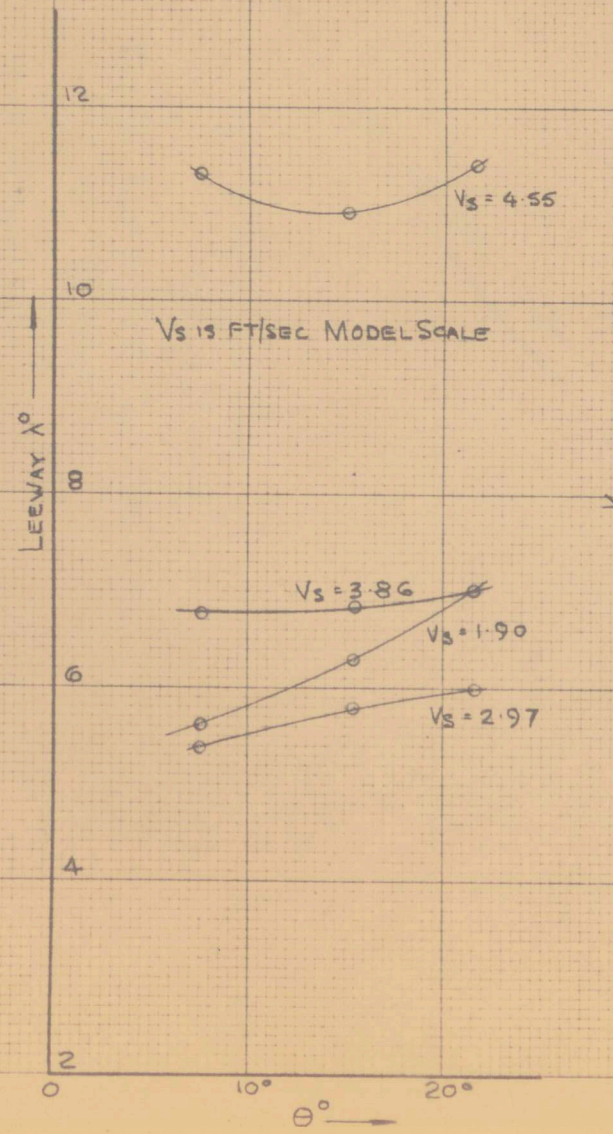

fig 79 variation in K_{xw} with heel at $\frac{C_{Yw}}{C_{Xw}} = 6.0$

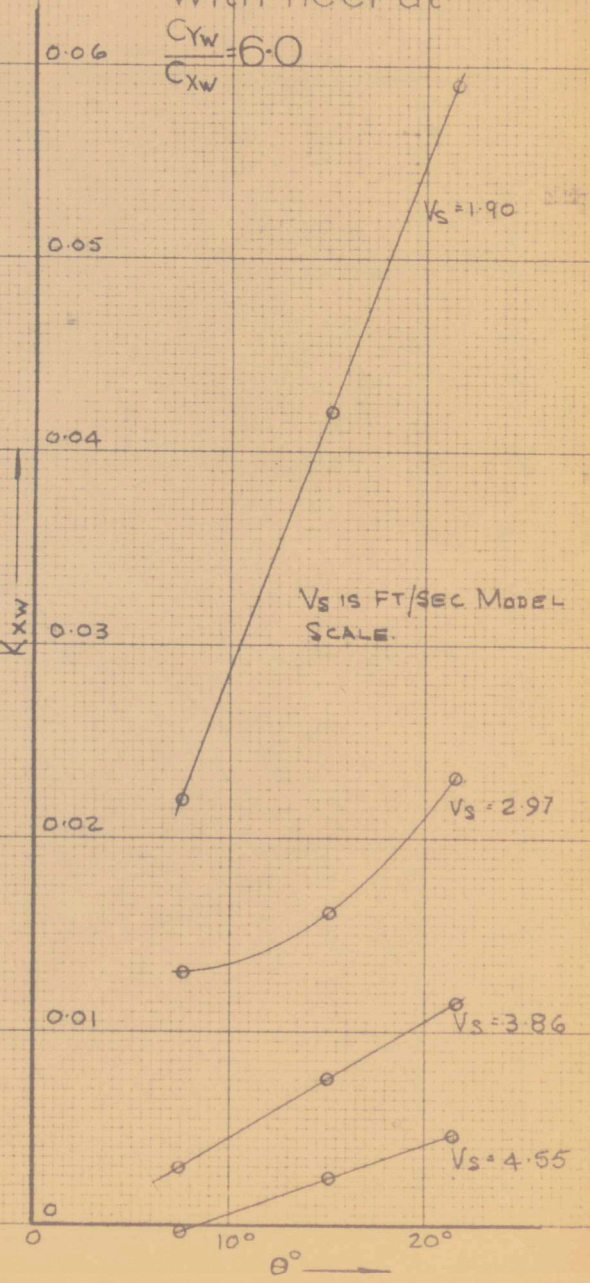

fig82 variation in C_{xw} with leeway, heel, course velocity.

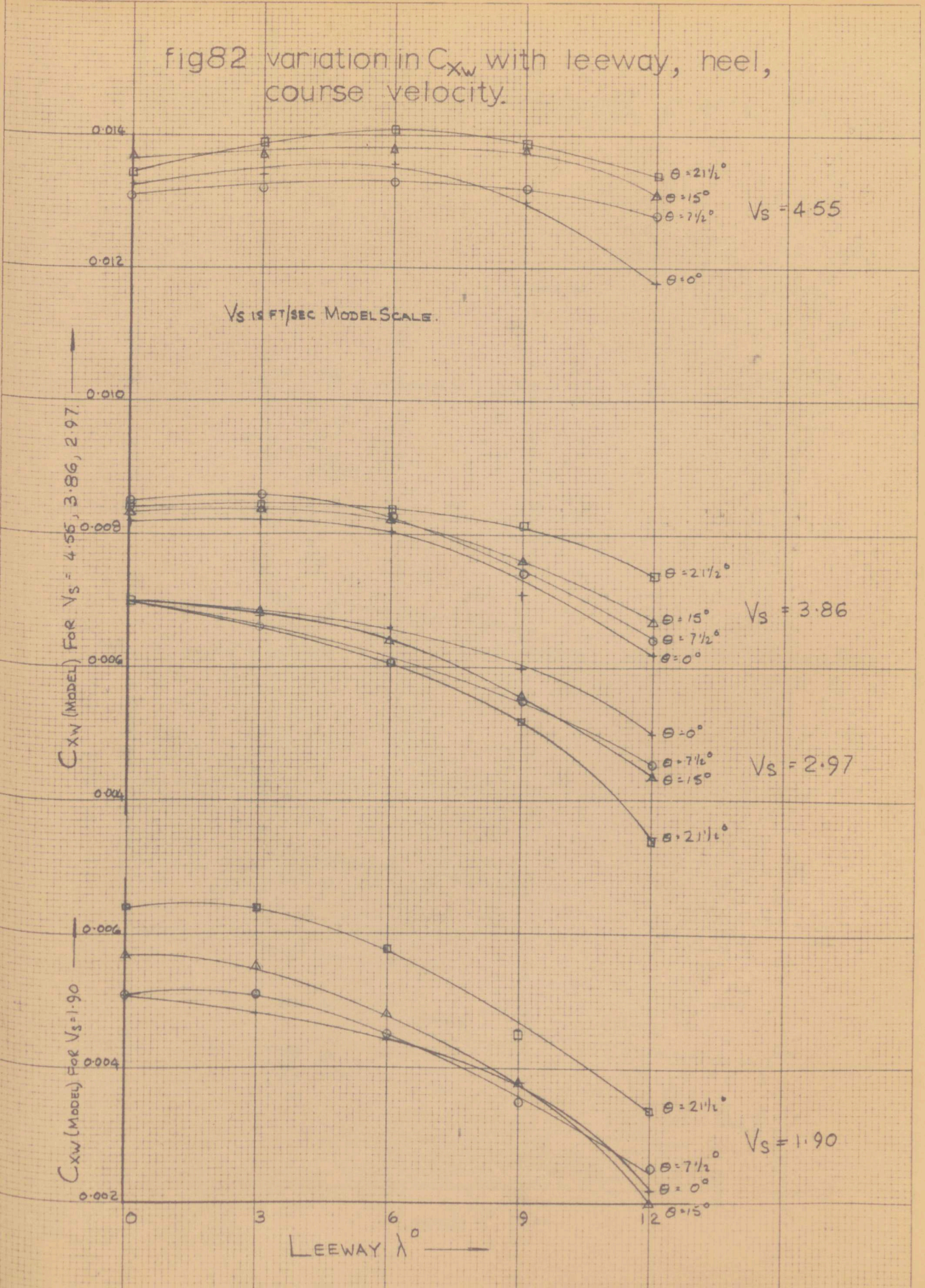

fig 84 stability— K_{xw} at 3° leeway variation with heel.

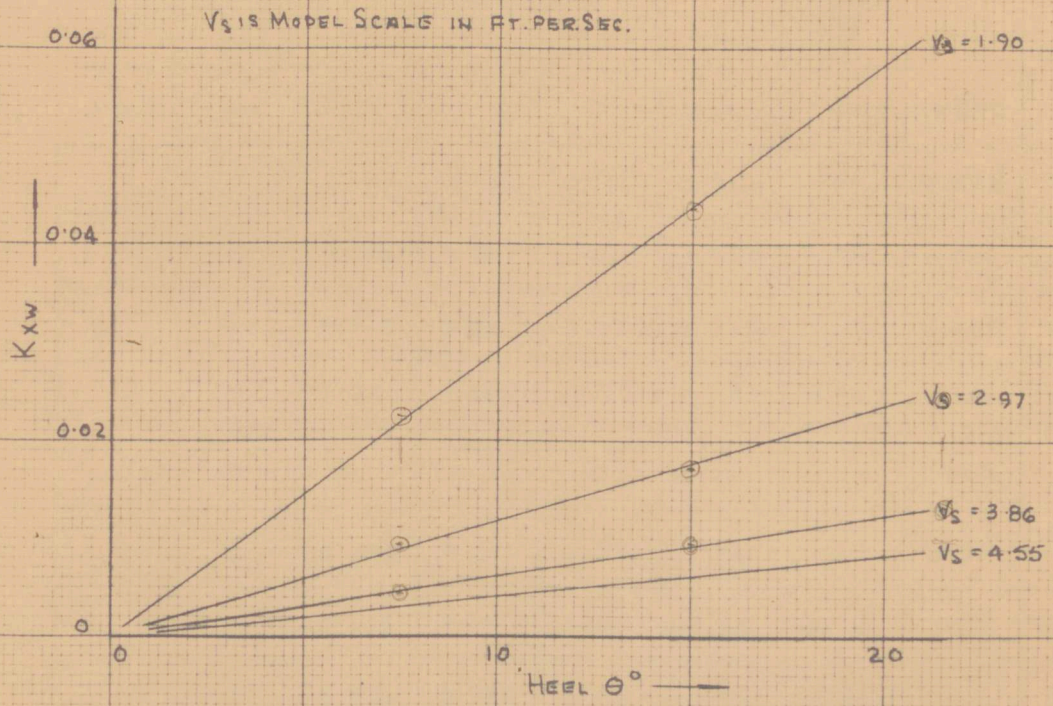

fig 85 stability K_{xw} at 3 leeway variation with velocity

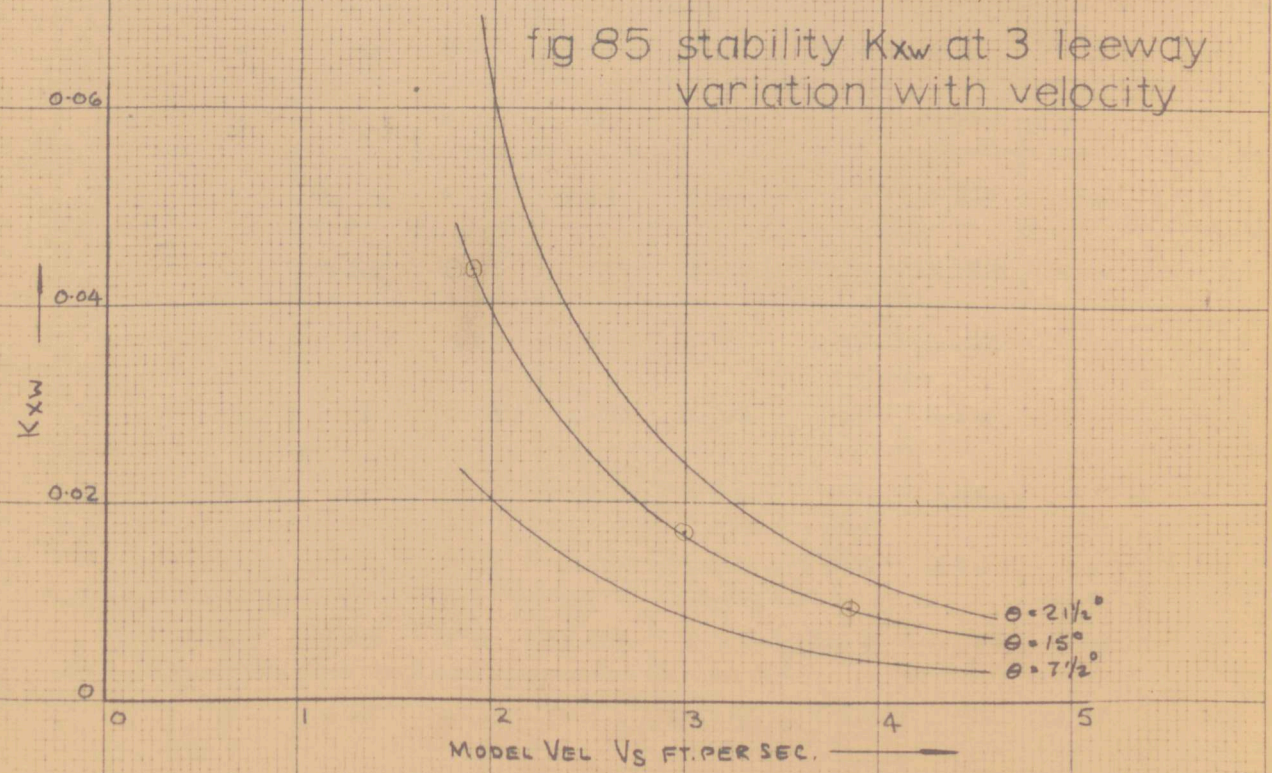

TABLE 7.

MODEL RESULTS FOR F_{YW} AND F_{XW} AT STANDARD CONDITION.

MODEL VELOCITY		1·90 FT/SEC		2·97 FT/SEC		3·86 FT/SEC		4·55 FT/SEC	
HEEL θ°	LEEWAY λ°	F_{YW} LB.	F_{XW} LB	F_{YW} LB	F_{XW} LB	F_{YW} LB	F_{XW} LB	F_{YW} LB	F_{XW} LB
0	0	0	0·11	0	0·265	0	0·525	0	1·18
	3	0·22	0·105	0·498	0·260	1·05	0·525	1·26	1·19
	6	0·49	0·10	1·17	0·250	2·04	0·515	2·87	1·20
	9	0·825	0·09	2·03	0·225	3·25	0·455	4·86	1·15
	12	1·21	0·065	3·26	0·19	4·70	0·40	6·58	1·04
7½	0	0	0·11	0	0·265	0	0·545	0	1·16
	3	0·206	0·11	0·53	0·25	1·23	0·55	1·24	1·17
	6	0·468	0·10	1·19	0·23	2·20	0·53	2·86	1·18
	9	0·821	0·085	2·06	0·21	3·54	0·47	4·73	1·16
	12	1·16	0·07	3·16	0·17	4·96	0·41	6·22	1·13
15	0	0	0·12	0	0·26	0	0·535	0	1·21
	3	0·176	0·116	0·49	0·26	1·05	0·54	1·54	1·21
	6	0·418	0·105	1·12	0·24	2·15	0·525	3·26	1·22
	9	0·737	0·09	1·84	0·21	3·49	0·485	5·11	1·22
	12	1·08	0·06	2·78	0·165	4·89	0·43	7·15	1·16
21½	0	0	0·13	0	0·265	0	0·54	0	1·19
	3	0·176	0·13	0·44	0·24	0·895	0·54	1·48	1·23
	6	0·418	0·12	1·00	0·23	2·15	0·535	3·08	1·25
	9	0·683	0·100	1·74	0·195	3·54	0·52	4·83	1·23
	12	0·991	0·084	2·59	0·15	5·10	0·47	6·75	1·18

TABLE 8. CYW AND CXW FOR FULL SCALE YACHT.

CYW APPLIES ALSO TO MODEL SCALE.

MODEL VELOCITY FT/SEC		1·90		2·97		3·86		4·55	
HEEL θ°	LEEWAY λ°	CYW	CXW	CYW	CXW	CYW	CXW	CYW	CXW
0	0	0	0·00519	0	0·00530	0	0·00663	0	0·01181
	3	0·0142	0·00507	0·0134	0·00520	0·0164	0·00663	0·0142	0·01193
	6	0·0317	0·00454	0·0309	0·00491	0·0321	0·00647	0·0324	0·01202
	9	0·0534	0·00390	0·0537	0·00425	0·0508	0·00552	0·0549	0·01145
	12	0·078	0·00229	0·0863	0·00332	0·0735	0·00466	0·0744	0·01023
7½	0	0	0·00519	0	0·00530	0	0·00694	0	0·01157
	3	0·0133	0·00519	0·014	0·00491	0·0192	0·00701	0·014	0·01172
	6	0·0302	0·00454	0·0314	0·00439	0·0345	0·00670	0·0323	0·01181
	9	0·0531	0·00358	0·0545	0·00385	0·0554	0·00576	0·0534	0·01157
	12	0·0748	0·00261	0·0835	0·00280	0·0776	0·00483	0·0703	0·01125
15	0	0	0·00584	0	0·00519	0	0·00678	0	0·01215
	3	0·0114	0·00564	0·013	0·00519	0·0164	0·00685	0·0174	0·0215
	6	0·0270	0·00487	0·0296	0·00465	0·0336	0·00662	0·0368	0·01227
	9	0·0476	0·00390	0·0486	0·00385	0·0546	0·006	0·0576	0·01227
	12	0·0696	0·00196	0·0735	0·00267	0·0765	0·00513	0·0809	0·01157
21½	0	0	0·00648	0	0·00530	0	0·00685	0	0·01193
	3	0·0114	0·00648	0·0118	0·00465	0·014	0·00685	0·0167	0·01237
	6	0·0270	0·00584	0·0264	0·00439	0·0336	0·00678	0·0348	0·1258
	9	0·0442	0·00455	0·0460	0·00346	0·0554	0·00655	0·0545	0·01237
	12	0·0640	0·00351	0·0685	0·00226	0·0798	0·00576	0·0763	0·01181

TABLE 9. CALCULATION OF C_{XW} FOR MODEL.

AT 1·9 FT/SEC. $A = 4.43$. $P/2 = 0.965$, $V^2 = 3.62$, $\therefore \frac{1}{2}\rho A V^2 = 15.5$.
AT. 2·97 FT/SEC, $V^2 = 8.84$ $\therefore \frac{1}{2}\rho A V^2 = 37.8$. AT 3·86 FT/SEC., $\frac{1}{2}\rho A V^2 = 63.9$. AT. 4·55 FT/SEC. $\frac{1}{2}\rho A V^2 = 88.5$.

MODEL VELOCITY. FT/SEC		1·90		2·97		3·86		4·55	
HEEL $\theta°$	LEEWAY $\lambda°$	F_{XW} (MODEL) LBS	$C_{XW} = \frac{F_{XW}}{\frac{1}{2}\rho A V^2}$	F_{XW} model. LBS.	$C_{XW} = \frac{F_{XW}}{\frac{1}{2}\rho A V^2}$	F_{XW} model	$C_{XW} = \frac{F_{XW}}{\frac{1}{2}\rho A V^2}$	F_{XW} model	$C_{XW} = \frac{F_{XW}}{\frac{1}{2}\rho A V^2}$
0	0	0·11	0·0071	0·265	0·007	0·525	0·00822	1·18	0·01334
	3	0·105	0·00678	0·260	0·0069	0·525	0·00822	1·19	0·01345
	6	0·10	0·00645	0·250	0·00661	0·515	0·00806	1·20	0·01355
	9	0·09	0·00581	0·225	0·00595	0·455	0·00711	1·15	0·01298
	12	0·065	0·00420	0·19	0·00502	0·40	0·00625	1·04	0·01176
7½	0	0·11	0·0071	0·265	0·007	0·545	0·00853	1·16	0·01310
	3	0·11	0·0071	0·25	0·00661	0·55	0·00860	1·17	0·01320
	6	0·10	0·00645	0·23	0·00609	0·53	0·00829	1·18	0·01334
	9	0·085	0·00549	0·21	0·00555	0·47	0·00735	1·16	0·01310
	12	0·07	0·00452	0·17	0·00450	0·41	0·00642	1·13	0·01278
15	0	0·12	0·00775	0·26	0·00689	0·535	0·00837	1·21	0·01368
	3	0·116	0·00755	0·26	0·00689	0·54	0·00844	1·21	0·01368
	6	0·105	0·00678	0·24	0·00635	0·525	0·00821	1·22	0·01380
	9	0·09	0·00581	0·21	0·00555	0·485	0·00759	1·22	0·01386
	12	0·06	0·00387	0·165	0·00437	0·43	0·00672	1·16	0·01380
21½	0	0·13	0·00839	0·265	0·007	0·54	0·00844	1·19	0·01345
	3	0·13	0·00839	0·24	0·00635	0·54	0·00844	1·23	0·01390
	6	0·12	0·00775	0·23	0·00609	0·535	0·00837	1·25	0·01411
	9	0·10	0·00646	0·195	0·00516	0·52	0·00814	1·23	0·01390
	12	0·084	0·00542	0·15	0·00396	0·47	0·00735	1·18	0·01334

TABLE 10(1) CALCULATION OF FULL SCALE C_{XW}

AT MODEL VEL. 1·90 f/s. R_e(model) = $5{\cdot}46 \times 10^5$, C_F(Schoenherr) = $4{\cdot}974 \times 10^{-3}$
R_e(F.S). = $7{\cdot}68 \times 10^6$. C_F(Schoenherr) = $3{\cdot}067 \times 10^{-3}$. C_F(model) − C_F(F.S) = $1{\cdot}91 \times 10^{-3}$
AT MODEL VEL 2·97 F/S. R_e(model) = $8{\cdot}57 \times 10^5$. C_F = $4{\cdot}549 \times 10^{-3}$.
R_e(F.S) = $1{\cdot}198 \times 10^7$, C_F = $2{\cdot}850 \times 10^{-3}$. C_F(model) − C_F(F.S) = $1{\cdot}70 \times 10^{-3}$

		MODEL VELOCITY 1·90 FT/SEC.			MODEL VELOCITY 2·97 FT/SEC.		
HEEL θ°	LEEWAY λ°	(1) C_{XW} model. $\times 10^3$	(2) C_F(model) − C_F(F.S) $\times 10^3$	C_{XW}(F.S) $\times 10^3$ (1) − (2)	(1) C_{XW} model $\times 10^3$	(2) C_F(model) − C_F(F.S). $\times 10^3$	C_{XW}(F.S) $\times 10^3$ (1) − (2)
0	0	7·10	1·91	5·19	7·0	1·70	5·30
	3	6·98		5·07	6·90		5·20
	6	6·45		4·54	6·61		4·91
	9	5·81		3·90	5·95		4·25
	12	4·20		2·29	5·02		3·32
7½	0	7·10		5·19	7·00		5·30
	3	7·10		5·19	6·61		4·91
	6	6·45		4·54	6·09		4·39
	9	5·49		3·58	5·55		3·85
	12	4·52		2·61	4·55		2·80
15	0	7·75		5·84	6·89		5·19
	3	7·55		5·64	6·89		5·19
	6	6·78		4·87	6·35		4·65
	9	5·81		3·90	5·55		3·85
	12	3·87		1·96	4·37		2·67
21½	0	8·39		6·48	7·00		5·30
	3	8·39		6·48	6·35		4·65
	6	7·75		5·84	6·09		4·39
	9	6·46		4·55	5·16		3·46
	12	5·42		3·51	3·96		2·26

TABLE 10 (11) CALCULATION OF FULL SCALE C_{XW}.

AT MODEL VEL. 3·86 F/S. R_e (model) = $1{\cdot}11 \times 10^6$, $C_F = 4{\cdot}326 \times 10^{-3}$

R_e (F.S) = $1{\cdot}1557 \times 10^7$, $C_F = 2{\cdot}733 \times 10^{-3}$. C_F (model) − C_F (F.S) = $1{\cdot}59 \times 10^{-3}$.

AT MODEL VEL. 4·55 F/S. R_e (model) = $1{\cdot}31 \times 10^6$, $C_F = 4{\cdot}190 \times 10^{-3}$

R_e (F.S) = $1{\cdot}842 \times 10^7$, $C_F = 2{\cdot}663 \times 10^{-3}$. C_F (model) − C_F (F.S) = $1{\cdot}53 \times 10^{-3}$.

		MODEL VELOCITY 3·86 FT/SEC			MODEL VELOCITY 4·55 FT/SEC.		
HEEL θ°	LEEWAY λ°	(1) C_{XW} model $\times 10^3$	(2) C_F (model) − C_F (F.S) $\times 10^3$	C_{XW} (F.S) $\times 10^3$ (1) − (2)	(1) C_{XW} model $\times 10^3$	(2) C_F (model) − C_F (F.S) $\times 10^3$	C_{XW} (F.S) $\times 10^3$ (1) − (2)
0	0	8·22	1·59	6·63	13·34	1·53	11·81
	3	8·22		6·63	13·45		11·93
	6	8·06		6·47	13·55		12·02
	9	7·11		5·52	12·98		11·45
	12	6·25		4·66	11·76		10·23
7½	0	8·53		6·94	13·10		11·57
	3	8·60		7·01	13·25		11·72
	6	8·29		6·70	13·34		11·81
	9	7·35		5·76	13·10		11·57
	12	6·42		4·83	12·78		11·25
15	0	8·37		6·78	13·68		12·15
	3	8·44		6·85	13·68		12·15
	6	8·21		6·62	13·80		12·27
	9	7·59		6·00	13·80		12·27
	12	6·72		5·13	13·10		11·57
21½	0	8·44		6·85	13·45		11·93
	3	8·44		6·85	13·90		12·37
	6	8·37		6·78	14·11		12·58
	9	8·14		6·55	13·90		12·37
	12	7·35		5·76	13·34		11·81

TABLE II. VALUES OF M_{xw} & F_{yw} FOR MODEL; K_{xw} FOR MODEL AND YACHT

HEEL θ°	LEEWAY λ°	M_{xw} Lb.ft.	$\frac{1}{2}\rho AQV^2$	K_{xw}	F_{yw} Lb.	M_{xw} Lb.ft.	$\frac{1}{2}\rho AQV^2$	K_{xw}	F_{yw} Lb.
		MODEL VELOCITY 1·90 FT/SEC.				MODEL VELOCITY 2·97 FT/SEC			
0	3	-0·0254	53·9	-0·000472	0·22	-0·104	131·4	-0·00079	0·498
	6	-0·0792		-0·00147	0·49	-0·252		-0·00193	1·17
	9	-0·158		-0·00293	0·825	-0·418		-0·00318	2·03
	12	-0·254		-0·00472	1·21	-0·828		-0·0063	3·26
7½	3	1·225		+0·0227	0·206	+1·135		+0·00864	0·53
	6	1·18		0·0219	0·468	1·038		0·00790	1·19
	9	1·065		0·0196	0·821	0·749		0·00570	2·06
	12	0·965		0·0179	1·16	0·465		0·00354	3·16
15	3	2·35		0·0436	0·176	2·24		0·017	0·49
	6	2·27		0·0420	0·418	2·045		0·0156	1·12
	9	2·155		0·0399	0·737	1·833		0·0139	1·84
	12	2·060		0·382	1·08	1·610		0·0122	2·78
21½	3	3·29		0·0610	0·176	3·18		0·0242	0·44
	6	3·20		0·0594	0·418	2·92		0·0222	1·00
	9	3·10		0·0575	0·683	2·686		0·0204	1·74
	12	2·78		0·0515	0·991	2·47		0·0188	2·59
		MODEL VELOCITY 3·86 FT/SEC				MODEL VELOCITY 4·55 FT/SEC			
0	3	-0·178	222	-0·00080	1·05	-0·253	308	-0·00082	1·26
	6	-0·546		-0·00246	2·04	-0·633		-0·00255	2·87
	9	-1·04		-0·00468	3·25	-1·159		-0·00376	4·86
	12	-1·608		-0·00724	4·70	-1·73		-0·00562	6·58
7½	3	+0·982		+0·00447	1·23	+0·992		+0·00322	1·24
	6	0·695		0·00313	2·20	0·566		0·00184	2·86
	9	0·291		0·00131	3·54	0·04		0·0013	4·73
	12	-0·158		-0·000711	4·96	-0·524		-0·00171	6·22
15	3	2·085		0·00939	1·05	1·974		0·00642	1·54
	6	1·740		0·00783	2·15	1·532		0·00497	3·26
	9	1·33		0·00599	3·49	1·0		0·00308	5·11
	12	0·925		0·00417	4·89	0·51		0·00166	7·15
21½	3	2·95		0·0133	0·893	2·57		0·00835	1·48
	6	2·55		0·0115	2·15	2·25		0·00730	3·08
	9	2·12		0·0955	3·54	1·72		0·00558	4·83
	12	1·79		0·00806	5·10	1·24		0·00399	6·75

CHAPTER 22: UPRIGHT RESISTANCE

The upright, zero leeway, resistance (F_{Xw}) of the hull was measured over a speed range between 1.54 ft/sec. and 4.55 ft/sec. model scale ($V/\sqrt{L}$ from 0.489 to 1.44) at the 'standard' weight and C.G. location. A similar curve is available from the tank evaluation work of Part 2 at an A.U.W. of 18.31 lb. with the C.G. at 2.76 ins. below datum and 30.2 ins. from the A.E.

Fig. 86 shows the measured resistance of the model at both values of A.U.W. and it may be seen that they follow the normal pattern for change in resistance with speed. As the L.C.G. and hence trim of the model at 18.31 lb. A.U.W. varied from that at the standard condition, the curves do not represent a direct measure of change in resistance with displacement between the weights; this is considered in more detail in Chapter 25.

Referring to the results from the experiments C_{Xw} is equivalent to C_T, the Total Resistance Coefficient, so that:

$$C_T = \frac{\text{Resistance}}{\frac{1}{2} \cdot \rho \cdot A \cdot V^2}$$

and $C_T = C_F + C_R$

where C_F is the friction resistance coefft.
C_R is the residuary resistance coefft.

In order to assess the full scale resistance coefficient for the hull when applied to a 'Dragon' class yacht, the same assumptions

have been used as in the general series of tests for close-hauled characteristics discussed in Chapter 4, i.e.:

(1) Schoenherr Friction Formulation

(2) Hull wetted surface assumed constant at the upright, static value of 4.43 sq.ft.

(3) The wetted length for computation of Reynolds No. has been taken as the waterline length for the static, upright condition.

(4) No correction has been made for the stimulator penalty or the laminar deficit; the full scale boundary layer has been assumed fully turbulent.

The full scale C_T is therefore:

$$C_T \text{ (full scale)} = C_T \text{ (model)} - C_F \text{ (model)} + C_F(\text{full Scale})$$

Table 12 gives the data and calculation of full scale coefficients for both conditions of A.U.W. and Fig. 87 shows C_T for model and full scale yacht plotted against $V/\sqrt{L}$.

The uppermost curve in Fig. 87 shows C_T for the model at the standard condition and it may be seen that at low speeds it follows the curve of friction coefficient at the model scale, with a 'hump' around $V/\sqrt{L}$ 0.8 before beginning to rise sharply at around $V/\sqrt{L}$ 1.0.

When allowance is made for the friction scale effect, C_T for the full size yacht is that shown; the level of the curves on the plot can be considered as approximate only, due to the simple method of model to ship extrapolation.

Curves for model and yacht are also shown for the lower A.U.W. of 18.31 lb. model scale, and as expected fall below those at the standard weight. Slight differences between the curve shape might be expected due to the difference in L.C. G. location.

The results of further experiments to assess the effect of changing A.U.W. and L.C.G. location are discussed in Chapter 25 and the results for upright resistance are compared with previous work using the same model and with tests on other hull forms in Chapter 23.

fig 86 :model upright resistance.

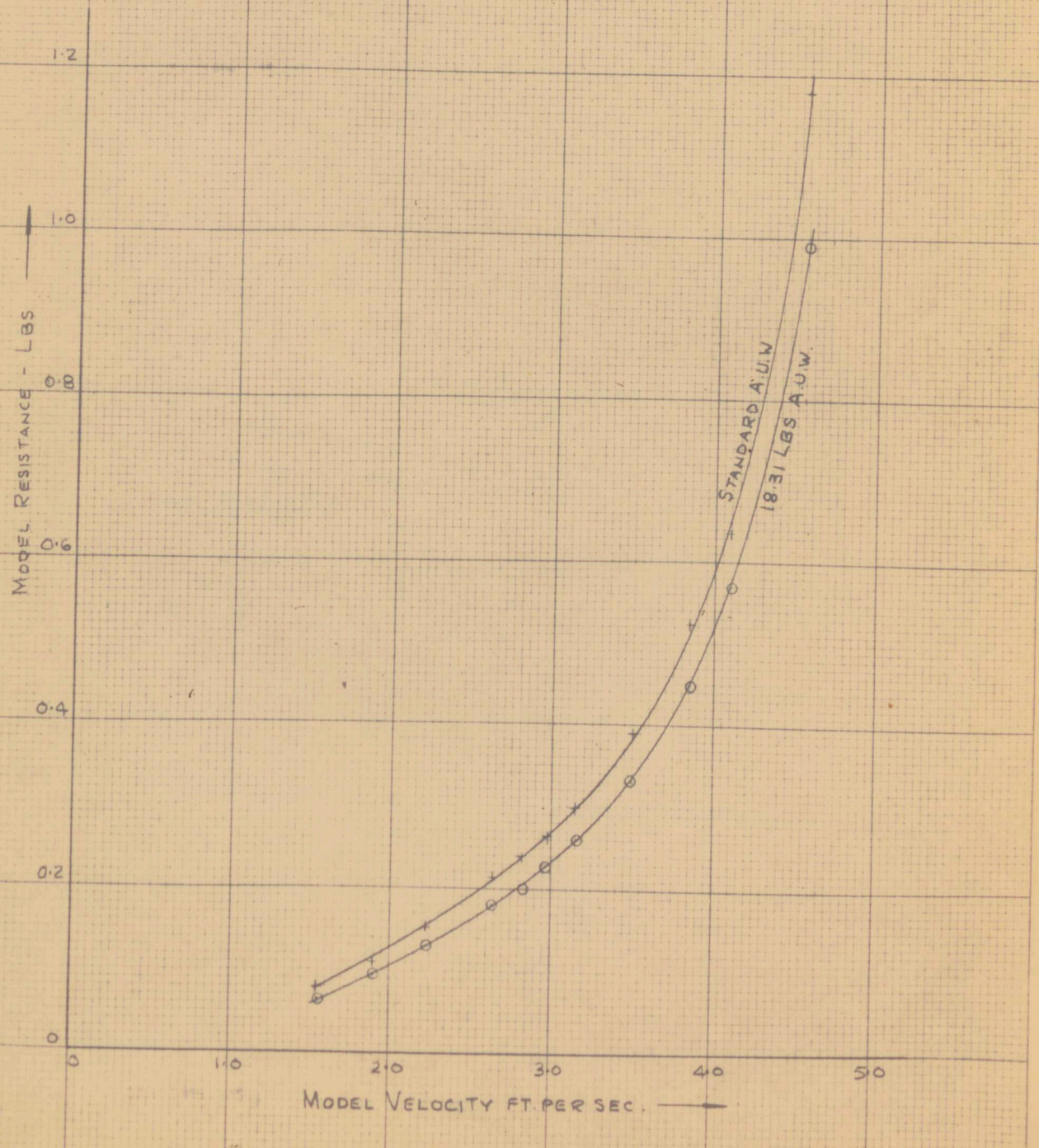

fig 87 C_T for model and full scale

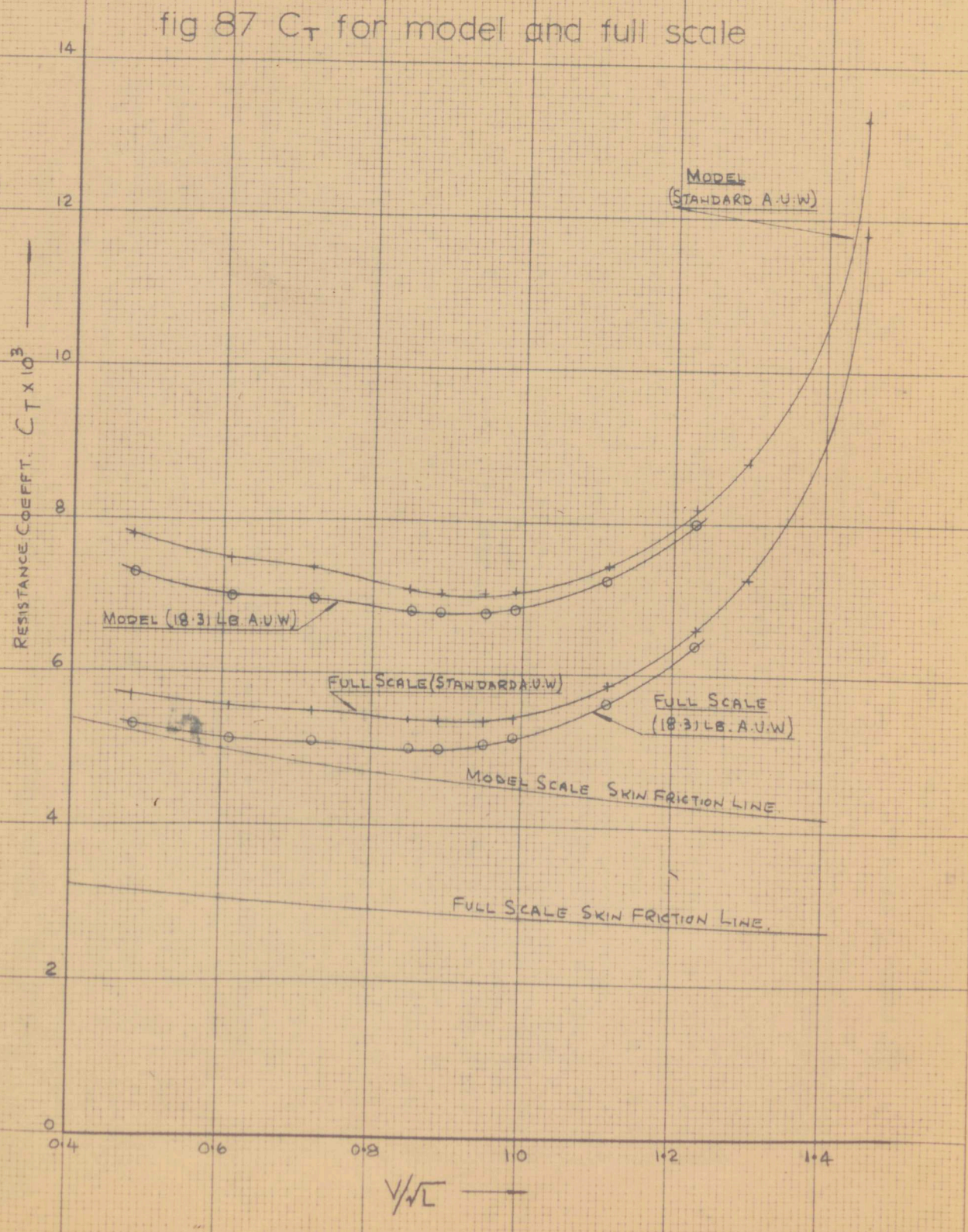

TABLE 12 DATA FROM UPRIGHT RESISTANCE EXPERIMENTS.

Model Velocity Ft/Sec.	$\frac{V}{\sqrt{L}}$	Model R_e $\times 10^{-5}$	C_F Model $\times 10^3$	F.S. R_e $\times 10^{-5}$	C_F F.S. $\times 10^3$	Scale Effect $\times 10^3$	Standard Condition				18·31 Lbs. A.U.W.				$V_{F.S.}$ Knots
							Model Resist. Lb.	$\frac{1}{2}\rho AV^2$	C_T Model	C_T F.S.	Model Resist. Lb.	$\frac{1}{2}\rho AV^2$	C_T Model	C_T F.S.	
1·54	0·489	4·43	5·185	62·3	3·117	2·068	0·08	10·2	0·0078	0·0057	0·065	8·82	0·00738	0·00531	2·23
1·90	0·604	5·46	4·974	76·9	3·067	1·907	0·110	15·5	0·0074	0·0055	0·095	13·45	0·00705	0·00514	2·76
2·23	0·719	6·42	4·815	91·7	2·979	1·836	0·155	21·3	0·0073	0·0055	0·130	18·50	0·00705	0·00521	3·28
2·67	0·848	7·68	4·648	107·9	2·900	1·748	0·215	30·4	0·0071	0·0053	0·180	26·50	0·00680	0·00505	3·87
2·82	0·895	8·11	4·594	114·0	2·875	1·719	0·240	34·1	0·00705	0·0053	0·200	29·60	0·00675	0·00503	4·09
2·97	0·944	8·57	4·547	120·2	2·842	1·705	0·265	37·8	0·007	0·0053	0·225	32·85	0·00685	0·00514	4·31
3·14	0·997	9·04	4·504	126·9	2·826	1·678	0·300	42·3	0·0071	0·0054	0·255	36·70	0·00695	0·00522	4·55
3·49	1·11	10·03	4·407	141·3	2·776	1·631	0·390	52·2	0·00745	0·00582	0·330	45·40	0·0073	0·00567	5·07
3·86	1·23	11·10	4·334	156·8	2·730	1·604	0·525	63·9	0·00820	0·0066	0·450	55·60	0·0081	0·00650	5·62
4·1	1·302	11·79	4·275	166·0	2·706	1·569	0·635	72·0	0·0088	0·00723	0·570	62·70	0·00918	0·00761	5·95
4·55	1·445	13·10	4·191	181·5	2·669	1·522	1·18	88·5	0·0133	0·0118	0·990	77·20	0·0128	0·0113	6·60

STANDARD CONDITION

$\rho/2 = 0.965$, WETTED AREA (A) = 4·43 SQ. FT.

$\frac{1}{2}\rho AV^2 = 4.27\,V^2$

18·31 LB. A.U.W.

$\rho/2 = 0.965$, A = 3·85 SQ. FT.

$\frac{1}{2}\rho AV^2 = 3.72\,V^2$

CHAPTER 23: RESULTS OF PRESENT WORK COMPARED WITH PREVIOUS TESTS USING THE SAME MODEL AND ALSO WITH OTHER HULL FORMS

23.1 Close Hauled Hull Characteristics

Previous experimental work in connection with yacht hulls has expressed the results in terms of Lift and Drag, using Sea axes. Results from the present work have therefore been placed in terms of C_L and C_D to allow comparison with previous work on the same and other hulls and to provide a clearer picture of the effect of heel, velocity and leeway to emerge in the light of similarity between the yacht keel and the aerofoil.

A consideration of the Sea and Body/Sea systems of axes shows that:

$$C_L = C_{Y_W} \cdot \text{Cos}\,\lambda - C_{X_W} \cdot \text{Sin}\,\lambda$$

$$C_D = C_{Y_W} \cdot \text{Sin}\,\lambda + C_{X_W} \cdot \text{Cos}\,\lambda$$

As the scale effect in extrapolation from model to full size has been assumed to vary only with velocity, either model or full scale values could be used to show the effect of heel and leeway; here, the values refer to the model scale.

Lift Coefficient

The variation of C_L with heel, leeway and model course velocity may be seen in Fig. 88, the use of separate plots for each velocity

avoids confusion due to superimposition of curves covering the ranges of heel and leeway.

The variation of C_L with leeway in the range considered is similar at all speeds, being a curve of increasing slope, although there is some tendency towards linearity as λ increases. The overall slope of the curves does however change with heel, increasing as heel decreases at the lower speeds but showing more variation at higher speeds.

Fig. 89 shows curves of C_L plotted against heel for each model velocity used during the experiments and three leeway angles covering the range within which the hull might expect to operate during windward sailing; at the lower velocities, C_L falls as heel increases, the effect being greater as leeway increases. At the higher speeds, experimental points are less fair although C_L appears first to rise and then to fall as heel increases.

Fig. 89 shows also that C_L generally rises as the course velocity is increased.

Comparison of test C_L with previous results for the model

Values of C_L from the original tests at the Saunders Roe Div. are given in Ref. 12 and shown here in Fig. 90. They appear to follow a more linear distribution than in the present experiments.

Previous work was undertaken for the prediction of performance

by the 'Gimcrack' technique and followed the usual practice in such experiments by measuring only at values of speed, leeway and heel near likely full scale sailing conditions. The Saunders Roe values shown in Fig. 90 are for a full scale speed of 3 knots and the appropriate spread of heel angle is shown by the square brackets.

The reason for this apparent linear distribution appears when comparison is made with results from the present work. The nearest full scale speed to 3 knots in the present tests used a model velocity of 1.90 ft/sec. and choice of a sutiable scale for C_L leads to the curves from Fig. 88 being superimposed on the Saunders Roe points. The two scales for C_L are necessary due to the different speeds and areas used in deriving coefficients and also take into account any scaling problems.

It is seen that the curves from Fig. 88 at $7\frac{1}{2}°$, 15° and $21\frac{1}{2}°$ pass through the equivalent areas of heel in the Saunders Roe results, confirming that the reason for apparent linearity of the latter is the combination of heel and leeway resulting from the test philosophy.

The comparison made here also demonstrates reasonable agreement between the two series of experiments and tanks in terms of C_L.

Results compared with other work

In his original work (Ref. 9, Fig. 15) Davidson gives curves of C_L against λ for the Six-metre yacht 'Jill' over a wide range of leeway extending beyond zero, and for two heel angles; these show

an angle of leeway for zero lift well beyond zero at both angles of heel, indicating that the hull produces considerable lift due to its assymetrical form when heeled; the same figure shows that the Lift varies linearly with heel but the slope of the curve reduces as heel increases.

In the present tests, there was no indication that the No-Lift leeway angle was beyond zero, and a series of runs made with the model set at 20° heel and leeway angles each side of zero confirmed that the Lift curve passed through the Origin; also the Lift curve is seen to be non-linear. It was however, found that the Lift curve slope reduced as heel increased at the two lower velocitites.

Crewe (Ref. 3, Fig. 15) shows curves of No-Lift Coefficient against an effective leeway angle taken from an assumed No-Lift value obtained by producing measured values backwards to the axis; it is unfortunate here that the number of test points is very great without indication being given of the velocities and heel angles to which they refer; the variation is shown as linear, but scatter is of the same type as in the 'Dragon' tests discussed earlier, and it may well be that a re-analysis would show a distribution varying with speed and heel.

In a more recent paper (Ref. 15, Fig. 4) Crewe shows values of Lift Force against leeway at various course velocities, scaled for

the full size yacht. Although no experimental points are shown and the same velocity appears for only two consecutive curves at a time, the variation is non-linear and gives No-Lift angles beyond zero at the higher angles of heel. The values are said to be typical of a 'large fin keeled yacht'; presumably a Twelve Metre.

In Ref. 11, Tanner shows results of his tank tests on the hull of an International ten Square Metre Class Canoe; this is a different type of hull and Lift producing mechanism, having a high aspect ratio centreboard; he found that the Lift curve is a straight line passing through the origin at all speeds; only the upright condition was considered, this being the attitude in which the hull normally works.

In considering the differences between the No-Lift angles at large heel angles found in the present experiments and those from the work discussed above, it is interesting to note the differences between the hull types involved, the 6-metre and 12 metre being fine craft where the keel faired into the bottom of the hull and the canoe has a centreboard projecting out of the hull; it may be possible to compare the canoe directly with an aerofoil plus end plate, and the fine craft with a low aspect ratio aerofoil piercing the surface while the dragon might be considered as a low aspect ratio aerofoil with some end plate effect.

Results from a typical Commercial tank test are contained in Ref. 5; the ranges of speed, leeway and heel tested are taken to

provide data for use in a 'Gimcrack' type full scale performance prediction, and as such do not permit a true analysis of the hull characteristics; the scatter and restricted ranges could well lead to erroneous interpretation. An attempt could be made to extend the results from the test ranges by extrapolation using either a straight line variation of Lift Force found by Davidson for the 6-Metre with a No-Lift angle beyond zero, or by reference to the slope of the curves from the present work; considerable difference would be found in the hull characteristics using each method and in this case it is essential to have more test points over a greater spread of leeway at each heel angle and speed before considering further analysis.

Drag Coefficient

Figure 91 illustrates the variation of C_D with heel, leeway and course velocity, and it is seen that the curves follow almost exactly a square law. Fig. 92 compares the curve of C_D for 0° heel at a model course velocity of 1.90 ft/sec. with a curve of $C_D \propto \lambda^2$. Some of the experimental curves at other values of velocity and heel show a better fit and some a slightly worse fit, although in several cases rotation is necessary to achieve agreement.

The principal effect of heel is seen to be a rotation of the $C_D \sim \lambda$ curve clockwise as heel increases and in some cases there is also a small vertical displacement.

Due to the differences in technique used for the two series of experiments it is impracticable to compare results of the present work with the Saunders Roe results under conditions of heel, and leeway, but some comparison between the predicted upright, zero leeway, resistance is possible and this is included in Section 23.2 which follows.

Plot of $C_D \sim C_L^2$

If the Lift Coefficient varied linearly with leeway and the Drag Coefficient followed a square law, the C_D plotted against C_L^2 would produce a straight line at each speed and heel, the slope of which is likely to vary. Results from the present experiments are plotted in this manner in Fig. 93 from which it can be seen that the variation is non-linear, showing considerable curvature at low leeway, a result to be expected following the non-linearity of Lift Coefficient with leeway. The vertical position of the curves on the plot will vary with speed in the same manner as the component quantities.

Ref. 5 indicates that the assumption of linearity for this curve is used to fair tank test data during routine work, and in Ref. 15, Fig. 17, linearity is assumed although the scatter of points is such that the variation could well be non-linear and there are indications that at low values of C_Y^2 the curves turn over in a

similar manner as those found from the present work.

It therefore appears dangerous to assume linearity for C_D plotted against C_L^2 for a particular hull especially one of 'traditional keel yacht' shape, without adequate experimental proof.

23.2 Upright Resistance

Ref. 1 gives predicted resistance curves for a Dragon at a full scale displacement of 43 cwts. and 39 cwts., and these are reproduced in Fig. 94a. According to the text of Ref. 1, these values were obtained by use of the Schoenherr Friction Line corrected for stimulator drag but not for the laminar area forward of the stimulators; no figures are given for the model scale so that comparison is possible only on the basis of predicted curves and those from the present work, as discussed in Chapter 22, which are for the 'standard' condition equivalent to a full scale displacement of 48 cwts. and at 18.31 lbs. model A.U.W. equal to a full scale displacement of 35.4 cwts., also shown in Fig. 94a.

It is clear immediately that the shape of these predicted curves from both series of experiments is similar, indicating general agreement between the series, but that they differ in level on the plot.

This difference in level may be explained by consideration of the following:

(a) The upper curve from the present series is for an A.U.W. some 5 cwts. grater that the upper curve from the Saunders Roe results; a difference of 4 cwts. in the latter series gives a difference in C_T of approx 0.0002, so that there may well be a difference of 0.00025 in levels due to this.

(b) In the present tests the stimulator penalty has been assumed equal to the laminar deficit, while previously no correction was made for the laminar deficit; which from the text of Ref. 1 could raise the curves by between 0.0004 and 0.0006, assuming a fully turbulent boundary layer on the yacht.

(c) Blockage effects have been ignored in the present work and the model resistance is likely to be high due to this.

(d) Comment has already been made concerning the condition of the model and its surface at the time of the present work and this could affect the level of the curves.

It must therefore be considered gratifying that the curves are eseentially identical in shape, and surprising that the difference in level is relatively small when the above factors are considered. There does not seem any reason to doubt the results obtained from the

present experiments, although a true correlation is desirable and could be obtained by running the same model in both tanks and correcting to a standard condition.

Comparison between Dragon hull and other forms.

Fig. 94b shows C_T against $V/\sqrt{L}$ for the dragon and two other hulls.

Ref. 10 gives results for the model of an International One Design Class yacht which was of similar size to the model used in the present series (L.W.L. of 3.226 ft.) so that comparison may be made between this curve and that for the Dragon.

Ref. 5 gives the predicted full scale resistance curve for a fairly shallow draught sketch having an L.W.L. of 50 ft. from a 1/12 scale model; the shape of this curve may be compared with that for the Dragon for which the full scale predictions from both series of tests are included.

Curves of friction coefficient for model and full scale have been omitted due to the difference in Reynolds No. and scale of the craft involved.

Fig. 94b indicates that the Dragon form is more successful than that of the other two vessels in prolonging an increase in wave making resistance when in the upright, zero leeway condition.

fig 88 lift coefficient for hull – variation with leeway

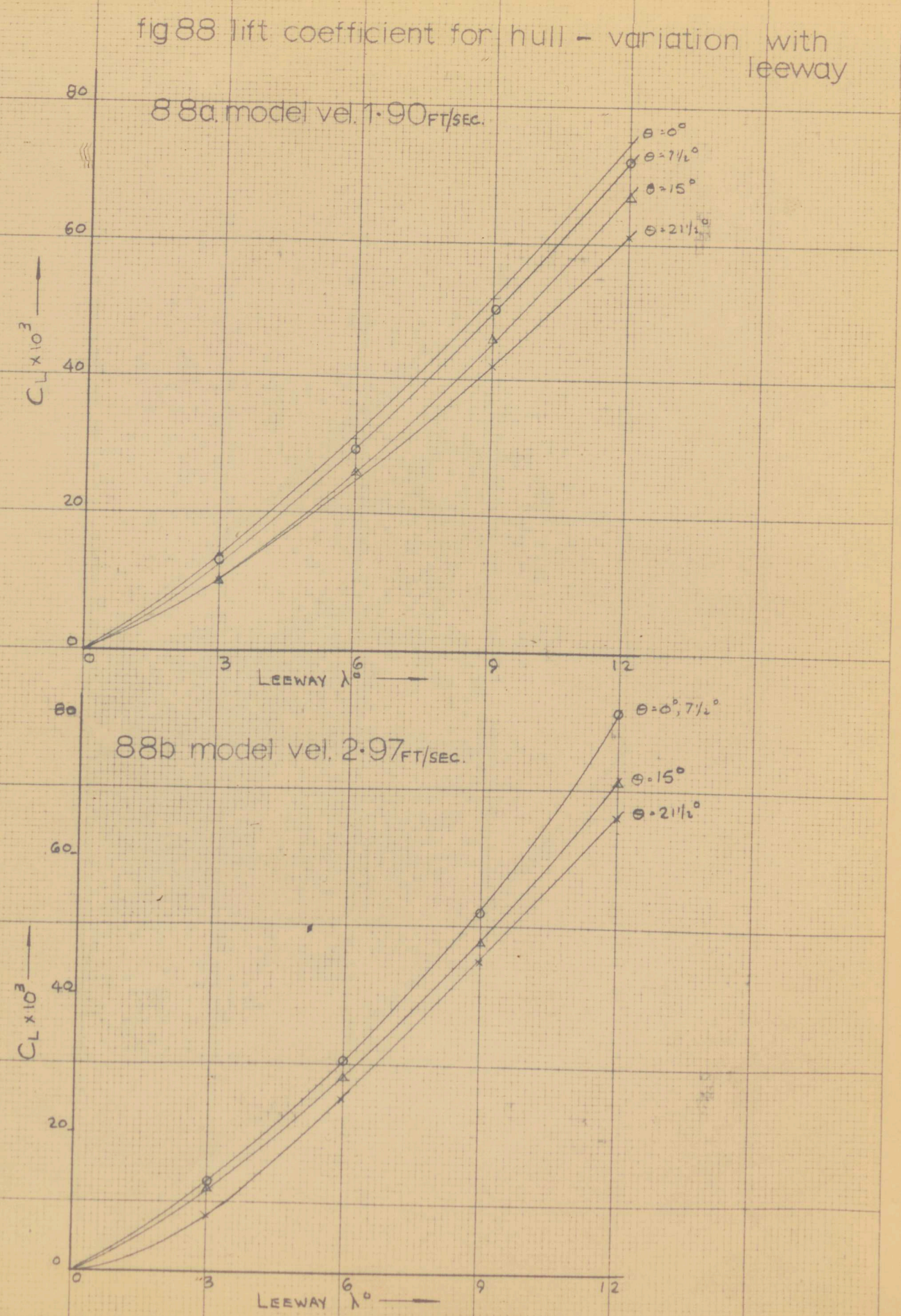

fig 88 lift coefficient for hull – variation with leeway.

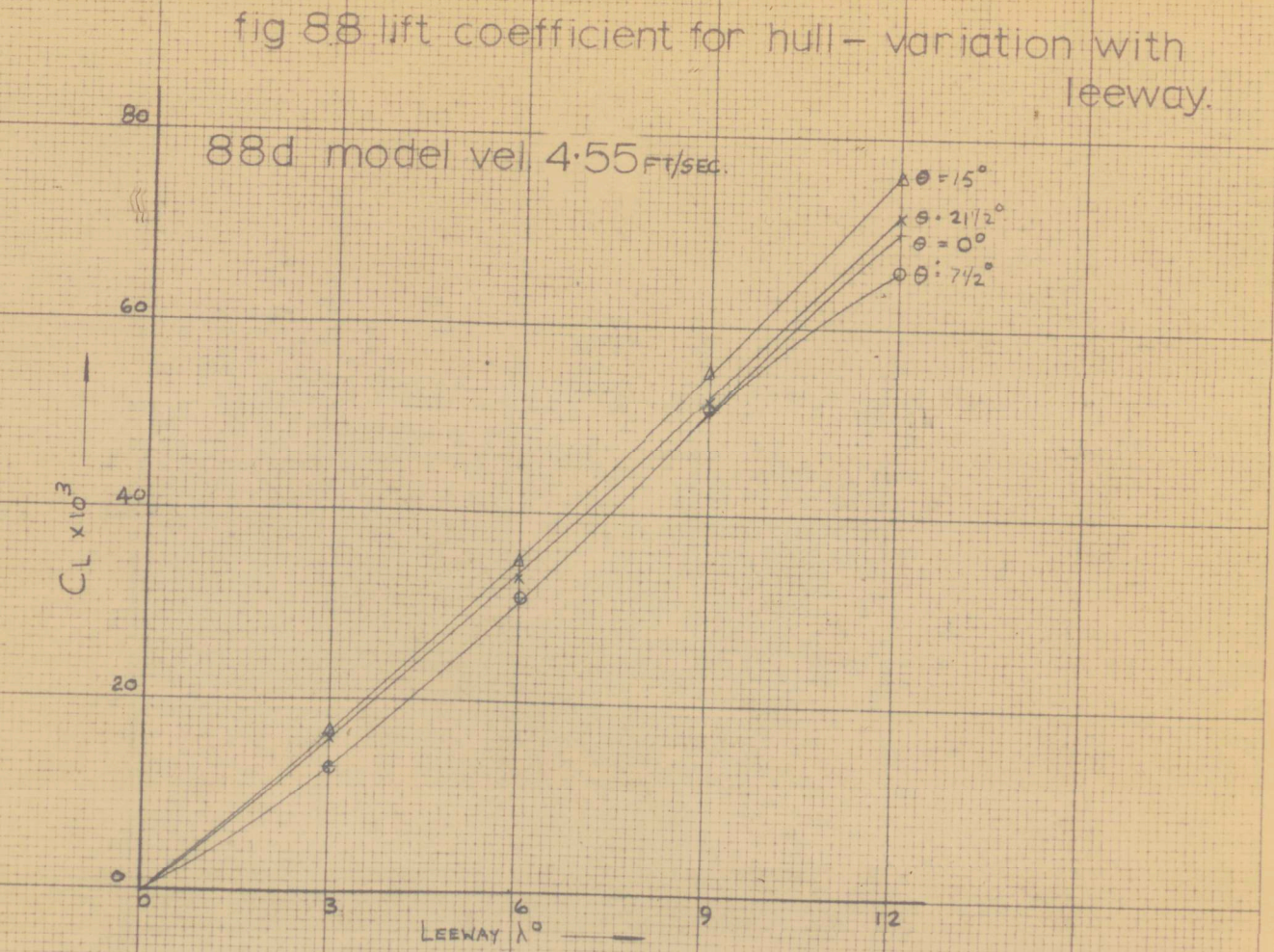

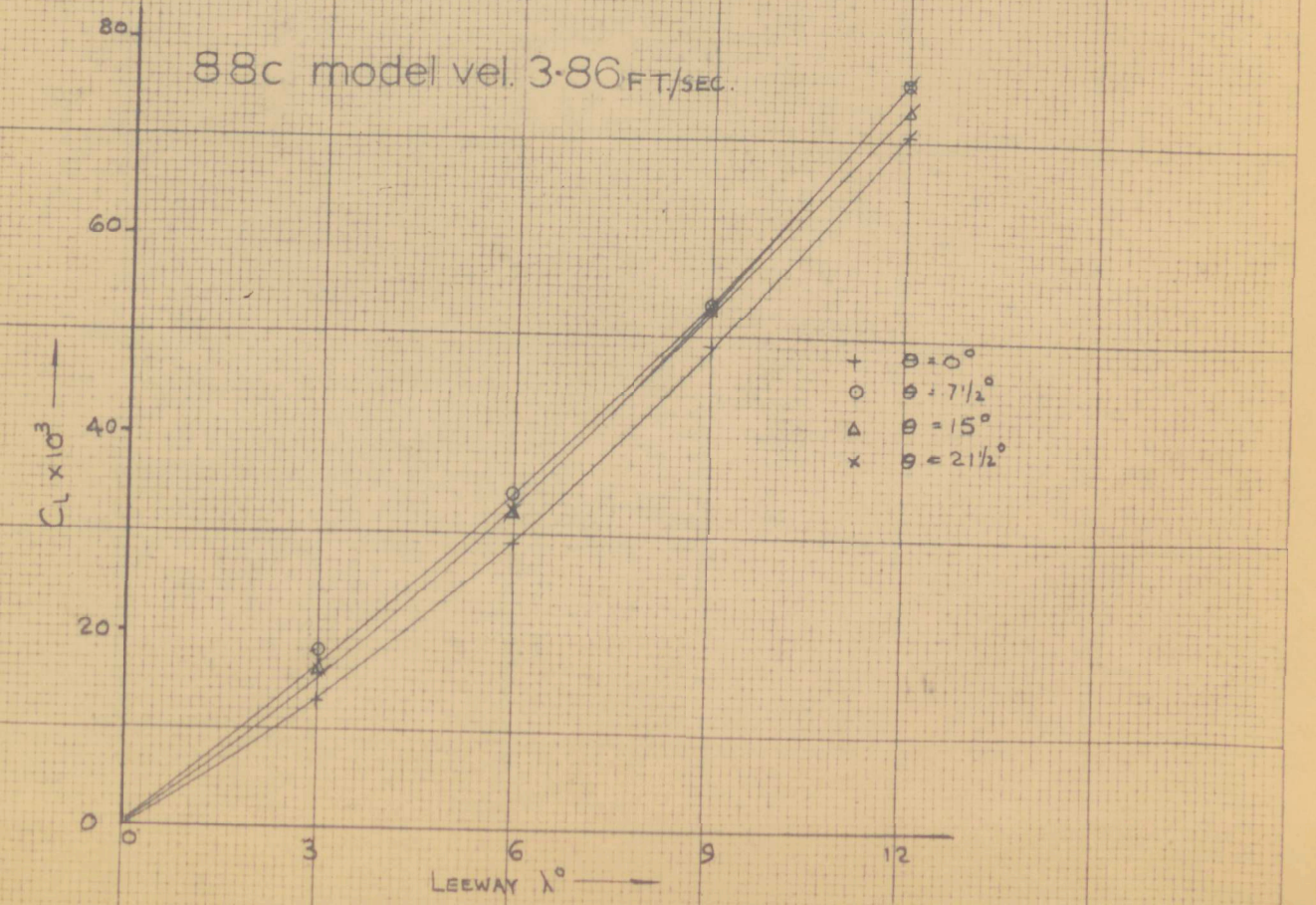

fig 89 illustration of velocity and heel effect on C_L.

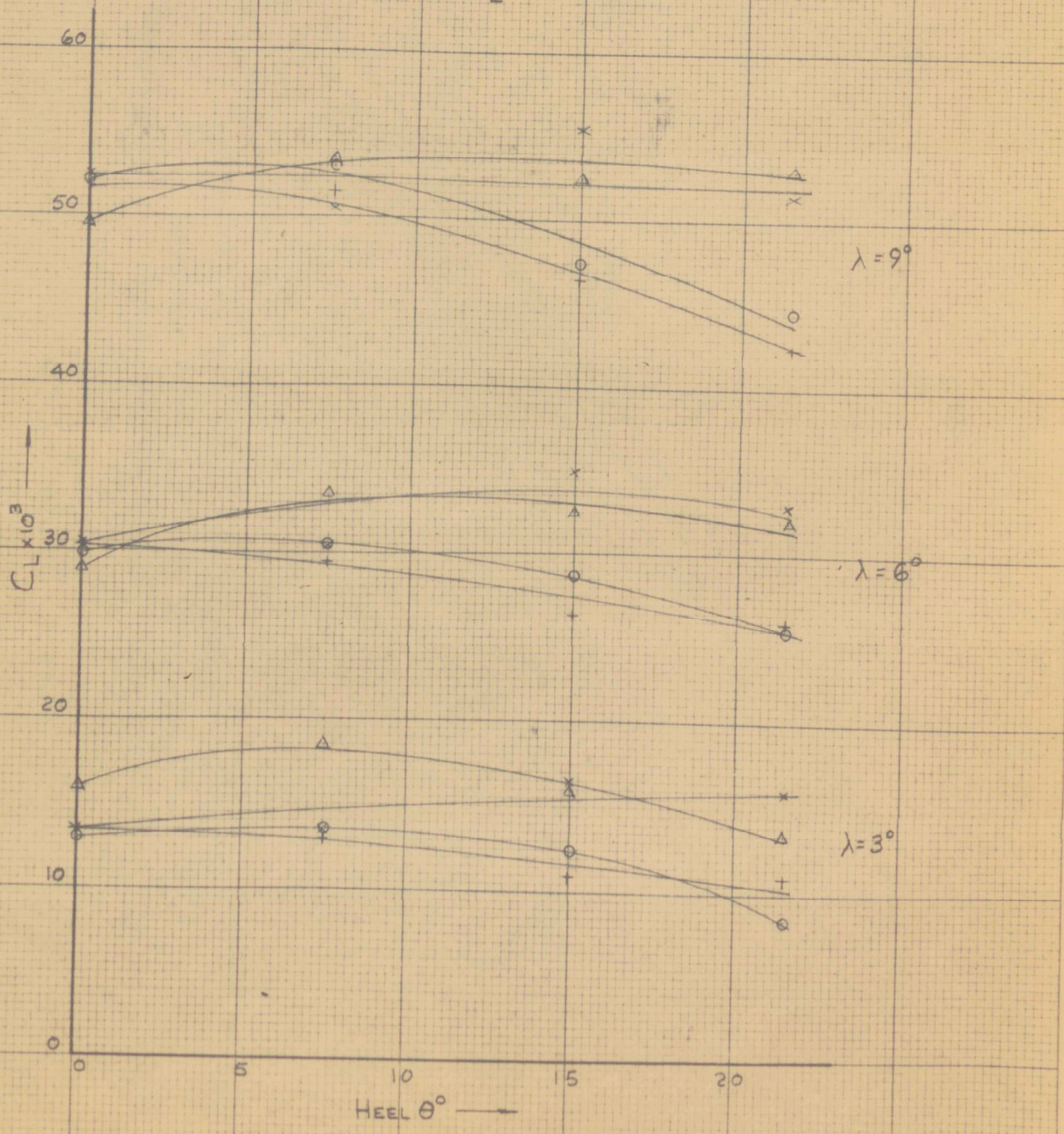

fig 90 lift coefficient from present work compared with that from previous tests at saunders roe division

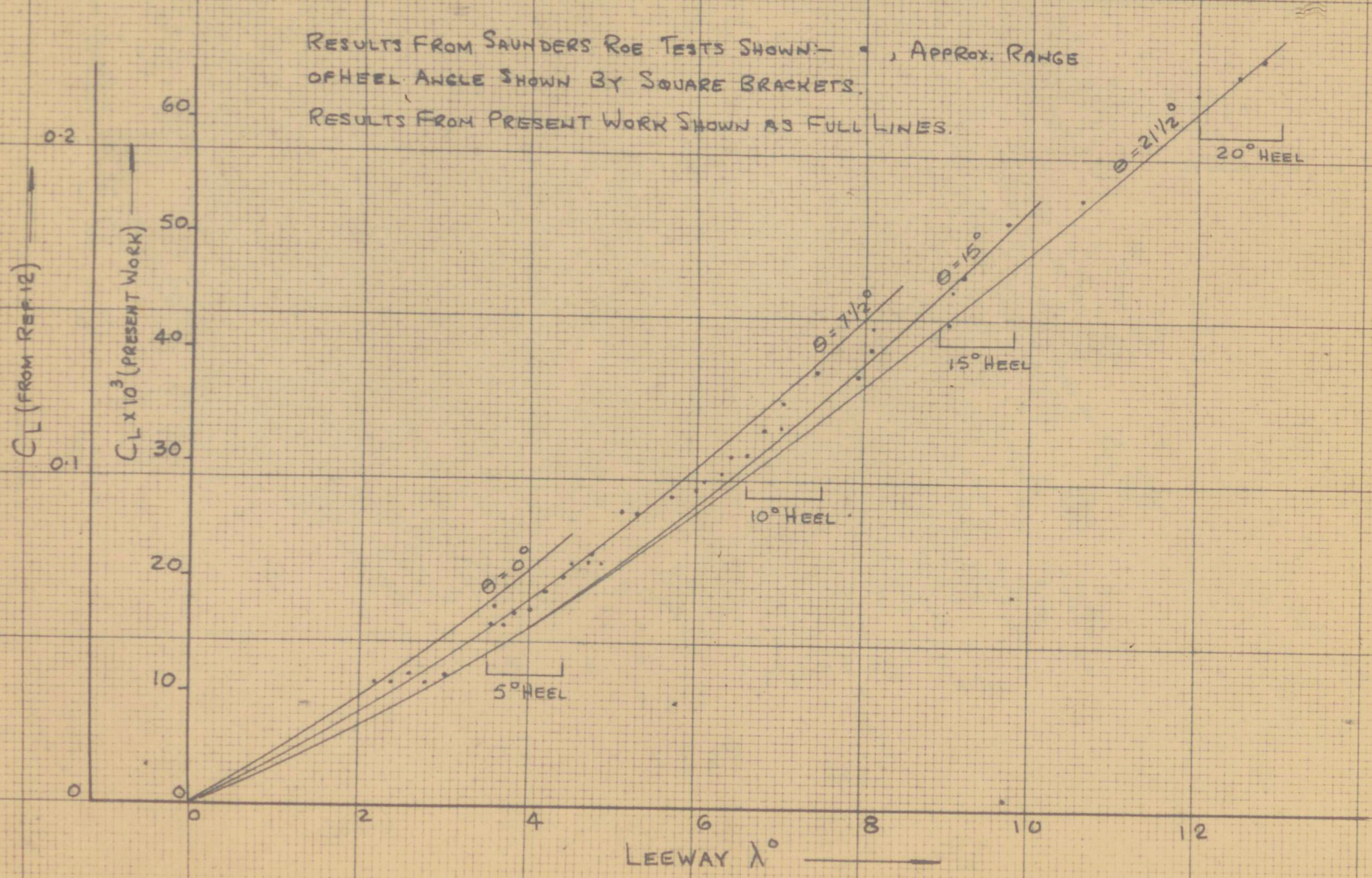

fig 91 drag coefficient for hull variation with leeway

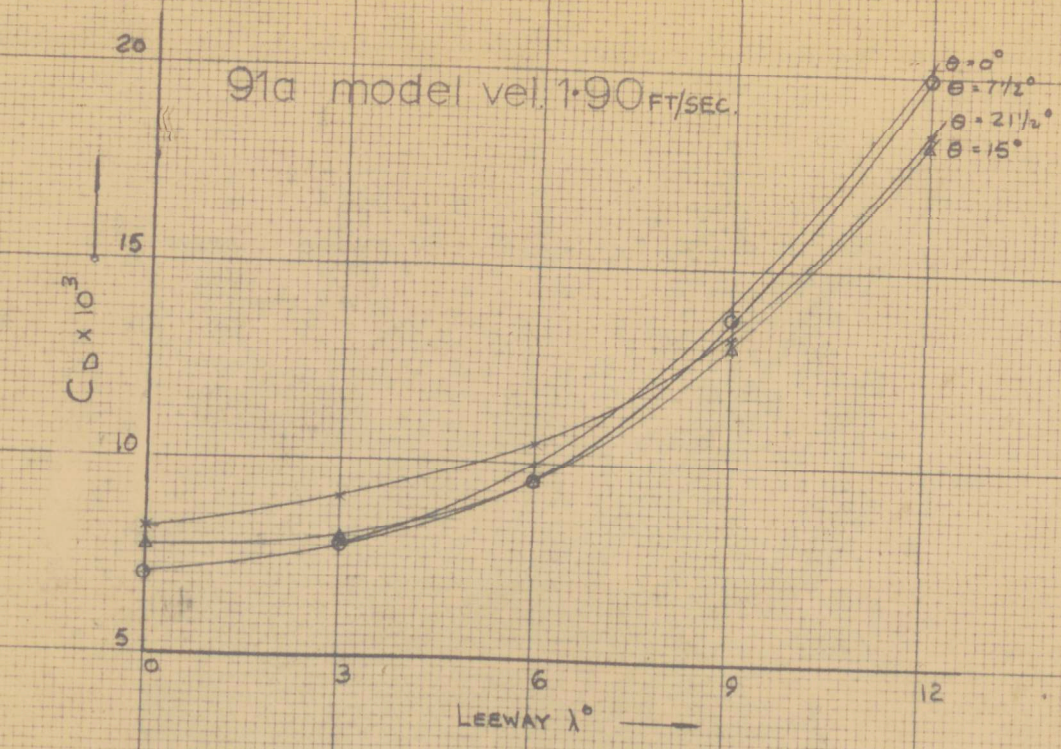

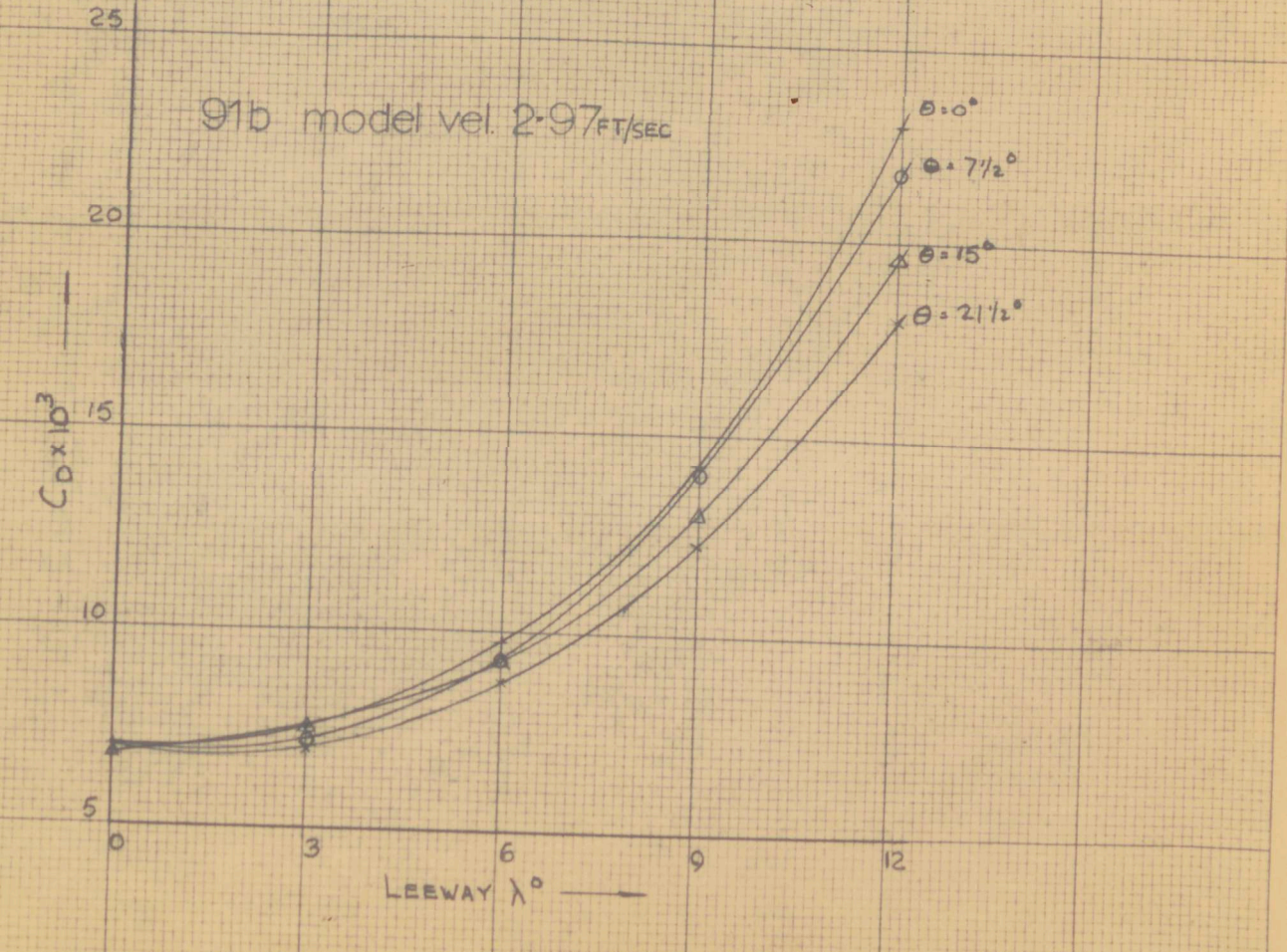

fig 91 drag coefficient for hull - variation with leeway

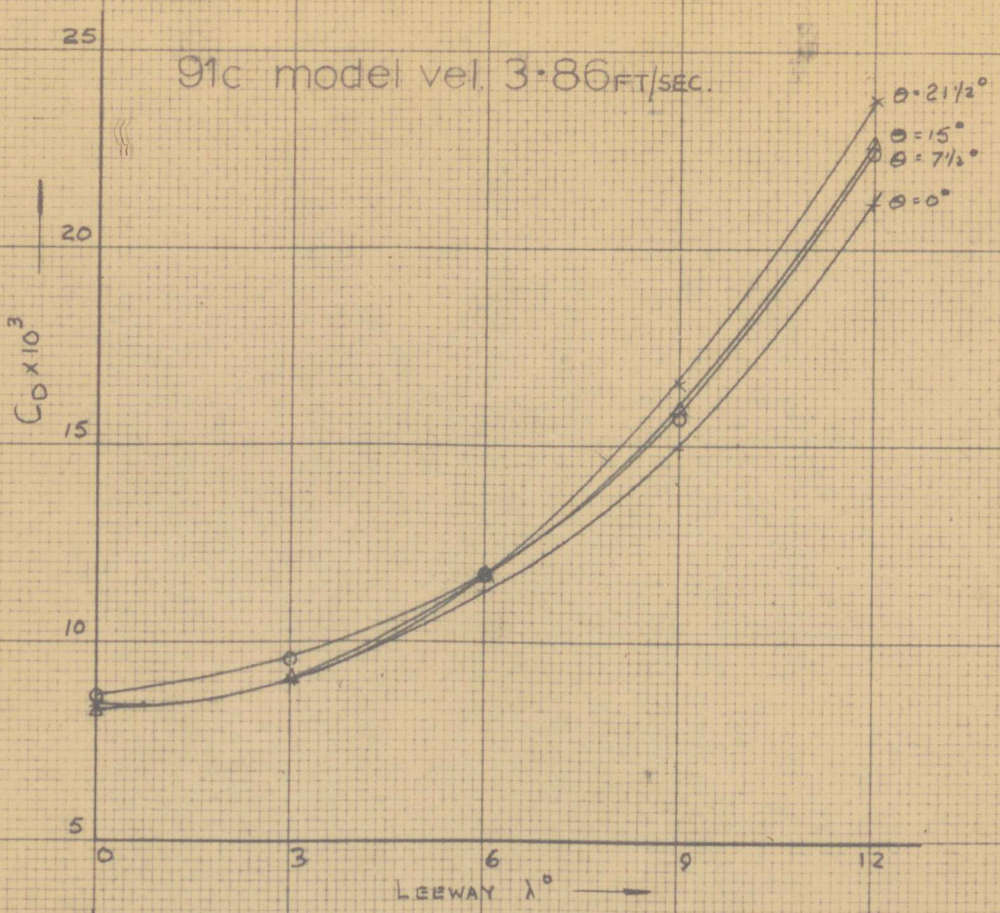

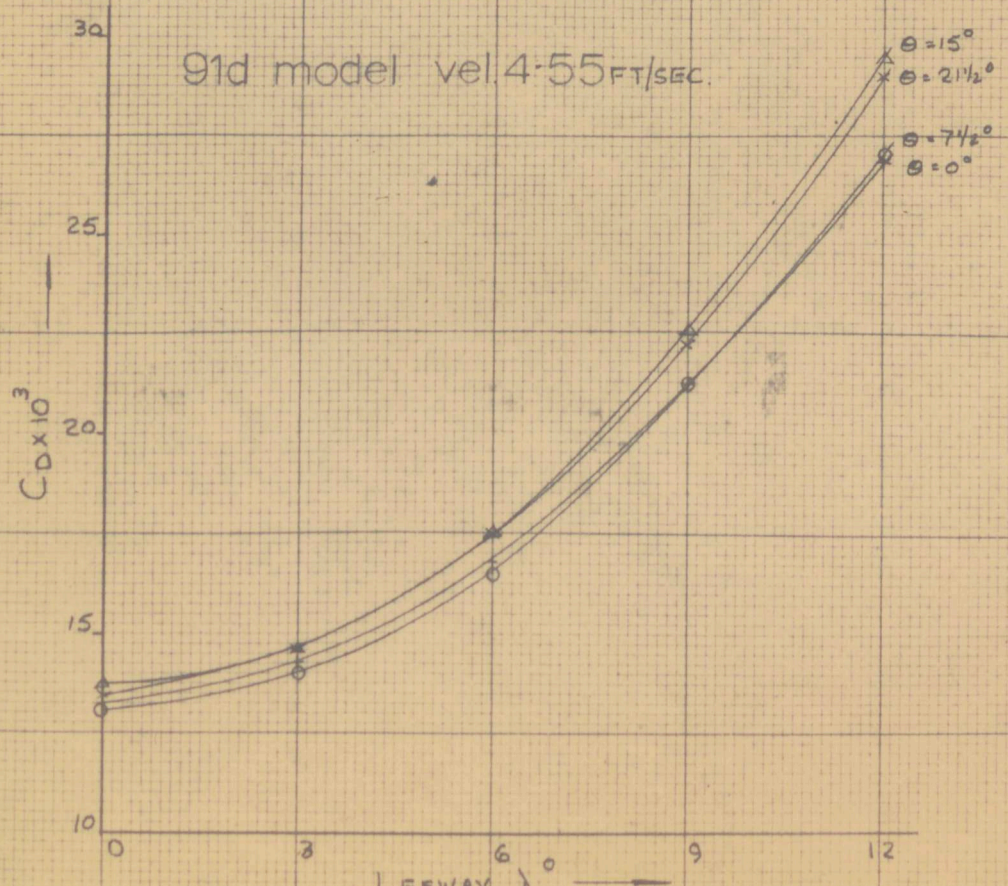

fig 92 comparison between typical $C_D - \lambda$ curve and square relationship.

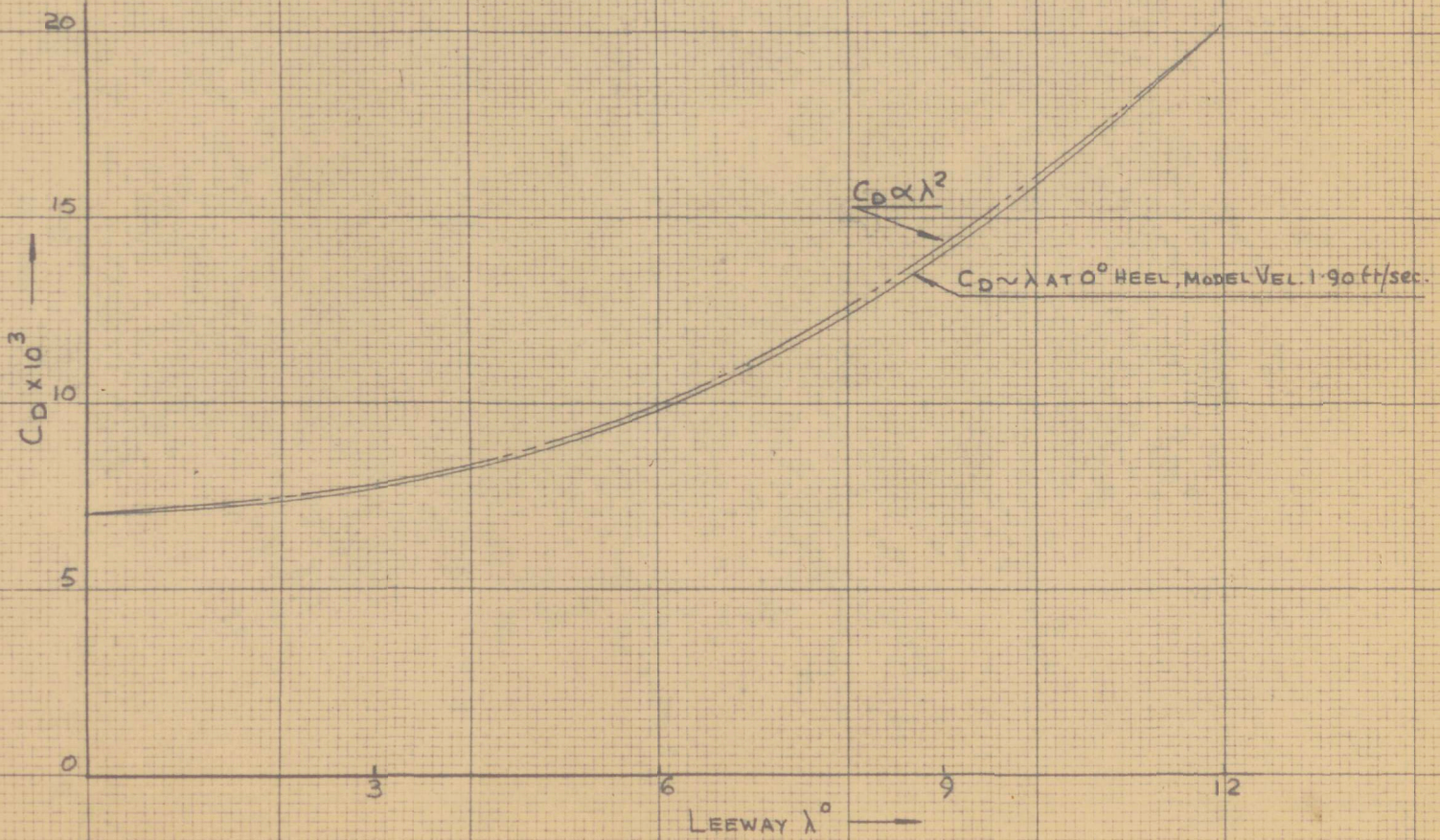

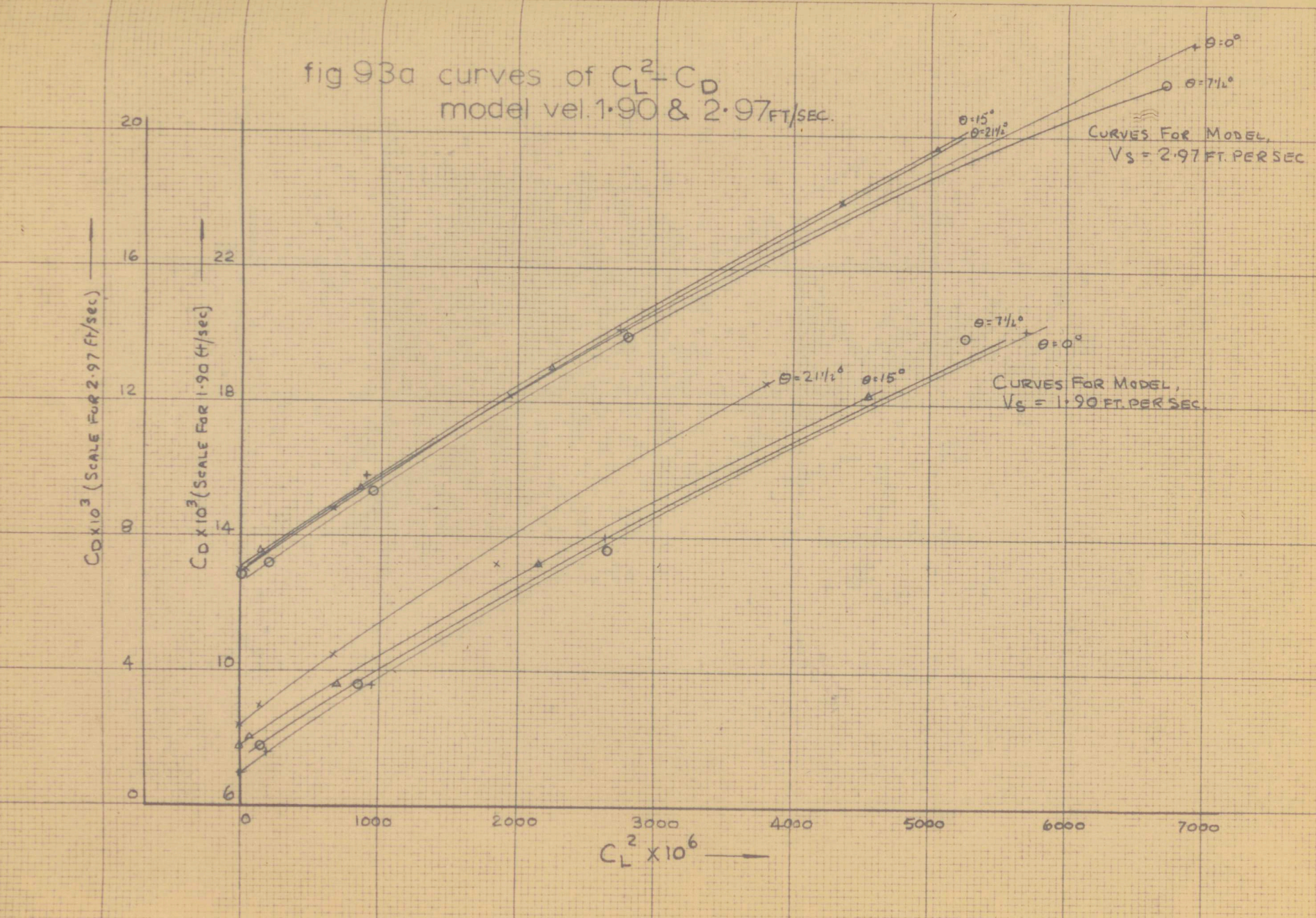
fig 93a curves of $C_L^2 - C_D$
model vel. 1·90 & 2·97 FT/SEC.
θ=0°
θ=7½°
θ=15°
θ=21½°
CURVES FOR MODEL,
Vs = 2·97 FT. PER SEC
θ=7½°
θ=0°
θ=21½°
θ=15°
CURVES FOR MODEL,
Vs = 1·90 FT. PER SEC.
$C_D \times 10^3$ (SCALE FOR 2·97 FT/SEC)
$C_D \times 10^3$ (SCALE FOR 1·90 FT/SEC)
$C_L^2 \times 10^6$
0
4
8
12
16
20
6
10
14
18
22
0
1000
2000
3000
4000
5000
6000
7000

fig 93b curves of $C_L^2 - C_D$
model vel. 3·86 & 4·55 FT/SEC.

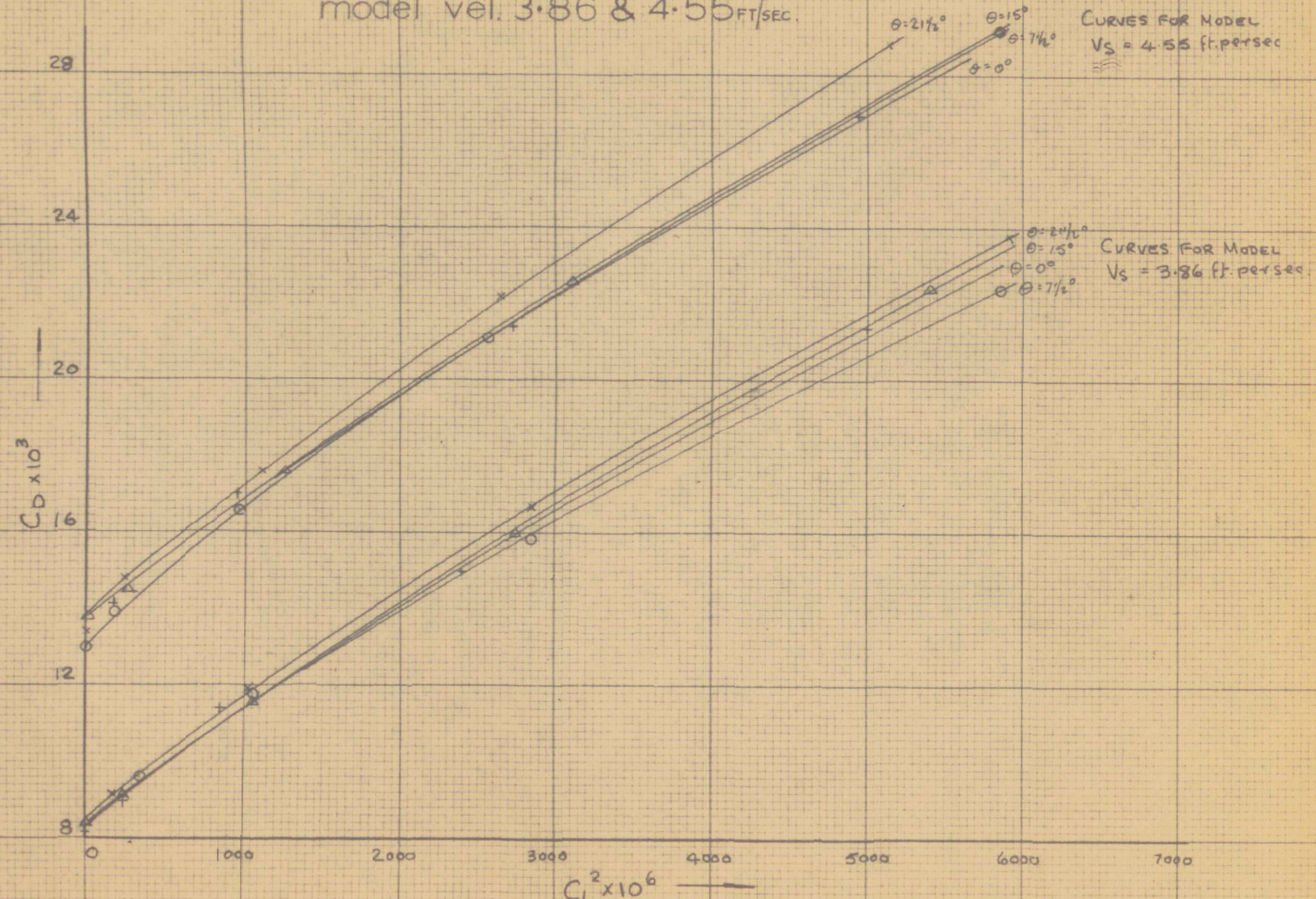

fig 94a C_T for model and full scale compared with that from saunders roe tests.

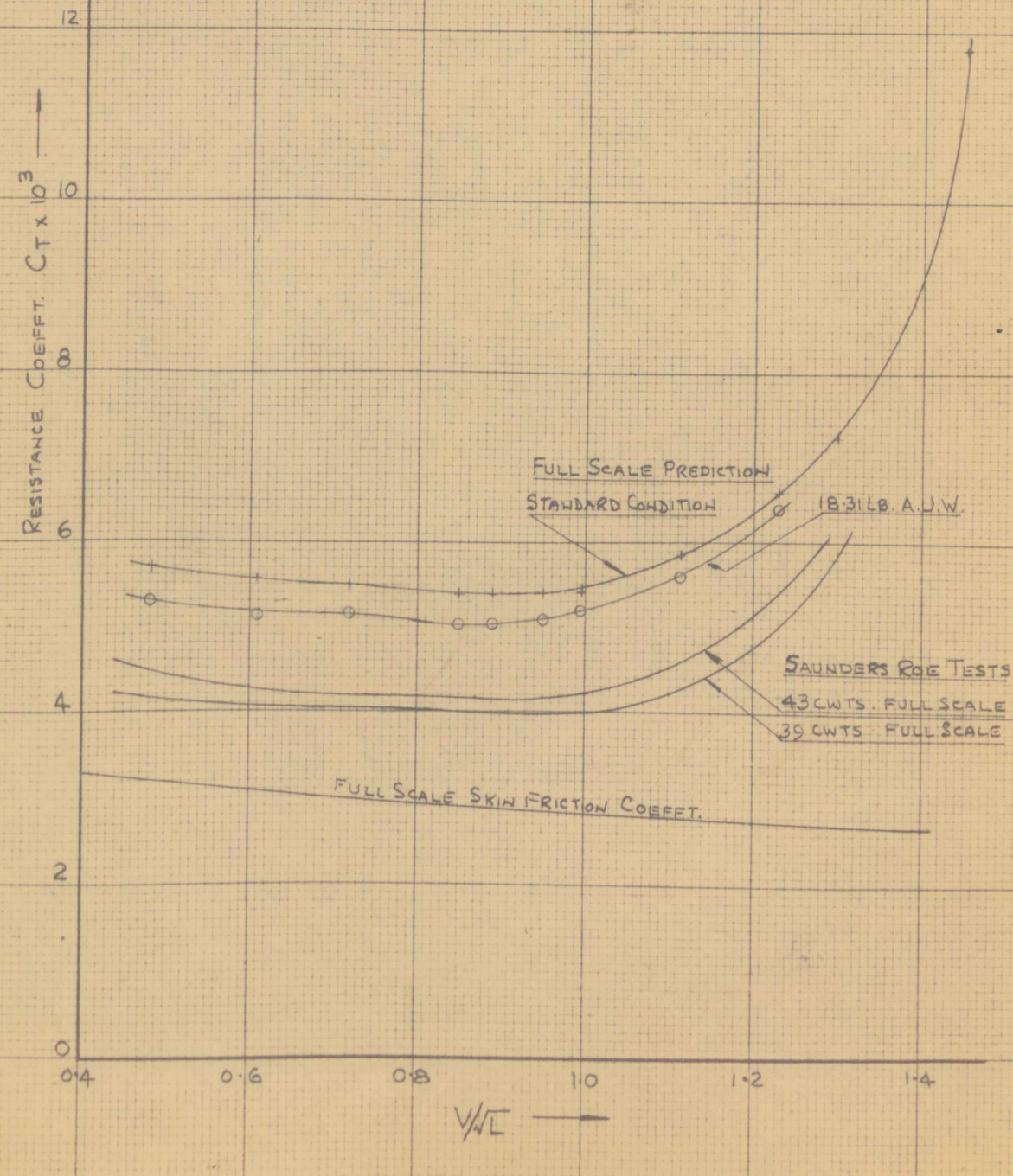

fig 94b C_T - comparison of 'dragon' with other hull forms.

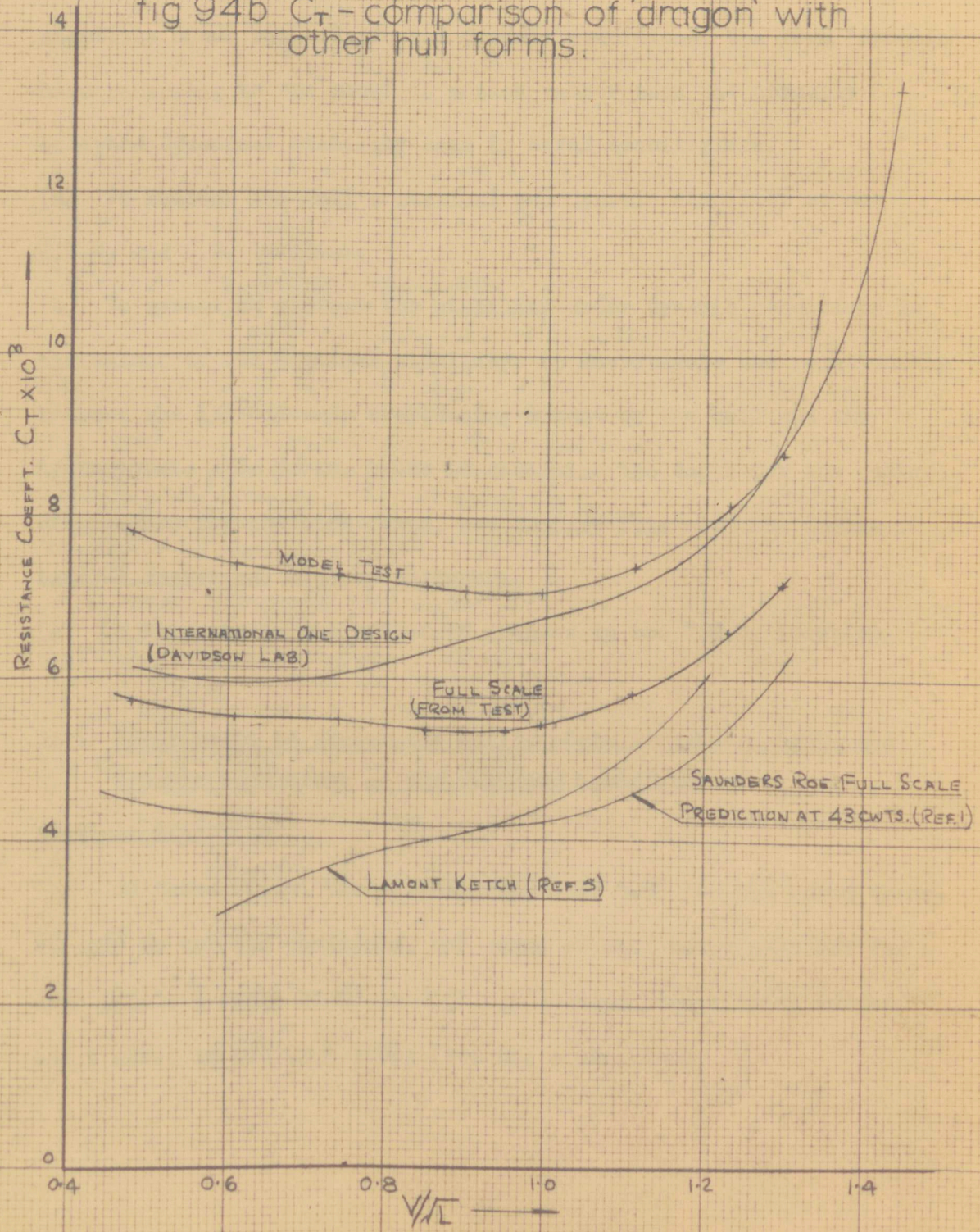

CHAPTER 24: TRANSVERSE STABILITY

Experiments were undertaken to establish the model's transverse stability under both static and dynamic conditions; the term 'dynamic' here referring to the model in motion rather than the normally accepted Dynamical Stability used in Naval Architecture.

(a) To measure the hull's statical and dynamic stability at one A.U.W. and C.G. location.

(b) To establish whether the stability under dynamic conditions is equivalent to the statical stability; to investigate the relationship between the hydrodynamic overturning moment on the hull and the hydrodynamic side force, hence to determine the depth for the centre of pressure for the side force, and compare this with the Centre of Lateral Resistance used by designers.

(c) To investigate the effect of changes in the V.C.G. location.

24.1 Experiments to measure the hull's stability under static and dynamic conditions at the Standard Condition

Statical Stability

In these tests, the sliding weight of 6.33 lbs was moved transversely to various positions, the angle of heel being read off for each point; a range of 0° to 21½° was covered, the sliding weight being moved in two inch steps from the centreline.

Fig. 95 shows the hull's statical stability in terms both of the distance of the sliding weight from the centreline and of the Applied moment given by:

$$M_{Xw} = \frac{6.33}{12} . x . \cos\theta \qquad \text{lb.ft.}$$

where x is the distance of the sliding weight from the centreline (model upright).

Stability under dynamic conditions

The hull was run at the desired condition of speed and leeway the sliding weight being moved in intervals of two inches, and the resulting heel angle measured. In addition the position of the sliding weight to maintain the model upright was obtained for each condition of speed and leeway.

Model velocities used were: 1.90, 2.97, 3.86, and 4.55 ft/sec., and the leeway was increased from zero to 12° in 3° steps.

Figs. 96 to 99 show the measurements from tests in terms of the sliding weight position and resulting heel angle.

Force measurements, described in Chapter 21, were made at four heel angles: 0°, 7½°, 15°, and 21½° so that in order to allow further analysis of the stability, it was necessary to calculate the Applied Moment M_{Xw} on the hull at each condition of speed and leeway for these four inclinations.

In each case the applied moment was found from:

$$M_{Xw} = \frac{6.33.x.\text{Cos}\,\theta}{12} \quad \text{lb.ft.}$$

by reading the positions of the sliding weight to maintain the four heel angles under each condition of course velocity and leeway from Figs. 90 to 93.

The values of these moments are shown in Table 11.

24.2 Comparison of statical and dynamic stability, and relationship between applied moment and F_{Yw}

M_{Xw} is the moment required to maintain the yacht at a certain heel angle, and does not represent the hull's stability under dynamic conditions, although a simple relationship does exist between these quantities.

If, for a heel angle θ, the yacht's dynamic stability is M_D and the hydrodynamic overturning moment is M_o, then:

$$M_D = M_{Xw} + M_o$$

or $$M_D = M_{Xw} + F_{Yw}.h$$

where h is the depth of action of F_{Yw} below the pivot. F_{Yw} is usually assumed by designers to act at the geometric centroid of the underwater hull profile: the C.L.R.

In standard commercial performance tests using hull measurements and assumed sail coefficients of the 'extended Gimcrack type', and also in more basic performance studies it is often assumed that F_{Yw} acts at a fixed distance below the waterline. (ref.3)

Crewe (Ref. 1) gives some measure of justification for this use in Ref. 3 by using assumed sail coefficients, but it has never been verified by an extensive series of experiments similar to those described here.

Also, it is generally assumed that the yacht's stability under dynamic conditions is equivalent to the statical stability at the relevant heel; this also has never been investigated previously.

If this were true, then the previous equation may be re-written as:

$$h = \frac{M_S - M_{Xw}}{F_{Yw}}$$

where M_S is the statical stability at the heel angle considered.

By plotting M_{Xw} against F_{Yw} however, the assumption is unnecessary, while its validity can be checked and the depth of action for F_{Yw} obtained.

Fig. 100 shows this plot for the various model velocities and heel angles considered, the result being a series of straight lines, the slope of which increases with heel, while velocity does not appear to cause any appreciable departure from the linear variation.

If the original equation is re-written as:

$$M_{Xw} = M_D - F_{Yw}.h$$

then M_D is the intercept of each line on the M_{Xw} axis and h is the slope of each line.

The statical stability is marked in Fig. 100, and it may be seen that the dynamic stability is in each case slightly greater than the equivalent statical stability, the difference increasing with heel; h increases with heel, particularly at the larger heel angles.

When the model is heeled, a hydrodynamic overturning moment is provided by both the horizontal and vertical components of the total hydrodynamic force, the relative magnitude of that from the vertical component increasing with heel.

Davidson (Ref. 9) assumed that the total component of hydrodynamic force in the travsverse plane acts at right angles to the yacht's centreline plane, and this has been maintained by many writers. If this were true, then it is equivalent to $\frac{F_{Yw}}{Cos\theta}$, and h should now be measured at $\theta°$ to the upright.

Fig. 101 shows the value of $h_1 = h.Cos\theta$, where h is taken from Fig. 100; h_1 is now the depth of action of $\frac{F_{Yw}}{Cos\theta}$ from the pivot point measured down the centre-line plane.

If the assumption were correct, the value of h_1 at all heel angles should be the same, but in fact this is not so. Indications are that the component, in the transverse plane, of the total hydrodynamic force does not act at right angles to the yacht's centreline plane; and this is further confirmed by the results of force measurements discussed in Chapter 21, where F_{Yw} should vary by a Cosine law with heel if the assumption were correct, but was not found to be so.

Comparison between h_1 and the designers assumed depth for C.L.R.

The shape of the underwater profile and the standard waterline for the experiments is shown in Fig. 102, the depth of the designer's C.L.R. below the waterline is equivalent to the depth of the centroid of this profile.

Two methods of calculation were used to determine this depth:

(a) Use of Simpsons First Rule with nine ordinates.

(b) Splitting the area into a number of rectangles and triangles.

Due to the discontinuity of the profile curve, it was felt that the Simpsons Rule method might give an erroneous result, but remarkable agreement was obtained between the two methods, giving a mean value for the depth of C.L.R. as 3.14 ins. The detailed Calculations are shown in Tables 13 & 14 which should be studied in conjunction with Fig. 102.

For the hull upright, the experimental results for h_1 may be compared directly with the depth above. It is seen that the experiments gave the depth of action for F_{Yw} as 3.33 ins, below the pivot point. In this standard condition, the pivot was 0.41 ins. above the waterline so that the depth of action is 2.92 ins. below the waterline, some 0.2 ins. above the designer's assumed C.L.R.

The maximum draught of the hull is some 8.42 ins. and on placing both depths in terms of a percentage of this, the difference between them is about 2½%.

There appears good reason to believe therefore, that, certainly as a first approximation, the force component F_{Yw} may be assumed to act at or very near to the geometric centroid of the hull below water profile, equivalent to the 'designer's C.L.R.'

24.3 Change in Location of the V.C.G. and resulting effect on Stability

Fig. 103 shows a yacht having an A.U.W. of W, with an upright waterline w-l, heeled through an angle θ to a waterline w_1-w_1. The centre of buoyancy has moved from B to B_1 (static condition).

If the vertical location of the yacht's C.G. is G_1, then the restoring couple tending to bring the yacht towards the upright is $W.G_1Z_1$, and if the vessel is to be maintained at θ° heel, then an

overturning moment of $M_1 = W.G_1Z_1$ must be applied.

With the hull stationary in still water, if the C.G. is raised to G_2 the the restoring couple will support only a decreased overturning moment $M_2 = G_2Z_2$, and the restoring moment is reduced by:

$$M_1 - M_2 = W(G_1Z_1 - G_2Z_2) = W.G_1G_2. \text{Tan}\theta$$

ie. there is a linear relationship between the movement of C.G. and the available restoring moment.

When the yacht is making way, the inherent restoring moment (as distinct from the nett moment when the overturning effect of the side force is taken into account) will alter due to the effect of the pressure distribution on the waterline and underwater form, these effects becoming more important as velocity, heel, and leeway increase.

It is assumed normally in standard yacht testing (Refs. 4 & 8) that change in inherent stability due to pressure variation is negligible and that the same relationship holds between the V.C.G. and restoring moment as with the hull stationary.

A short series of experiments was undertaken to assess whether this assumption is satisfactory.

By altering the height of the sliding weight and its supporting structure, the V.C.G. of the hull was arranged in three vertical

positions: 0.91, 1.3, and 1.61 ins. below the datum level, and the restoring moment measured for both static and dynamic conditions.

Before these runs were undertaken, the model had been modified for the rudder tests described in Chapter 25; a new rudder was fitted together with tiller and securing arrangements, resulting in an increase of model weight to 25.23 lb. with L.C.G. 29.1 ins. from the after end.

Statical Stability

With the model stationary, the sliding weight was moved athwartships in two inch increments from the centreline, and the resulting angle of heel measured, with the V.C.G. at each of the three locations.

Figs. 104a and 104b show the result; the restoring moment (equal to the applied moment) varies linearly with the height of the V.C.G. (Fig. 104b) as would be expected from theory, the variation being given by:

$$\text{Change in Moment} = W.G_1G_2.\ \text{Tan}\theta$$

Stability Under Way

A number of runs were made with the model at the three V.C.G. positions to assess the effect on stability at three velocities: 1.90, 2.97, and 3.86 ft/sec., while leeway was maintained at 3° and 6°.

With the hull fixed at one value of leeway, the sliding weight

was moved in two inch increments, and the resulting heel angle measured for each speed and V.C.G. Results in terms of applied moment (equal to restoring moment) and heel are given in Fig. 105.

Assessment of the results under dynamic conditions is complicated by the overturning effect of F_{Yw}; this will, however, be indentical for all V.C.G. locations at one value of heel and leeway, and in Fig. 106 the applied moment required to maintain the hull at 15° heel for leeway of 3° and 6° is plotted against V. C.G. for each speed. The effect of including the hydrodynamic overturning moment would be to displace curves vertically on the plot without altering their shape.

It may be seen that the variation of restoring moment with V.C.G. is no longer linear, the curvature increasing with speed, and showing the same trends at both leeway angles used during the test runs.

The increase in inherent stability resulting from a fall in V.C.G. from 0.91 to 1.3 ins. below datum is greater than that from statical considerations, ($W.G_1G_2.\ Tan\theta$ = 2.625 lb. ins) while the increase for a further 0.39 ins fall in V.C.G. is less than that under static conditions.

It must therefore be questionable whether the assumption that inherent stability under way when making leeway and heel is identical

with the statical stability, can be considered sufficiently accurate for normal use.

fig 95 statical stability of 'dragon' hull model.

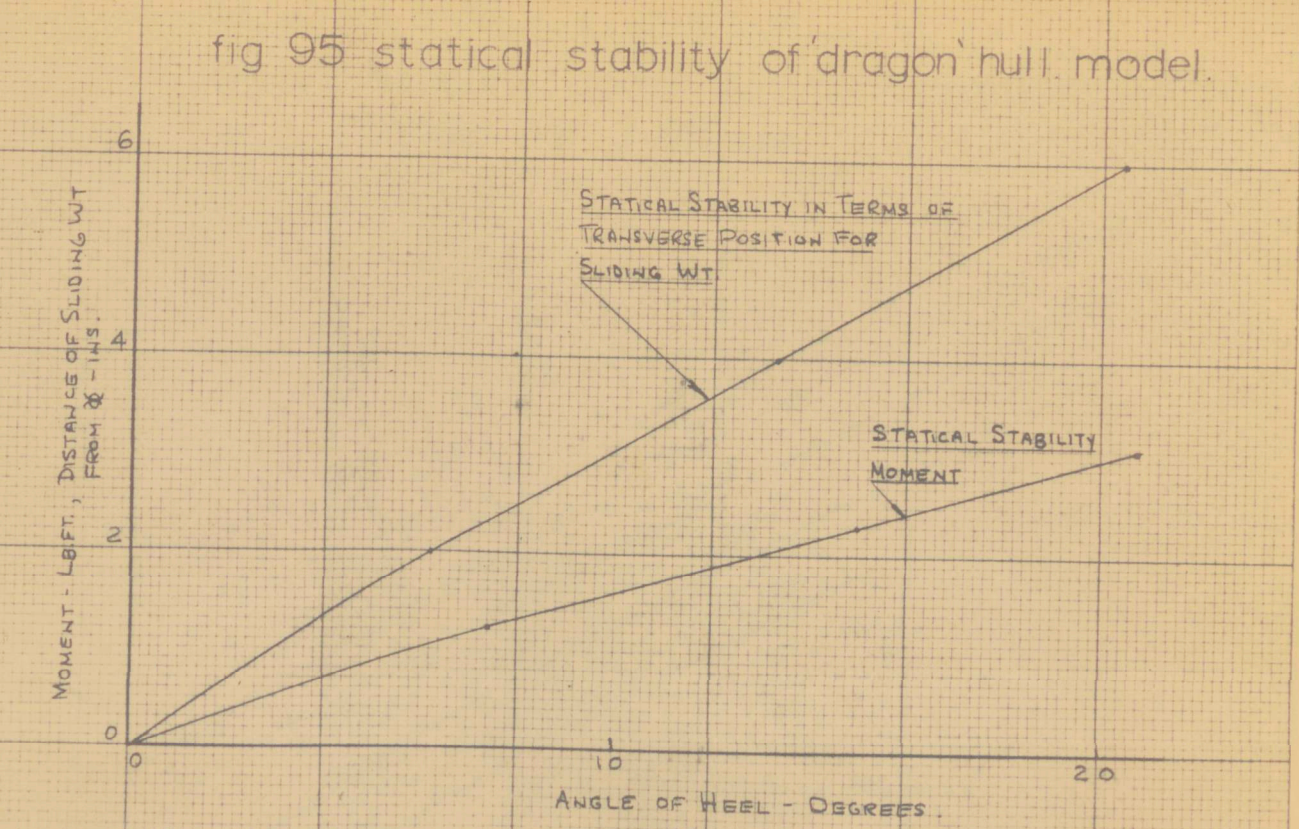

fig 96 stability under dynamic conditions.
model vel 4·55 FT/SEC.

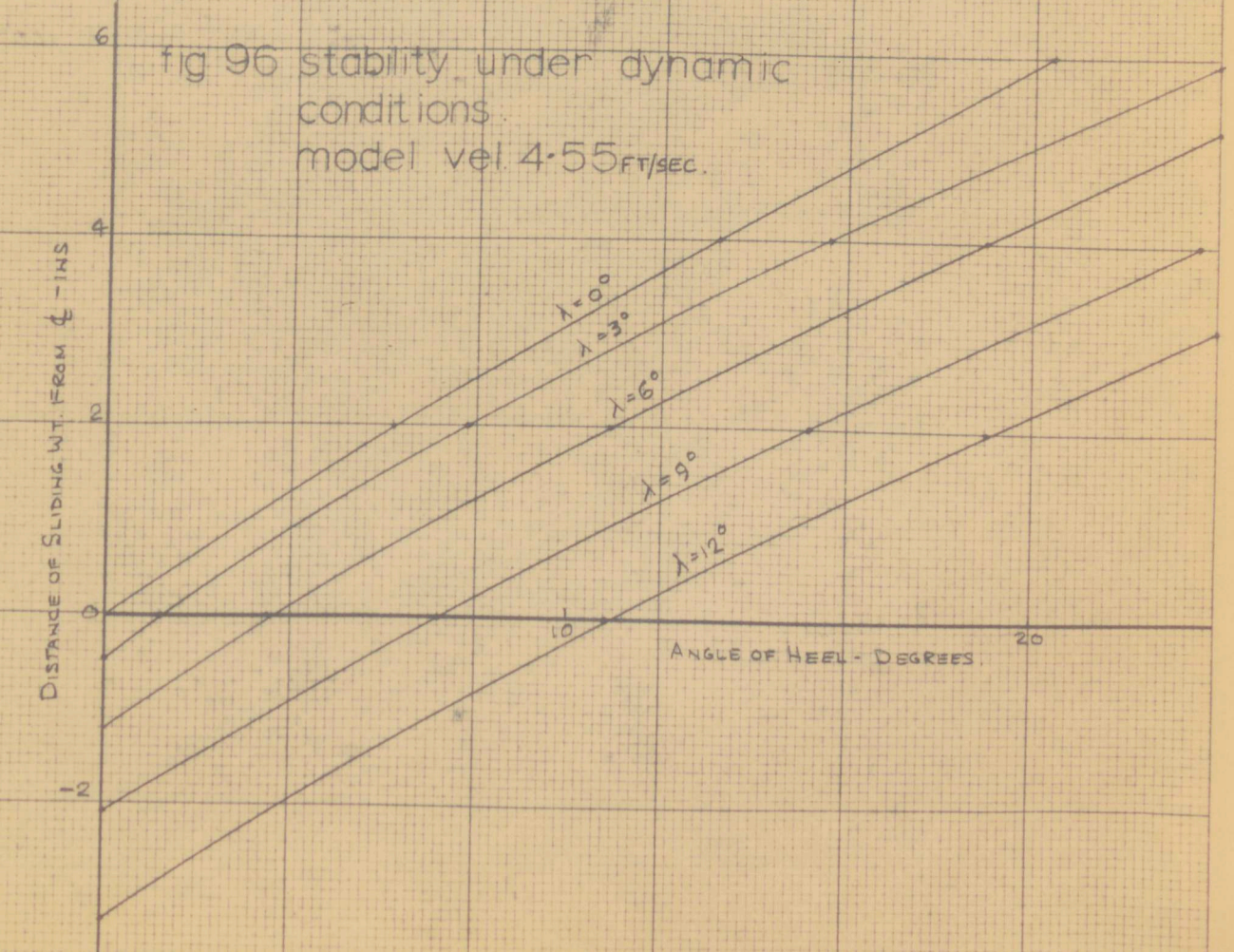

fig 97 stability under dynamic conditions.
model vel. 3·86 FT/SEC.

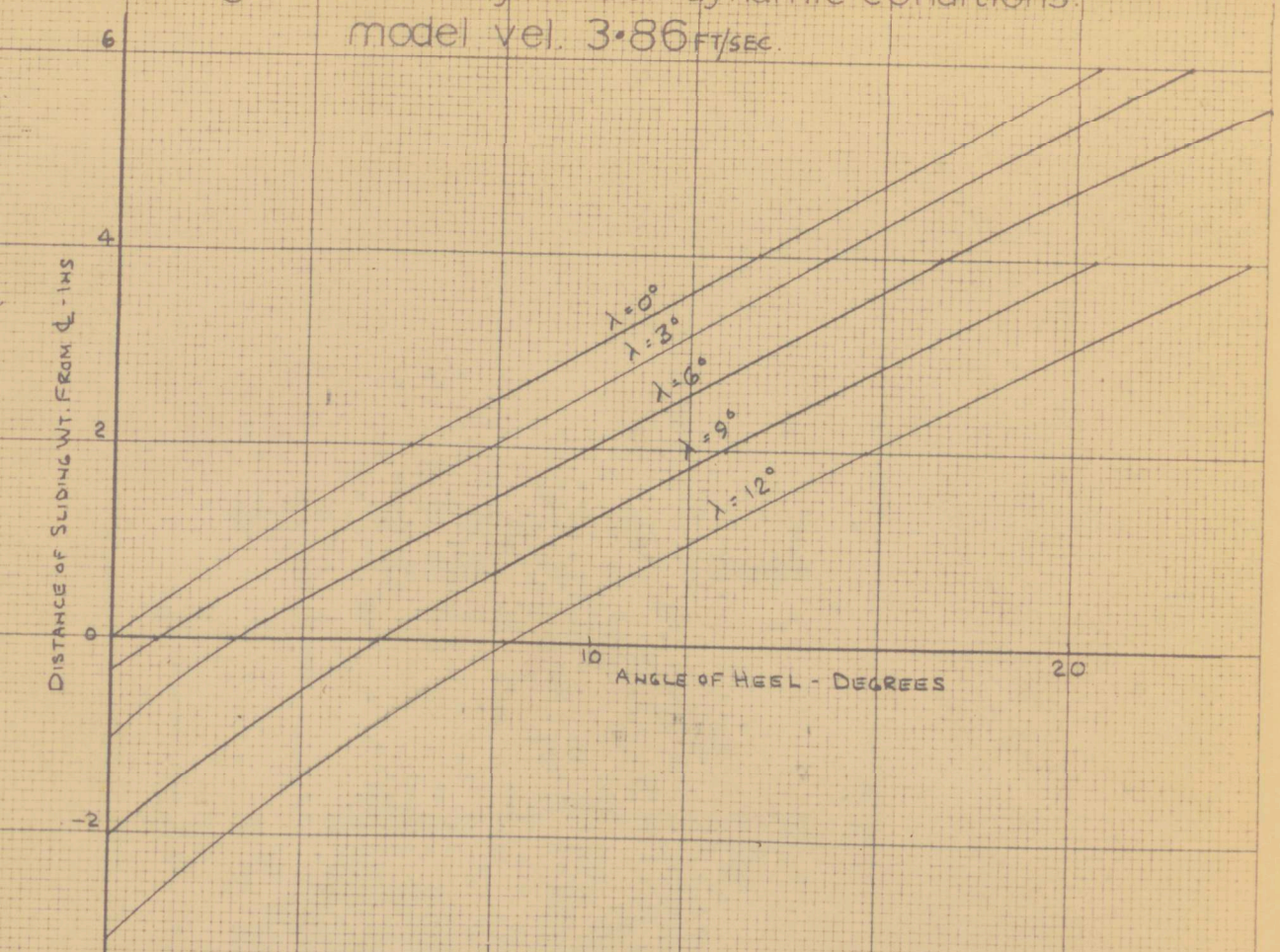

fig 98 stability under dynamic conditions.
model vel. 2·97 FT/SEC.

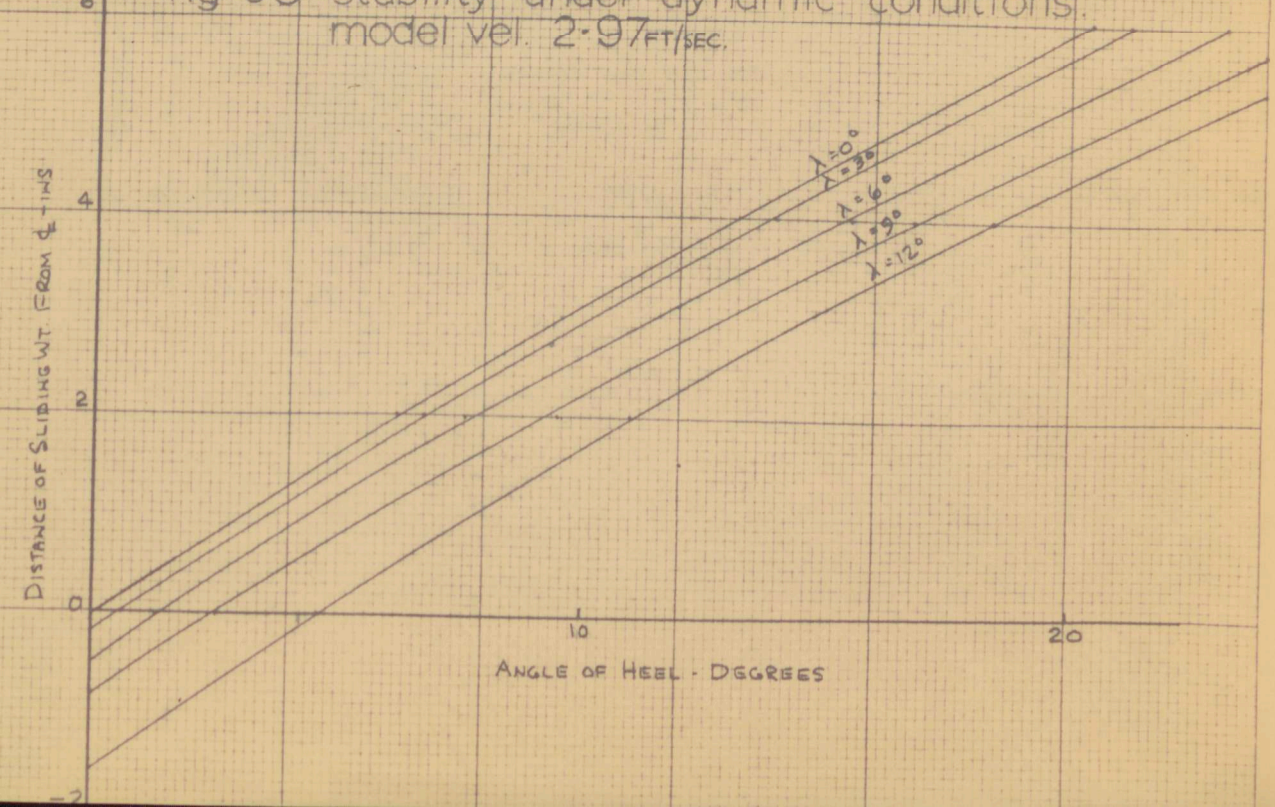

fig 99 stability under dynamic conditions.
model vel. 1·90 FT/SEC.

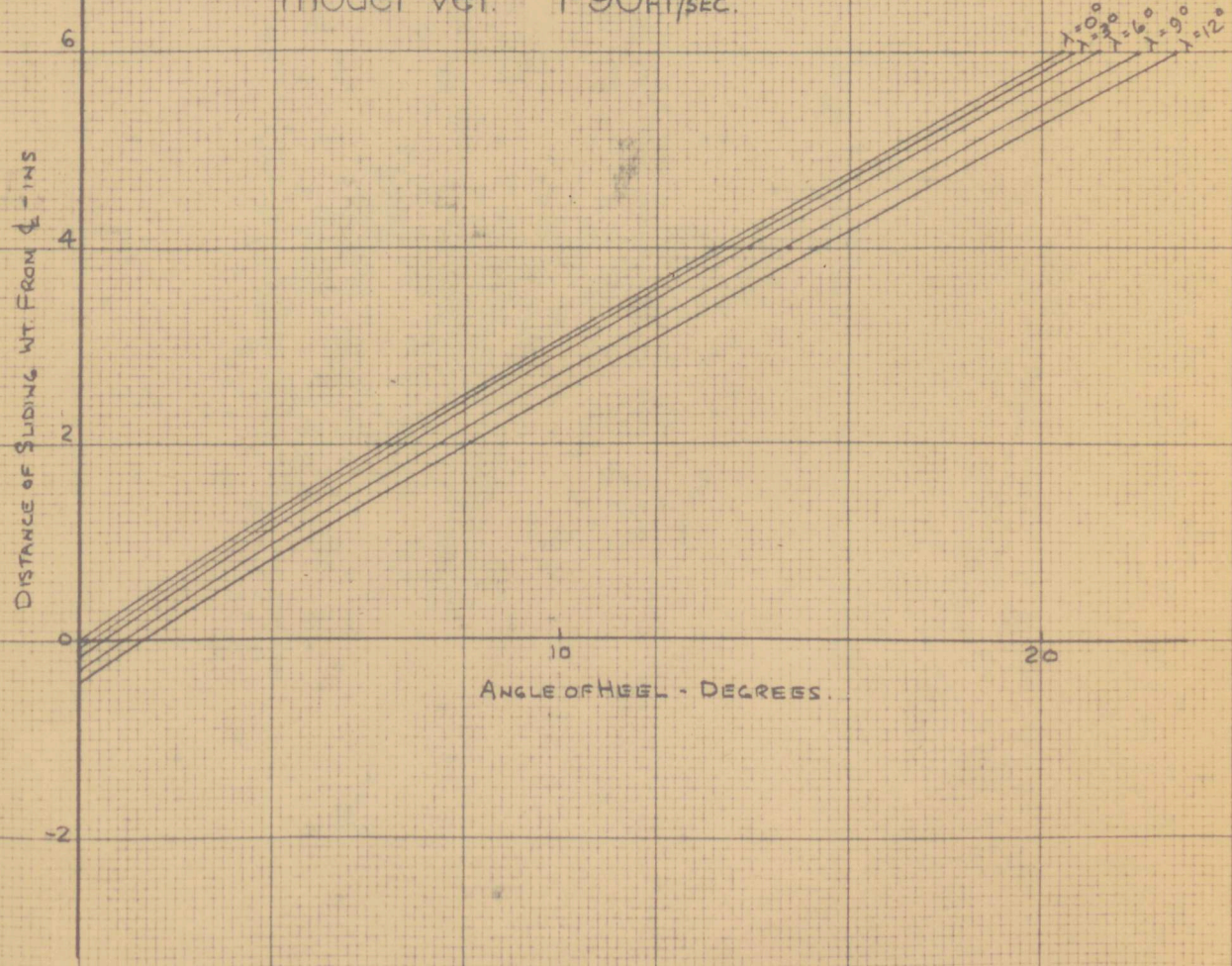

fig 100 stability. applied moment - sideforce

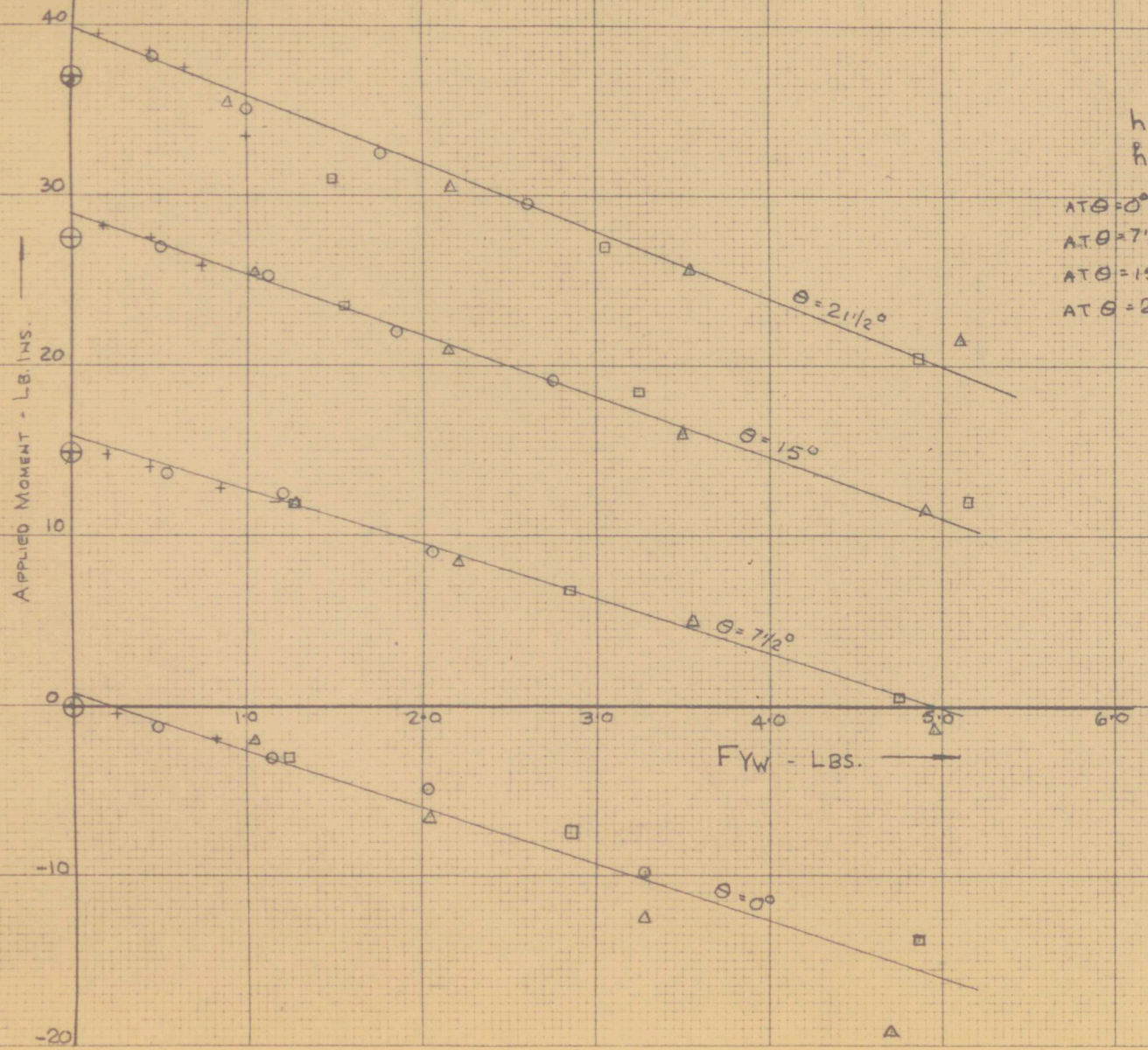

h = SLOPE OF LINES
ĥ = DEPTH OF ACTION FOR FYW

AT θ = 0°, ĥ = 3·33
AT θ = 7½°, h = 3·25
AT θ = 15°, h = 3·62
AT θ = 21½°, h = 4·0

+ V_S = 1·9 FT/SEC
⊙ V_S = 2·97 FT/SEC
Δ V_S = 3·84 FT/SEC
□ V_S = 4·55 FT/SEC.

ALL AT MODEL SCALE

fig 101 depth of action for sideforce.
$h_1 = h.\cos\theta$ against heel.

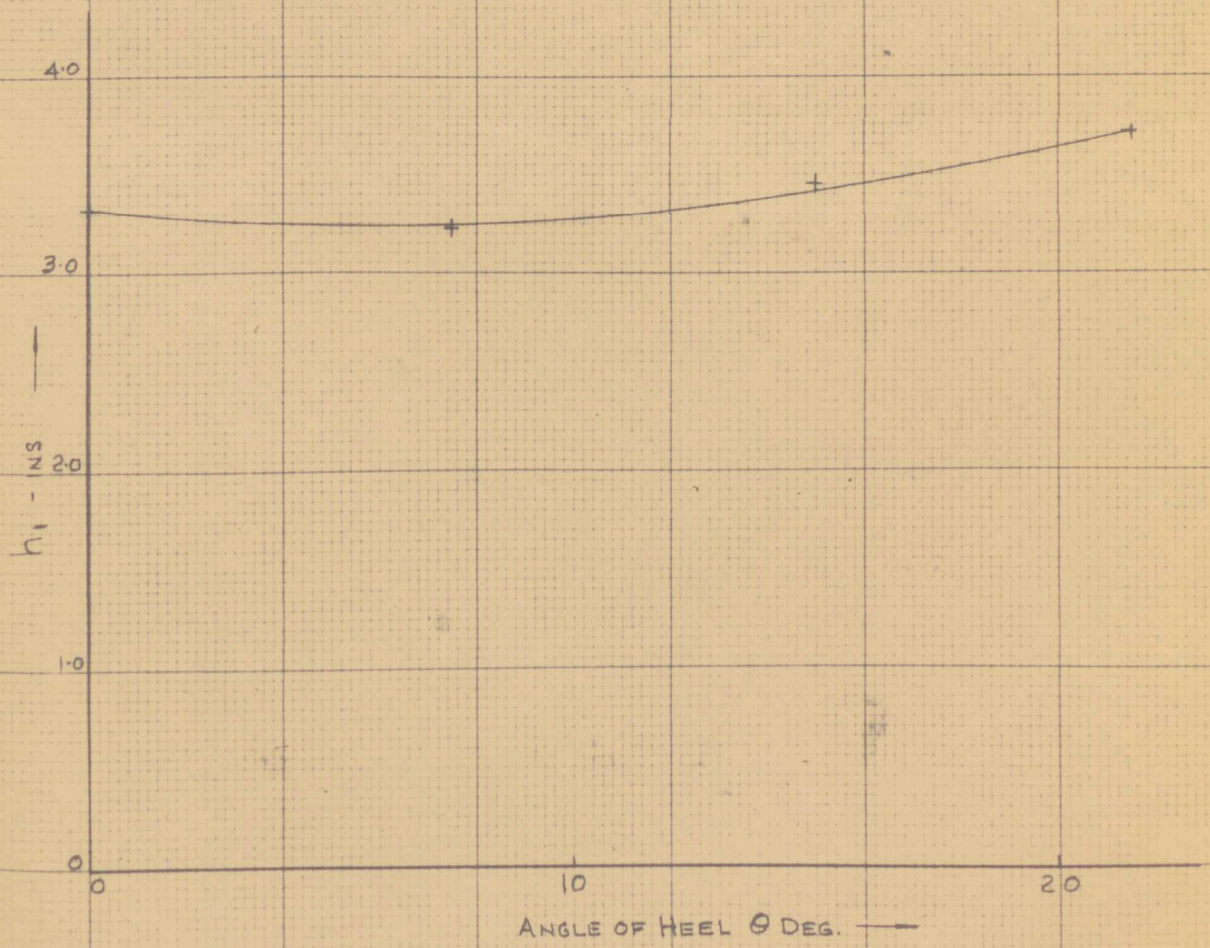

fig 102 calculation of area and centroid for underwater profile.

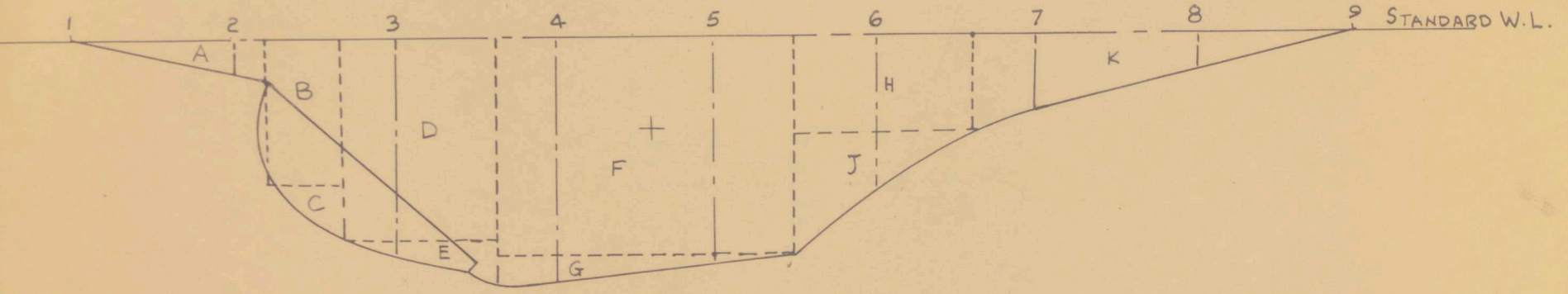

METHOD 1:- DIVISION INTO RECTANGLES AND TRIANGLES.

METHOD 2:- SIMPSONS RULES.

fig 103 effect of change in V.C.G. on statical stability, theory.

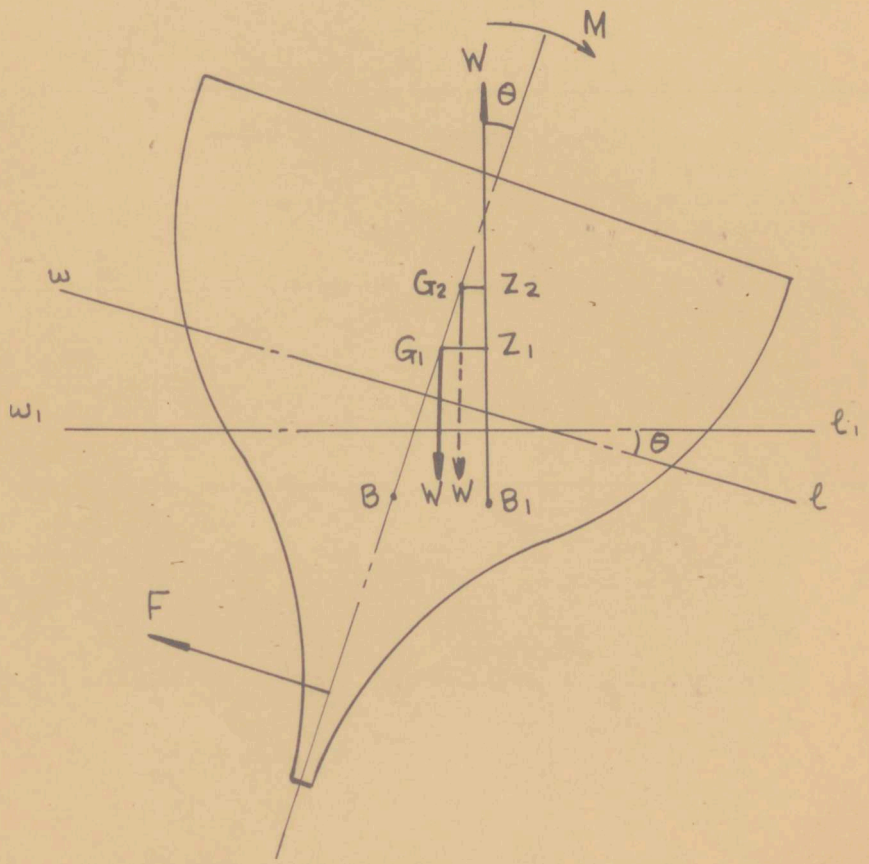

fig 104 effect of V.C.G. on statical stability, experiment.

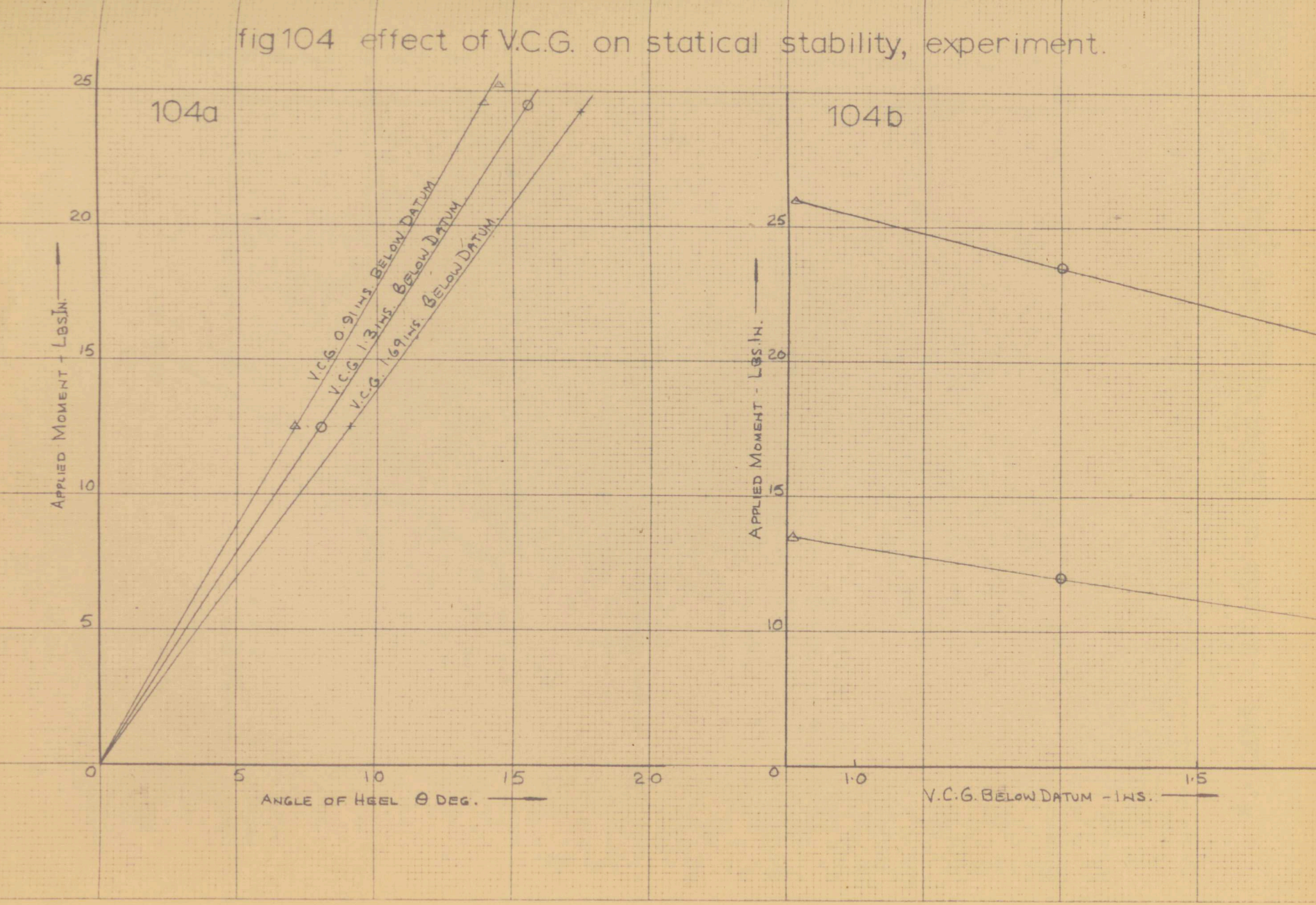

fig 105 effect of V.C.G. on dynamic stability.

fig 105a model vel. 1·90 FT/SEC.

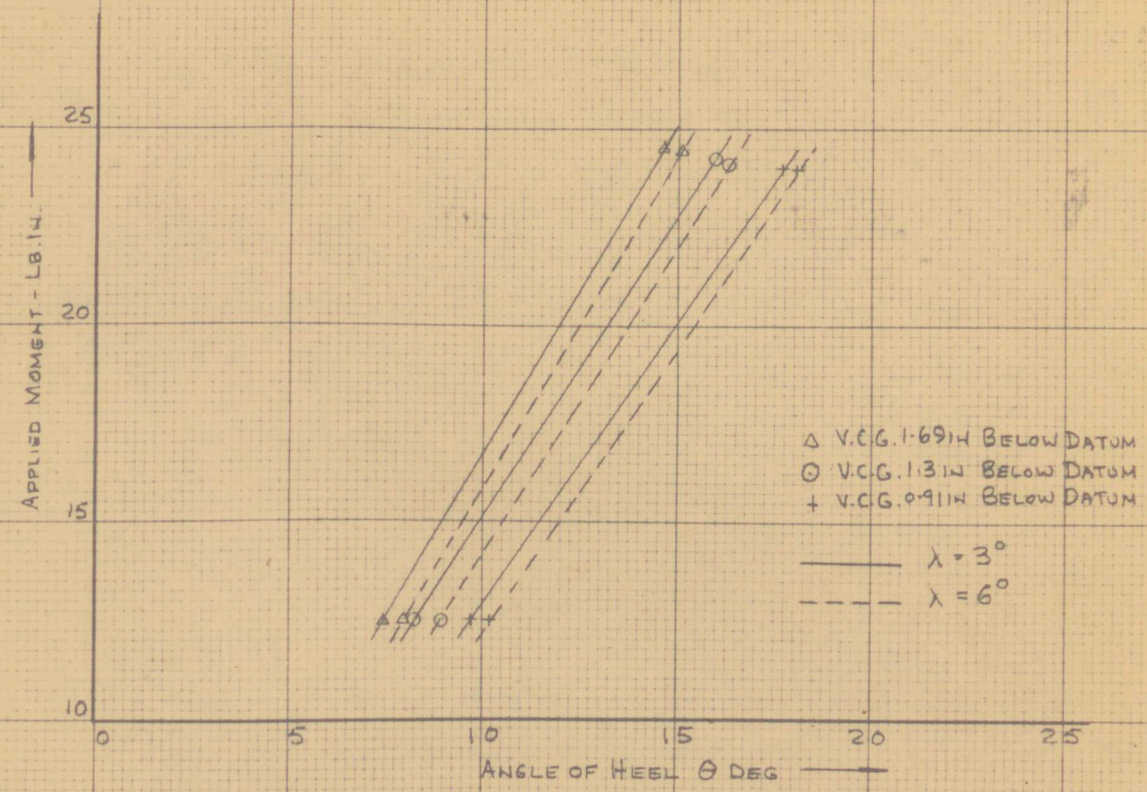

fig 105b model vel. 2·97 FT/SEC.

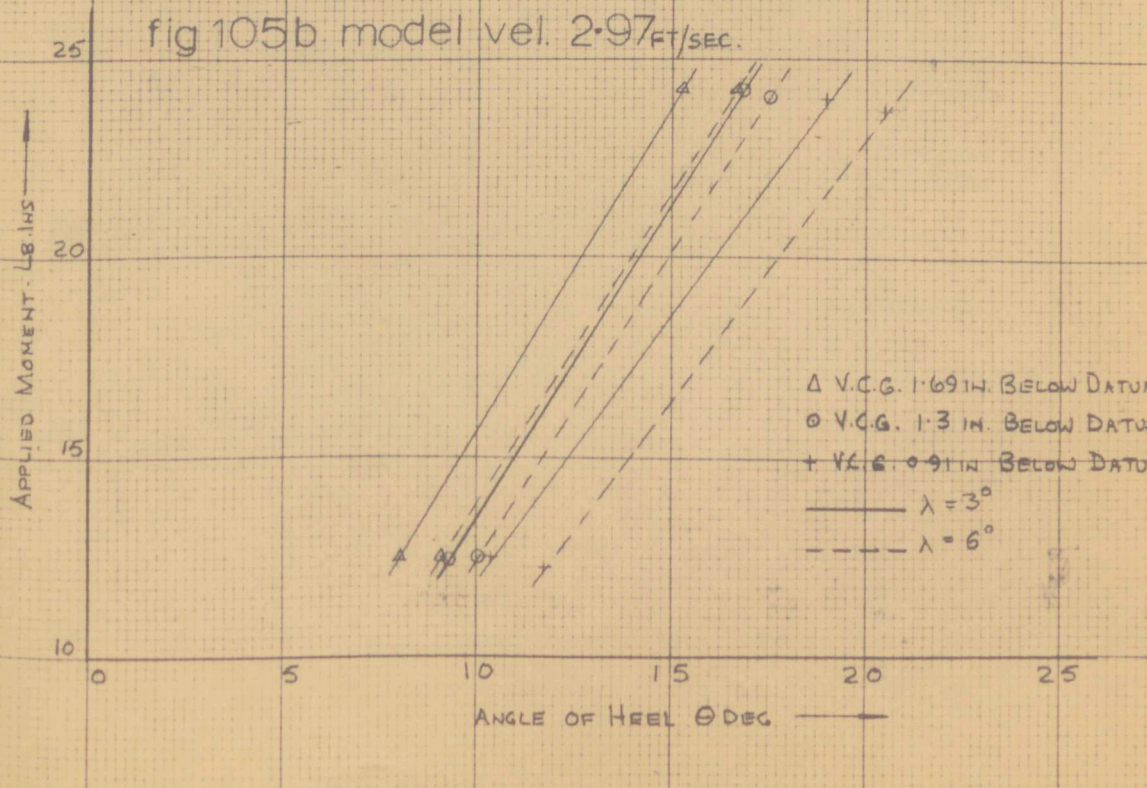

fig 105 effect of V.C.G on dynamic stability.

fig 105c model vel. 3·86 FT/SEC.

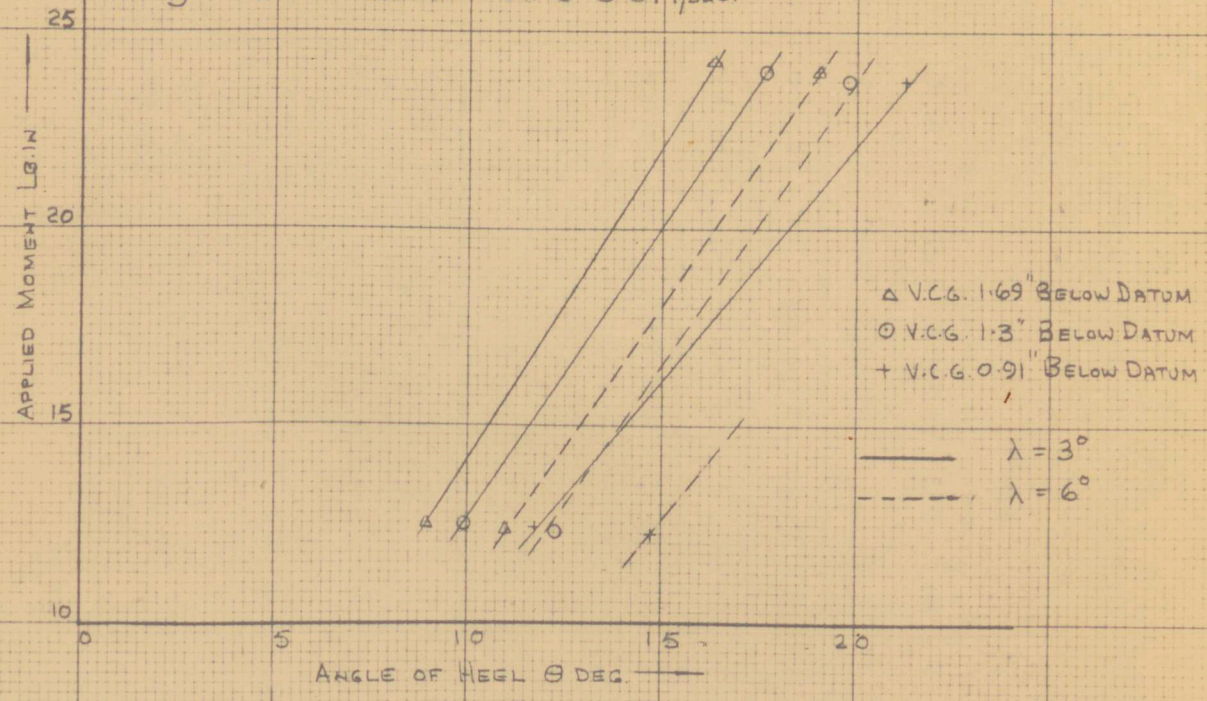

fig 106 effect of V.C.G. on dynamic stability
applied moment —
V.C.G. location.

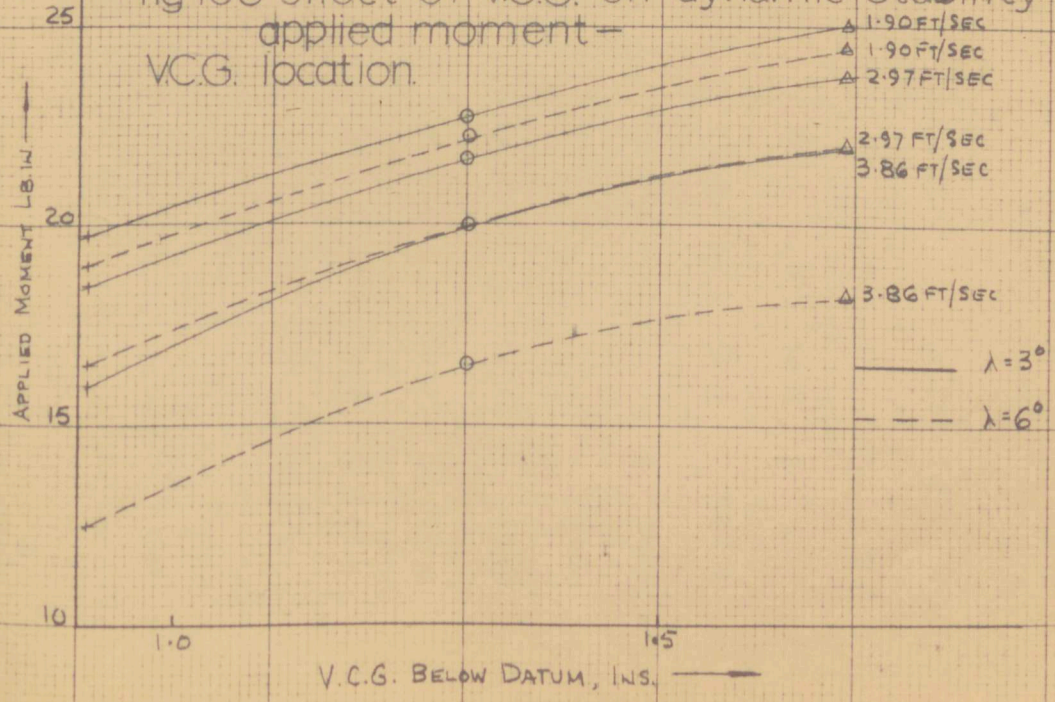

TABLE 13. CALCULATION FOR DEPTH OF C.L.R.

USING SIMPSON'S FIRST RULE.

ORD No.	ORD (INS)	S.M.	AREA FUNC.	MOM. MULT. (½ × ORD)	MOM. FUNC.
1	0	½	0	0	0
2	1·17	2	2·34	0·58	1·36
3	7·34	1	7·34	3·17	23·22
4	8·34	2	16·68	4·17	69·50
5	7·68	1	7·68	3·84	29·44
6	5·08	2	10·16	2·54	25·80
7	2·43	1	2·43	1·22	2·97
8	1·13	2	2·26	0·57	1·29
9	0	½	0	0	0
TOTALS (× ②)			48·89		153·58

C.I = 5·23 INS. AREA OF PROFILE

$= \frac{1}{3} \times 5{\cdot}23 \times 48{\cdot}89 \times ② = 171 \text{ IN}^2$.

DEPTH OF CENTROID BELOW W.L.

$= \frac{153{\cdot}58}{48{\cdot}89} = 3{\cdot}13$ INS.

TABLE 14 CALCULATION FOR DEPTH OF C.L.R.

USING SIMPLE GEOM. FIGS.

FIG.	LENGTH OF BASE INS.	AREA (DIMS. IN INS)	AREA IN²	C.G. BELOW STD. W.L. INS	MOMENT OF FIGURE
A	6·34	$\frac{6{\cdot}34 \times 1{\cdot}33}{2}$	4·21	0·44	1·85
B	2·33	2·33 × 4·67	10·88	2·34	25·40
C	-	$\frac{2{\cdot}2 \times 1{\cdot}87}{2}$	2·06	5·30	10·90
D	5	5 × 6·68	33·40	3·34	111·50
E	-	½ × 5 × 1·53	3·82	7·19	27·4
F	9·78	9·78 × 7·25	70·80	3·62	256·0
G	-	½ × 9·661 × 1	4·83	7·59	36·60
H	5·80	5·80 × 3	17·40	1·50	26·10
J	-	½ × 5·8 × 3·83	11·10	4·28	47·50
K	12·5	12·5 × 3 × ½	18·75	1·0	18·75
TOTALS			177·25		562·0

AREA OF PROFILE = 177·25 IN²

DEPTH OF CENTROID BELOW W.L.

$= \frac{562{\cdot}0}{177{\cdot}25} = 3{\cdot}16$ INS.

CHAPTER 25: A SHORT INVESTIGATION TO ASSESS THE EFFECT OF L.C.G. LOCATION, A.U.W. AND RUDDER APPLICATION ON HULL CHARACTERISTICS.

Properties of the hull in a simple form as required for the performance analysis of Part 1 have been discussed in Chapter 21, with the hull at one 'standard' condition of A.U.W. and C.G. location, and with the rudder locked amidships. It was considered desirable therefore to determine how any departure from this condition might affect the vessel's performance.

A complete investigation would require a very considerable amount of experimental work and analysis as the full hull characteristics would have to be obtained in a form similar to those of Chapter 21, for each change in condition; several short series of experiments were therefore devised, using representative values of model velocity, leeway and heel for closehauled sailing; spot measurements were made also for the upright, zero leeway case referring to a vessel 'on the run'.

25.1 Effect on Model Characteristics of variation in L.C.G.

A short series of experiments was performed to measure the changes in upright resistance, hydrodynamic force components while sailing close-hauled, and stability, due to changes in L.C.G. location.

The model was maintained at the standard A.U.W. of 24.89 lb.

throughout, with the V.C.G. at 1.74 ins. below datum.

By changing the longitudinal position of the 6.33 lb. sliding weight and its supporting structure, the model L.C.G. was moved forward and aft as shown in Fig. 107; this figure also shows the associated trims and static waterlines. Measurements with the model at Standard L.C.G. acted as confirmation of those from the more extensive series described in Chapter 21.

Upright Resistance

Runs were made with the model at each L.C.G. for velocities of 1.9, 2.97, and 3.86 ft/sec. Results are shown in Fig. 108, from which it can be seen that when the model is trimmed by the stern, there is considerable increase in resistance over that at level trim, the likely cause being the increased immersion of the long after overhang, expecially at higher speeds. This agrees with the original Saunders Roe experiments (Fig.11, Ref. 1).

With the model trimmed by the head, it was noticeable that the wave profile was less prone to creep up the overhang as speed increased, and this is reflected in Fig. 108 where the resistance shows less tendency to increase, and at higher speeds appears to fall slightly below that at level trim.

From these results it appears reasonable to conclude that at the higher speeds (higher wind velocities) some trim is beneficial while on the run, if it can be tolerated from the general sea-keeping of the yacht.

Close-hauled Characteristics

Runs were made at course velocities of 1.9, and 2.97 ft/sec., at each C.G. location, with the model maintained at 10° heel and $4\frac{1}{2}$° leeway to represent a close-hauled sailing condition.

Measurements of F_{Yw} and F_{Xw} are shown in Fig. 109; at a model velocity of 1.9 ft/sec, an increase in F_{Yw} appears when trim by the bow is applied, but this is less evident in the case of trim by the stern. F_{Xw} appears to remain essentially constant.

At 2.97 ft/sec., an increase in F_{Yw} is obtained with trim by the stern; F_{Xw} increases when the vessel is brought out of level trim, the effect being more pronounced in the case of astern trim.

While the increase in F_{Xw} with trim by the head is likely to be associated with the increased side-force, the increase resulting from trim by the stern is again likely to be due to immersion of the overhang, and is considerable despite the reduction in side-force and hence induced drag.

In terms of Lift and Drag, the characteristics are given in Fig. 110, and follow the same trends as the curves of F_{Yw} and F_{Xw}.

It may be concluded from the curves of Fig. 110 that at 1.9 ft/sec., trim by the head appears advantageous as the available Lift of the hull is increased while Drag remains constant; at the same time, trim by the stern would not seem to effect the performance

detrimentally.

At the higher speed, trim by the stern is an obvious disadvantage, the available Lift decreasing while the Drag increases; there appears to be no disadvantage in trim by the head however, both Lift and Drag lying above the values for level trim.

Stability

The transverse movement of the sliding weight to produce heel angles of 5° and 10° is shown in Fig. 111 for various L.C.G. locations. Experiments were made under static and dynamic conditions at the two velocities, the hull being maintained at $4\frac{1}{2}^{o}$ leeway.

The statical stability is seen to be less when trimmed than when level (from Fig. 111).

Measurements for the sideforce F_{Yw} at 10° heel have been given previously; reference to these allows some discussion concerning the stability under dynamic conditions: the applied moment necessary to heel the yacht to 10° while underway is seen to fall sharply with trim by the head; this will be due partly to the lower statical stability and partly to the increased F_{Yw}. It might be expected that the dynamic stability would be increased as the hull is trimmed by the stern, especially at higher speeds, where the wide overhang becomes immersed; this is evident at the lower test velocity, but at 2.97 ft/sec., the stability shows a considerable decrease despite the reduced F_{Yw}.

The results of these experiments indicate that under certain conditions especially when running, some increase in performance might be achieved by adjustments to the trim. When close-hauled, although some increase in the hydrodynamic efficiency of the hull seems possible, it would be at the expense of stability, so that more work is required before any definite conclusions are possible. A more extensive investigation could well prove useful, and indicate areas within the performance envelope where adjustment to the trim could be advantageous.

25.2 Effect on Model Characteristics of Variation in A.U.W.

It is to be expected that the hydrodynamic force components would increase as the A.U.W. and displacement increases; a brief investigation was undertaken to confirm this and assess the changes for a range in A.U.W. from the 'standard'to a 'Light' condition. (Bare hull A.U.W. 18.13 lb.)

Runs were made with the model at A.U.W.'s of 24.89 (standard), 21.56, and 19.56 lb. The variation in A.U.W. was effected by changing the sliding weight, which was also shifted longitudinally as necessary to maintain the model at its'standard' L.C.G. of 29.3 ins. from the A.E.

Measurements were taken of the upright resistance and close-hauled characteristics at $4\frac{1}{2}^{\circ}$ leeway and 5° heel; this heel was the

maximum achievable with the smallest sliding weight (1 lb.) used. The results at standard A.U.W. served as a further check on the overall results and accuracy of measurement from the tank.

Model Course velocities of 1.9, 2.97, and 3.86 ft/sec. were used to provide a reasonable coverage of speed.

Upright Resistance

Results from the runs are shown in Fig. 112, the resistance decreasing as the A.U.W. is reduced; in addition to the experimental points, the upright resistance curve at 18.31 lb. given in a previous section is also included. Some disparity in spacing appears between the latter curve and the series of curves from the present experiments; this is due to the difference in L.C.G. at the low weight, which would cause trim by the head and hence a reduction in resistance at higher speeds as shown by Fig. 108 (see Section 25.1).

Close-Hauled Characteristics

Fig. 113 shows the results in terns of F_{Yw} and F_{Xw} and Fig. 114 in terms of Lift and Drag for the hull, which show similar variations.

Generally, both Lift and Drag appear to vary linearly with A.U.W., the difference being more pronounced at the higher velocities.

There is no indication that the forces are in direct proportion to A.U.W., and a complete performance analysis using data for each model weight would be necessary to determine the changes in windward performance.

25.3 Rudder Application, and its Effect on Hull Characteristics

With a yacht under way, especially when close-hauled, it is often necessary to apply a certain amount of helm to 'balance' the vessel and maintain a desired course.

Usually, a small amount of 'weather' helm is considered desirable by yachtsmen to ensure the yacht will tack readily and be under control; weather helm may be defined as the rudder angle to leeward (or tiller angle to windward) necessary to prevent a vessel turning into the wind, or alternatively as the the torque on the rudder under these circumstances; usually the rudder will require torque even when central, and as it is the angle which determines the hydrodynamic characteristics, the angular definition will be used here. This application of rudder will alter the characteristics of the hull and usually the yacht's performance.

Published data on the effect of rudders is available from work at the Davidson Laboratory (Ref. 14) which is concerned with the effect of rudder application on 'balance' and the rudder angle desirable to maintain balance with minimum resistance for particular yachts; this indicates that a small amount (1° to 2°) of weather helm is desirable.

The tests at Davidson Laboratory were made with hull side force and heel maintained constant, the case for a yacht sailing steadily to windward, and are not in a form suitable to show the variation of

hydrodynamic characteristics as the rudder angle is varied.

A short series of experiments was therefore undertaken with the 'Dragon' hull to determine the variation of F_{Yw} and F_{Xw}, and hence Lift and Drag, with rudder angle.

The rudder fitted to the hull is of conventional pattern, situated at the after end of the keel and in its wake; due to rake in the forward edge (hinge line), rudder movement will produce a trimming moment in addition to a yawing moment.

It must be considered doubtful if the flow state around the rudder on the model scale bears a direct relationship to that full size, due to the possibilities of differences in the flow separation, and this may have an effect on the results and their expansion to full scale.

For these experiments a new rudder was manufactured and fitted to the hull as a replacement for that existing, which had become damaged; arrangements were made to hinge the rudder, and the stock passed through the hull, via a gland, to a tiller which enabled the rudder angle to be varied and secured up to 20° each side of the central position.

As a result of these alterations, A.U.W. for the experiments was 23.23 lb., with V.C.G. 1.69 ins. below datum and L.C.G. 29.1 ins. from the A.E.

Runs were made with the model upright at zero leeway and, in a condition to simulate close-hauled sailing, with 10° heel and $4\frac{1}{2}$° leeway; F_{Yw} and F_{Xw} were measured in each case at velocities of 1.9, and 2.97 ft/sec. while the rudder was moved in two steps from 0° to 20°.

Results for the upright condition are shown in Fig. 115, and in this case F_{Yw} and F_{Xw} were equivalent to Lift and Drag.

When the rudder is moved from its central position, the chord shape of the immersed hull is changed and the whole hull is set at an effective angle of incidence; the effect of both these factors will become greater as the rudder angle is increased, so that Lift and Drag would be expected to grow with increasing rudder angle. Fig. 115 shows that although the curves are similar to those when leeway is varied, see Chapter 21, with rudder locked, the Drag curve does not appear to follow a parabolic form.

In the close-hauled case, Fig. 116 shows the results for F_{Yw} and F_{Xw}; here the rudder is likely to suffer less from the flow differences between model and full scale, and Fig. 117 indicates that Lift increases with weather helm and decreases with lee helm, as might be expected from considerations of the changing chord shape and incidence of the modified hull form.

The Drag curve now follows parabolic form with minimum Drag occurring at some angle of lee helm which appears to increase with speed.

The slope of the Lift curve around the position of zero rudder angle is indeterminate, due to the small number of experimental points, but the variation in hull chord shape and incidence could lead to a change of curvature at this point without a noticeable change in the Drag curve.

Minimum Drag occurs therefore with lee helm, the angle necessary increasing with speed; at the same time however, the Lift is reduced and this state is unlikely to be of use in practice; also a yacht sailing close-hauled with large lee helm could be dangerous to sail and tack especially at the higher true wind velocities, where large lee helm would be required.

In practice, a yacht will sail close-hauled with a certain Lift Force required for the hull; if this Lift can be maintained while Drag is reduced, then imporved performance will result. The Davidson Laboratory work of Ref. 14 which utilised this fact by running tests at constant Lift, found that minimum Drag occurred under these circumstances with small weather helm.

It appears therefore, that the increased Lift of the hull from this weather helm more than outweighs the increase in Drag, and that

the hull does not operate most efficiently at the condition of minimum Drag.

Although the experiments described here give a general idea of the effect of rudder application on the hull characteristics, more extensive work is necessary to determine in detail the changes to be expected over a wide range of hull attitude. Such work would make possible a full assessment of the effect of conventional rudders.

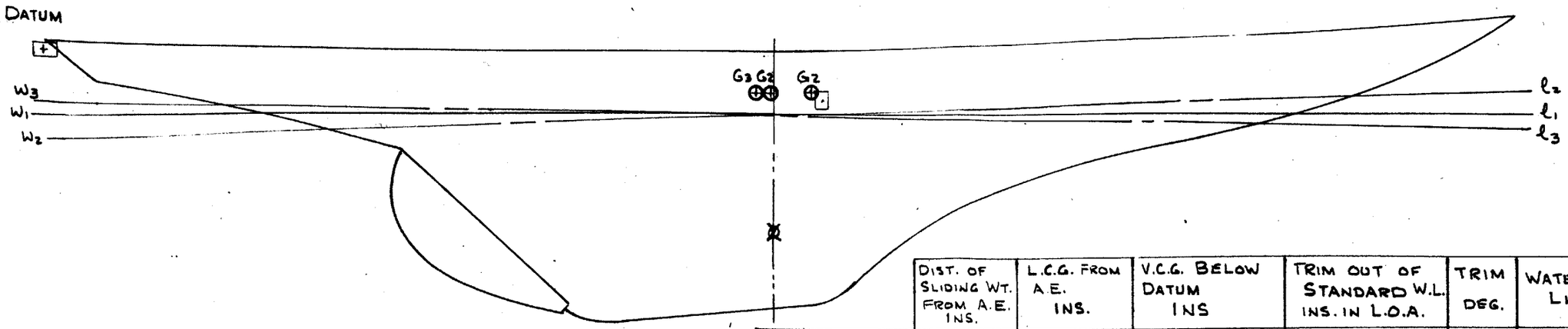

fig 107 data for L.C.G. experiments.

	Dist. of Sliding Wt. from A.E. Ins.	L.C.G. from A.E. Ins.	V.C.G. below Datum Ins	Trim out of Standard W.L. ins. in L.O.A.	Trim deg.	Water-Line
Standard Condition	27	G1 29.3	1·74	0	1·8°	$w_1 l_1$
Trim by Head	33	G2 30.92	1·74	1¾"	1·78°	$w_2 l_2$
Trim by Stern	24	G3 28·49	1·74	¾"	0·75°	$w_3 l_3$

fig 108 effect of model L.C.G. and trim on upright resistance

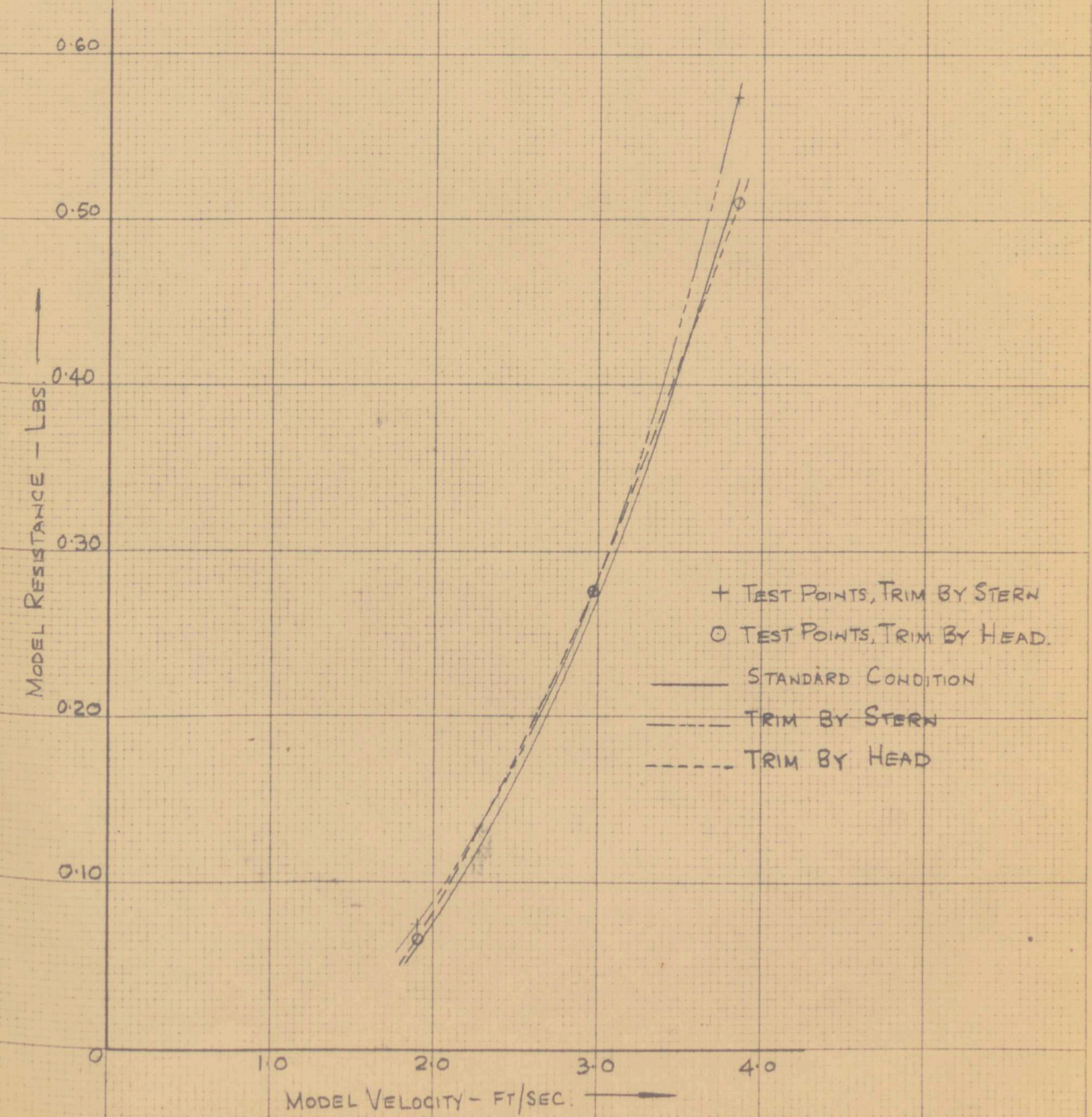

fig109 effect of L.C.G. and trim on close hauled model characteristics.
heel 10°, leeway 4½°

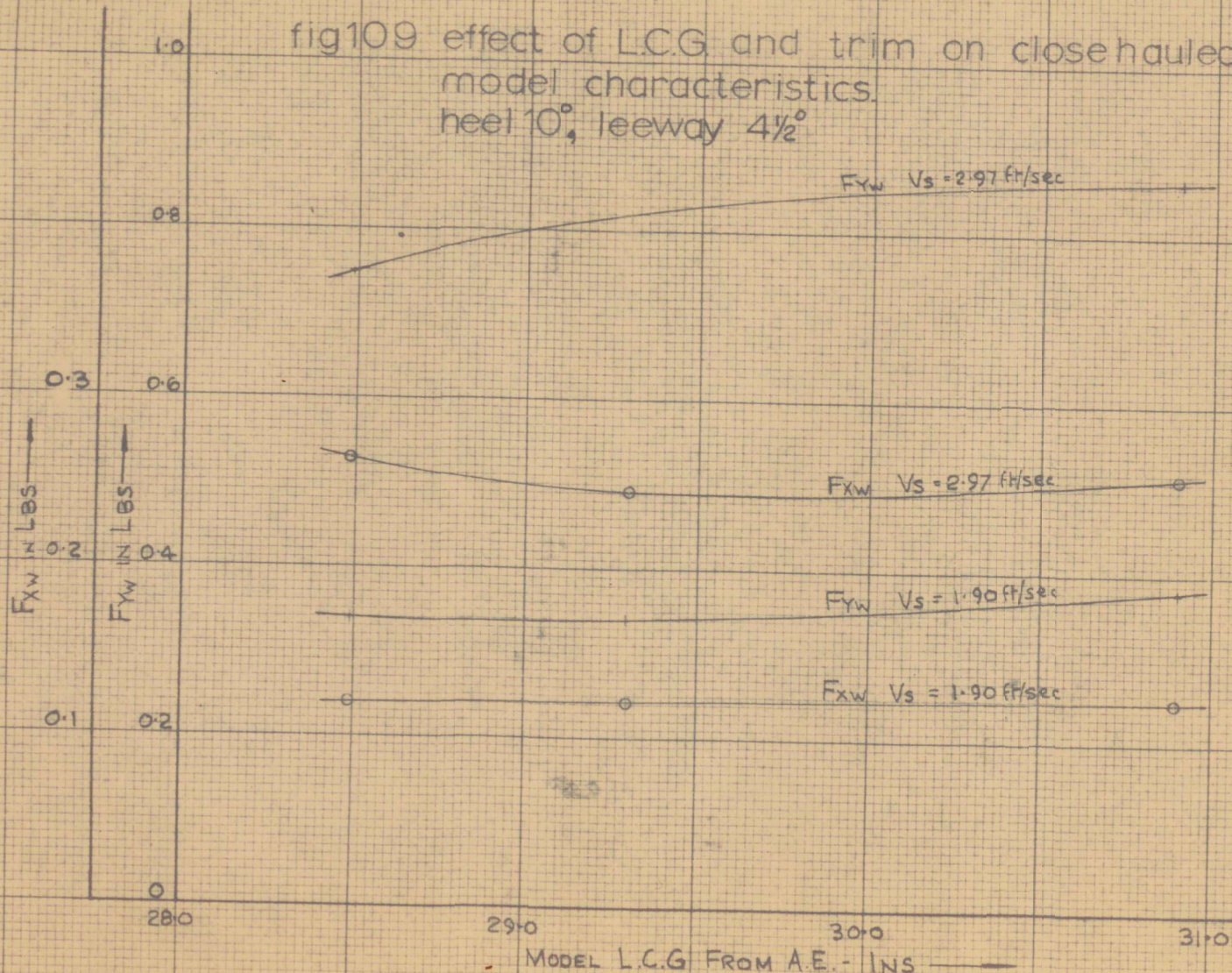

fig 110 effect of L.C.G. and trim on closehauled lift and drag.

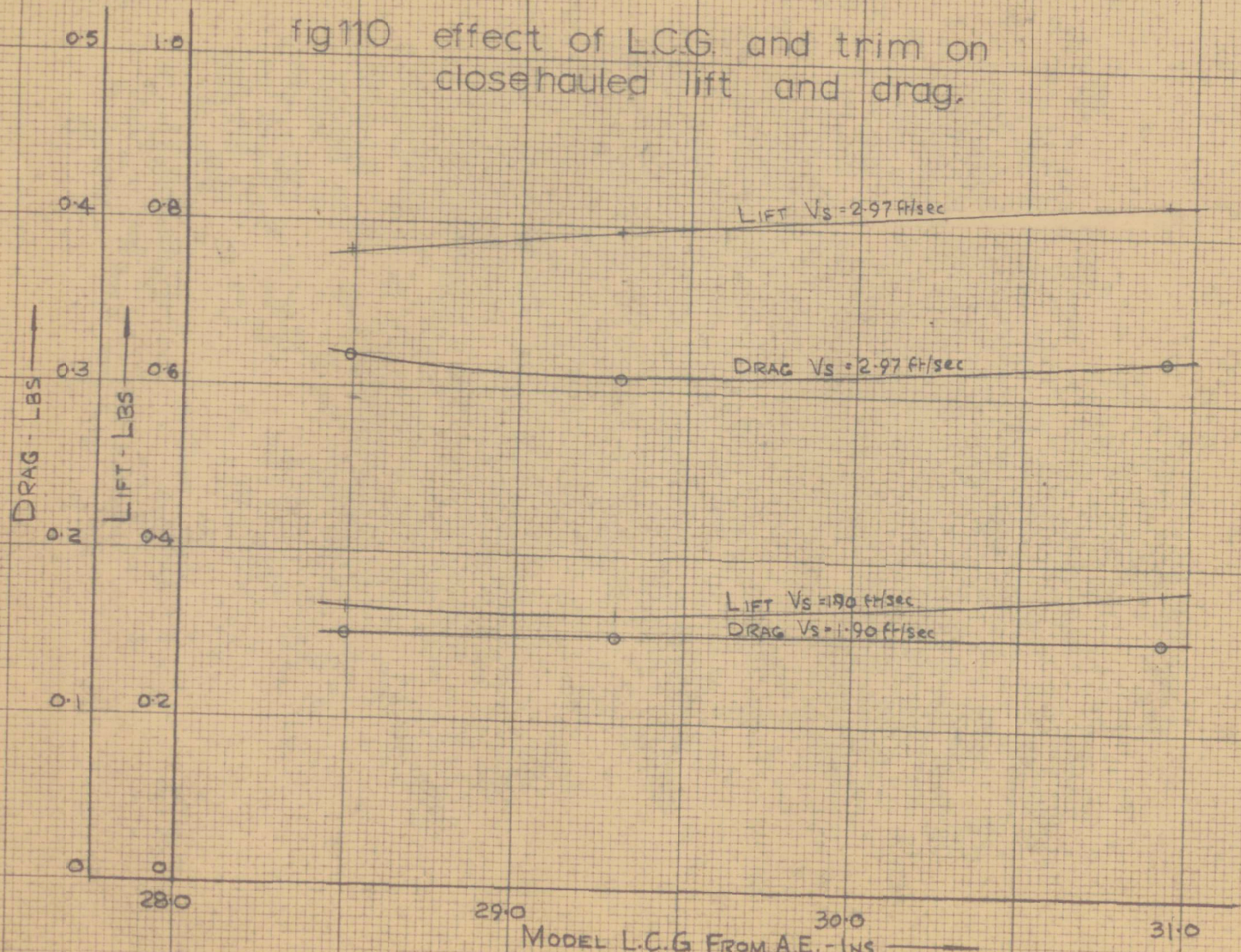

fig 111 effect of L.C.G. on dynamic stability.
movement of sliding weight from c.l.
to give heel stated.

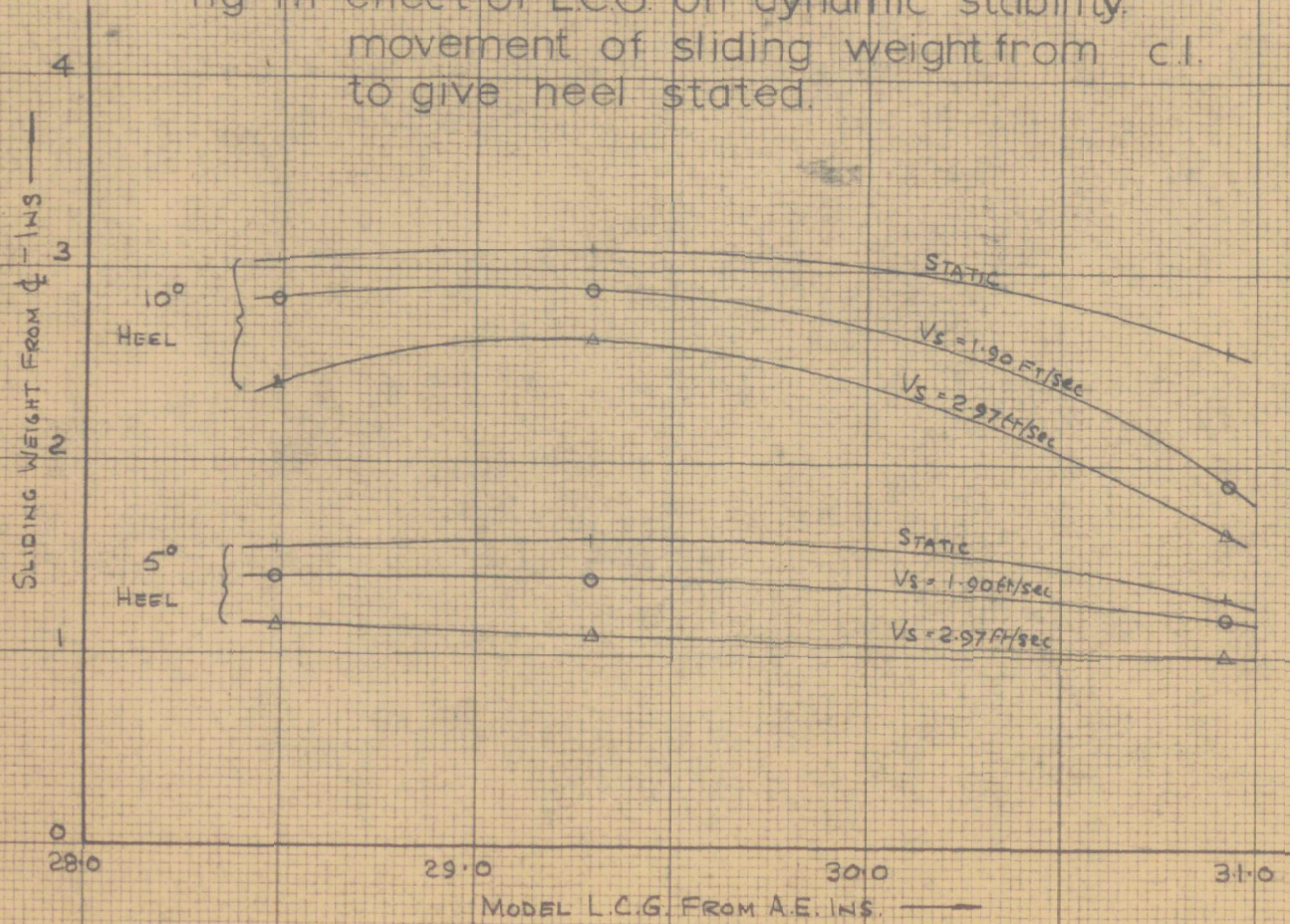

fig 112 effect of A.U.W. on upright resistance.

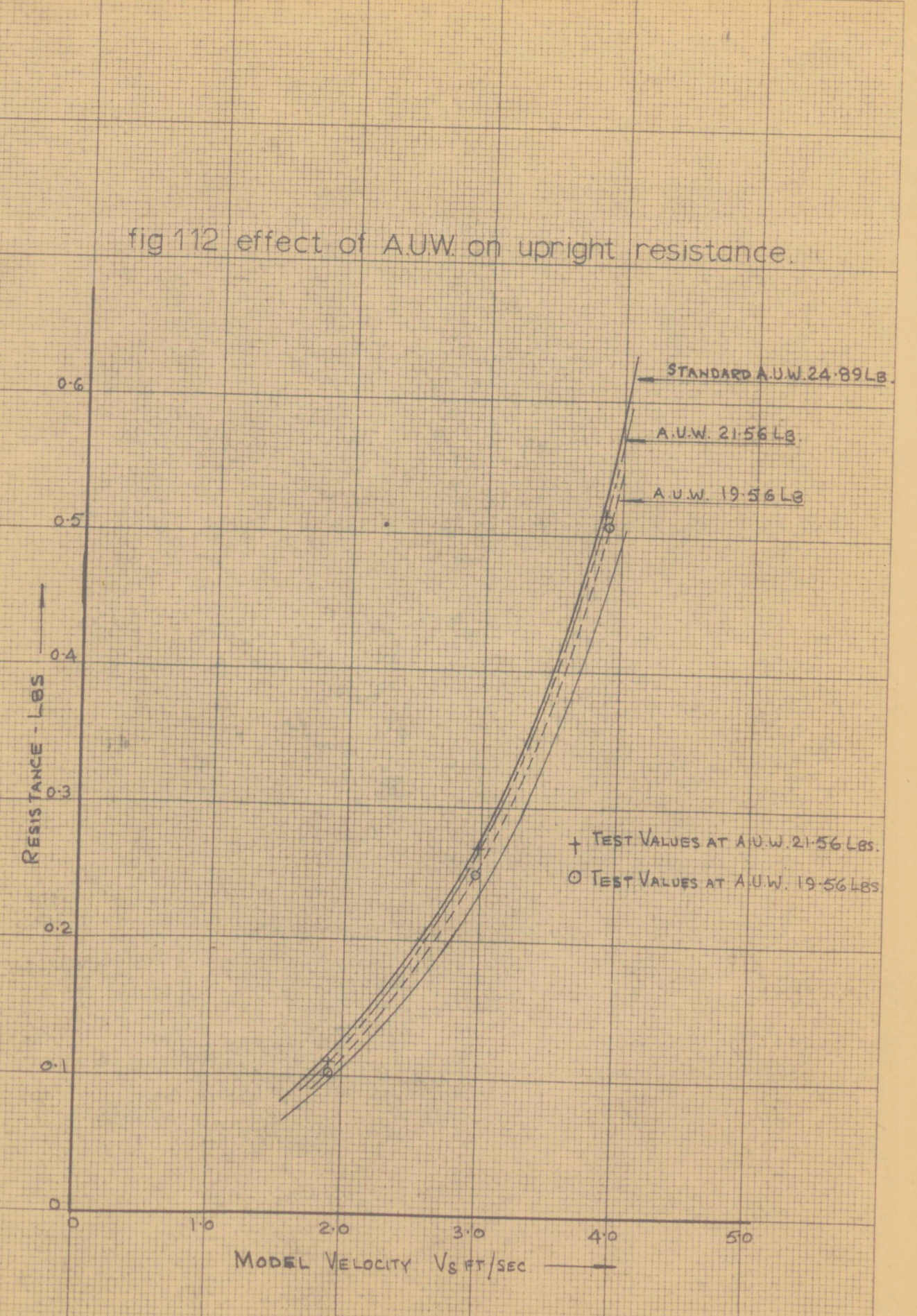

fig113 effect of A.U.W. on close-hauled model characteristics.

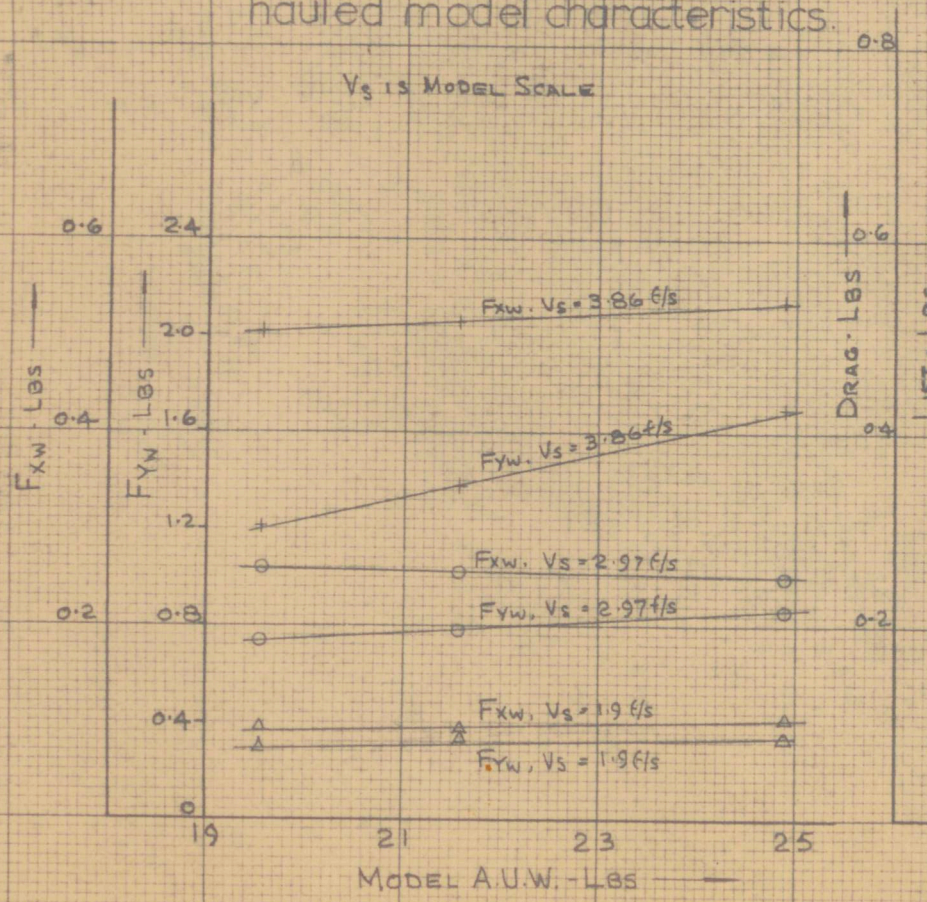

fig114 effect of A.U.W. on close-hauled lift and drag.

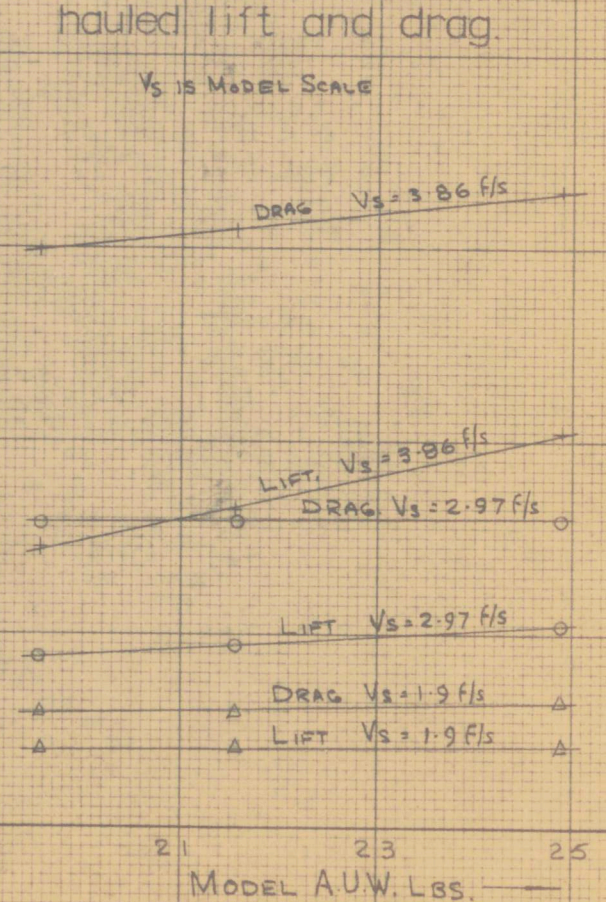

fig115 effect of rudder application. lift and drag upright, zero leeway.

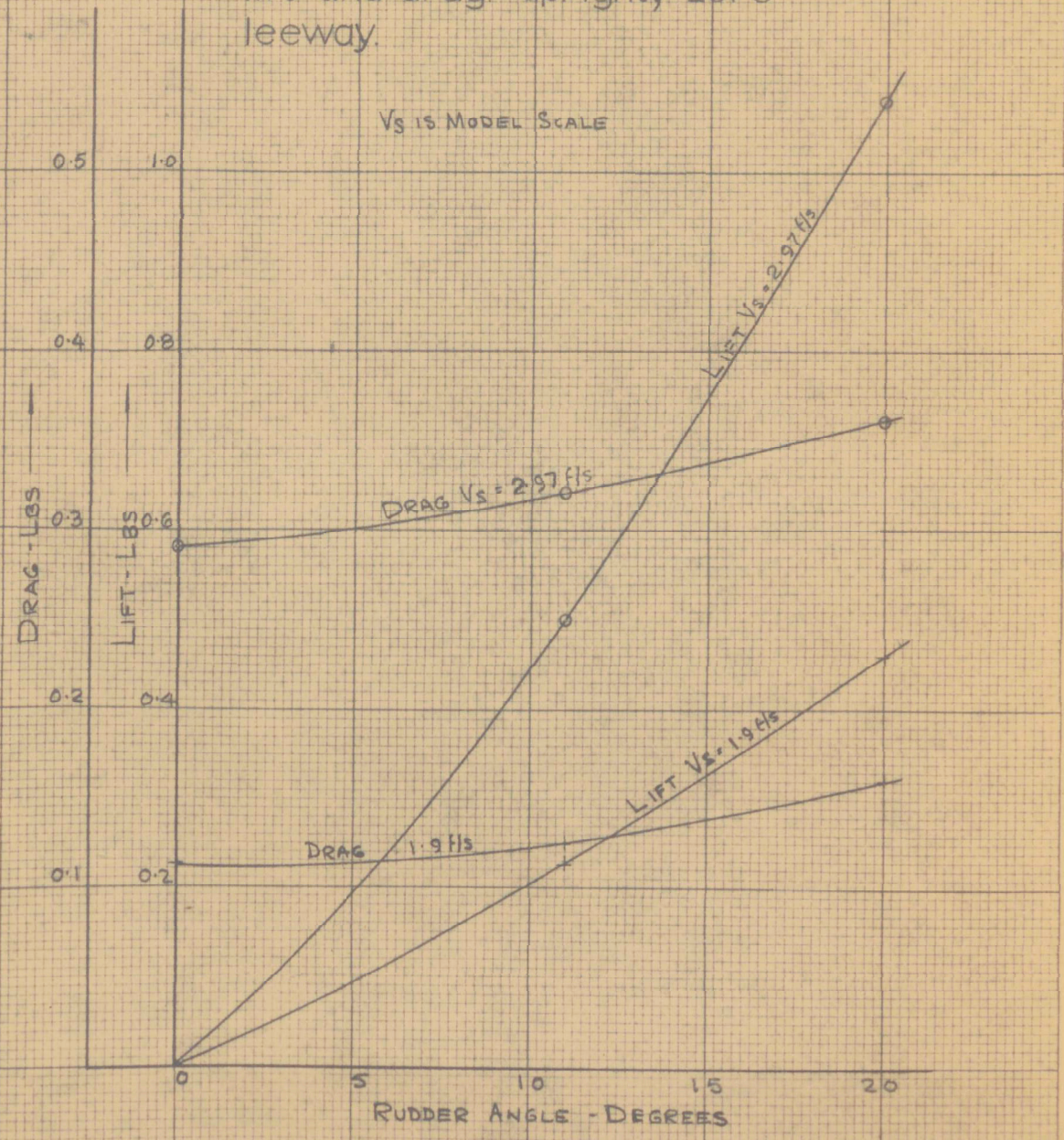

fig 116 effect of rudder on close-hauled characteristics.
leeway 4½° heel 10°

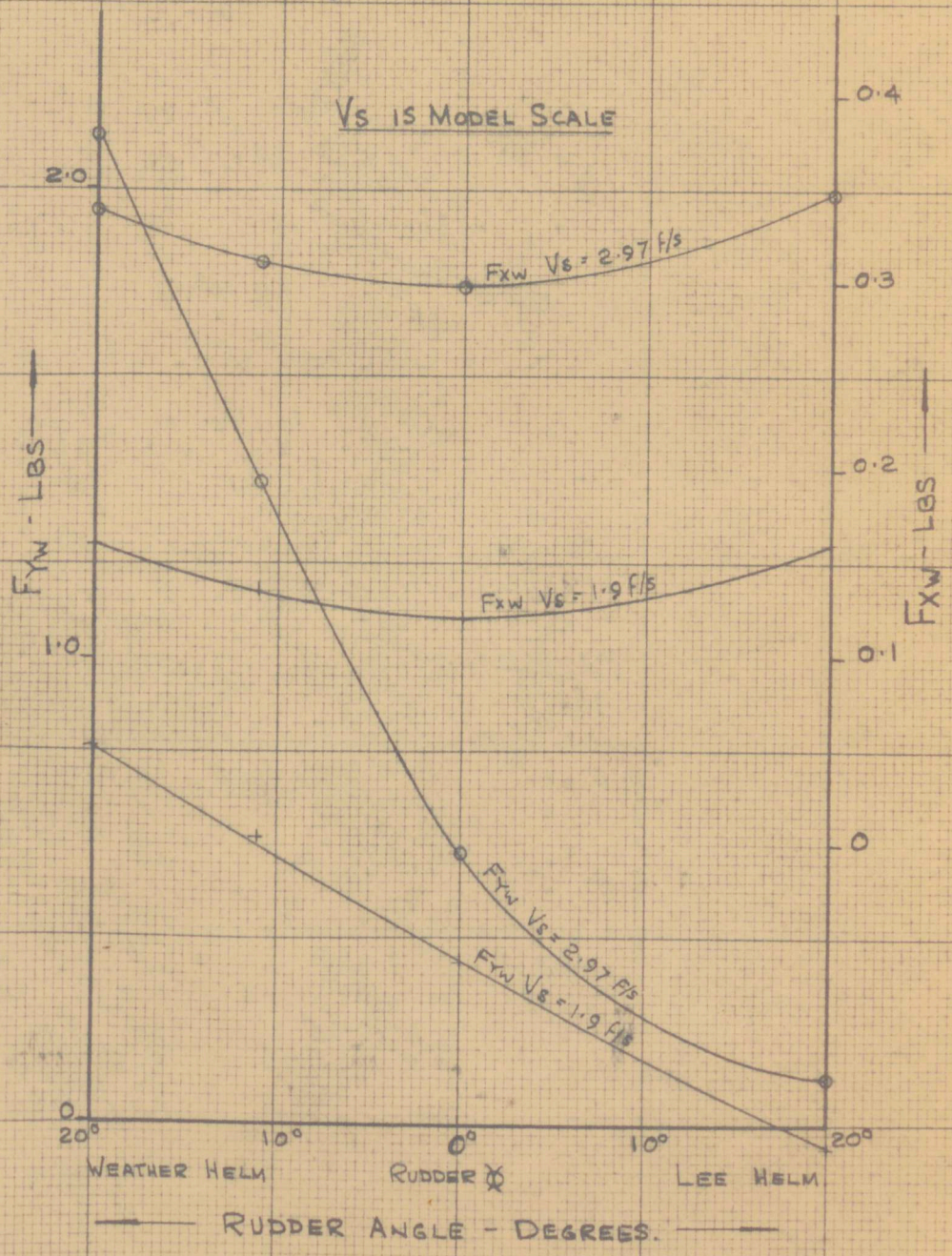

fig 117 effect of rudder on close-hauled lift and drag leeway 4½°, heel 10°.

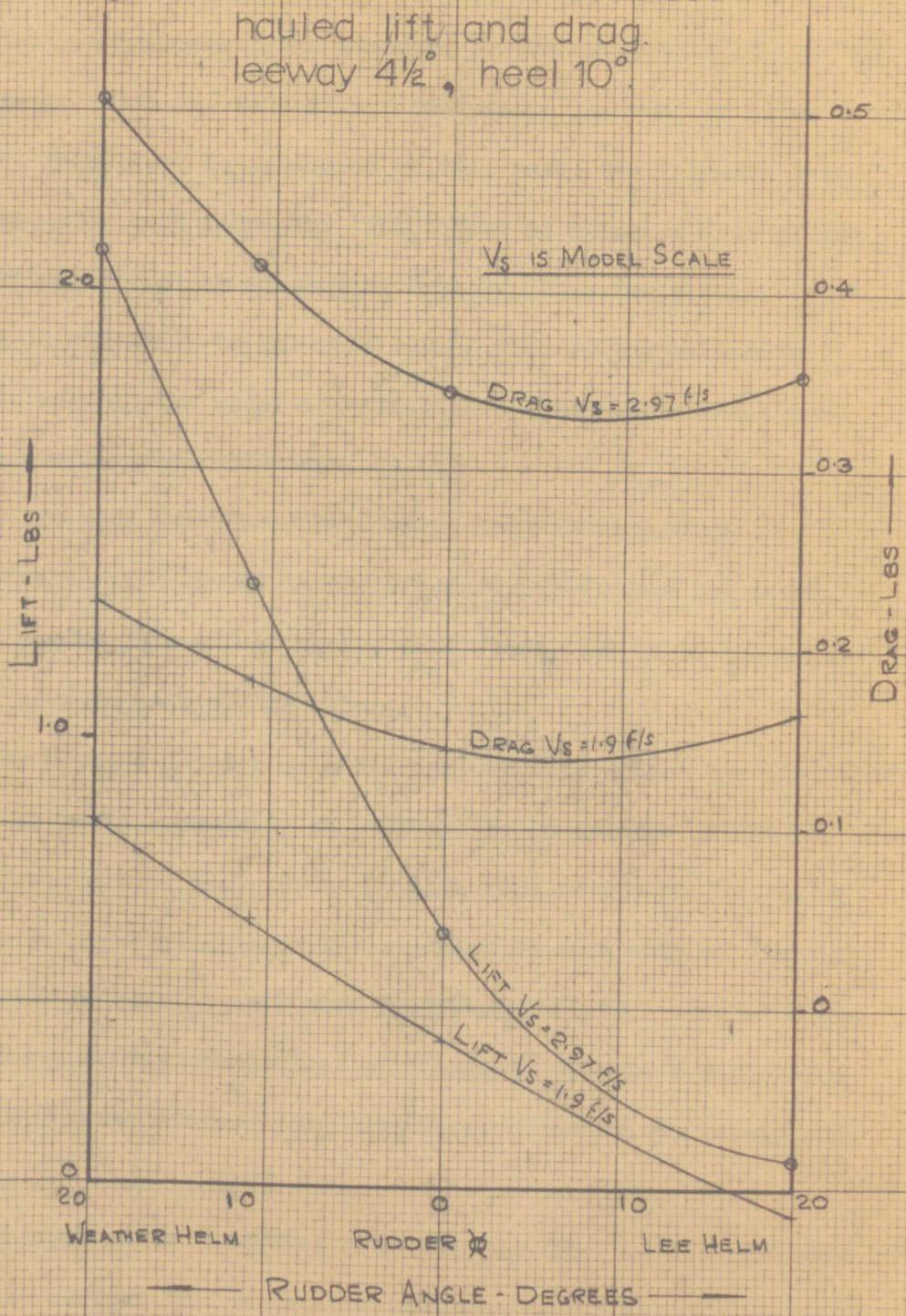

CHAPTER 26: WETTED SURFACE AREA

When use is made of the standard Froude conception of separating friction and wave making resistance in order to allow model test results to be scaled up to full size, the friction Drag is estimated for both model and 'ship' from estabilshed data giving the friction coefficient at varying Reynolds No., for planks.

It is necessary to know the wetted area of the hull with reasonable accuracy in order to establish a tolerably correct prediction of full scale resistance.

In the more usual case of a ship, the wetted surface is likely to vary slightly due to the pressure field round the model producing waves; this effect varies with speed, the waves taking the same form on each side of the ship.

With a yacht model, two other factors will affect the pressure distribution around the hull, so influencing to a large extent the wave formation: leeway and heel, both of which tend to the production of wave forms having a non-symmetrical pattern on each side of the ship, the unequal pressure distribution providing Lift to conteract side-force from the sails. The effect will tend to promote a difference in the wetted area under varying conditions of velocity, leeway and heel.

The experiments described here were designed to determine the order of any changes in the total wetted surface of the hull under

different conditions and also to establish the order of importance of the three quantities velocity, leeway, heel in affecting the wetted surface area.

Determination of Change in Wetted Surface Area

The outer hull surface of the Dragon model was divided into equally spaced strips as shown in the various photographs, by means of 1/8 inch wide lengths of waterproof plastic adhesive tape.

Because of the complex curvature of the hull surface and the shape at the end overhangs, these strips were not horizontal except at one datum waterline, but when looking at the model in profile appeared to close up towards the ends of the hull.

The datum horizontal waterline for the strips was that shown on the official drawings of the Dragon Class. In fact the upright waterline for the tests was deeper than this, being that used also for the measurement of hydrodynamic characteristics, so that when floating in the standard condition, the waterline cut several of the equi-distant tape lines above the datum as shown in Fig. 118.

The hull surface above and below the datum waterline was expanded in terms of the equi-distant tape lines and the stations shown on the Official Drawings. This expansion is shown in Fig. 119 where it will be seen that the equi-distant lines have been maintained horizontal, the distance between them representing $\frac{1}{2}$ inch. The station

lines are parallel over the amidships region where the hull curvature is relatively small, but become distorted towards bow and stern where curvature is considerable.

The longitudinal distance between stations was measured on the model along each line of tape to give the expansion, which represents one side of the hull surface from the deck line to the approximate line where the hull merges into the keel, so covering the complete variation of waterline obtained.

No. 4 tape line on Fig. 119 represents the topmost full length line on the model in Fig. 118.

Photographs of both the windward and leeward sides of the hull were taken for each speed, leeway and heel considered, to show the actual waterline resulting from the wave formation in each condition.

By transferring the shape of this waterline to the surface expansion chart and comparing it with the upright static waterline, the change in wetted surface area in the condition considered could be found for both windward and leeward sides of the hull.

Fig.120 shows this procedure applied to the model heeled at 10° and stationary; the photographs for this condition are given in Fig. 121.

The red curve lying for the main part just beneath No. 3 tape line is the waterline in the upright static condition, and is the

datum from which the area changes are measured.

The upper black curve represents the leeward waterline at 10° heel which, as would be expected, lies nearer the deck edge than the red datum line, so indicating an increase in wetted surface for this side of the hull.

The windward waterline is shown by the lower black curve; being below the original datum line, it indicates a lower wetted area for this side of the hull.

Decrease in wetted area to windward is given by the area lying between the red line and lower black line, while the increase in wetted area to leeward is given by that area between the upper black line and the red datum. The leeward surface has been taken as positive and the windward surface as negative, the nett increase or decrease being given by the difference between the two areas.

Transferring Waterlines to Expansion Chart

The following method was adopted for transferring the waterline shape from photographs to the chart:
Originals of the photographs were enlarged so that in all prints the model appeared at a standard length of eleven inches. By placing a transparent sheet, on which station lines were drawn to the same scale, over the print it was possible to determine the shape of the waterline on the expansion chart in terms of the stations and tape lines. In practice it proved most satisfactory to take each station

in turn and plot the actual position of the waterline by reference to the tape lines.

The method was quite satisfactory except at the extreme after end where in some cases a little difficulty was experienced in judging the waterline endings, due to lack of contrast in the photographs; because of this small errors are likely in the waterline shapes at the after end.

Coverage of Tests

A total of fifty six photographs were taken covering the following combinations of speed, leeway and heel:

Velocity: 0, 1.9, 2.97, 3.86 ft/sec ($V/\sqrt{L}$: 0, 0.6, 0.94, 1.22)

Leeway: 0°, 5°, 10°.

Heel: 0°, 10°, 20°. (heel was restricted by immersion of deck edge)

Calculation of Area from Chart

The change in wetted surface as plotted on the charts was found by use of Simpsons Rules, the number of ordinates being chosen to cover each area adequately. This was found to give satisfactory results.

Results

The increase or decrease in wetted surface area with speed, leeway and heel are given in Table 15 for each side of the hull separately and together with the nett over-all variation.

The Static Condition

In this condition the wetted area would be expected to vary only slightly with heel due to the hull section shape; any increase in wetted surface to leeward being balanced by a corresponding decrease to windward.

This is confirmed, the variation being some 1.4% of the total wetted area of 639 ins. in the upright static state (The calculation of this static upright area is given later).

'Underway Condition'

Effect of Leeway

At speed, the pressure distribution around the hull will cause surface waves to be set up, which change the shape of the wetted area. In the upright, zero leeway, position this wave formation would be similar to that for a normal ship, but when the yacht is sailing heeled and making leeway, the pressure distribution will change, pressure increasing to leeward and decreasing to windward. The effect of this pressure change will be to modify the normal 'ship style' waves, especially over the amidship section where the keel is of particular importance, so that the surface is raised to leeward and lowered to windward, the effect varying with leeway at any particular angle of heel.

Observation of the model running in the tank indicated that

this occurred as may be seen in the series of photographs. (Fig. 112).

This figure shows the model at a course velocity of 2.97 ft/sec. which is conveniently near the speed with one wave length in the hull length, so enabling any change in waterline due to pressure variation to be seen easily.

Both the windward and leeward side of the hull are shown at 10° heel in the still condition and at speed with leeways of 0° and 10°

Taking the leeward side first, the change in waterline with speed is seen from photographs 17 and 25; at speed, the wave formation has crests near the forward and after ends of the hull with a trough between. On referring to photo. 29 it can be seen that at 10° leeway the water level is higher near amidships so reducing the trough and indicating a rise in pressure.

Photos. 18, 26 and 30 for the windward side show that the trough amidships is deepened, indicating a fall in pressure to windward of the hull.

Effect of Heel

As the heel increases, the wetted surface to leeward will increase due to deeper immersion, and that on the windward side will decrease. The change will depend on the hull section shape and

form at each speed and leeway. There will also be some change due to the pressure distribution round the hull when the waterline shape becomes more assymmetrical as the heel increases.

Fig. 123 shows this effect at a speed of 3.86 ft/sec. and a leeway of 5°.

Effect of Course Velocity

At low values of $V/\sqrt{L}$, there will be more than one wavelength in the hull length, until at around $V/\sqrt{L}$ between 0.8 and 0.9, one wavelength will exist; above this speed there will always be less than one wavelength in the hull length.

This is confirmed by ovservations during the experiments and is illustrated by Fig. 124 which shows the wave formation as the speed is increased in the upright, zero leeway, case.

The wave profile, as discussed previously, will be modified by heel and leeway, the effect of which may be considered as superimposed on the general wave system.

Numerical Effect of Speed, Leeway and Heel for Windward and Leeward Sides of the Hull.

Decrease in Wetted Surface to Leeward (Windward)

Fig. 125 shows the effect of speed, leeway and heel, indicating that the most important factor affecting the reduction in wetted surface while under way is heel. The area appears to reduce linearly

as heel increases, to approximately 100 in^2 below the upright static value, a reduction of some 15½% in the total wetted area.

Both course velocity and leeway appear to have relatively little effect, the maximum spread in results at any heel angle being only some 2% of the total, even outside the region 0° to 6° leeway.

Increase in Wetted Surface to Leeward

Fig. 126 shows the effect of speed, leeway and heel on the leeward wetted area, indicating that the increase is more variable and of greater magnitude than the windward decrease.

The greatest increase is due to heel, but this is only linear at low speeds. The maximum effect of heel is approximately 11% between 10° and 20° heel at zero leeway, course speed 3.86 ft/sec.

Speed causes the greatest variation at high and low angles of heel, the effect being smaller at medium heel (around 10°). The maximum increase due to speed is 50 sq. ins. (8 % of static upright area).

Leeway has the least effect especially at low speeds between 0° to 6°, a normal sailing range. The maximum increase in wetted surface is some 3½% for a 5° change in leeway.

Over-All Numerical Effect

As might be expected, on combining the results for windward and leeward sides of the hull as shown in Figs. 125 and 126, the

over-all effect is entirely variable, see Fig. 127.

Generally, the wetted surface increases with leeway over the whole speed range for low and high heel, while remaining relatively constant, decreasing slightly, at moderate heel (around 10°). The maximum variation is at 3.86 ft/sec. and amounts to some 6½% of the static upright area.

While the wetted area is least at moderate heel angles, it increases with both high and low values of heel. The maximum variation occurring at 10° leeway and 3.86 ft/sec. and being some 8% of the static upright area for a 10° alteration in heel.

Fig. 127 indicates that the total wetted area falls as the speed increases up to about 0.6 $V/\sqrt{L}$ with low and moderate heel, but tends to remain constant, or increase, at large heel angles.

Above $V/\sqrt{L}$ of 0.6 however, the total wetted surface increases rapidly as the wave profile creeps up the large ovehang aft, the effect being less noticeable at moderate than at small or large heel angles.

At a course velocity of 3.86 ft/sec., the wave profile lies near the top or the stern so that very little increase is possible here, and it is to be expected that all the curves will tend to turn over similarly to those for 10° heel. Indeed as the wetted surface amidships may decrease due to an enlarging hollow, the total wetted area could decrease at very high speeds, this is supported by the

shape of the curves for 10° heel.

The maximum variation in wetted surface due to velocity occurred at zero heel and 10° leeway, being some 62 sq. ins. over the speed range of the experiments, equivalent to nearly 10% of the static upright area.

The over-all variation in wetted surface area amounted to some 11% of the static upright value (70 sq. ins.)

The most important factor affecting the total wetted area, within normal conditions expected while sailing, is speed; heel is also important, while leeway is less so.

Variation on the full scale vessel will be similar at comparable speeds.

Estimate of Static Wetted Surface in Upright, Standard, Condition

This was calculated by the method of half girths which were taken from the Official Plans of the Dragon Class at each station. The girths were put through a Simpsons Rule calculation using the First Rule; the effect of longitudinal curvature in the hull surface bring taken into account by each half girth being multiplied by Cot ϕ , where ϕ is the average inclination of the waterlines at the appropriate station.

The calculation is shown in Table 16, resulting in a wetted surface area for the standard model condition during the experiments of 639 sq. ins. or 4.43 sq. ft.

The wetted surface at each test condition was then estimated by reference to Table 15. (set out in Table 17).

In order that the wetted surface can be read off simply in any desired condition, the curves for each speed are drawn separately as shown in Figs. 128 to 130.

The use of axes intersecting at 45° gives a better spread of results and enables curves of greater curvature to be drawn with a more likely distribution when only three points are available, than would the usual 90° axes.

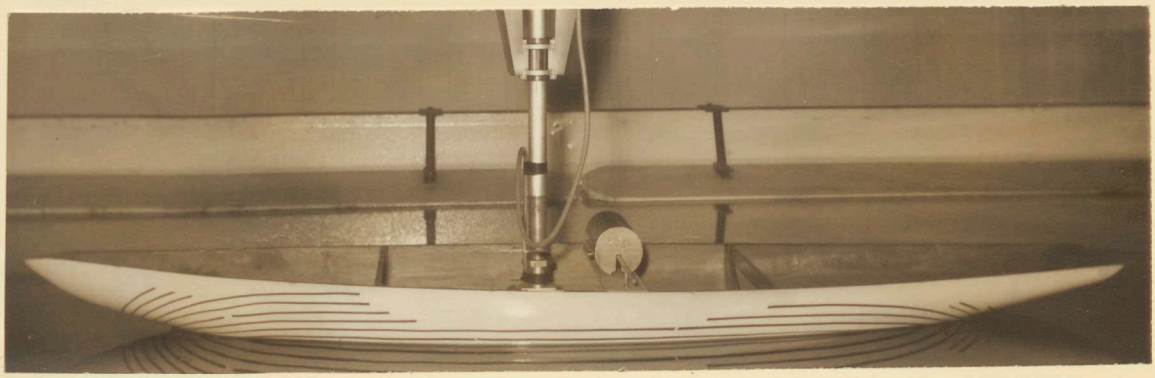

Fig.118. Arrangement of plastic adhesive strips, and still waterline for wetted surface experiments.

fig 119 hull surface expansion chart.

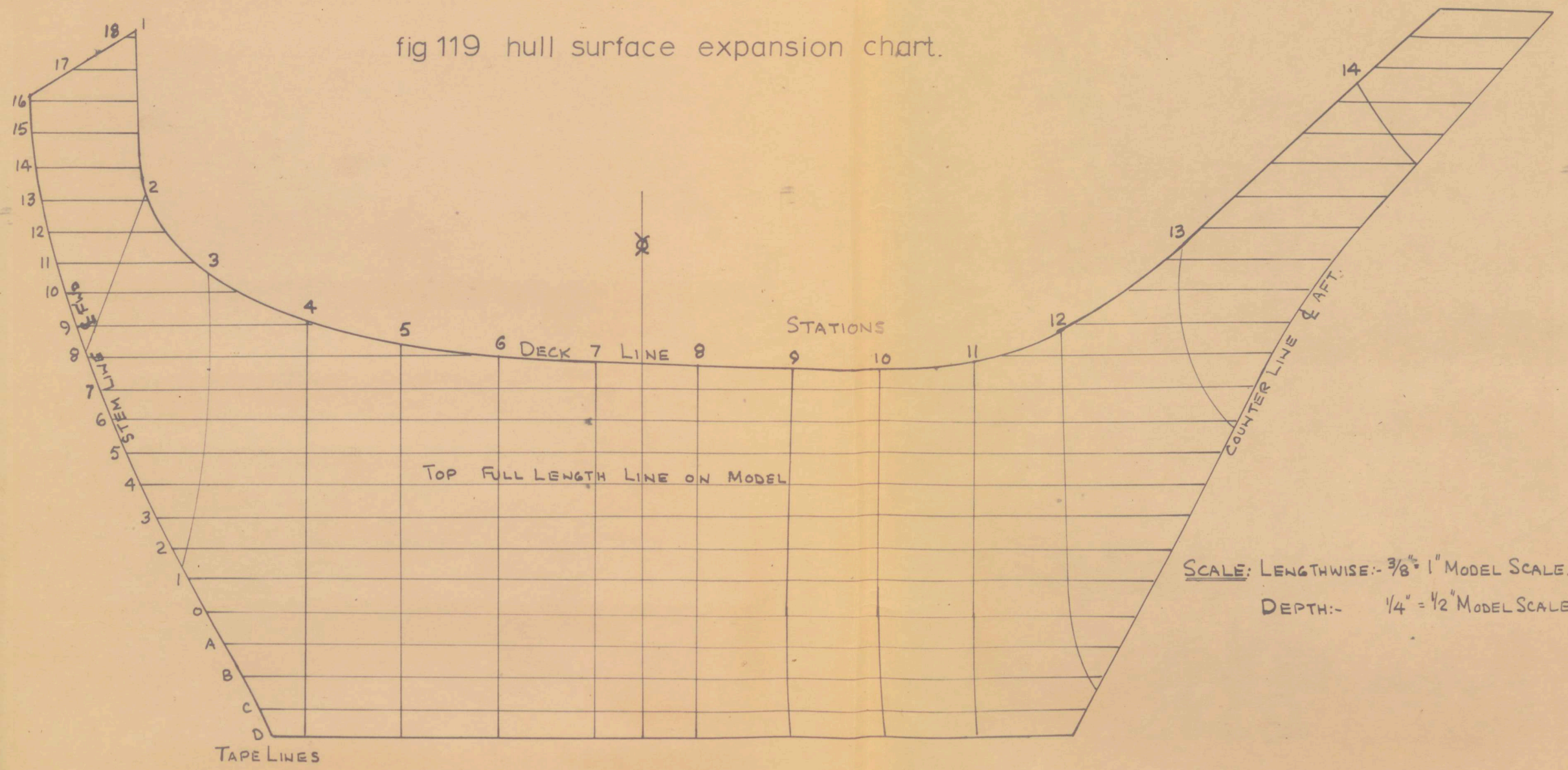

SCALE: LENGTHWISE:- 3/8" = 1" MODEL SCALE.

DEPTH:- 1/4" = 1/2" MODEL SCALE.

fig 120 waterlines on leeward and windward sides of hull.
heel 10°, model vel. 0 FT/SEC.

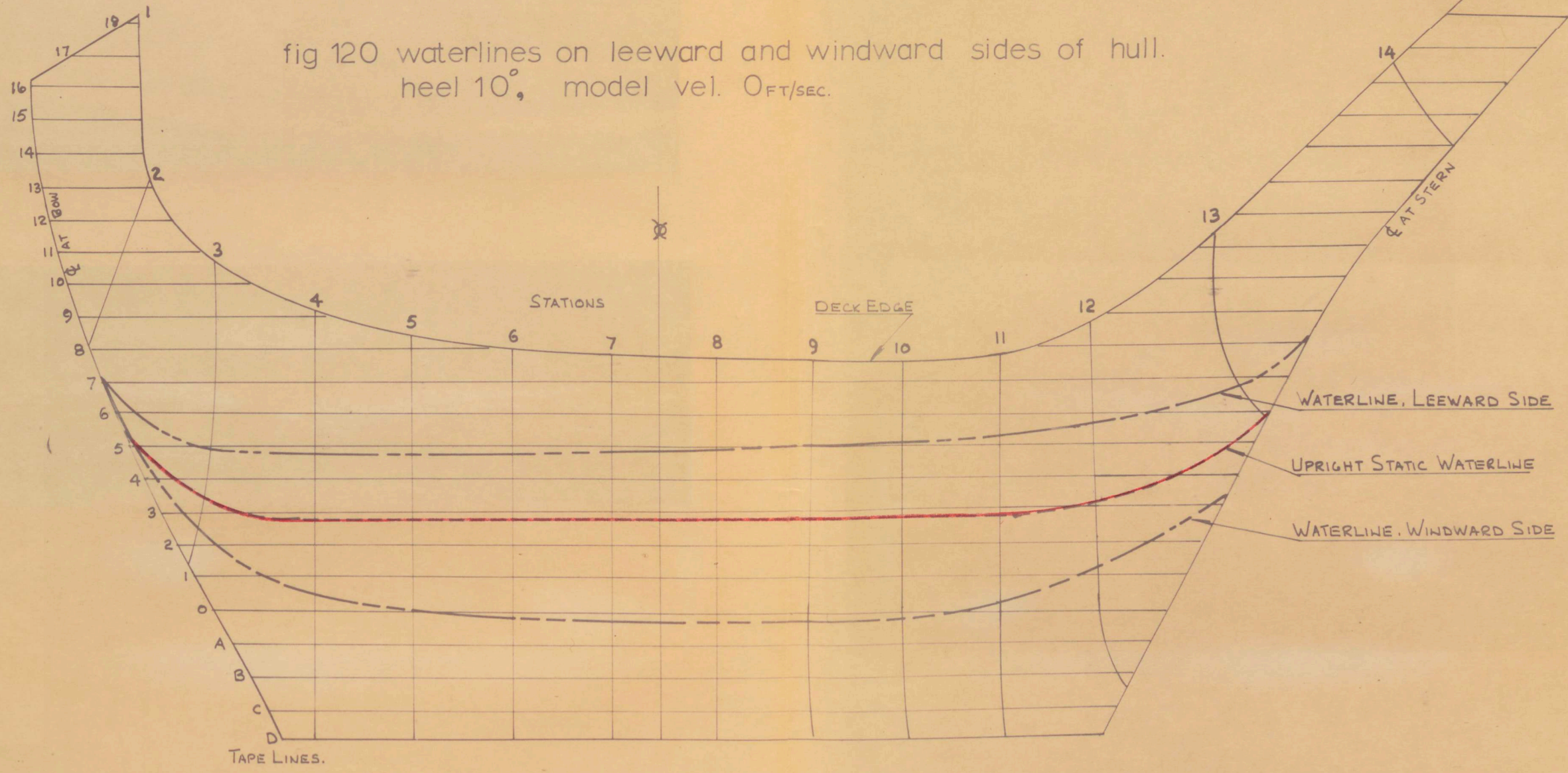

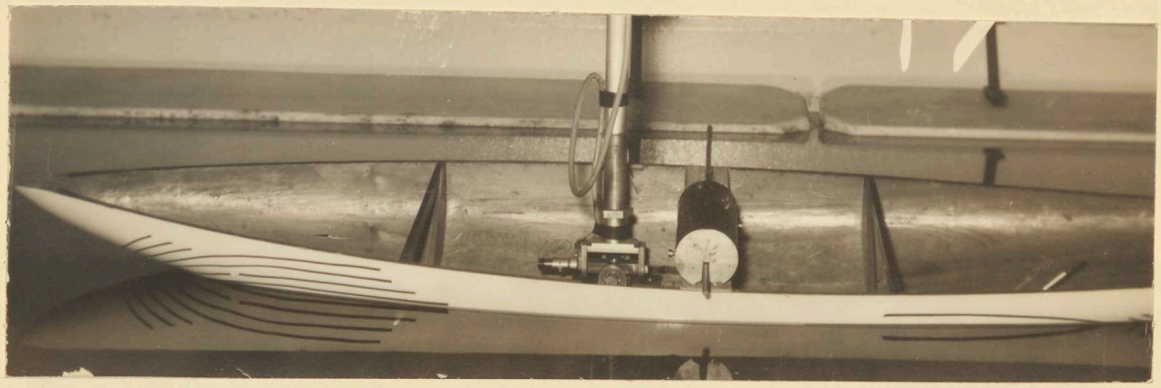

Photo No.17. Leeward side.

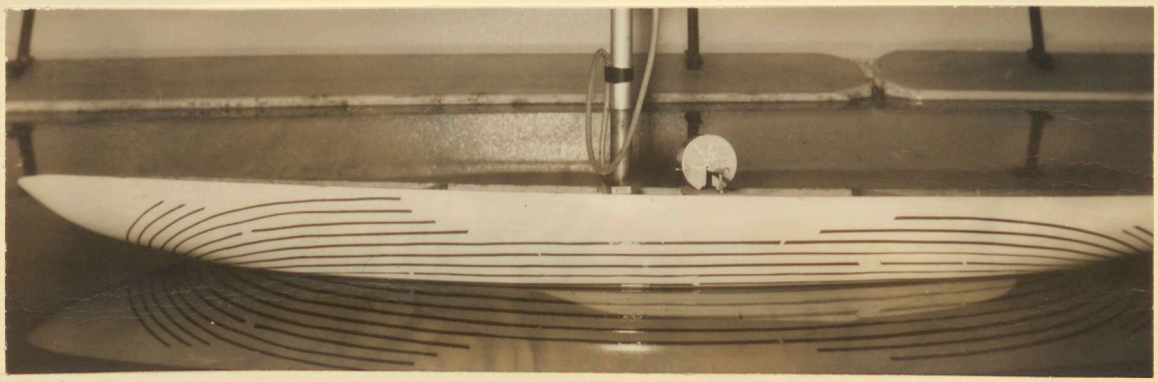

Photo No.18. Windward side.

Fig.121. Model static, heeled 10°.

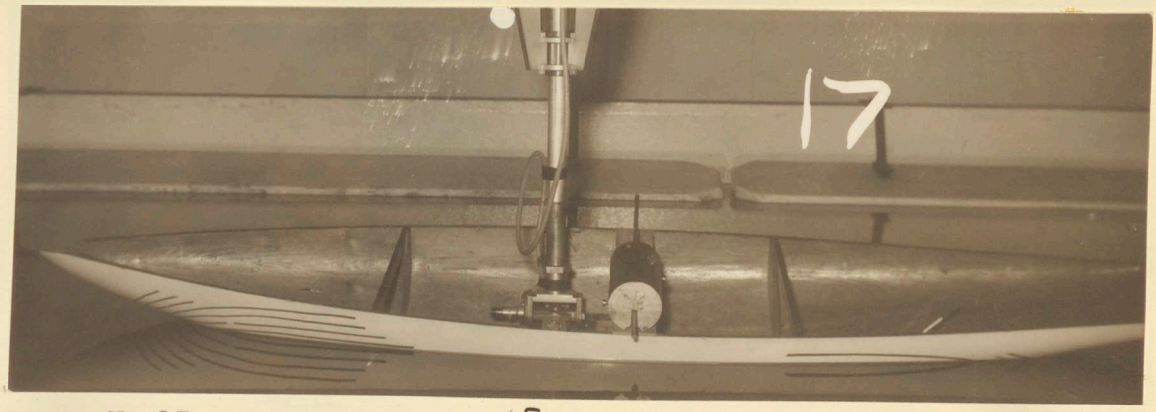

Photo No.17. Leeward side. $V/\sqrt{L}$ zero.

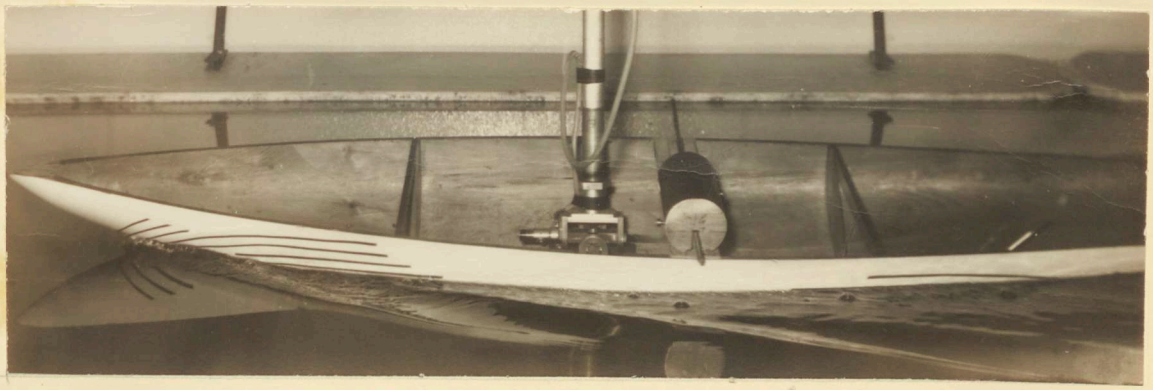

Photo No. 25. Leeward side, $V/\sqrt{L}$ 0.94, $\lambda = 5^{o}$.

Photo No.29. Leeward side. $V/\sqrt{L}$ 0.94, $\lambda = 10^{o}_{o}$.

Fig.122. effect of leeway on waterline.

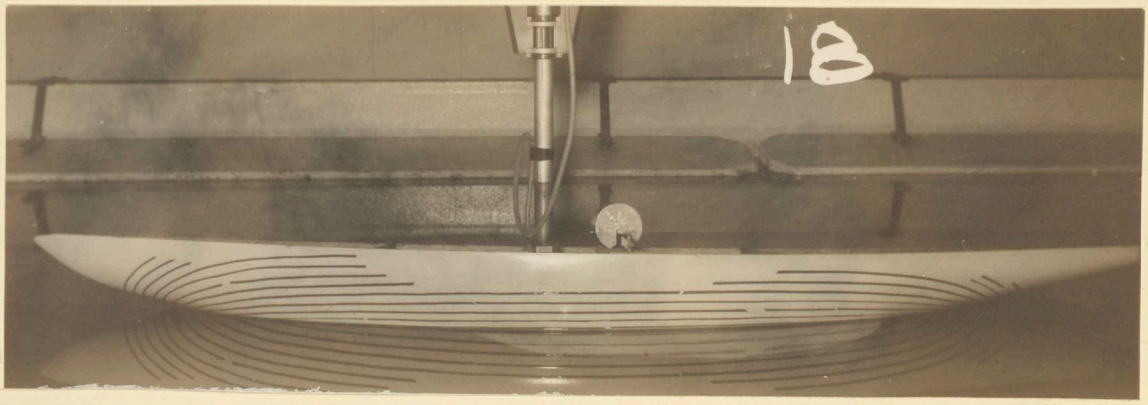

Photo No.18. Windward side. $V/\sqrt{L}$ zero.

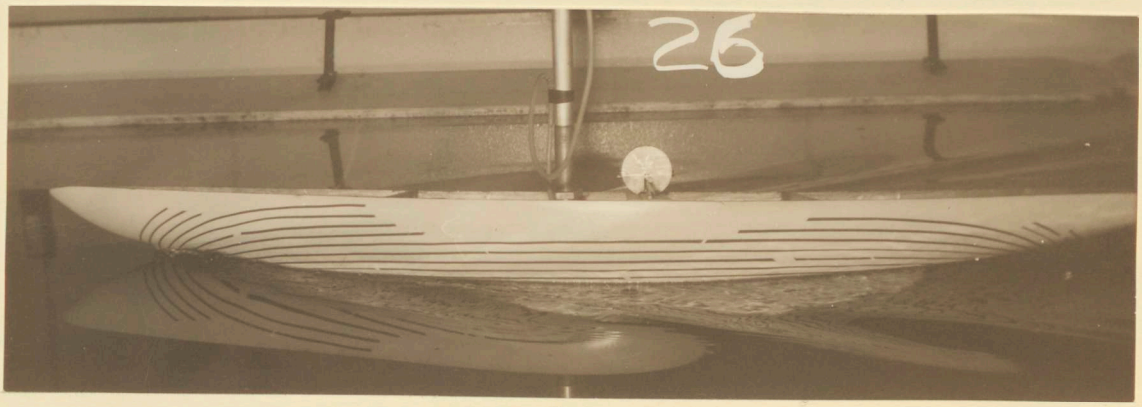

Photo No.26. Windward side. $V/\sqrt{L}$ 0.94, $\lambda = 5^{\circ}$.

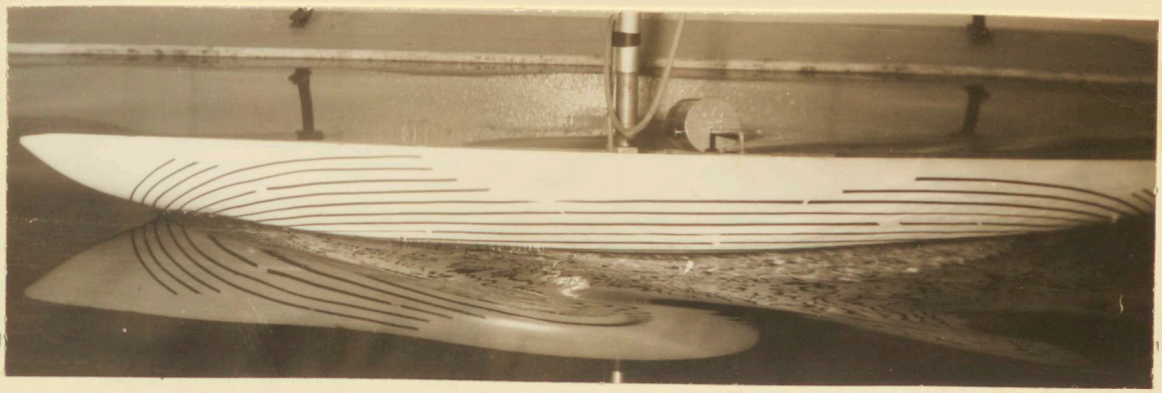

Photo No. 30. Windward side. $V/\sqrt{L}$ 0.94. $\lambda = 10^{\circ}$.

Fig.122. effect of leeway on waterline.

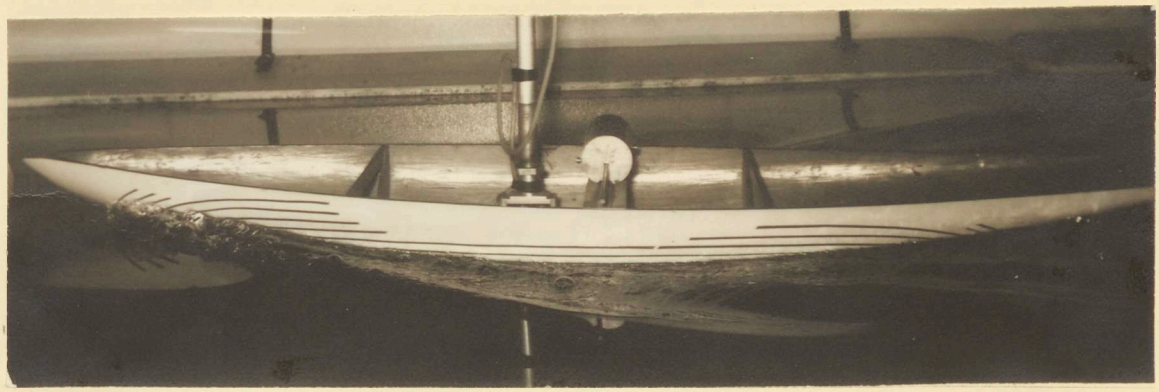

Photo No.13. Leeward side, $V/\sqrt{L}$ 1.44, $\theta = 0^{\circ}$

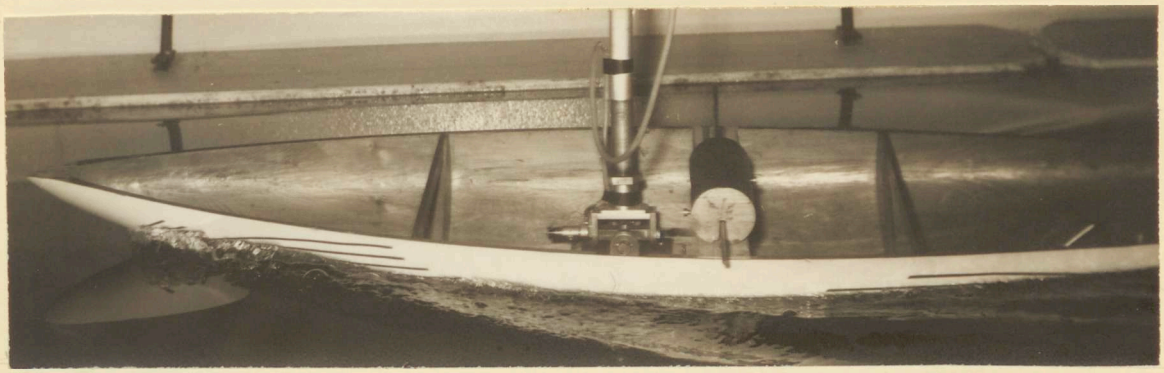

Photo No.33. Leeward side, $V/\sqrt{L}$ 1.44, $\theta = 10^{\circ}$

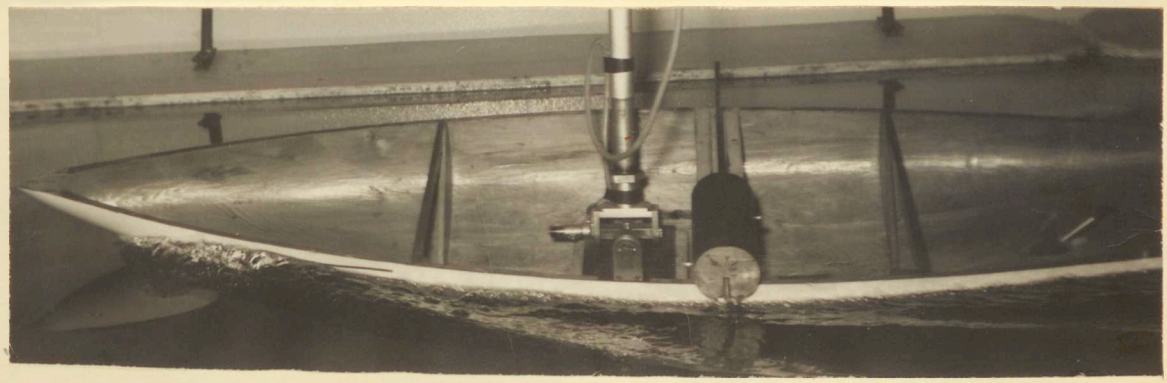

Photo No.53. Leeward side, $V/\sqrt{L}$ 1.44, $\theta = 20^{\circ}$

Fig.123. Effect of heel on waterline.

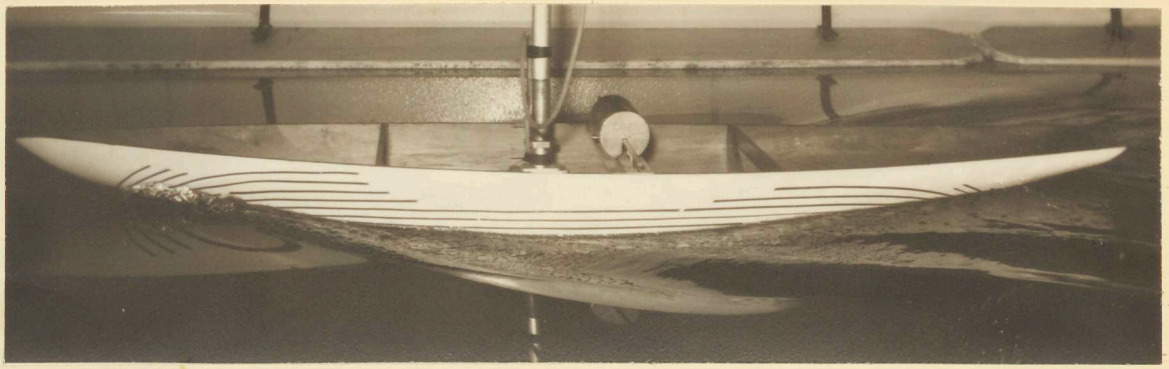

Photo No.14. Windward side $V/\sqrt{L}$ 1.44, $\theta = 0^{\circ}$.

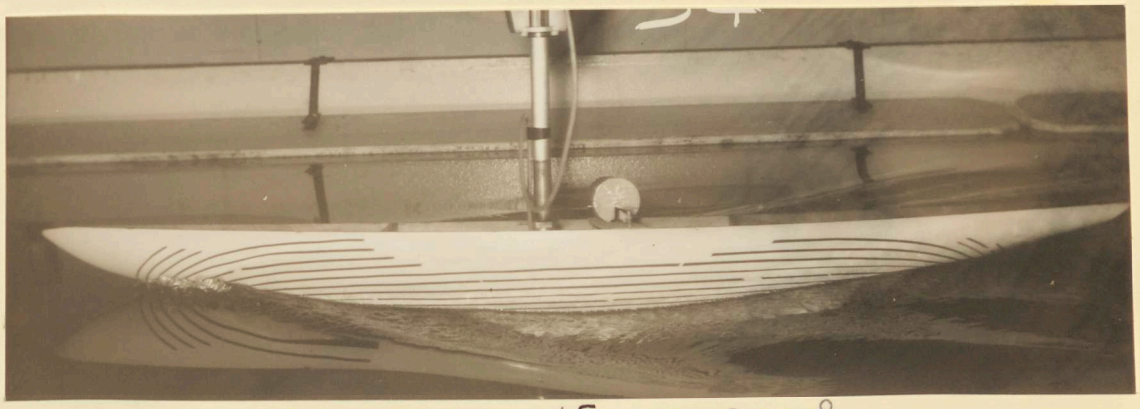

Photo No.34. Windward side. $V/\sqrt{L}$ 1.44, $\theta = 10^{\circ}$.

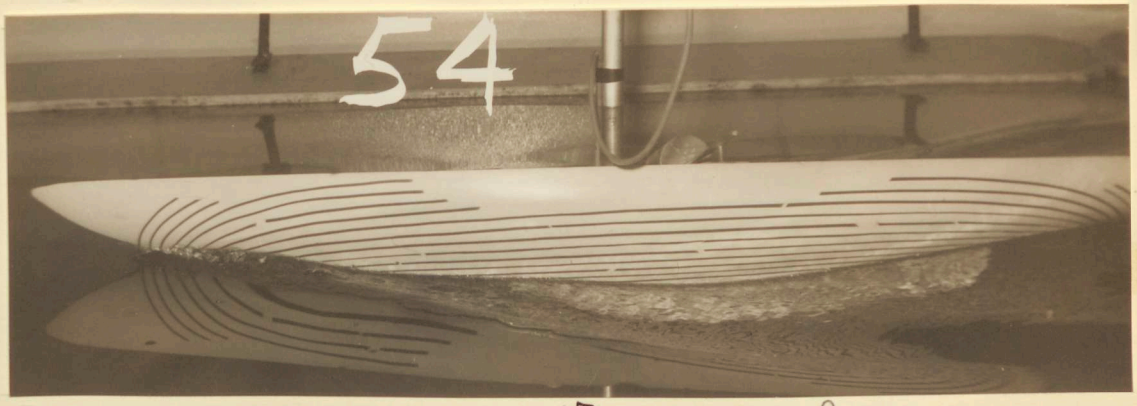

Photo No.54. Windward side. $V/\sqrt{L}$ 1.44, $\theta = 20^{\circ}$

Fig.123. Effect of heel on waterline.

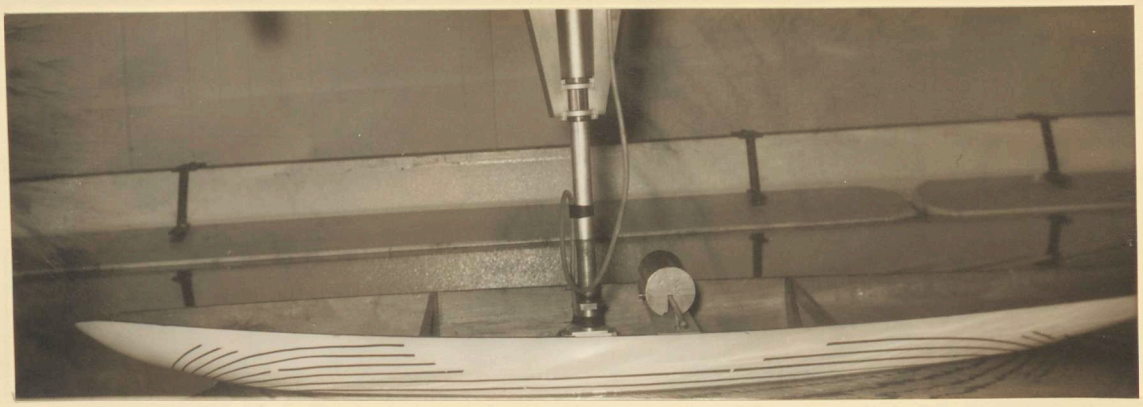

Photo No.2 Model upright, $V/\sqrt{L}$ 0.6, zero leeway.

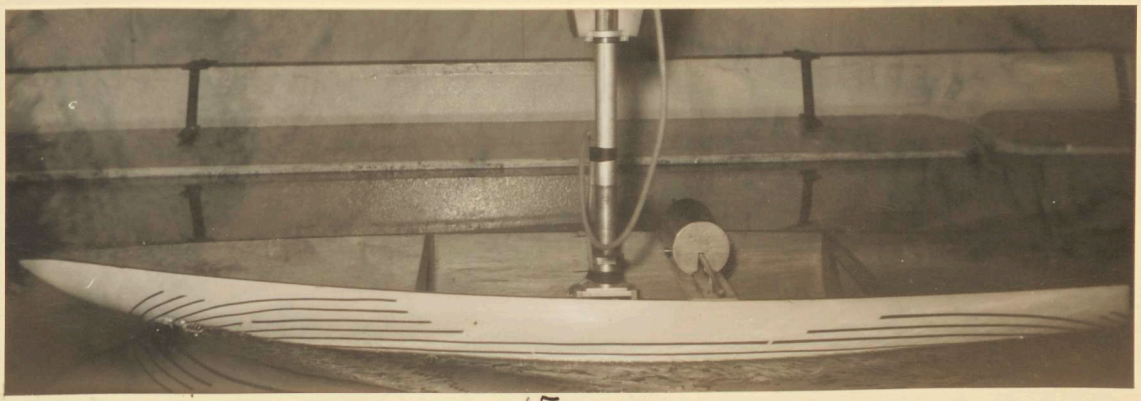

Photo No.7. Model upright, $V/\sqrt{L}$ 0.94, zero leeway.

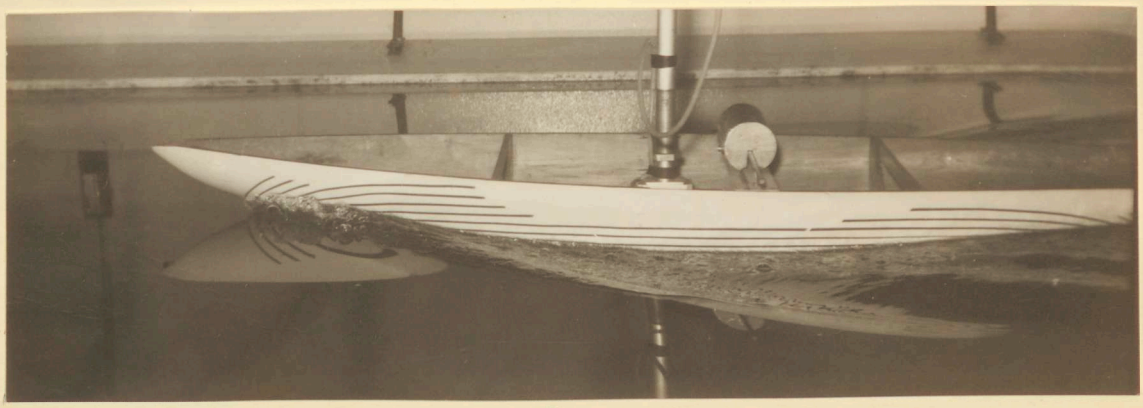

Photo No.12. Model upright, $V/\sqrt{L}$ 1.44. zero leeway.

Fig.124. Effect of speed on waterline.

fig 125 decrease in wetted surface - windward side.

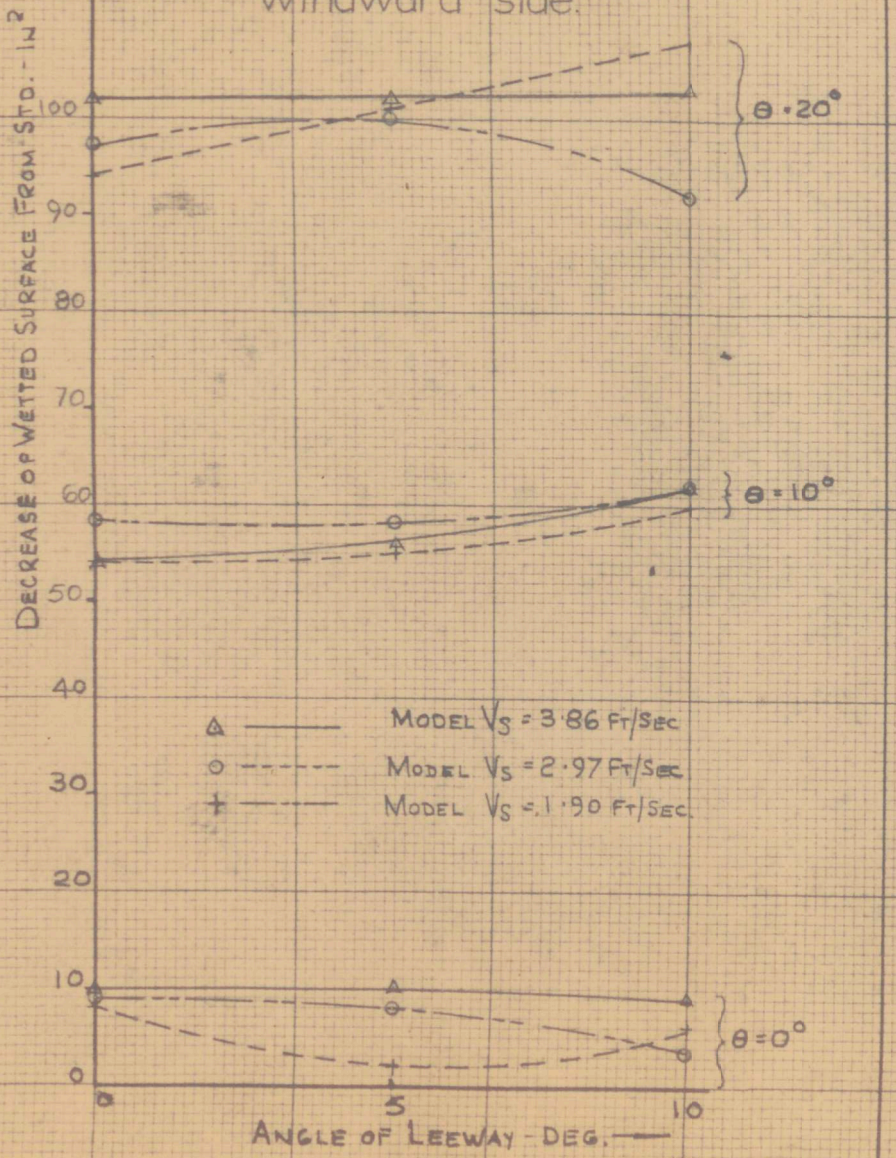

fig 126 increase in wetted surface - leeward side

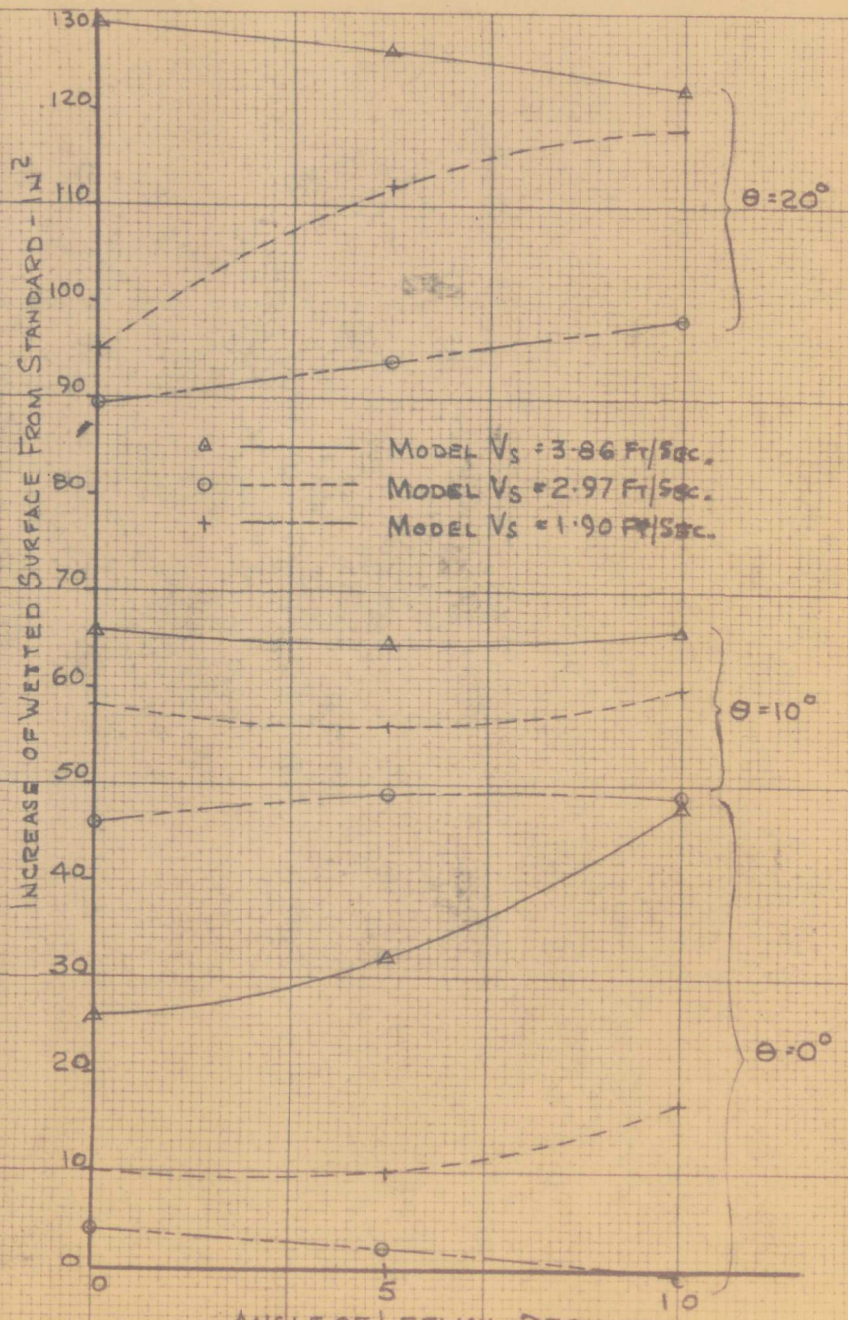

fig 127 variation in wetted surface area with speed, leeway and heel

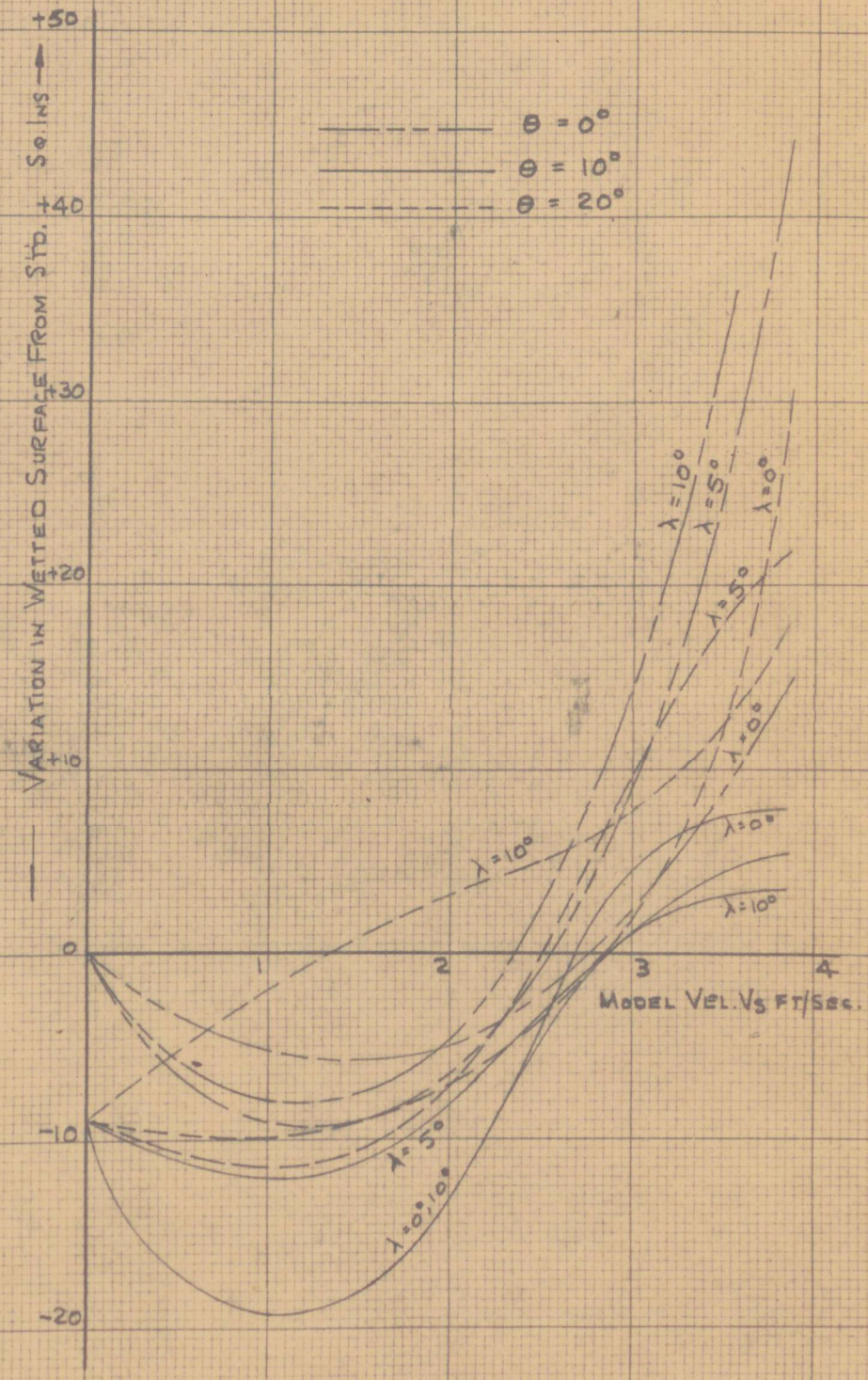

fig 128 'dragon' model - standard condition
wetted surface at 1·90 & 0 FT/SEC.

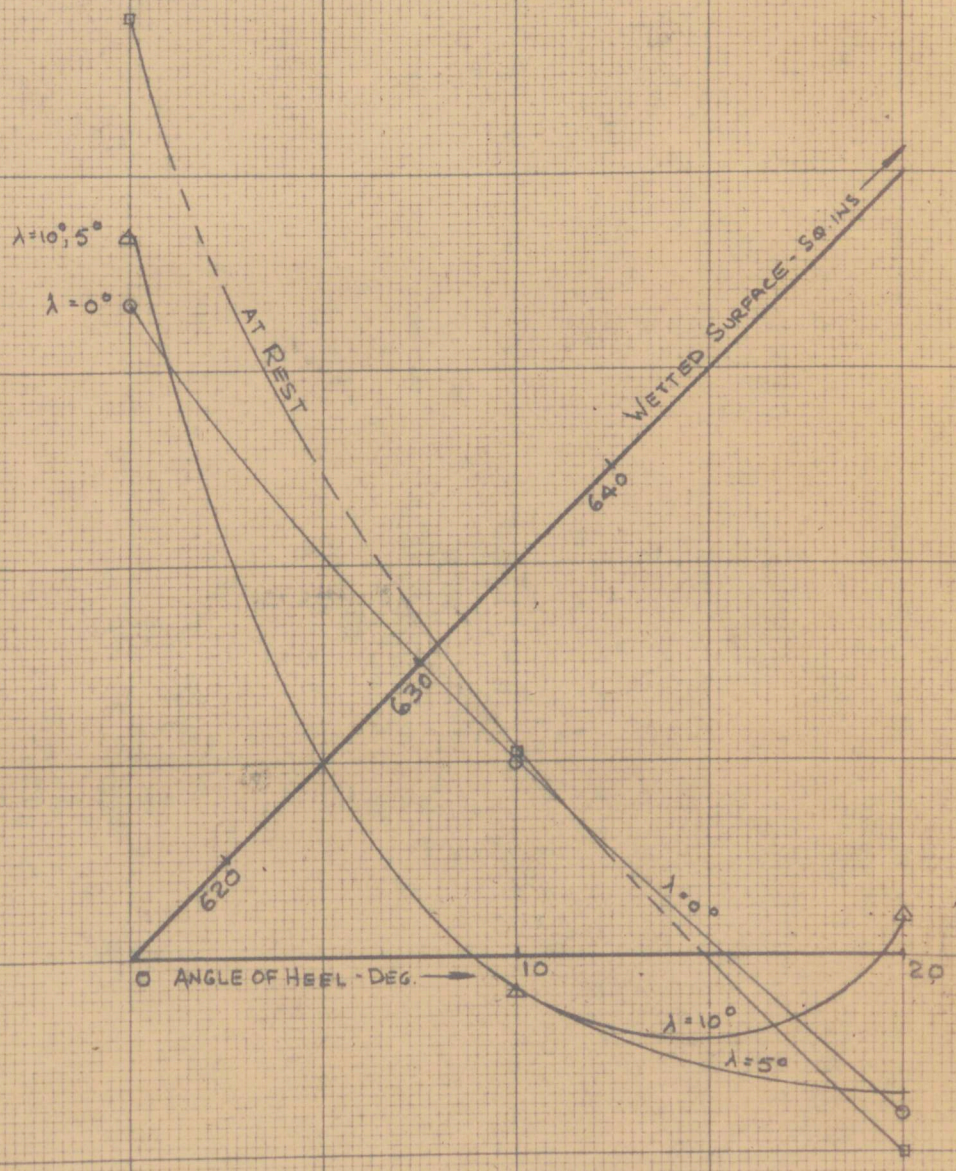

——— MODEL VEL. V_S = 1·90 FT/SEC.
——— - - - ——— MODEL VEL. V_S = 0 FT/SEC

fig 130 'dragon' model standard condition.
wetted surface at 3·86 FT/SEC.

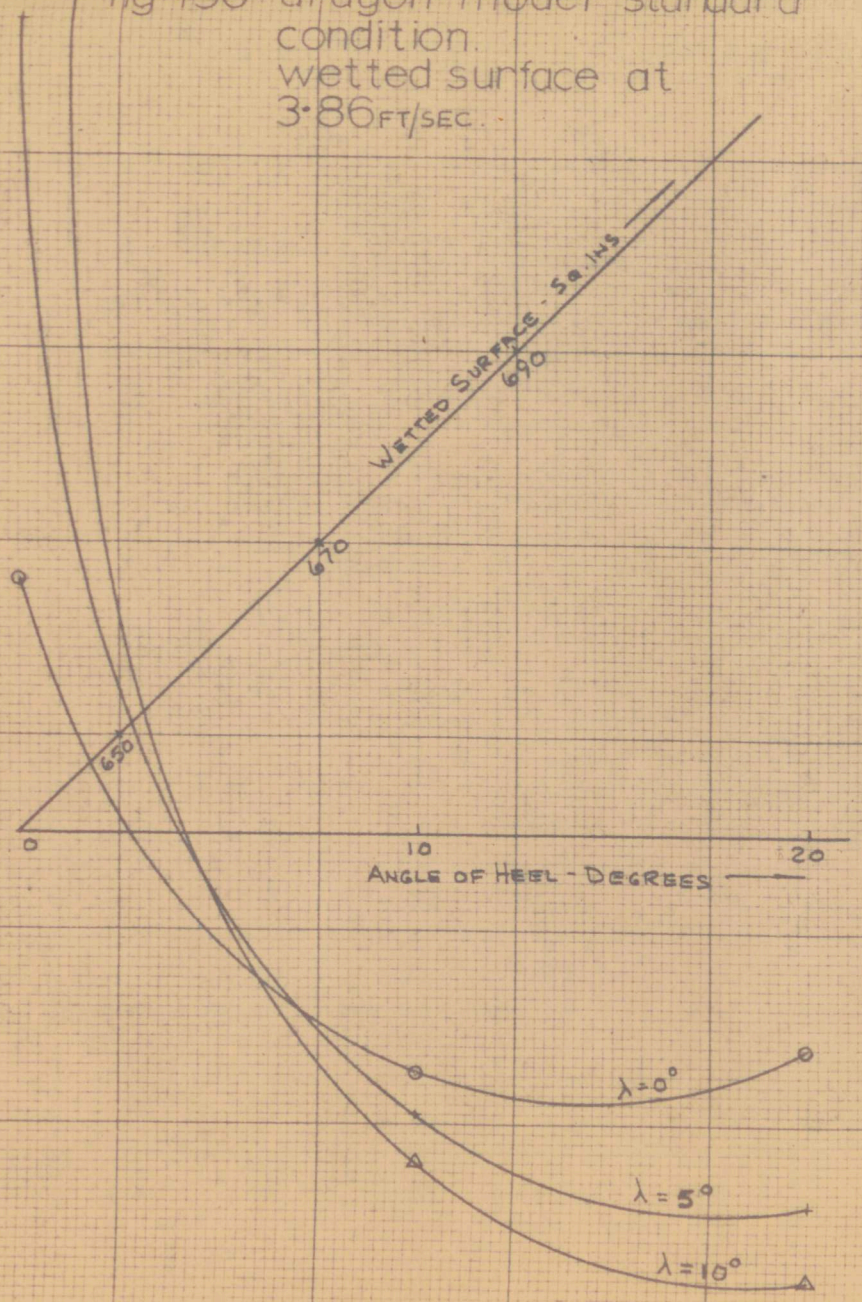

fig 129 'dragon' model standard cond'n.
wetted surface at 2·97 FT/SEC.

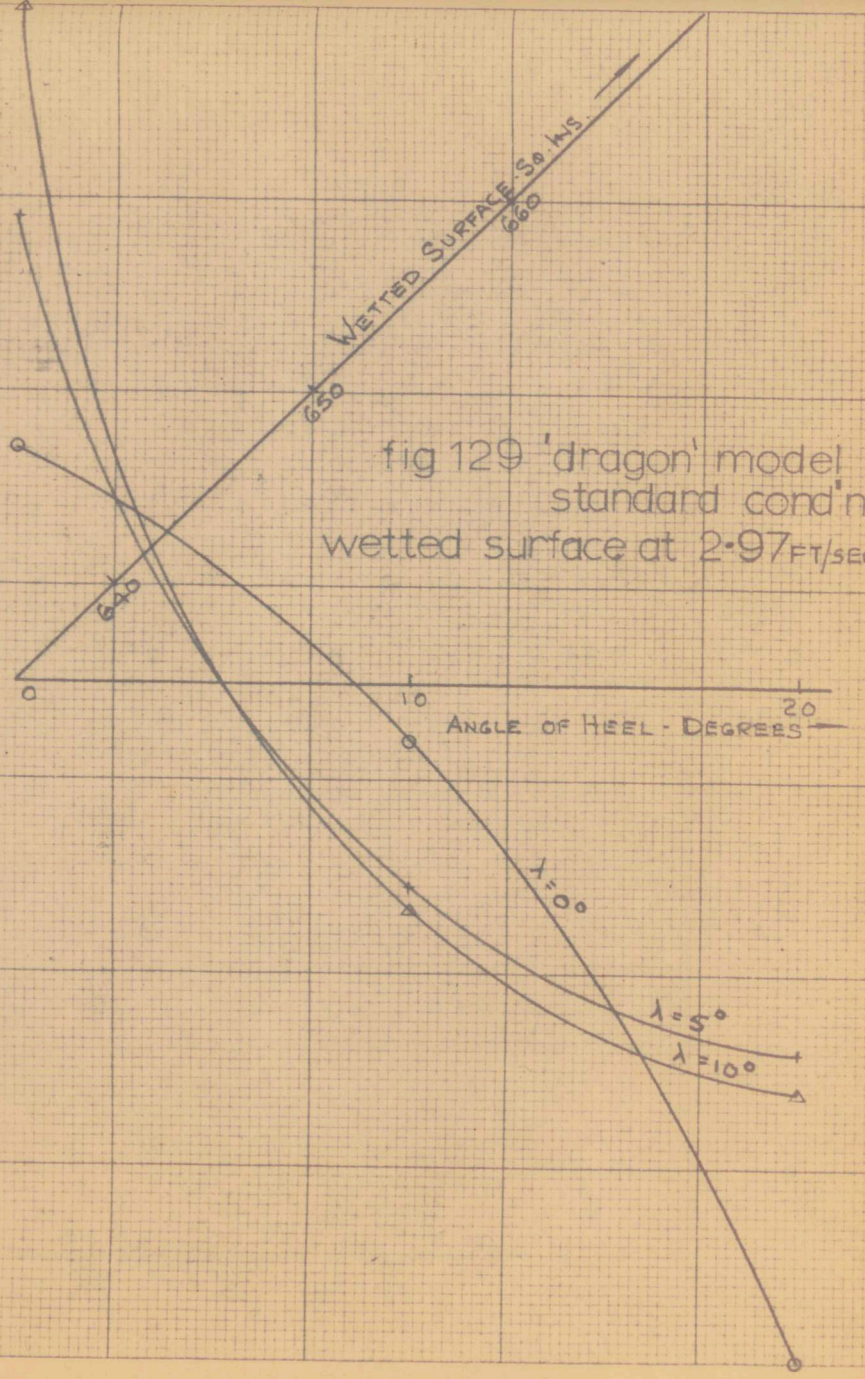

TABLE 15 WETTED SURFACE VARIATION.

HEEL θ°	LEEWAY λ°	MODEL VELOCITY 1·90 FT/SEC			MODEL VELOCITY 2·97 FT/SEC			MODEL VELOCITY 3·86 FT/SEC.		
		LEEWARD SIDE. W.S. FROM STD. IN^2	WINDWARD SIDE. W.S. FROM STD. IN^2	TOTAL DEVIATION FROM STD. IN^2	LEEWARD SIDE. W.S. FROM STD. IN^2	WINDWARD SIDE W.S. FROM STD. IN^2	TOTAL DEVIATION FROM STD. IN^2	LEEWARD SIDE. W.S. FROM STD. IN^2	WINDWARD SIDE W.S FROM STD. IN^2	TOTAL DEVIATION FROM STD. IN^2
0	0	+3·5	-9·0	-5·5	+10·04	-8·25	+1·79	+25·8	-11·6	+14·2
	5	+1·0	-8·0	-7·0	+9·4	-1·2	+8·2	+32·32	+10·95	+43·27
	10	-1·6	-3·8	-5·4	+18·7	-5·08	+13·6	+47·1	+9·7	+56·8
10	0	+44	-59	-15	+59	-54·5	+4·5	+62·3	-54·8	+8·0
	5	+48·5	-57·8	-9·3	+56·5	-55·7	+0·8	+64·5	-59	+5·5
	10	+46·5	-61·5	-15	+60·2	-61·3	-1·0	+66·1	-62·5	+3·6
20	0	+89·7	-97·2	-7·5	+95	-94	+1·0	+132	-102	+30
	5	+94	-102	-8·0	+112	-103	+9·0	+125	-103	+22
	10	+96·5	-93·5	+3·0	+117	-109	+8·0	+121·5	-103·5	+18
0	—	—	—	—	STATIC.					
10	—	+46	-55	-9						
20	—	+85	-94	-9						

TABLE 16. CALCULATION OF STATIC, UPRIGHT, WETTED SURFACE

STANDARD DISPLACEMENT.

FREEBOARD:- F'WD 3 5/8", AFT 2 5/8".

DRAWING STATION No.	1/2 GIRTH INS.	ϕ°	SEC ϕ	CORRECTED 1/2 GIRTH INS	S.M.	PRODUCTS	S.M.	PRODS.
2	0	-	-	0	1	0		
3	* 2·7	24	1·095	2·96	4	11·84		
4	4·4	22	1·079	4·75	2	9·50		
5	5·8	19	1·058	6·12	4	24·48		
6	7·3	11	1·02	7·43	2	14·86		
7	10·5	5	1·004	10·53	4	42·12		
8	11·3	0	1·0	11·3	2	22·60		
9	11·6	6	1·006	11·67	4	46·68		
10	9·9	18	1·05	10·4	2	20·80		
11	6·4	28	1·133	7·25	4	29·00	−1	−7·25
12	4·2	34	1·206	5·05	1	0	8	40·40
13	0	-	-	-			5	0
	②					231·88		33·15

* MULT BY 0·8 AS ACTUAL C.I. IS LESS THAN 4INS. W.L. ENDS ABAFT STN 2.

ϕ IS MEAN INCLINATION OF W.L.'S. TO ℄. AT EACH STATION.

TOTAL W.S. AREA. = $② \times \frac{4}{3} \times 232 + \frac{4}{12} \times 33.15 \times ② = 639 \text{ IN}^2 = \underline{4.43 \text{ FT}^2}$.

TABLE 17. ACTUAL WETTED SURFACE.

(STANDARD UPRIGHT WETTED SURFACE = 639 SQ. INS.)

HEEL θ°	LEEWAY λ°	MODEL VELOCITY 1·90 FT/SEC		MODEL VELOCITY 2·97 FT/SEC.		MODEL VELOCITY 3·86 FT/SEC.	
		VAR^N OF W.S. FROM S'TD. IN^2	ACTUAL W.S. IN^2	VAR^N OF W.S. FROM S'TD. IN^2	ACTUAL W.S. IN^2	VAR^N OF W.S. FROM S'TD IN^2	ACTUAL W.S. IN^2.
0	0	−5·4	633·5	+1·8	641·0	+14·6	653·0
	5	−7·15	632·0	+8·25	647·0	+43·27	682·0
	10	−5·42	633·5	+13·62	652·5	+56·8	696·0
7	0	−15·0	624·0	+4·35	643·5	+8·0	647·0
	5	−9·3	630·0	+0·8	640·0	+5·5	645·0
	10	−15·0	624·0	+1·0	640·0	+3·6	643·0
20	0	−7·5	631·5	+1·0	640·0	+30·0	669·0
	5	−8·0	631·0	+9·0	648·0	+22·0	661·0
	10	+3·0	636·0	+8·0	647·0	+18·0	657·0
0	–	0	639·0				
10	–	−9·0	630·0				
20	–	−9·0	630·0				

CHAPTER 27: GENERAL CONCLUSIONS AND RECOMMENDATIONS

The results of experiments described in the previous chapters have provided an over-all picture of the hull's hydrodynamic and stability characteristics, and demonstrated their variation with various factors under direct or indirect control of the designer and helmsman.

The limited comparison possible between the experimental results and previous work on the same model at Saunders Roe Divn. showed general agreement, no obvious discrepancy appearing. It would be extremely useful however, to establish a correlation between measurements from both the Saunders Roe and University tanks, and this could be achieved by undertaking experiments on one particular hull in both tanks at identical model velocities, inclinations, A.U.W., and C.G. location. Such work should also allow an assessment of the blockage effects in the University Tank which will be more pronounced than at Saunders Roe.

Although a clear picture emerges of the variation in hydrodynamic force components with leeway, their change with heel and course velocity is more irregular, a situation which is hardly surprising when consideration is taken of the superimposition and combination of the pressure fields round the hull, due to velocity, heel and leeway.

In the light of experiments on this hull and the discussions which followed, it appears that caution should be observed in any assumption concerning the variation of Lift coefficient with leeway, heel and velocity, and that it is inadvisable to assume linearity for the curve of $C_D \sim C_L^2$.

The experimental results, when compared with the samll amount of other available published data, indicate that apparent linearity of the Lift curve from results of routine commercial tank tests may be due to assumed sailing conditions in which the values of leeway and heel vary with speed.

Comparison of the present results with those of Davidson's original paper (Ref. 9) show that the Lift curve may be linear or curvilinear, so that it is apparent that for any yacht hull tank tested, a number of test runs should be made to establish the shape of curves for C_L, C_D, and $C_L^2 \sim C_D$, before any assumptions are made. As the present experiments indicate a similar variation with leeway for these quantities over a wide range of heel and speed, it is probable that the same pattern would occur with other hulls, and that only a small number of extra runs would be required at one speed and heel, measuring Lift and Drag over the range of leeway used in the present work.

In particular, the use of assumed linearity for $C_L^2 \sim C_D$

in order to fair experimental results must be questionable, unless an experiment on the lines described has proved the variation.

Marchaj (Ref. 16) has shown from wind tunnel measurements that the 'centre of effort' for the sails is very near that normally assumed by designers: a geometric centroid of sail area. The present experiments indicate that the depth for the 'centre of pressure' of the hull is also very close to the designer's assumed 'centre of lateral resistance'. Surprisingly, the depth of action for F_{Yw}, as found, lies slightly above the geometric centroid, suggesting that the hull, as distinct from the fin, plays a large part in producing Lift; the opposite indication appears however, from the fact that the 'Dragon' hull does not appear to develop lift due to heel at zero leeway.

There is a need for further, more detailed work to study the hydrodynamic overturning moment on the hull.

Inherent stability while under way is seen to differ from that expected due to hydrostatic considerations; results indicate that more attention should be given to this during routine experiments for performance prediction; this is a further area of study where more detailed work is desirable.

The experiments of H.M. Barkla at ehe Davidson Laboratory are reported to have been an attempt to assess the variation in performande with hull shape in terms of length beam and depth, using sail

coefficients of the 'Gimcrack' type.

In fact, the performance of any particular hull can only be analysed fully by combining the hull characteristics with those of the particular sail plan in a similar manner to the work of Part 1; in this way the effect of different sail plans and cuts, together with different hull and fin shapes may be obtained. The measurement of hull characteristics should now be expended to craft of other forms and hull/ fin combinations.

It can be envisaged that at some future date, designers will have access to charts determing the hydrodynamic and stability characteristics for hulls of varying properties, which can be used with similar charts for sail plans in order to find the correct combination for a particular yacht. Naturally, the results of the various possible combinations would have to be assessed in conjunction with other requirements for a particular vessel, e.g. sea-keeping, capacity, use, so that the need for skilled and experienced designers is still apparent.

The production of such charts for the hull requires a considerable amount of experimental work on the model scale to measure the characteristics of a wide range of hull proportions and forms, similar to that reported to have been undertaken by Barkla, but on a far wider basis.

Once results on the model scale are available from which charts of hull characteristics could be prepared, there remains the

problem of applying the figures to a full size yacht. This problem has been discussed briefly in Chapter 20 and in the light of this, there is an obvious and urgent need for further work on the scaling of force components using both the Sea and Body/Sea axes systems.

The traditional method of extrapolating resistance has been developed to such an extent in 'large ship' work, that it can be used to provide a reasonably accurate prediction; in this field a considerable amount of research is being undertaken in hydrodynamic establishments throughout the World, so that the basic work necessary regarding resistance and its components is in progress.

The application of these methods to yacht forms and sizes requires investigation, as does the expansion of Lift from model to full scale. Concurrently, the scaling effects on F_{Yw} and F_{Xw} should emerge.

Feed back from large ships is principally, because of their size, from data obtained during speed trials, although various experiments have been undertaken by either towing or using jet propulsion; e.g. Refs. 6 & 7.

In the case of yachts, the size is such that full scale runs could be made in one of the large tanks now available, e.g. The Ship Hydrodynamics Laboratory at Feltham, for a vessel the size of a 'Dragon'. Here under controlled conditions, accurate measurement is

possible of the full scale resistance and Lift, and a survey of the boundary layer flow state could be obtained under both calm and distrubed sea states.

From the discussion of Chapter 20, it is considered that the boundary layer investigation is certainly as important as force measurements, and the use of 'Hot film' turbulence detectors would enable accurate measurement of laminar and turbulent areas to be obtained.

A problem difficult to overcome in such experiments is caused by the large Lift developed by a yacht hull; as tank carriages and associated apparatus are usually designed for measuring forces acting along the tank length, they are not equipped to support or measure large lift forces. It might prove more acceptable to use a whirling arm support, so that the major part of the Lift is in the radial direction.

If it proved impossible to run the hull in a tank, a boundary layer investigation could be undertaken on a yacht, while sailing, by means of turbulence detection probes. Although such work would present more problems than in the controlled conditions of a laboratory, the results should enable a reduction in one uncertainty during the scaling operation.

Other methods of measuring the full scale hull forces have been discussed by Crago in Ref. 8; the only direct method being that of

towing a full size hull, which is considered impracticable. Other methods involved the use of measured sail forces from which the hull components could be deduced, or the calculation of hull forces from full scale sailing trials. The latter method was used by Davidson (Ref. 9) and with the 12-Metre yacht 'Norsaga' for which the data has not been published.

This method of approaching the problem may provide useful data for applying hull measurements in the comparison of full scale performance for commercial work; whether it can be used to confirm the actual full scale hull forces is doubtful, due to the number of assumptions and steps in the calculations necessary to reduce the data.

A first study of wetted surface variation is given in Chapter 26; this is another region where the difficulty in scaling for yachts could be reduced by further study on the model scale.

LIST OF REFERENCES

1. An Investigation into the Performance of a Dragon Class Yacht. Saunders Roe Report T/O 142.

2. An Investigation into the Performance of a Dragon Class Yacht. Y.R.C. Report No. 2

3. Chapter 5, of Papers presented at the Conference on Yacht Design and Research. Held at the University of Southampton 28th to 30th, March 1962.

4. Chapter 7, of Papers presented at the Conference on Yacht Design and Research. Univ. of Southampton 28th to 30th, March 1962.

5. Tank Tests on a 50 ft. W.L. Auxiliary Centreboard Ketch. Saunders Roe Divn. T/N 8125 and PRC/DCM/AN/SN/4139.

6. B.S.R.A. Resistance Experiments on the Lucy Ashton. R.I.N.A. 1955 et seq.

7. Scale Effect Experiments on Victory Ships and Models. R.I.N.A. 1955 et seq.

8. The Prediction of Yacht Performance from Tank Tests. W.A. Crago R.I.N.A. 1963.

9. Some Experimental Studies of the Sailing Yacht. K.S.M. Davidson. S.N.A.M.E. 1936.

10. Sailing Yacht Calculation Procedure Davidson Laboratory T.M. 108.

11. Full Scale Tank Tests of an International 10 sq. metre Class Canoe. T.Tanner R.I.N.A. 1961

12. Analysis of Data obtained from Tank Tests of a Model Dragon Class Yacht. W.A. Crago. A.C.Y.R. Paper 8.

13. Full Scale Performance Trials of the 5.5 metre yacht Yeoman. Y.R.C. Report No. 1.

14. Correlation of Data on Yacht Rudder Characteristics. Davidson Laboratory T.M. 37.

References (Cont.)

15. Estimation of the Effect of Sail Performance on yacht close-hauled behaviour.
P.R. Crewe. R.I.N.A. 1964

16. Wind Tunnel Tests on a one third scale model of an 'X' One Design Class Yacht's Sails.
C.A. Marchaj, University of Southampton 1963

17. National Physical Laboratory, New Ship Hydrodynamics Laboratory.
Allan, R.I.N.A. 1957

18. Methods for inducing trubulence for small models at Davidson Laboratory.
Davidson Laboratory Note. No. 549

19. Basic Naval Architecture
Barnaby

20. Proceedings of the Symposium on the Towing Tank Facilities, Instrumentation, and measuring techniques;
Zagreb, 22nd. to 25th. Sept. 1959.

21. Ship Model Size and Tank Boundary Correction.
Emmerson, N.E.C. Inst. of England & Shipbuilders. 1959

22. Davidson Laboratory Note N509

23. The Behaviour of the Sailing Yacht.
Barkla, R.I.N.A. 1961

24. The Geometry of Sailing to Windward
T. Tanner, R.I.N.A. 1961

25. Yacht Testing
Allan, Doust & Ware, R.I.N.A. 1957

26. Some Notes on the use of the Yacht Test Tank.
Chapleo, University of Southampton 1963.

27. Proposals for a System of Basic Equations for Yacht Steady Sailing performance, together with useful Simplifying Assumptions.
P.R. Crewe, University of Southampton 1962

28. Chapter 3 of Papers Presented at Conference on Yacht Design and Research, University of Southampton, 28th. to 30th. March 1962.